Evolutionary Economics and Social Complexity Science 6

Jun Tanimoto

Fundamentals of Evolutionary Game Theory and its Applications

Springer

Evolutionary Economics and Social Complexity Science

Volume 6

The Japanese Association for Evolutionary Economics (JAFEE) always has adhered to its original aim of taking an explicit "integrated" approach. This path has been followed steadfastly since the Association's establishment in 1997 and, as well, since the inauguration of our international journal in 2004. We have deployed an agenda encompassing a contemporary array of subjects including but not limited to: foundations of institutional and evolutionary economics, criticism of mainstream views in the social sciences, knowledge and learning in socio-economic life, development and innovation of technologies, transformation of industrial organizations and economic systems, experimental studies in economics, agent-based modeling of socio-economic systems, evolution of the governance structure of firms and other organizations, comparison of dynamically changing institutions of the world, and policy proposals in the transformational process of economic life. In short, our starting point is an "integrative science" of evolutionary and institutional views. Furthermore,we always endeavor to stay abreast of newly established methods such as agent-based modeling, socio/econo-physics, and network analysis as part of our integrative links.

More fundamentally, "evolution" in social science is interpreted as an essential key word, i.e., an integrative and/or communicative link to understand and re-domain various preceding dichotomies in the sciences: ontological or epistemological, subjective or objective, homogeneous or heterogeneous, natural or artificial, selfish or altruistic, individualistic or collective, rational or irrational, axiomatic or psychological-based, causal nexus or cyclic networked, optimal or adaptive, microor macroscopic, deterministic or stochastic, historical or theoretical, mathematical or computational, experimental or empirical, agent-based or socio/econo-physical, institutional or evolutionary, regional or global, and so on. The conventional meanings adhering to various traditional dichotomies may be more or less obsolete, to be replaced with more current ones vis-à-vis contemporary academic trends. Thus we are strongly encouraged to integrate some of the conventional dichotomies.

These attempts are not limited to the field of economic sciences, including management sciences, but also include social science in general. In that way, understanding the social profiles of complex science may then be within our reach. In the meantime, contemporary society appears to be evolving into a newly emerging phase, chiefly characterized by an information and communication technology (ICT) mode of production and a service network system replacing the earlier established factory system with a new one that is suited to actual observations. In the face of these changes we are urgently compelled to explore a set of new properties for a new socio/economic system by implementing new ideas. We thus are keen to look for "integrated principles" common to the above-mentioned dichotomies throughout our serial compilation of publications.We are also encouraged to create a new, broader spectrum for establishing a specific method positively integrated in our own original way.

More information about this series at http://www.springer.com/series/11930

Jun Tanimoto

Fundamentals of Evolutionary Game Theory and its Applications

Springer

Jun Tanimoto
Graduate School of Engineering Sciences
Kyushu University Interdisciplinary
Fukuoka, Fukuoka
Japan

ISSN 2198-4204 ISSN 2198-4212 (electronic)
Evolutionary Economics and Social Complexity Science
ISBN 978-4-431-54961-1 ISBN 978-4-431-54962-8 (eBook)
DOI 10.1007/978-4-431-54962-8

Library of Congress Control Number: 2015951623

Springer Tokyo Heidelberg New York Dordrecht London

Printed on acid-free paper

Springer Japan KK is part of Springer Science+Business Media (www.springer.com)

Preface

For more than 25 years, I have been studying environmental issues that affect humans, human societies, and the living environment. I started my research career by studying building physics; in particular, I was concerned with hygrothermal transfer problems in building envelopes and predictions of thermal loads. After my Ph.D. work, I extended my research field to a *special scale* perspective. This extension was motivated by several factors. One was that I noticed a reciprocal influence between an individual building environment and the entire urban environment. Another was that the so-called urban heat island problem began to draw much attention in the 1990s. Mitigation of urban heating contributes to energy conservation and helps improve urban amenity; hence, the urban heat island problem became one of the most prominent social issues of the time. Thus, I started to study urban climatology because I was mainly concerned with why and how an urban heat island forms. The problem was approached with sophisticated tools, such as wind tunnel experiments, field observations, and computational fluid dynamics (CFD), and was backed by deep theories concerning heat transfer and fluid dynamics. A series of such studies forced me to realize that to obtain meaningful and reasonable solutions, we should focus not only on one area (e.g., the scale of building physics) but also on several neighboring areas that involve complex feedback interactions (e.g., scales of urban canopies and of urban climatology). It is crucially important to establish new bridges that connect several areas having different spatiotemporal scales.

This experience made me realize another crucial point. The term "environment" encompasses a very wide range of objects: nature, man-made physical systems, society, and humanity itself. One obvious fact is that we cannot achieve any significant progress in solving so-called environmental problems as long as we focus on just a single issue; everything is profoundly interdependent. Turning on an air conditioner is not the final solution for feeling comfortable. The operation of an air conditioner increases urban air temperatures; therefore, the efficiency of the overall system inevitably goes down and more energy must be provided to the system. This realization might deter someone from using an air conditioner. This

situation is one intelligible example. The decisions of any individual human affect the environment, and the decisions of a society as a collection of individuals may substantially impact the environment. In turn, the environment reacts to those decisions made by individuals and society, and some of that feedback is likely to be negative. Such feedback crucially influences our decision-making processes. Interconnected cycling systems always work in this way.

With this realization, I recognized the concept of a combined human–environmental–social system. To reach the crux of the environmental problem, which includes physical mechanisms, individual humans, and society, we must study the combination of these diverse phenomena as an integrated environmental system. We must consider all interactions between these different systems at all scales.

I know well that this is easy to say and not so easy to do. I recognize the difficulties in attempting to establish a new bridge that connects several fields governed by completely different principles, such as natural environmental systems and human systems. I understand that I stand before a steep mountain path.

Yet, I have seen a subtle light in recent applied mathematics and physics that includes operations research, artificial intelligence, and complex science. These approaches help us model human actions as complex systems. Among those, evolutionary game theory seems to be one of the most powerful tools because it gives us a clear-cut template of how we should mathematically treat human decision making, and a thorough understanding of decision making is essential to build that new bridge. Thus, for the last decade, I have been deeply committed to the study of evolutionary game theory and statistical physics.

This book shares the knowledge I have gained so far in collaboration with graduate students and other researchers who are interested in evolutionary game theory and its applications. It will be a great pleasure for me if this book can give readers some insight into recent progress and some hints as to how we should proceed.

Interdisciplinary Graduate School of Engineering Sciences, Kyushu University
Fukuoka, Japan

Jun Tanimoto

Acknowledgments

This book owes its greatest debt to my coworkers who had been my excellent students. Chapter 2 relies at critical points on the contributions of Dr. Hiroki Sagara (Panasonic Factory Solutions Co. Ltd.) and Mr. Satoshi Kokubo (Mitsubishi Electric Corporation). Dr. Atsuo Yamauchi (Meidensha Corporation), Mr. Satoshi Kokubo, Mr. Keizo Shigaki (Rico Co. Ltd.), Mr. Takashi Ogasawara (Mitsubishi Electric Corporation), and Ms. Eriko Fukuda (Ph.D. candidate at Kyushu University) gave very substantial input to the content of Chap. 3. Chapter 5 would not have been completed without the many new findings of Dr. Atsuo Yamauchi, Mr. Makoto Nakata (SCSK Corporation), Mr. Shinji Kukida (Toshiba Corporation), Mr. Kezo Shigaki, and Mr. Takuya Fujiki (Toyota Motor Corporation) based on the new concept that traffic flow analysis can be dovetailed with evolutionary game theory. Chapter 6 is the product of dedicated effort by Ms. Eriko Fukuda in seeking another interesting challenge that can be addressed with evolutionary game theory. I sincerely express my gratitude to these people as well as to Dr. Zheng Wang (JSPS [Japan Society for the Promotion of Science] Fellow at Kyushu University) who works with our group, is regarded as one of the keenest young scholars, and deals with game and complex network theory. Continuous discussions with all these collaborators have helped me advance our studies and realize much satisfaction from our efforts.

I am also grateful to Dr. Prof. Yuji Aruka at Chuo University for giving me the opportunity to publish this book.

Contents

Biography of the Author

Jun Tanimoto, Dr. Eng. was born in 1965 in Fukuoka, but he grew up in Yokohama. He graduated in 1988 from the Department of Architecture, Undergraduate School of Science & Engineering, at Waseda University. In 1990, he completed his master's degree, and in 1993, he earned his doctoral degree from Waseda. He started his professional career as a research associate at Tokyo Metropolitan University in 1990, moved to Kyushu University and was promoted to assistant professor (senior lecturer) in 1995, and became an associate professor in 1998. Since 2003, he has served as professor and head of the Laboratory of Urban Architectural Environmental Engineering. He was a visiting professor at the National Renewable Energy Laboratory (NREL), USA; at the University of New South Wales, Australia; and at Eindhoven University of Technology, the Netherlands. Professor Tanimoto has published numerous scientific papers in building physics, urban climatology, and statistical physics and is the author of books including *Mathematical Analysis of Environmental System* (Springer; ISBN: 978-4-431-54621-4). He was a recipient of the Award of the Society of Heating, Air-Conditioning, and Sanitary Engineers of Japan (SHASE), the Fosterage Award from the Architectural Institute of Japan (AIJ), the Award of AIJ, and the IEEE CEC2009 Best Paper Award. He is involved in numerous activities worldwide, including being an editor of several international journals including *PLOS One* and the *Journal of Building Performance Simulation*, among others; a committee member at many conferences; and an expert at the IEA Solar Heating and Cooling Program Task 23. He is also an active painter and novelist, and has been awarded numerous prizes in fine art and literature. He has created many works of art and published several books. He specializes in scenic drawing with watercolors and romantic fiction. For more information, please visit http://ktlabo.cm.kyushu-u.ac.jp/.

Chapter 1
Human–Environment–Social System and Evolutionary Game Theory

Abstract In this chapter, we discuss both the definition of an environmental system as one of the typical dynamical systems and its relation to evolutionary game theory. We also outline the structure of each chapter in this book.

1.1 Modeling a Real Complex World

We define the word "system" as a collection of elements, all of which are connected organically to form an aggregate of elements that collectively possess an overall function. We know that most real systems are not time constant but time variable, i.e., they are "dynamical systems." According to the common sense of the fields of science and engineering, a dynamical system can be described by space and time variables, i.e., $\mathbf{x}$ and t. Therefore, a dynamical system has a spatiotemporal structure.

Any system in the real world looks very complex. An environmental system is a typical example. If an environmental system is interpreted literally, considering every system involved with the environment, we can see there is a lot of variety within it.

This variety arises from interactions between different environments (e.g., natural, human, and social) and differences in spatial scale (i.e., from the microscopic world weaved by microorganisms to the global environment as a whole, see Fig. 1.1). To reach the crux of an environmental problem, we must observe and consider diverse phenomena together, as an integrated environmental system, considering all interactions between the different systems and scales (Fig. 1.1). Accordingly, we have coined the phrase "**human–environmental–social system**" to encompass all these diverse phenomena.

One important aspect that is revealed when you shed some light on the human–environment–social system is that human intention and behavior, either supported by rational decision making, in some cases, or irrational decision making, in others, has a crucial impact on its dynamics. In fact, what is called "global warming," as one example of a global environmental problem, can be understood because of

J. Tanimoto, *Fundamentals of Evolutionary Game Theory and its Applications*,
Evolutionary Economics and Social Complexity Science 6,
DOI 10.1007/978-4-431-54962-8_1

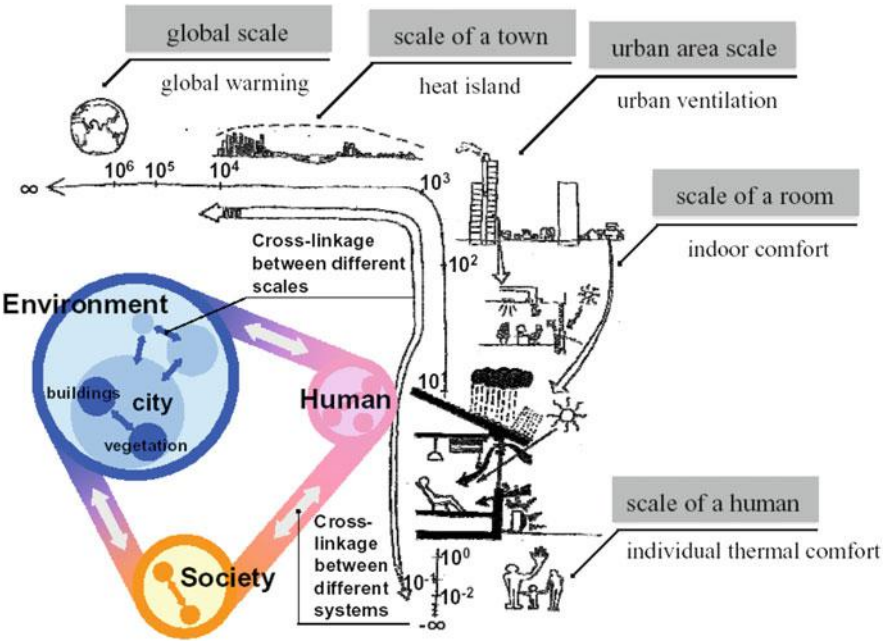

Fig. 1.1 Wide range of spatial scales over which environmental systems act, and the concept of the human–environmental–social system (Tanimoto 2014)

human overconsumption of fossil fuels over the course of the past couple of centuries, which seems rational for people only concerned with current comfort but seems irrational for people who are carefully considering long-term consequences. Hence, in seeking to establish a certain provision to improve environmental problems, one needs to consider complex interactions between physical environmental systems and humans as well as social systems as a holistic system of individuals. In general, the modeling of the human decision-making process or actual human behavior is harder than that of the transparent physical systems dealt by traditional science and engineering, because the governing mathematical models are usually unknown. What we can guess concerning these processes is not expressed as a set of transparent, deterministic, and explicit equations but black box-like models or, in some cases, stochastic models. At any rate, in order to solve those problems in the real world, we must build a holistic model that covers not only environment as physical systems but also human beings and society as complex systems. Although this may be a difficult job, we can see some possibility of progress in the field of applied mathematical theory, which can help to model complex systems such as human decision-making processes and social dynamics. Even if it is almost impossible to obtain an all-in-one model to perfectly deal with the three spheres, i.e., environmental, human, and societal, which have different spatiotemporal scales as well as different mechanisms, it might be possible to

establish bridges to connect the three. One effective tool to do this is evolutionary game theory.

1.2 Evolutionary Game Theory

Why do we cooperate? Why do we observe many animals cooperating? The mysterious labyrinth surrounding how cooperative behavior can emerge in the real world has attracted much attention. The classical metaphor for investigating this social problem is the prisoner's dilemma (PD) game, which has been thought most appropriate, and is most frequently used as a template for social dilemma.

Evolutionary game theory (e.g. Weibull 1995) has evolved from game theory by merging it with the basic concept of Darwinism so as to compensate for the idea of time evolution, which is partially lacking in the original game theory that primarily deals with equilibrium.

Game theory was established in the mid-twentieth century by a novel contribution by von Neumann and Morgenstern (von Neumann and Morgenstern 1944). After the inception they provided, the biggest milestone in driving the theory forward and making it more applicable to various fields (not only economics but also biology, information science, statistical physics, and other social sciences) was provided by John Nash, one of the three game theorists awarded the Nobel Prize. He did this by forming the equilibrium concept, known as Nash Equilibrium (Nash 1949). Another important contribution to evolutionary game theory was provided, in the 1980s, by Maynard Smith (Maynard Smith 1982). He formulated a central concept of evolutionary game theory called the evolutionarily stable strategy. In the 1990s, with the rapid growth of computational capabilities, multi-agent simulation started to strongly drive evolutionary game theory, allowing one to easily build a flexible model, free from the premises that previous theoretical frameworks presumed.[1] This enables game players in these models to behave more intelligently and realistically. Consequently, many people have been attracted to seeking answers for the question of why we can observe so much evidence of the reciprocity mechanism working in real human social systems, and also among animal species, even during encounters with severe social dilemma situations, in which the theory predicts that game players should act defectively. As one example, the theory shows that all players would be trapped as complete defectors in the case of PD, which will be explained later in this book. However, we can observe a lot of evidence that opposes this in the real world, where we ourselves and even some animal spices show social harmony with mutual cooperation in the respective social context (Fig. 1.2).

[1] The classical game theory assumes infinite population and perfect anonymity among those players. This is called well-mixed situation. Also, the players are presumed to act in an ideally rational way.

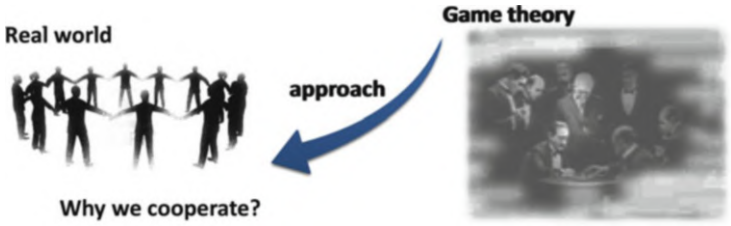

Fig. 1.2 How are humans able to establish reciprocity when encountering a social dilemma situation in the real world?

Since these developments, thousands of papers have been produced on research performed by means of computer simulations. Most of them follow the same pattern, in which each of the new models they build a priori is shown with numerical results indicating more enhanced cooperation than what the theory predicts. Those are meaningful from the constructivism viewpoint, but still less persuasive in answering the question: "What is the substantial mechanism that causes mutual cooperation to emerge instead of defection?"

Nowak successfully made progress in understanding this problem, to some extent, with his ground-breaking research (Nowak 2006). He proved theoretically that all the reciprocity mechanisms that bring mutual cooperation can be classified into four types, and all of them, amazingly, have similar inequality conditions for evolving cooperation due to the so-called Hamilton Rule. Nowak calls all these fundamental mechanisms "social viscosity." The Hamilton Rule (Hamilton 1964) finally solved the puzzle, which was originally posed by Charles Darwin's book—The Origin of Species (1859)—of why sterile social insects, such as honey bees, leave reproduction to their sisters by arguing that a selection benefit to related organisms would allow the evolution of a trait that confers the benefit but destroys the individual at the same time. Hamilton clearly deduced that kin selection favors cooperative behavior as long as the inclusive fitness surge due to the concept of relatedness is larger than the dilemma strength. This finding by Nowak, though he assumed several premises in his analytical procedure, elucidates that all the reciprocity mechanisms ever discussed can be explained with a simple mathematical formula, very similar to the Hamilton Rule, implying that "Nature is controlled by a simple rule." The Nowak classifications—kin selection, direct reciprocity, indirect reciprocity, network reciprocity, and group selection—successfully presented a new level to the controversy, but there have still been a lot of papers reporting "how much cooperation thrives if you rely on our particular model"-type stories, because Nowak's deduction is based on several limitations, and thus the real reciprocity mechanism may differ from it. In fact, among the five mechanisms, network reciprocity has been very well received, since people believe complex social networks may relate to emerging mutual cooperation in social system.

This is why this book primarily focuses network reciprocity in Chap. 3.

1.3 Structure of This Book

This book does not try to cover all the developments concerning evolutionary games, not even all the most important ones. In fact, it strives to describe several fundamental issues, a selected set of core elements of both evolutionary games and network reciprocity, and self-contained applications, which are drawn from our studies over the last decade.

Chapter 2 describes some theoretical foundations for dealing with evolutionary games in view of so-called social dilemma games. Some points such as universal scaling for dilemma strength might be useful from a theoretical viewpoint.

In Chap. 3, we focus on network reciprocity. We provide a transparent discussion on why limiting game opponents with a network helps the emergence of cooperation.

The remaining chapters demonstrate real-life applications of evolutionary games. Chapter 4 touches on the story of what triggers evolving communication among animal species. Chapter 5 demonstrates that social dilemma seems ubiquitous, even in traffic flow, which has been thought to be one of the typical applications that fluid dynamics deals with. Chapter 6 concerns spreading epidemics and social provision for this by vaccination through the vaccination game, one of the hottest areas in evolutionary games.

References

Hamilton, W.D. 1964. The genetical evolution of social behavior I and II. *Journal of Theoretical Biology* 7: 1–16, 17–52.

Maynard Smith, J. 1982. *Evolution and the theory of games*. Cambridge: Cambridge University Press.

Nash, J.F. 1949. Equilibrium points in n-person games. *Proceedings of the National Academy of Science of the United States of America* 36(1): 48–49.

Nowak, M.A. 2006. Five rules for the evolution of cooperation. *Science* 314: 1560–1563.

Tanimoto, J. 2014. *Mathematical analysis of environmental system*. Tokyo: Springer.

Von Neumann, J., and O. Morgenstern. 1944. *Theory of games and economic behavior*. Princeton: Princeton University Press.

Weibull, J.W. 1995. *Evolutionary game theory*. Cambridge: MIT Press.

Chapter 2
Fundamental Theory for Evolutionary Games

Abstract In this chapter, we take a look at the appropriate treatment of linear dynamical systems, which you may be familiar with if you have taken some standard engineering undergraduate classes. The discussion is then extended to non-linear systems and their general dynamic properties. In this discussion, we introduce the 2-player and 2-strategy (2×2) game, which is the most important archetype among evolutionary games. Multi-player and 2-strategy games are also introduced. In the latter parts of this chapter, we define the dilemma strength, which is useful for the universal comparison of the various reciprocity mechanisms supported by different models.

2.1 Linear Dynamical Systems

Let us start with an example. Consider the dynamics of an arbitrary linear thermal system.[1] One typical case is a thermal field of semi-infinite soil, as shown in Fig. 2.1. The x-coordinate axis takes the ground surface as its origin and measures depth underground. Underground heat propagates only by conduction, but convective heat transfer occurs on the ground surface, which is exposed to the external temperature. Also, radiation, evaporative cooling, and incoming solar radiation have an effect on the surface. As can be seen in Fig. 2.1, a discretization of space has been imposed, and thus the system is no longer continuous. The system featured, with thermal mass **M**, is affected by thermal conduction, convection, liberalized radiation, evaporative cooling, and solar radiation. Therefore, the temperature field is variable with time (t). All thermal balance equations, located on nodes designated in the thermal system, can be expressed with a single matrix–vector equation, the **system state equation**:

[1] Concerning detail of this discussion, you should consult with Tanimoto (2014).

J. Tanimoto, *Fundamentals of Evolutionary Game Theory and its Applications*,
Evolutionary Economics and Social Complexity Science 6,
DOI 10.1007/978-4-431-54962-8_2

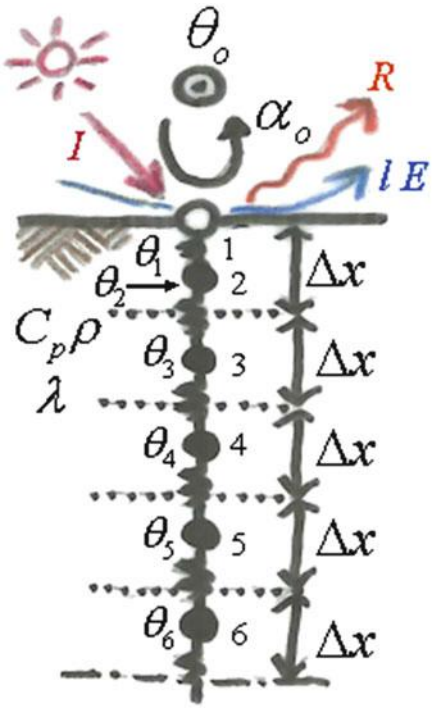

Fig. 2.1 Space discretization model based on Control Volume Method in which the surface layers of the semi-infinite soil are lumped parameterized

$$\mathbf{M}\frac{\mathrm{d}\boldsymbol{\theta}}{\mathrm{dt}} = \mathbf{C}\boldsymbol{\theta} + \mathbf{C_o}\boldsymbol{\theta_o} + \mathbf{f}. \tag{2.1}$$

Here, $\boldsymbol{\theta}$ is a vector of unknown variables, which is each temperature of the nodes of the underground. $\mathbf{M}$ is called the heat capacitance matrix. $\mathbf{C}$ is called the heat conductance matrix, and the vector–matrix product $\mathbf{C}\boldsymbol{\theta}$ expresses the influence of heat conduction. Another vector–matrix product $\mathbf{C_o}\boldsymbol{\theta_o}$ means the influence derived from heat convection. The vector $\mathbf{f}$ indicates other thermal influences given by a form of heat flux. Thermal influences other than conduction happening with in the system, expressed by $\mathbf{C_o}\boldsymbol{\theta_o} + \mathbf{f}$, are called boundary condition. One extremely important thing is that the system state equation has universal form. Regardless of what particular problem you have, as long as linear system it would be, what you see as a final equation is always same as expressed in Eq. (2.1). It might be understood by the fact that Eq. (2.1) can be likened to the Newton's equation of motion for a particle, where $\frac{\mathrm{d}\boldsymbol{\theta}}{\mathrm{dt}}$ implies first derivation of velocity; namely acceleration, $\mathbf{M}$ is literally "mass", and the terms appeared in the right side; $\mathbf{C}\boldsymbol{\theta} + \mathbf{C_o}\boldsymbol{\theta_o} + \mathbf{f}$ imply respective forces acting on the particle.

By the concept of time discretization, the left side of Eq. (2.1) is easily discretized as

$$\mathbf{M}\frac{\mathrm{d}\boldsymbol{\theta}}{\mathrm{dt}} = \frac{1}{\Delta t}\,\mathbf{M}\left(\boldsymbol{\theta}^{i+1} - \boldsymbol{\theta}^{i}\right). \tag{2.2}$$

The superscripted indices in the above equation are not exponentials, but represent the discretised time steps i and $i+1$. The right side of Eq. (2.1) is slightly problematic because we must decide at what point in time the vectors $\boldsymbol{\theta}$, $\boldsymbol{\theta}_{\mathbf{o}}$, and $\mathbf{f}$ should be discretized; more specifically, whether they should be computed at the i th or $(i+1)$ th time step. The former is a forward-difference computation; the latter constitutes backward difference, respectively summarized by;

$$\text{Time-forward scheme; } \boldsymbol{\theta}^{i+1} = \left[\frac{1}{\Delta t}\mathbf{M}\right]^{-1}\left\{\left[\frac{1}{\Delta t}\mathbf{M} + \mathbf{C}\right]\boldsymbol{\theta}^{i} + \mathbf{C}_{\mathbf{o}}\boldsymbol{\theta}_{\mathbf{o}}{}^{i} + \mathbf{f}^{i}\right\}. \tag{2.3}$$

$$\text{Time-backward scheme; } \boldsymbol{\theta}^{i+1} = \left[\frac{1}{\Delta t}\mathbf{M} - \mathbf{C}\right]^{-1}\left\{\left[\frac{1}{\Delta t}\mathbf{M}\right]\boldsymbol{\theta}^{i} + \mathbf{C}_{\mathbf{o}}\boldsymbol{\theta}_{\mathbf{o}}{}^{i+1} + \mathbf{f}^{i+1}\right\}. \tag{2.4}$$

In any cases, after the time discretization, we can transform Eq. (2.1) into;

$$\boldsymbol{\theta}^{i+1} = \mathbf{T}\boldsymbol{\theta}^{i} + (\text{heat impact on the system based on boundary conditions}). \tag{2.5}$$

Hence, the true impact of the aforementioned system is expressed as $\mathbf{T} = \left[\frac{1}{\Delta t}\mathbf{M} - k\mathbf{C}\right]^{-1}\left[\frac{1}{\Delta t}\mathbf{M} + (1-k)\mathbf{C}\right]$, where the forward and backward schemes are specified by $k = 0$ and $k = 1$, respectively. The matrix $\mathbf{T}$ is a **transition matrix**, so-called, because it embodies the characteristics of the time transition. If the second term on the right side in row 3 of Eq. (2.5) is ignored, $\boldsymbol{\theta}^{i+1} = \mathbf{T}\boldsymbol{\theta}^{i}$, equivalent to geometric progression in scalar recursions. We now ask: what is the necessary and sufficient condition for convergence and stability of the general terms in the following geometric progression?

$$\{a_1, a_2, a_3, \ldots, a_n\} = \left\{a, ar, ar^2, \ldots, ar^{n-1}\right\} \Leftrightarrow a_n = r \cdot a_{n-1}$$

Here knowledge from junior high school may be useful, that is, a series converges if its geometric ratio r satisfies $|r| \leq 1$. The same idea applies to vector matrix recurrence formulae. However, the problem of how to measure the size of the transition matrix $\mathbf{T}$ arises. The answer lies in the **eigenvalues** of $\mathbf{T}$. Generally, an $n \times n$ square matrix has n eigenvalues. For convergence, it could be argued that the absolute value for the maximum eigenvalue should not exceed 1. In other words,[2]

$$|\mathrm{Max}[\mathrm{eigen}[\mathbf{T}]]| \leq 1. \tag{2.6}$$

[2] This argument derives from the fact that the time evolution of the error between the numerical solution and the explicit solution obeys the original equation.

Let us back to Eq. (2.1), that is the form before time discretization process. To discuss about its dynamics, it is an acceptable idea that the boundary conditions are not considered. As already explained, a boundary condition operates externally to the system (in this case, via a "temperature raising" mechanism) and is not related to the intrinsic dynamics of the system. If it is the case, we are allowed to discuss in a general form;

$$\frac{\mathrm{d}\mathbf{x}}{\mathrm{dt}} = \dot{\mathbf{x}} = \mathbf{A}\mathbf{x}. \tag{2.7}$$

Equation (2.7) is in a linear format. By linear format[3] we mean that the time evolution of the system is described by a vector matrix operation. In other words, in a linear system, the elapsed time in the system (dynamics) can be described by the familiar linear algebra introduced at senior school.

What happens to in Eq. (2.7) as $t \to \infty$? One might imagine that changes will occur until $\frac{\mathrm{dx}}{\mathrm{dt}} = \mathbf{0} \Leftrightarrow \dot{\mathbf{x}} = \mathbf{0}$, denoting a state of no further change. This eventual state, called steady state in many engineering fields, is called **equilibrium** in physical dynamical systems (or in fields such as economics). Hence, the equilibrium state is defined as $\dot{\mathbf{x}} = \mathbf{0}$. The equilibrium point is frequently expressed as $\mathbf{x}^*$.

By treating Eq. (4.1) as an ordinary scalar differential equation, its solutions are obtained as

$$\frac{\mathrm{d}\mathbf{x}}{\mathrm{dt}} = \mathbf{A}\,\mathbf{x} \Leftrightarrow \frac{1}{\mathbf{x}}\,\mathrm{d}\mathbf{x} = \mathbf{A}\mathrm{dt} \Leftrightarrow \mathbf{x} = \exp[\mathbf{A}\,t] + \mathbf{c}, \tag{2.8}$$

where $\mathbf{c}$ is an integration constant vector. At equilibrium, $\dot{\mathbf{x}} = \mathbf{0} \Rightarrow \mathbf{A}\mathbf{x}^* = \mathbf{0} \Leftrightarrow \mathbf{x}^* = \mathbf{0}$. Under what circumstances will $\mathbf{x} \to \mathbf{0}$as $t \to \infty$ in Eq. (2.8)? Let us once again use the analogy with scalar cases. Evidently, the solutions $x(t) = \exp[a\,t] \to 0$ as $t \to \infty$ if and only if $a < 0$. Vector matrix systems of equations are solved similarly, by finding the eigenvalues of the matrix$\mathbf{A}$. If the equilibrium point in Eq. (2.7) is to satisfy $\mathbf{x} \to \mathbf{0}$, all n eigenvalues of the $n \times n$ matrix$\mathbf{A}$ must be negative. Thus, to explain the equilibrium situation in Eq. (2.7), we should examine each eigenvalue in the transition matrix$\mathbf{A}$, which determines the time evolution of the system.

To simplify the discussion without loss of generality, we suppose that $\mathbf{A}$ is a 2×2 matrix with eigenvalues λ_1 and λ_2. Three sign combinations of these eigenvalues are possible; both positive, both negative, or one positive and one negative. The signs of the eigenvalues determine the stability of the equilibrium point $\mathbf{x}^* = \mathbf{0}$ in our current problem, as illustrated in Fig. 2.2. When all eigenvalues are negative, the equilibrium point $\mathbf{x}^*$ is stable (in Eq. (2.7), $\mathbf{x}^* = \mathbf{0}$). In stable equilibrium, $\mathbf{x}^*$ behaves like a jug whose potential is minimized at its base, so that all points

[3] The "linear" quality of a system is truly beneficial in engineering. No sharp fluctuations develop over time; therefore, future behavior is easily extrapolated from currently available information.

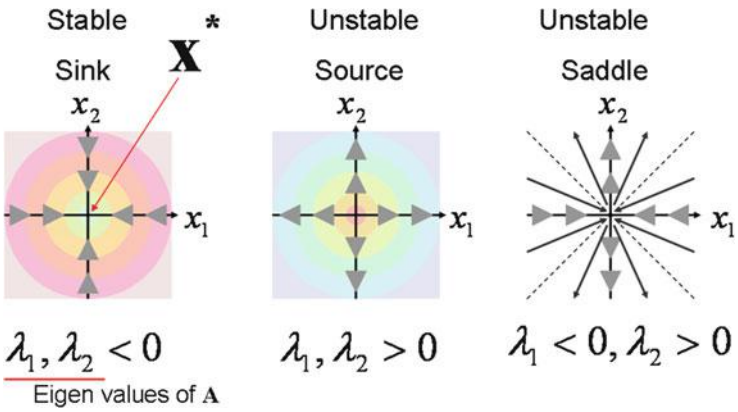

Fig. 2.2 Characteristics of equilibrium point

surrounding $\mathbf{x}^*$ are drawn toward it. In Eq. (2.7), with a single equilibrium point at $\mathbf{x}^* = \mathbf{0}$, the system eventually converges to $\mathbf{x}^* = \mathbf{0}$ regardless of the initial conditions. If all eigenvalues are positive then $\mathbf{x}^* = \mathbf{0}$ behaves like the peak of a dune (see central panel of Fig. 2.2). In this case, regardless of the initial conditions, the system never attains $\mathbf{x}^* = \mathbf{0}$, and the system is unstable. If both positive and negative eigenvalues exist, $\mathbf{x}^* = \mathbf{0}$ converges in one direction but diverges in a linearly independent direction, as shown in the right panel of Fig. 2.2. Such an equilibrium point is called a **saddle point** (viewed three-dimensionally in Fig. 2.3), and is also unstable.

In summary, the equilibrium point is the solution of the given system state equation satisfying $\dot{\mathbf{x}} = \mathbf{0}$. The signs of the eigenvalues of the transition matrix determine whether the equilibrium point $\mathbf{x} = \mathbf{x}^*$ is a source, a sink, or a saddle point. Negative and positive eigenvalues give rise to sinks and sources, respectively, while mixed eigenvalues signify a saddle point. This seemingly trivial fact is of critical importance. Once the nature of the equilibrium points of a system is determined, laborious numerical calculations to find stationary solutions are not required. Estimating the system dynamics by closely examining the eigenvalues is known as the deductive approach. To reiterate, if a deductive approach is possible, there is no requirement for numerical solutions.

Thus far, Eq. (2.7) has been considered as continuous in time. We now reinterpret (2.7) as a time-discretized system and investigate its behavior. The essence of time discretization was explained in Eqs. (2.1, 2.2, 2.3, 2.4, 2.5, and 2.6).

Initially, we adopt a forward difference scheme in time. Equation (2.7) becomes

$$\mathbf{x_{k+1}} - \mathbf{x_k} = \Delta t \cdot \mathbf{A}\,\mathbf{x_k} \Leftrightarrow \mathbf{x_{k+1}} = (\Delta t \cdot \mathbf{A} + \mathbf{E})\mathbf{x_k}. \tag{2.9}$$

In physical dynamical systems, a recurrence equation such (2.9), in which a linear continuous equation is discretized in time, is sometimes called a **linear mapping**. The transition matrix $\Delta t \cdot \mathbf{A} + \mathbf{E} \equiv \mathbf{T}$ of Eq. (2.9) is essentially equal to Eq. (2.3).

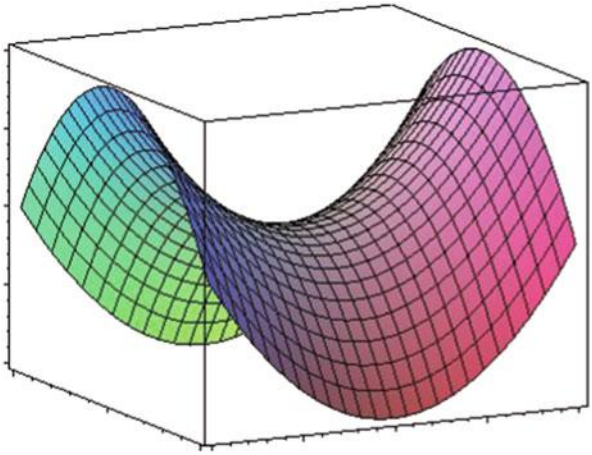

Fig. 2.3 Saddle

For this linear mapping to be stable (non-diverging), the absolute value of the maximum eigenvalue of the transition matrix must not exceed 1. Again, the necessary and sufficient stability criterion is as follows:

$$|\text{Max}[\text{eigen}[\mathbf{T}]]| \leq 1.$$

Now, let us assume stability as an original system characteristic. In other words, assume that the following is true:

$$\text{Max}[\text{eigen}[\mathbf{A}]] \leq 0. \tag{2.10}$$

The eigenvalue of the unit matrix **E** is 1. We know that if the eigenvalues λ_D of a matrix **D** are known, the eigenvalues of a function of **D**, $f(\mathbf{D})$, are $f(\lambda_D)$. Applying this rule under the assumptions of Eq. (2.10), the transition matrix of the linear mapping becomes

$$\text{Max}[\text{eigen}[\mathbf{T}]] < -1. \tag{2.11}$$

Equation (2.11) suggests that even when Eq. (2.10) holds, $|\text{Max}[\text{eigen}[\mathbf{T}]]| \leq 1$ is not necessarily satisfied. Thus, the linear mapping of an originally stable system may be unstable. This is a surprising result. It implies that even though the original qualities were good, the calculations fail because of errors introduced in subsequent "time discretization" operations. This potential instability, generated when continuous time is mapped to a discrete system, is exactly the numerical instability. We now consider the same linear mapping under backward difference time discretization. In this case, the mapping is

$$\begin{aligned} &\mathbf{x_{k+1}} - \mathbf{x_k} = \Delta t \cdot \mathbf{A}\, \mathbf{x_{k+1}} \\ \Leftrightarrow\ &\mathbf{x_{k+1}} = [1 - \Delta t \cdot \mathbf{A}\,]^{-1}\mathbf{x_k} = \mathbf{T}\mathbf{x_k} \end{aligned} \tag{2.12}$$

from which we obtain

$$0 < \mathrm{Max}[\mathrm{eigen}[\mathbf{T}]] < 1. \tag{2.13}$$

This linear mapping never diverges and will not cause the numerical fluctuations. Thus, if the original qualities are good, it appears that the integrity of the system is retained under backward difference time discretization.

2.2 Non-linear Dynamical Systems

Consider a continuous dynamical system in which the system state equations are expressed by a non-linear function **f**:

$$\frac{\mathrm{d}\mathbf{x}}{\mathrm{dt}} = \dot{\mathbf{x}} = \mathbf{f}(\mathbf{x}). \tag{2.14}$$

The subsequent procedure is typical of how nonlinearities are treated in all types of analyses. Non-linear functions are approximated to linear functions over infinitesimal intervals by Taylor expansion. Expanding the right hand side of Eq. (2.14), we get

$$\begin{aligned} &\mathbf{f}(\mathbf{x}) = \mathbf{f}\left(\mathbf{x}^*\right) + \mathbf{f}'\left(\mathbf{x}^*\right)\left(\mathbf{x} - \mathbf{x}^*\right) + \frac{\mathbf{f}''\left(\mathbf{x}^*\right)}{2!}\left(\mathbf{x} - \mathbf{x}^*\right)^2 + \cdots \\ \Leftrightarrow\ &\mathbf{f}(\mathbf{x}) \cong \mathbf{f}\left(\mathbf{x}^*\right) + \mathbf{f}'\left(\mathbf{x}^*\right)\left(\mathbf{x} - \mathbf{x}^*\right). \end{aligned} \tag{2.15}$$

From the definition of equilibrium point, $\mathbf{f}\left(\mathbf{x}^*\right) = 0$ (this should be evident by substituting $\frac{\mathrm{dx}}{\mathrm{dt}}\big|_{\mathbf{x}=\mathbf{x}^*} = 0$ in Eq. (2.14)), Eq. (2.15) is approximately equal to

$$\mathbf{f}(\mathbf{x}) = \mathbf{f}'\left(\mathbf{x}^*\right)\left(\mathbf{x} - \mathbf{x}^*\right). \tag{2.16}$$

Equation (2.16) is approximated to a linear equation as follows:

$$\mathbf{f}(\mathbf{x}) = \mathbf{f}'\left(\mathbf{x}^*\right)\left(\mathbf{x} - \mathbf{x}^*\right) = \mathbf{f}'\left(\mathbf{x}^*\right)\mathbf{x} - \mathbf{f}'\left(\mathbf{x}^*\right)\mathbf{x}^*. \tag{2.17}$$

The first term on the right of (2.17) is first-order in **x**, while the second term is constant. Now we can apply the deductive approach introduced in the previous section. Clearly the transition matrix is $\mathbf{f}'(\mathbf{x}^*)$. We must determine the signs of the eigenvalues corresponding to the equilibrium points of this matrix.

The transition matrix is the **Jacobian matrix** of tangent gradients of the multivariable vector function.

$$\mathbf{f}'\left(\mathbf{x}^*\right) = \left.\frac{\partial\,\mathbf{f}(\mathbf{x})}{\partial\mathbf{x}}\right|_{\mathbf{x}=\mathbf{x}^*} = \left[\begin{array}{ccc} \frac{\partial f_1(\mathbf{x})}{\partial x_1} & \cdots & \frac{\partial f_1(\mathbf{x})}{\partial x_n} \\ \vdots & \ddots & \vdots \\ \frac{\partial f_n(\mathbf{x})}{\partial x_1} & \cdots & \frac{\partial f_n(\mathbf{x})}{\partial x_n} \end{array}\right]_{\mathbf{x}=\mathbf{x}^*}. \tag{2.18}$$

Let us apply the deductive procedure of Sect. 2.1 to the non-linear system state Eq. (2.14). First, we seek the equilibrium points of Eq. (2.14), which are solutions to $\dot{\mathbf{x}} = \mathbf{0}$ in the given system state equation. A system may contain one or several equilibrium points. In general, quadratic and quartic non-linear functions possess two and four equilibrium points, respectively. Whether each of these equilibrium points ($\mathbf{x} = \mathbf{x}^*$) is a source, a sink, or a saddle point is determined by the sign of the eigenvalues of the transition matrix (2.18). As before, if all n eigenvalues are negative, the equilibrium point is a stable sink, if all are positive, it is an unstable source, and if a mix of signs is found, it is an unstable saddle point. The stability characteristics of the equilibrium points apply only within the vicinity of the equilibrium points (as assumed in the Taylor expansion). Hence, when several equilibrium points exist, the behavior of the system as $t \to \infty$ depends on the starting point of the dynamics, i.e., the initial values. Because the linear system in Sect. 2.1 possessed a single equilibrium point at $\mathbf{x}^* = \mathbf{0}$, this type of initial condition dependency was irrelevant, but non-linear systems can depend heavily on the initial conditions.

2.3 2-Player & 2-Stratey (2×2) Games

In this section, the **2-player 2-strategy game** (abbreviated as **two-by-two game** or **2×2 game**) is presented as an example of a non-linear system. As the reader will come to appreciate, this apparently esoteric two-by-two game is related to environmental problems.

As previously explained, the two-by-two game is a branch of applied mathematics that models human decision making. It is a relatively new mathematical tool based on the pioneering work of von Neumann and Morgenstern entitled "Theory of games and economic behavior" published in 1944. The applications of the two-by-two game are extremely diverse, ranging from social sciences such as economics and politics to biology, information science, and physics. If a group of particles possessing binary strategies of cooperation or defection is imposed to develop a spatial structure, clusters of cooperation particles emerge abruptly. This seems similar to formation of crystallization or phase transitions in materials. Currently, these analogies have drawn huge interest from members of the statistical physics community.

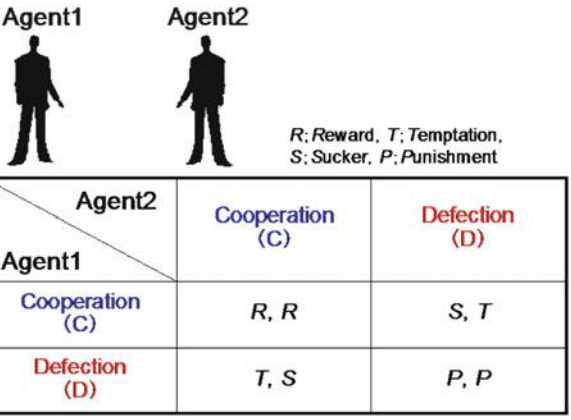

Fig. 2.4 Payoff matrix of 2×2 game

From an unlimited population, two individuals are selected at random and made to play the game. The game uses two discrete strategies (as shown in Fig. 2.4); cooperation (C) and defection (D). The pair of players receives payoffs in each of the four combinations of C and D. A symmetrical structure between the two players is assumed. In Fig. 2.4, the payoff of player 1 (the "row" player) is represented by the entries preceding the commas; the payoff of player 2 (the "column" player) by the entries after the commas. The payoff matrix is denoted by $\begin{bmatrix} R & S \\ T & P \end{bmatrix}$. A player can also be called an agent. Depending on the relative magnitudes of the matrix elements P, R, S, and T, the game can be divided into 4 classes; the **Trivial** game with no dilemma, the **Prisoner's Dilemma** (sometimes abbreviated to **PD**), **Chicken** (also known as Snow Drift Game or Hawk–Dove Game) and **Shag Hunt** (sometimes abbreviated to SH). The main aim of this section is to show that these four game classes can be derived from the eigenvalues of the system per deductible approach for non-linear system equation explained in the previous section.

Here, the gamble-intending dilemma (hereafter referred to as GID) and risk-averting dilemma (hereafter referred to as RAD) are introduced. The existence of these dilemmas is determined by D_g and D_r, defined as follows[4]:

$$\begin{aligned} D_g &\equiv T - R, \\ D_r &\equiv P - S. \end{aligned} \tag{2.19}$$

If $D_g > 0$, GID behavior results, while $D_r > 0$ leads to RAD. Each of the dilemma classes and the existence of GIDs and RADs are summarized in Fig. 2.5. Although, the reader may be overwhelmed at this point having been introduced to a large set of

[4] To precisely know about GID & RAD and D_g and D_r, you should consult with Tanimoto and Sagara (2007a).

Fig. 2.5 Class type in 2×2 game

Game class	Dilemma?	GID	RAD
Prisoner's Dilemma; PD	Yes	Yes	Yes
Chicken (Snow Drift; Hawk-Dove)	Yes	Yes	No
Stag Hunt; SH	Yes	No	Yes
Trivial	No	No	No

Fig. 2.6 Derivation method for Nash equilibrium with PD as an example

(a)

	C	D
C	5, 5	1, 7
D	7, 1	3, 3

(b)

	C	D
C	5, 5	1, 7
D	**7**, 1	**3**, 3

(c)

	C	D
C	5, 5	1, **7**
D	**7**, 1	**3**, **3**

(d)

	C	D
C	5, 5	1, **7**
D	**7**, 1	**3**, **3**

Nash equilibrium

qualities without proofs or detailed explanations, we request the reader to bear with this for just a little bit longer. GIDs are sometimes called Chicken dilemmas while RIDs can be referred to as SH dilemmas. Figure 2.5 shows that the PD game may be Chicken or SH (details will be provided later).

A couple of further explanations are needed here.

Figure 2.6(a) shows a game setup of the prisoner's dilemma (PD) class. Calculating D_g and D_r from Eq. (2.19), both eigenvalues are seen to be positive; thus, from Fig. 2.5, the game is PD, for reasons which will be explained later. For now, examine panel (b) in Fig. 2.6. The payoff values before the commas, i.e., those of

the row-represented agent, are shaded orange and green. In these situations, the column agent is fixed in strategy C or D. The larger of the two elements shaded with the same colour is marked in bold text. These bold values denote whether C or D is the more rational choice for the row agent. Panel (c) illustrates a similar scenario with fixed row agent, indicating whether C or D is the most rational strategy for the column agent. In panel (d), the element for which both row and column agents appears bold is shaded red. The state thus obtained (the game outcome) is known as the **Nash equilibrium**. In this example, the Nash equilibrium indicates the grouping of rational strategies adopted by an agent selected at random from an unlimited agents who participates in a single game. Figure 2.6 reveals that both agents exhibit D behavior, and defect each another to accept low profit P (also from that figure, the relationship $T > R > P > S$ is seen to hold in PD). Relating this outcome to the non-linear dynamics of the previous section, even if the unlimited agents began with an even division of cooperative and defection agents (50 % cooperators & 50 % defectors), once the game is started and the strategy of the agents reviewed according to a certain set of rules after every step[5]; as time progresses,[6] the system will stabilize into a state in which all members (despite the unlimited population size) exhibit defection behavior.

Figure 2.7 plots the payoffs for Agents 1 and 2 on the vertical and horizontal axis, respectively, and displays the payoff matrices for each of the four game classes. These diagrams show the **feasible solutions regions**. The pink areas within the feasible solutions of PD and Chicken reside in the 1st, 2nd, and 4th quadrant (around the central point R). When several plots exist in these regions, we hope to determine the most desirable game outcome between the equal outcomes of Agents 1 and 2. In reality, T and S are clearly the desirable outcomes for Agent 1 and his opponent, respectively. However, we have seen that both agents compromise by taking the fair option R, rather than seeking maximum payoffs for themselves. In this case, R is not the optimal solution but is merely a **fair Pareto optimum**. In contrast to this, in SH and Trivial games, R is the only possible outcome in the pink region (result not shown), and a unique optimal solution exists, R.

In Fig. 2.7, the open and filled circles ○ and ● indicate that Agent 1 (your own offer, say), adopts C and D strategies, respectively. The C and D strategies of Agent 2 (the opponent's offer) are delineated by gray and black dotted lines, respectively. With this visualization, the following discussion should be apparent. In the PD game (upper left panel of Fig. 2.7), if the strategy of the opponent's offer is fixed as C (region within the gray dotted lines), the most rational strategy for your hand is D, which lies further along the horizontal axis (indicating a higher payoff for Agent 1). If your opponent's offer is fixed on D, the same situation arises; within the D region of Agent 2, the D strategy of Agent 1 lies further along the horizontal axis than the C strategy. In other words, you should adopt the D strategy regardless of your opponent's behavior, and the system settles into Nash equilibrium. Similarly for the

[5] This is referred to as strategy adaptation.

[6] This is referred to as evolution.

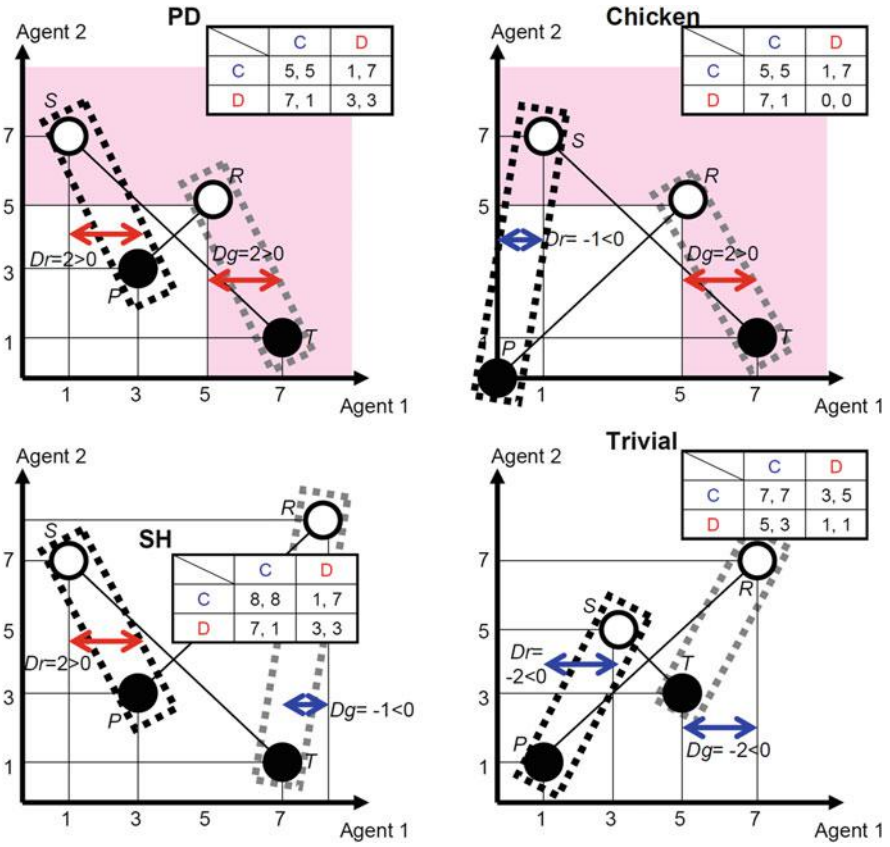

Fig. 2.7 Feasible solution regions of each game class and examples of D_g and D_r

Trivial game (lower right panel of Fig. 2.7), comparing the areas enclosed by black and grey dotted lines, we observe that Agent 1 should adopt the C strategy regardless of the opponent's offer, and that Nash equilibrium is the *R* outcome (C, C). The Nash equilibria in the Chicken and SH games are obtained from the payoff matrices as explained in Fig. 2.6. The Nash equilibria in Chicken are the *S* and *T* outcomes (C, D) and (D, C), while in SH, they are the *R* and *P* outcomes (C, C) and (D, D). In Chicken and SH, the Nash equilibria cannot be determined from the feasible solution regions in Fig. 2.7, but whether one's own strategy should change in response to the opponent's strategy (C or D) can be gauged from the horizontal axis's value of the plots surrounded by black or gray (see upper right and lower left panels of Fig. 2.7 for Chicken and SH games, respectively).

The above dilemmas, to which we have referred so extensively, are defined in the following paragraphs.

A dilemma, from mathematical meaning, is introduced whenever the Pareto optimum does not match the Nash equilibria. In PD, Chicken, and SH, the fair

Pareto optimums differ from the Nash equilibria. SH yields only partial match ((C, C) is one of Nash equilibria), but causes dilemma because other outcomes are also possible. The details are explained below.

In PD, the magnitudes of the outcomes are $T > R > P > S$. In reverse phrasing, the order $T > R > P > S$ characterizes the PD game class. Since D_g and D_r are both positive, GIDs and RADs coexist. The Chicken dilemma, an alternative name for the former, arises from the positive value of $D_g = T - R$. However, as evident from the regions of feasible solutions in the PD and Chicken games shown in Fig. 2.7, when this condition is satisfied, T and S always exist in the first, second, and fourth quadrants (assuming R as the center). Thus, it could be argued that "an incentive to exploit the opponent" exists. In a similar vein, positive $D_r = P - S$ leads to the SH dilemma. However, when this condition is satisfied (results not schematically shown with color highlight), the feasible solution regions in Fig. 2.7 become that T and S always exist in the second, third, and fourth quadrants (assuming P as the center), suggesting "an incentive of not being exploited by the opponent." In fact, this situation emerged in the PD dynamics discussed earlier; as $t \to \infty$, the entire population became defection. Such an equilibrium state is called **D-dominate**.

In the Chicken game, $T > R > S > P$. Since $D_g > 0$ and $D_r < 0$, the gamble-intending (Chicken-type) dilemma exists in the absence of the risk-averting (SH-type) dilemma. In this game, you incur little risk of being ruined by your opponent but you may gain an advantage by exploiting the opponent. The Chicken game is characterized by $S > P$. That is, the most convenient situation for yourself would arise if you and your opponent adopt the D and C strategies, respectively ($T > R$). Conversely, if you and your opponent both adopt the D strategy, the worst outcome (P, P) results. Being ruined by your opponent would be a more favorable scenario ($S > P$). The structure of environmental issues is very similar. The environment is a public property available to anyone, but if overused by all individuals, it gets depleted. To preserve the environment, individuals might benefit from not using it, and hence a social dilemma is created. This supposed environment may be regarded as a public pastureland, from which your cows may be permitted to consume an unlimited or restricted amount (corresponding to defection and cooperation strategies, respectively). In the short-term, the cooperative strategy restricts the cows' diet until the ground has recovered. This situation can be modelled as a multi-player Chicken game termed the **tragedy of commons** (Hardin 1968). The Nash equilibria of the Chicken game are (C, D) and (D, C), implying that if half of the population are initially cooperative,[7] as $t \to \infty$, cooperation and defection members exist in certain proportions (this does not mean that specific agents are restricted to C and D strategies, but rather that the proportions of individuals adopting C and D stabilize to fixed values). This scenario is called **coexistence** or **polymorphic equilibrium**.

[7] The proportion of cooperative members at the start of a series of games is 0.5.

The SH game is characterized by $R > T > P > S$. Since $D_g < 0$ while $D_r > 0$, risk-averting (SH-type) dilemmas exist in the absence of gamble-intending (Chicken-type) dilemmas. Although there is no incentive to exploit one's opponent (since R is optimal and $R > T$), an individual risks damage from an opponent ($P > S$). For instance, if two hunters cooperate to secure a large catch, such as a deer, a successful outcome is likely. However, if the opponent is not certain to cooperate (but instead might defect to cause trouble for the co-operator while knowingly losing their share of the catch), the dilemma of whether one should go on a rabbit hunt (which can be undertaken single-handedly, and is a defection strategy) arises. The name "deer hunting game" is derived from this episode in Chapter Two of "Discourse on Inequality" by Jean-Jacques Rousseau, who is famous for "The Social Contract" and "Émile." The deer hunting game epitomises SH. The Nash equilibria in SH are (C, C) and (D, D), but the dynamics depend on the initial proportion of cooperative individuals. As $t \to \infty$, the systems converge to either complete defection or complete cooperation. In other words, whether a dark, uncooperative society or a fully cooperative society emerges depends on the initial proportion of cooperators. This type of dynamics is known as **bi-stable**.

In the Trivial game, $R > T > S > P$, and D_g and D_r are both negative. This system is devoid of GIDs and RADs. The Nash equilibrium matches the optimal solution (C, C); thus, regardless of initial cooperation status, all members become cooperative as $t \to \infty$. This type of equilibrium is called **C-dominate**.

The PD game presents tough dilemmas containing both Chicken and SH-type dilemmas. Since a portion of the optimal SH solutions matches the Nash equilibria, the SH dilemma is weaker than the Chicken dilemma. As previously explained, whether a fully cooperating society emerges depends upon the initial values.

There are other several game classes. More precisely, Chicken game contains two sub-classes; one is **Leader Game** and another is **Hero Game**. Those two have polymorphic equilibriums, because $D_g > 0$ and $D_r < 0$, the gamble-intending (Chicken-type) dilemma exists in the absence of the risk-averting (SH-type) dilemma. The feasible solutions regions of those two are shown in Fig. 2.8.

Crucially important feature of those games is $S + T > 2R$ is always satisfied. Only the difference to identify those two is the order of T and S. If $T > S$ is valid, it is a Leader game. It is a Hero game, if $S > T$ is valid. Those two types of 2×2 games are very special. It is because, unlike PD ($D_g > 0$ & $D_r > 0$, and $S + T < 2R$) and pure Chicken ($D_g > 0$ & $D_r < 0$, and $S + T < 2R$), continuing mutual cooperation (continuously obtaining R; hereafter we call R-reciprocity) is not a fair Pareto optimum. The fair Pareto optimum in the cases is obtaining T (S) followed with S (T) in an entire alternating way (ST-reciprocity). In this point, we cannot evaluate a social efficiency by a cooperation rate, which is measured by cooperators fraction among the mother population, anymore. Instead, we have to take average payoff of all game players. Summing up, we should say that both Leader and Hero games have Chicken-type dilemma, and are expected to realize ST-reciprocity to attain the fair

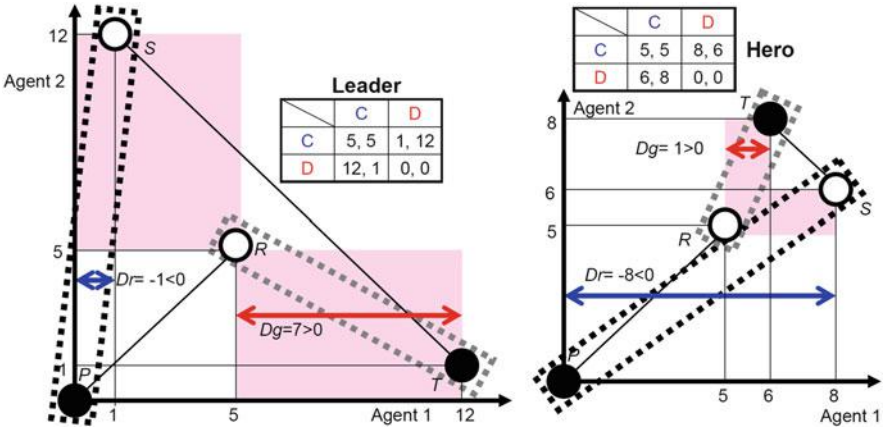

Fig. 2.8 Feasible solution regions of Leader and Hero Games

Pareto optimum unlike PD and pure Chicken favoring *R*-reciprocity. We will deliberately discuss about *R*-reciprocity and *ST*-Reciprocity latter.[8]

Another sub-game class to be noted is Donor & Recipient Game (sometimes abbreviated by D & R Game), where $D_g > 0$ & $D_r > 0$ and $D_g = D_r$ are satisfied. This means D & R game belongs to PD. This particular game has been used as one of the template models by theoretical biologist, because this game captures a social dilemma situation observed in many biological applications. Suppose you donate cost; c to help your game opponent. If your opponent is also willing to donate you by paying c, both of you and your opponent obtain benefit; b. Thus, the net payoff of both you and your opponent is $b - c$. Contrariwise, if your opponent rejects to donate even you offering donation, your net payoff is $-c$ (namely, you are exploited by your opponent) and that of your opponent is b. The asymmetric situation, where you and your opponent respectively offer D and C, gives you and your opponent; b and $-c$, respectively. Let alone, this story can be rewritten by; $P = 0$, $R = b - c$, $S = -c$ and $T = b$.

Although 2×2 games have four parterres; P, R, S and T, we can restrict the parameter area by fixing P and R. The most commonly accepted way is presuming $P = 0$ and $R = 1$. In this parameterization, games are expressed by remaining two variables; $T = 1 + D_g$ and $S = -D_r$. Thus, the games are parameterized by only D_g and D_r. Figure 2.9 shows all the game classes above mentioned in $D_g - D_r$ plane.

[8] To precisely know about *R*-reciprocity and *ST*-Reciprocity, you should consult with Tanimoto and Sagara (2007b).

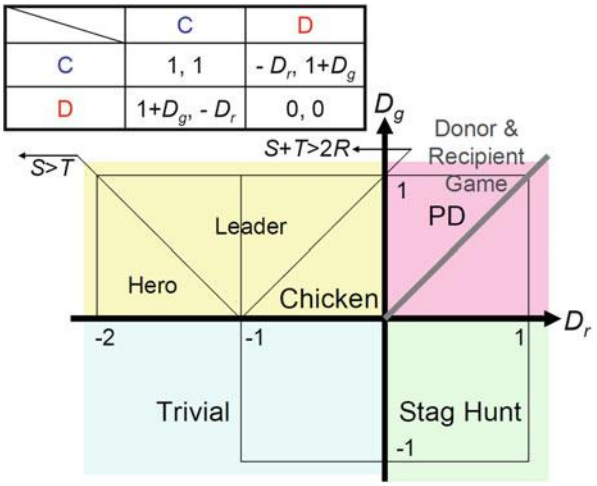

Fig. 2.9 Game classes of 2×2 game for varying D_g and D_r in case $R = 1$ and $P = 0$

2.4 Dynamics Analysis of the 2×2 Game

This section explores how the two-by-two game dynamics differ between the four game classes explained in the previous section, i.e., Trivial with no dilemmas, PD, Chicken, and SH with dilemmas. A deductive approach, relating to the non-linear system state equations derived in Sect. 2.2, is adopted.

As before, we assume unlimited group size (i.e., infinite number of agents) existing in a well-mixed state with no social viscosities. The strategies (offers) adopted by an agent are cooperation (C) or defection (D), expressed by the following state vectors:

$$\text{Strategy C;}\ {}^T\mathbf{e}_1 = (\,1 \quad 0\,), \tag{2.20-1}$$

$$\text{Strategy D;}\ {}^T\mathbf{e}_2 = (\,0 \quad 1\,). \tag{2.20-2}$$

The payoff matrix of the game structure is

$$\begin{bmatrix} R & S \\ T & P \end{bmatrix} \equiv \mathbf{M}. \tag{2.21}$$

Moreover, the proportions of agents adopting strategy C and strategy D at a given time (referred to as the strategy ratio) are defined by s_1 and s_2 respectively. These strategy ratios are expressed as

$${}^T\mathbf{s} = (\,s_1 \quad s_2\,). \tag{2.22}$$

From the condition of simplex we get

$$s_2 = 1 - s_1. \tag{2.23}$$

The validity of Eqs. (2.20-1, 2.20-2, 2.21, 2.22, and 2.23) should be understood from the following matrix equation describing the battle between two agents adopting strategy D, in which the outcome is P:

$$\pi_{\mathrm{DD}} = \begin{pmatrix} 0 & 1 \end{pmatrix} \cdot \begin{bmatrix} P & S \\ T & P \end{bmatrix} \begin{pmatrix} 0 \\ 1 \end{pmatrix} = P. \tag{2.24}$$

A variant form of Eq. (2.24) also computes the payoff when one strategy plays a game **M** against another with a different strategy. The expected payoff when an agent using strategy C battles with a randomly sampled agent at the present time expressed as strategy ratio **s** is

$${}^{T}\mathbf{e}_1 \cdot \mathbf{M}\,\mathbf{s}.$$

Similarly, the expected payoff when an agent using strategy D fights a randomly sampled agent at the present time expressed as strategy ratio **s** is

$${}^{T}\mathbf{e}_2 \cdot \mathbf{M}\,\mathbf{s}.$$

The **replicator dynamics** are defined as the strategy ratio dynamics of strategy i, expressed as

$$\frac{\dot{s}_i}{s_i} = {}^{T}\mathbf{e}i \cdot \mathbf{M}\,\mathbf{s} - {}^{T}\mathbf{s} \cdot \mathbf{M}\,\mathbf{s}. \tag{2.25}$$

The dimensionless quantity on the left hand side of (2.25), obtained by dividing $\dot{s}_i$ by the strategy ratio itself, indicates the level of change. As the reader should certainly appreciate, this quantity is determines by the extent to which the payoff for strategy i playing against the society average at a given time differs from the expected society payoff at that time. Recall how we discussed in page 17, "...even division of cooperative and defection agents (50 % cooperators & 50 % defectors), once the game is started and the strategy of the agents reviewed according to a certain set of rules after every step..." As part of this "set of rules," we investigate the evolution of the system under the replicator dynamics described in Eq. (2.25). Although other temporal dynamics can be supposed, replicator dynamics provide an adequate "set of rules" to govern evolution, for the following reason. After a game, the successful strategies (those achieving higher payoff than the average accumulated by the strategy ratio) will increase in the next time step, whereas less successful strategies will decrease. The ratio of this extent is thought to be decided by comparing with the aforementioned level of "success." In such a system, good conduct is rewarded whereas bad conduct is punished (a form of survival of the fittest). Selection mechanisms in the natural world (including human social systems) tend to operate in this manner. Alternative systems of rewarding the good and

punishing the bad exist in which the response to the acquired payoffs differs from that of Eq. (2.25) may be possible. Also randomness caused by luck may enter the dynamics (i.e., poor-scoring individuals could, if lucky enough, produce offspring). In any case, we suppose replicator dynamics as the "set of rules" in the following analysis.

Substituting Eqs. (2.20-1, 2.20-2, 2.21, and 2.22) into Eq. (2.25) and explicitly writing the elements, we obtain

$$\begin{cases} \dot{s}_1 = [(R-T)\cdot s_1 - (P-S)\cdot s_2]\cdot s_1 \cdot s_2, \\ \dot{s}_2 = -[(R-T)\cdot s_1 - (P-S)\cdot s_2]\cdot s_1 \cdot s_2. \end{cases} \tag{2.26}$$

Note that when the right hand side of (2.26) = 0, the equation becomes a cubic in s_1 and s_2; that is, the system contains three equilibrium points. Two of these are self-evident:

$$(s_1 \quad s_2) = (1 \quad 0) \equiv \mathbf{s}^*\big|_{\text{C-dominate}}, \tag{2.27-1}$$

$$(s_1 \quad s_2) = (0 \quad 1) \equiv \mathbf{s}^*\big|_{\text{D-dominate}}. \tag{2.27-2}$$

In the former, all individuals ultimately become cooperative; the latter leads to the defection state, implying C-dominant and D-dominant, respectively. The remaining equilibrium point is obtained by simultaneously solving Eq. (2.26), setting [. . .] on the right hand side to 0 and eliminating s_2 through Eq. (2.23) (the reader should confirm this for themselves):

$$(s_1 \quad s_2) = \left(\frac{P-S}{P-T-S+R} \quad \frac{R-T}{P-T-S+R} \right) \equiv \mathbf{s}^*\big|_{\text{Polymorphic}}. \tag{2.27-3}$$

This third equilibrium point lies within [0, 1] depending on the values of P, R, S, and T. In this case, the dynamics become polymorphic or bi-stable. Equation (2.27-3) defines an **internal equilibrium point**.

Once the three equilibrium points are obtained, the signs of the eigenvalues of the Jacobian matrix at each equilibrium point are determined, and the equilibrium points are assessed as sink, source, or saddle.

To this end, we re-write Eq. (2.26) as follows:

$$\dot{s}_1 \equiv f_1(s_1, s_2), \tag{2.28-1}$$

$$\dot{s}_2 \equiv f_2(s_1, s_2). \tag{2.28-2}$$

From Eq. (2.23), we observe that $f_1 = -f_2$. Hence, the Jacobian (2.18) is calculated as

$$\begin{cases} \dfrac{\partial f_1}{\partial s_1} = -\dfrac{\partial f_2}{\partial s_1} = 3(-R+S+T-P)s_1^{\,2} \\ \quad +2(R-2S-T+2P)s_1 + S - P \end{cases} \tag{2.29-1}$$

$$\begin{cases} \dfrac{\partial f_1}{\partial s_2} = -\dfrac{\partial f_2}{\partial s_2} = -3(-R+S+T-P)s_1^{\,2} \\ \quad -2(R-2S-T+2P)s_1 - S + P \end{cases} \tag{2.29-2}$$

The reader is encouraged to verify these equations. The Jacobian matrix $\mathbf{J} = \begin{bmatrix} \frac{\partial f_1}{\partial s_1} & \frac{\partial f_1}{\partial s_2} \\ \frac{\partial f_2}{\partial s_1} & \frac{\partial f_2}{\partial s_2} \end{bmatrix} = \begin{bmatrix} \frac{\partial f_1}{\partial s_1} & \frac{\partial f_1}{\partial s_2} \\ -\frac{\partial f_1}{\partial s_1} & -\frac{\partial f_1}{\partial s_2} \end{bmatrix}$ is a 2×2 matrix, so its eigenvalues (0 and $\frac{\partial f_1}{\partial s_1} - \frac{\partial f_1}{\partial s_2}$) are easily obtained using senior school mathematics (readers should try to recall and apply the eigenvalue calculations from their maths textbooks). Since 0 is unsigned, we need only obtain the sign of $\frac{\partial f_1}{\partial s_1} - \frac{\partial f_1}{\partial s_2}$ to establish the equilibrium conditions. Explicitly, these eigenvalues are

$$\begin{aligned} \lambda = \frac{\partial f_1}{\partial s_1} - \frac{\partial f_1}{\partial s_2} &= 6(-R+S+T-P)s_1^{\,2} \\ &\quad + 4(R-2S-T+2P)s_1 + 2(S-P) \end{aligned} \tag{2.30}$$

1. The necessary and sufficient condition for the equilibrium point $\mathbf{s}^*|_{\text{C-dominate}}$ to be sink is $\lambda < 0$ when substituting $(s_1 \quad s_2) = (1 \quad 0)$ into Eq. (2.30). The following conditions are sought:

$$T - R = D_g < 0. \tag{2.31}$$

2. The necessary and sufficient condition for the equilibrium point $\mathbf{s}^*|_{\text{D-dominate}}$ to be a sink is $\lambda < 0$ when substituting $(s_1 \quad s_2) = (0 \quad 1)$ into Eq. (2.30). We now require that

$$P - S = D_r > 0. \tag{2.32}$$

3. The necessary and sufficient conditions for the equilibrium point $\mathbf{s}^*|_{\text{Polymorphic}}$ to be a sink is $\lambda < 0$ with $(s_1 \quad s_2) = \left(\frac{P-S}{P-T-S+R} \quad \frac{R-T}{P-T-S+R}\right)$ substituted into Eq. (2.30). Noting that $\lambda = 2\frac{(R-T)(P-S)}{R-S-T+P}$, we seek the following conditions:

$$P < S \wedge R < T \Leftrightarrow P - S = D_r < 0 \wedge T - R = D_g > 0. \tag{2.33}$$

The above conditions are summarized in Table 2.1, with the following substitution:

Table 2.1 2×2 game dynamics derived analytically

Game class	Phase	Nash equilibrium	Sign of D_g	Sign of D_r	Each point sink, source, or saddle		
					(1,0)	(0,1)	$\left(\frac{D_r}{D_g - D_r} \quad \frac{-D_g}{D_r - D_g}\right)$
PD	**D**-Dominate	(0,1)	+	+	Source	Sink	Saddle
Chicken	Polymorphic	$\left(\frac{D_r}{D_g - D_r} \quad \frac{-D_g}{D_r - D_g}\right)$	+	−	Source	Source	Sink
SH	Bi-stable	(0,1) or (1,0)	−	+	Sink	Sink	Source
Trivial	**C**-Dominate	(1,0)	−	−	Sink	Source	Saddle

$$\mathbf{s}^*\big|_{\text{Polymorphic}} = \left(\frac{P-S}{P-T-S+R} \quad \frac{R-T}{P-T-S+R}\right) = \left(\frac{D_r}{D_g-D_r} \quad \frac{-D_g}{D_r-D_g}\right).$$

Defining D_g and D_r in Eq. (2.19), the four game classes were established as PD, Chicken, SH, and Trivial (see Fig. 2.5). Here, these divisions are represented by the difference between the signs of the three equilibrium points.

In PD, $\mathbf{s}^*|_{\text{C-dominate}}$ and $\mathbf{s}^*|_{\text{D-dominate}}$ are source and sink, respectively; hence, regardless of the initial cooperation proportion in [0, 1] the ultimate state is one of complete defection at $t \to \infty$.

In Chicken, $\mathbf{s}^*|_{\text{C-dominate}}$ and $\mathbf{s}^*|_{\text{D-dominate}}$ are both sources. In this case $\mathbf{s}^*|_{\text{Polymorphic}}$ (value in [0, 1]) is a sink, so regardless of initial cooperation proportion, as $t \to \infty$, the system settles to the internal equilibrium point $\mathbf{s}^*|_{\text{Polymorphic}}$. As previously mentioned, this state does not imply that specific agents are fixed into cooperation or defection strategies, but that when the infinitely large group is viewed as a whole, the proportions of cooperation and defection players are (dynamically) steady.

In SH, the internal equilibrium point $\mathbf{s}^*|_{\text{Polymorphic}}$ is a source, while $\mathbf{s}^*|_{\text{C-dominate}}$ and $\mathbf{s}^*|_{\text{D-dominate}}$ are both sinks. Therefore if the initial proportion of cooperative players is smaller (or larger) than $\mathbf{s}^*|_{\text{Polymorphic}}$, the ultimate state is pure defection, (or pure cooperation), and the system is bi-stable.

In Trivial, $\mathbf{s}^*|_{\text{C-dominate}}$ is a sink and $\mathbf{s}^*|_{\text{D-dominate}}$ is a source, so regardless of the initial cooperation proportion, the pure cooperation state is inevitable. For this reason, Trivial is a game with no dilemmas.

The above discussion is summarized schematically in Fig. 2.10.

Here, we have fully characterized the 2×2 replicator dynamics, expressed as non-linear cubic equations.

The following is provided for interest only. A two by two game has two strategies, so the dynamics are relatively simple, and one of the equilibrium points inevitably acts as a sink. If the number of strategies is increased, more degrees of freedom are introduced, leading to **perturbation** dynamics (which display periodic behavior) or **chaos** (which is deterministic but unpredictable). The interested reader should take a look at related literatures (Weibull 1997; Nowak 2006a).

2.5 Multi-player Games

Though we have so far assumed that there are two game players, a multi-player situation is more typical in a realistic context. It is therefore natural that the discussion can now be extended to multi-player games.

First, we outline the so-called Public Goods Game (PGG), which has been used most often in the field as a template for multi-player games. This game is based on a social dilemma around a public good that can only be sustained by a reasonable number of moral-minded cooperators through their donations. This means players have an incentive not to donate but also to want to get their share of the cooperative fruits brought about by the donations of others.

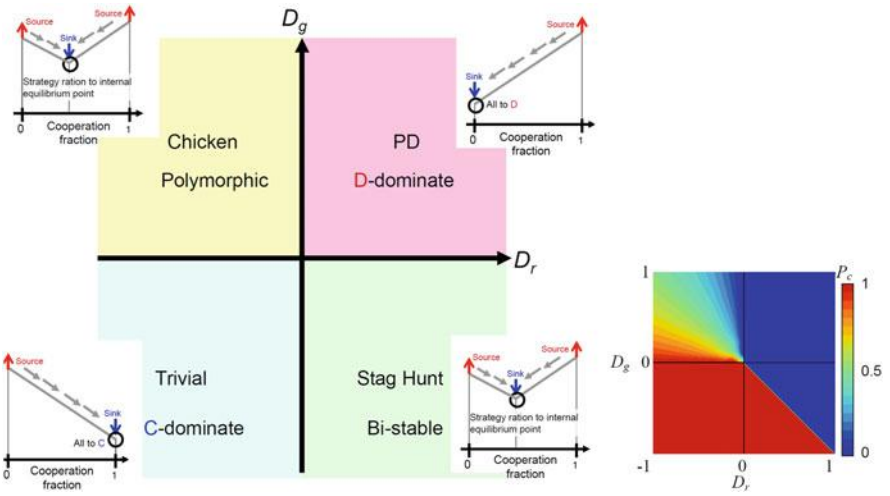

Fig. 2.10 Phase diagram of dynamics classified by D_g and D_r of two-by-two game and a summary of dynamics of each game class (*left panel*). *Right panel*; Cooperation fraction at equilibrium when an infinite and well-mixed population with replicator dynamics is assumed when initial cooperation fraction; P_c of 0.5 presuming. PD and Trivial are colored with *blue* and *red*, respectively, since D-dominate and C-dominate phases are established. In Chicken game region, gradually shifting of cooperation fraction at equilibrium is observed due to polymorphic phase. In SH game region, bi-stable shows twofold phases; either absorbed all cooperation bor all defection

Suppose G players participate in a single multi-player game, where a cooperator is requested to donate a cost c (in most cases, as in Fig. 2.11, assuming $c = 1$) to a public pool. The number of cooperators is denoted by n_c. After collecting the donations from all cooperators among the G players, the total pooled donation is multiplied by an amplifying factor, r. Thus, the public good is amplified. The fruits of this public good are distributed equally to all game participants irrespective of whether they are a cooperator or defector. In this sense, a defector can be called a free-rider.[9] Here, we can define the payoff structure functions for both cooperators and defectors as shown in Fig. 2.11, which can be drawn from the cooperation fractions in the lower panel of Fig. 2.11. One important thing is that the defectors' payoff is always larger than that of the cooperators at any particular cooperation fraction. This schematic relation is redrawn more precisely in Fig. 2.12, where the cooperator and defector plots indicate the respective payoffs at discrete cooperation fractions, where $P_c = n_c/G$. The figure obviously suggests that, as long as $\pi_D(n_c - 1) > \pi_C(n_c)$ is satisfied, a cooperator has no incentive to keep cooperating at any cooperation fraction, and thus the cooperation fraction is always declining regardless

[9] Precisely speaking, we should call it a 1st order free-rider, because in the models considering the punishment mechanism, which many previous studies have investigated, there are 1st order free-riders, meaning simple defectors, as well as 2nd order free-riders, implying cooperators who are not punishing other defectors.

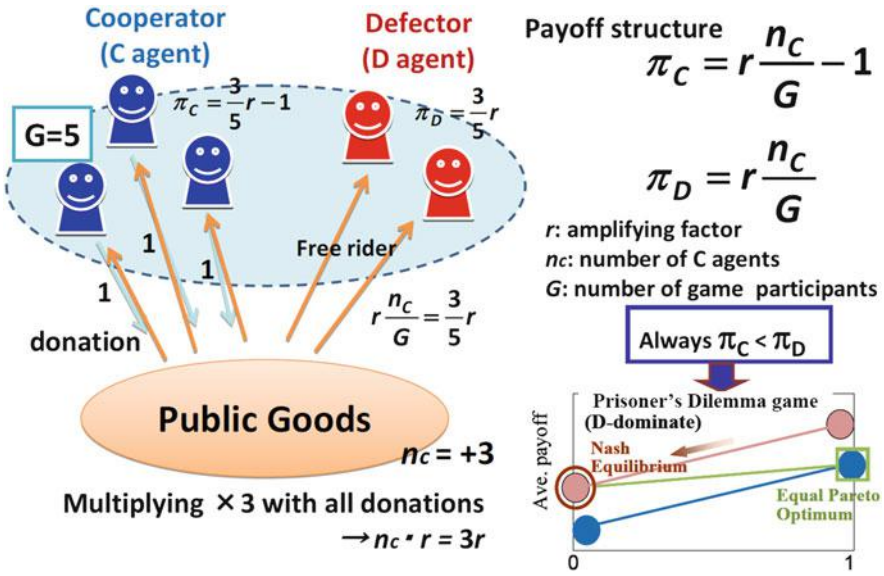

Fig. 2.11 Public Goods Game (PGG); N-Prisoner's Dilemma Game

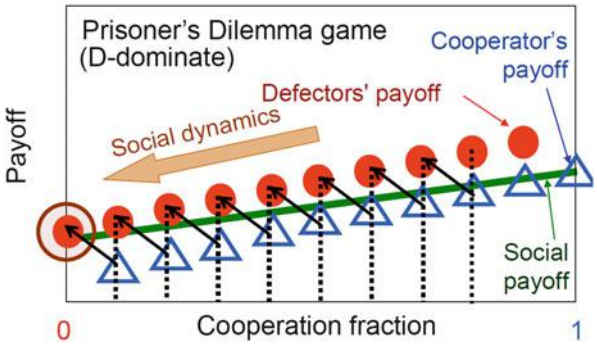

Fig. 2.12 Payoff structure function of multi-player PD

of the initial cooperation fraction. Consequently, Nash equilibrium is absorbed by an all defectors state, i.e., $P_c = 0$. On the other hand, the maximum social payoff, or fair Pareto optimum, appears at the all cooperators state, $P_c = 1$. This is why we can basically identify PGG as multi-player Prisoner's Dilemma (N-PD) game. Comparing with 2×2 PD games, it can be seen that $\pi_D(0) = P$ and $\pi_C(1) = R$.

Noting the relative geometric relationship between the payoff structure functions for cooperators and defectors, we can summarize the classes of multi-player games as in Fig. 2.13.

Multi-player Chicken (N-Chicken) is featured when the cooperator's payoff function crosses with the defector's one at a certain cooperation fraction, which is called an internal equilibrium point, as in 2×2 Chicken. As mentioned before, a

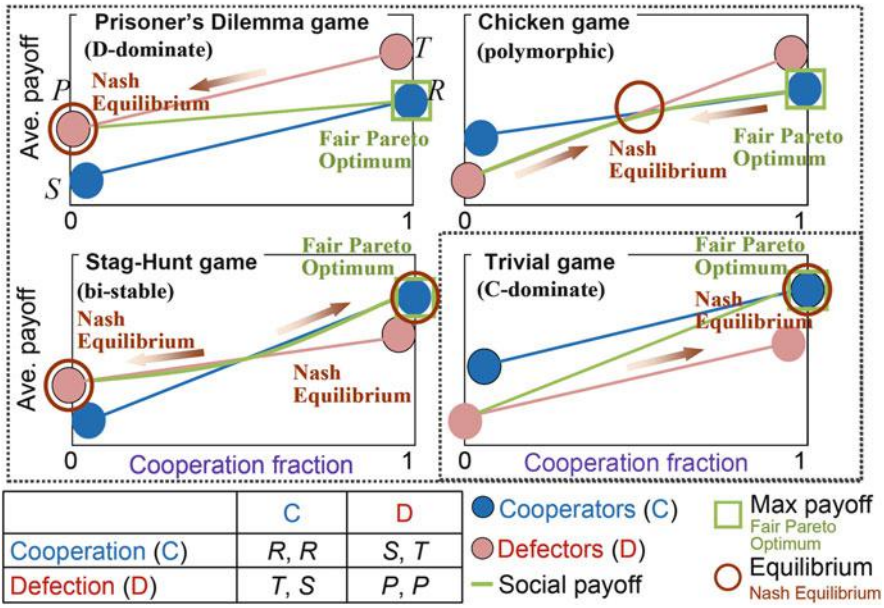

Fig. 2.13 Four game classes and payoff structure functions of multi-players games

multi-player Chicken game termed "the tragedy of commons" has been accepted as one of the typical template models for describing a social dilemma caused by environmental problems.[10] Multi-players Stag Hunt (N-SH) games also have a crossing point between the two payoff functions. But the dynamics differ from those of N-Chicken, as shown schematically in the figure. Multi-player Trivial (N-Trivial) has no social dilemma, since cooperation dominates defection meaning the cooperator's payoff exceeds the defector's one at any cooperation fraction.

2.6 Social Viscosity; Reciprocity Mechanisms

As long as an infinite and well-mixed population is assumed, the theory correctly predicts the dynamics of any symmetric 2-strategy game as well as its equilibrium as we discussed in Sects. 2.5 and 2.6.

Although the fundamental theory seems transparent and unsurprising, the interdisciplinary field around the study of evolutionary games has been persistent, with a new paper appearing every day, or even every hour or minute. What has aroused this enthusiasm to study the field in mathematicians, biologists, physicists,

[10] But there have been several indications that "tragedy of commons", or say a multi-players Chicken game is insufficient to model with general environmental problems on the ground that the model does not consider any dynamics of the environment. Even though a grass field or fishing field temporarily becomes exhaustive, it can gradually recover according to dynamics the environment has. More intimately, you can consult with Tanimoto (2005).

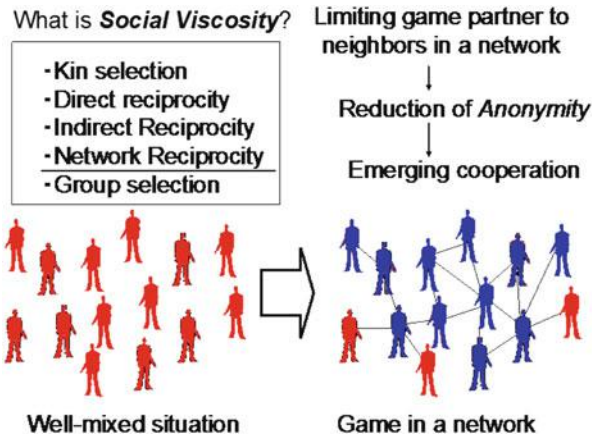

Fig. 2.14 Five basic mechanisms of dilemma resolution and example of Network Reciprocity

information scientists, and even common foot soldiers such as the author? At the end of the day, it comes down to a single question: What additional mechanisms will promote the ultimate cooperation among agents if a pair of agents is randomly selected from an unlimited group (i.e., an infinite and well-mixed selection) and forced into a specified game (such as PD)? In the natural world, cooperative behavior is found not only in human societies, but also among social insects such as ants and bees. This question invokes the mysteries of biological evolution, and invites analogies with the statistical physics of crystal structure and phase transitions. Solutions may lead to suggestions for an improved human society.

From recent theoretical studies, the puzzle of what can be "supplementary framework" of dilemma resolution has been unfolded. Nowak (2006b) showed there are the five fundamental protocols to mitigate or cancel dilemmas,[11] summarized as in Fig. 2.14. The mechanisms of these activities are governed by very ordinary and beautiful mathematical expressions similar to those of kin selection (Hamilton 1963). Nowak refers to these mechanisms as "**Social Viscosity**." Under these circumstances, the population is initially well-mixed as before, and each game is played by a single person whose next encounter is unknown. But, in repeated game battles between a pair of individuals (direct reciprocity),[12] or observing the tag of the opponent (indirect reciprocity), the behaviour of opponent; cooperation or defection, can be distinguished. Or, when players play games against only the neighboring players throughout the network, information relating to strategy is obtained (network reciprocity). All these enable the agents to overcome the dilemmas and create a cooperative society.[13] These processes essentially reduce

[11] Strictly speaking PD satisfying $D_g = D_r$.

[12] This situation accords with common sense. If a game is played against the same partner each time rather than against an unknown one, both individuals should accept the cooperation option to avoid strategies leading merely to short term profit. If both individuals take the defection option P, neither will benefit long-term. Our daily behavior follows the former pattern.

[13] Many of these dynamics can be verified by simulation. Games are repeated between multiple agents in a simulated society; this approach is known as multi-agent simulation.

the anonymity from that of an infinite and well-mixed population (which exists in a total anonymous state) and authenticate the battle opponent. By carefully studying the authentication of others through indirect reciprocity, it may be possible to elucidate how notable features of organisms (such as colour differences in bird crests) evolve, or evolution of language, which is the ultimate third party identification system. Network reciprocity may also help us understand the structure of special network topologies such as the scale-free graphs observed in many natural phenomena, as well as human social systems; in particular, how cooperation self-organizes in such networks.

2.7 Universal Scaling for Dilemma Strength in 2 × 2 Games

As long as an infinite and well-mixed population is presumed with the replicator dynamics, an evolutionary trail can be stipulated strictly by what Table 2.1 shows. In a nutshell, whenever both D_g and D_r are fixed, the evolutionary dynamics are determined. In this sense, D_g and D_r are scaling parameters of dilemma strength, and the dynamics of equilibrium are determined by their values.

However, D_g and D_r are not sufficient for indicating the dilemma strength when a certain specific reciprocity mechanism is introduced into a game. For example in Fig. 2.15, we show the equilibrium cooperation fractions of spatial PD games on a lattice network with degree $k = 8$ (the details of simulation setting are described later). Although these three games have the same D_g and D_r, cooperation fractions in Fig. 2.15 are completely different depending on the value of $R - P$. The larger $R - P$ becomes, the higher is the equilibrium cooperation fraction.

Thus, in a game with a certain reciprocity mechanism, the dilemma strength cannot be quantified only by D_g and D_r, which can be sufficient indicators in an infinite well-mixed population game. Let us assume two PDs having the same D_g and D_r, as shown in Fig. 2.16, which visually explains the preceding discussion. As $R - P$ becomes larger relative to D_g and D_r, we can regard $T \to R$ and $P \to S$

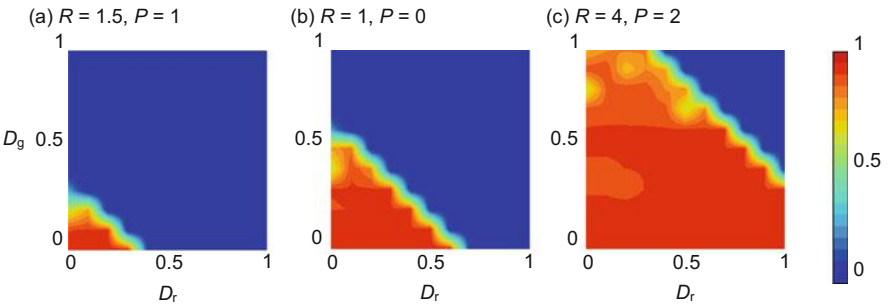

Fig. 2.15 Averaged cooperation fraction $D_r - D_g$ diagrams for (**a**) $R = 1.5$, $P = 1$, (**b**) $R = 1$, $P = 0$, and (**c**) $R = 4$, $P = 2$. Games are played on 8-neighbor lattice. Imitation Max (IM) is adopted as the strategy update rule

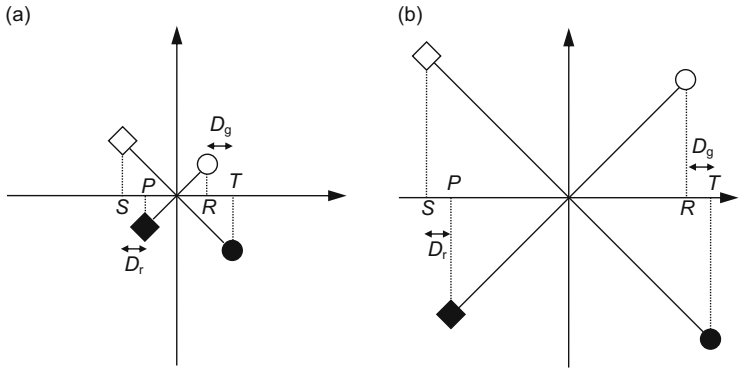

Fig. 2.16 Two PD games having the same D_g and D_r but different $R-P$; (**a**) smaller $(R-P)$ and (**b**) larger $(R-P)$

asymptotically. This is similar to the Avatamasaka game, defined by Akiyama and Aruka (2004), wherein a focal player's gain becomes irrelevant to his own offer, but is entirely dominated by his opponent's offer. Thus, in game (b), the payoff increment of the focal player by his offering either cooperation (C) or defection (D) is relatively lower than that of whether his opponent offering cooperation (C) or defection (D). This is because the focal player's payoff is affected more by his opponent's offer than by his own decision, whether C or D. Thus, we can say that game (b) has a relatively higher incentive to establish a reciprocal relationship than does game (a). Therefore, we should take $R-P$ into a new index parameter to evaluate dilemma strength when a game is played in a situation with social viscosity, wherein an agent might play with the same opponent in several rounds; because of a reciprocity mechanism.

In the discussion about the five reciprocity mechanisms in explained Sect. 2.6, Nowak assumed PD games of $D_g = D_r$, which is a Donor and Recipient (D & R) game as shown in Fig. 2.9 (Nowak 2006a, 2006b). In a D & R game, the game structure can be described by two parameters, *benefit* (b) and *cost* (c) of cooperation. Nowak reported that any reciprocity mechanism among the five can be expressed by; (cooperation fraction; P_c) = function(c/b). Thus, in short, universal scaling is possible for D & R game by using c/b. Assuming $P=0$, $R=b-c$, $S=-c$, and $T=b$, we can derive $c/b = D_g/(R-P+D_r)$. Therefore, Nowak's scaling parameter c/b has already quantified $R-P$ as well as D_g and D_r. Despite his work implying that c/b can work as a scaling parameter to express dilemma strength, Nowak's discussion is restricted to D&R games.

Inspired by Nowak's scaling concept, Tanimoto (2009) proposed a set of universal scaling parameters defined as b/c_c and b/c_d. This concept can extend Nowak's scaling to the general PD game by considering two parameters—c_c and c_d—implying the *focal player's costs* when his opponent offers C and D, respectively. However, Tanimoto's report assumed only PD games, and he did not demonstrate any theoretical plausibility.

This section shows a new set of universal scaling parameters that can be applicable to all 2×2 games, i.e., from those with an infinite well-mixed population, which is the premise for the replicator dynamics, to those having a population with any of the five reciprocity mechanisms.

2.7.1 Concept of the Universal Scaling for Dilemma Strength

We consider 2×2 games composed of N agents. Let us denote the payoff matrix as;

$$\mathbf{A} \equiv [a_{ij}] = \begin{matrix} \\ \text{C} \\ \text{D} \end{matrix} \begin{matrix} \begin{matrix} \text{C} & \text{D} \end{matrix} \\ \begin{pmatrix} R & S \\ T & P \end{pmatrix} \end{matrix}. \tag{2.34}$$

When we consider an infinite well-mixed population ($N \to \infty$) and denote $x_i(t)$ as the frequency of strategy i at time t, the expected payoff of strategy i is given by $f_i = \sum_{j=1}^{2} x_j a_{ij}$. Hence, the average payoff is given by $\varphi = \sum_{i=1}^{2} x_i f_i$. The replicator dynamics can be written by;

$$\dot{x}_i = x_i(f_i - \varphi). \tag{2.35}$$

From the definition of the payoff matrix; Eq. (2.34), we note $i = 1$ and $i = 2$, representing C and D strategies, respectively. Since the simplex condition; $x_1 + x_2 = 1$ is kept for any time, we can reduce the two variables by introducing $x_1 = x$. Recalling (2.27-1, 2.27-2, and 2.27-3), we can deduce the three of equilibrium x^* for Eq. (2.34) by;

$$x^* = 0, \quad 1, \quad \frac{P - S}{R - S - T + P}. \tag{2.36}$$

It is worthwhile to note again that in a finite well-mixed population or a population with any of reciprocity mechanisms, the equilibrium under the replicator dynamics can no longer be given by Eq. (2.36).

According to Eq. (2.19), the payoff matrix; Eq. (2.34) can be re-written as;

$$\mathbf{A} = [a_{ij}] = \begin{matrix} \\ \text{C} \\ \text{D} \end{matrix} \begin{matrix} \begin{matrix} \text{C} & \text{D} \end{matrix} \\ \begin{pmatrix} R & P - D_r \\ R + D_g & P \end{pmatrix} \end{matrix}. \tag{2.37}$$

We also note that the third equilibrium of Eq. (2.36), which is the so-called internal equilibrium, can be given as follows:

$$x^* = \frac{D_r}{D_r - D_g}. \tag{2.38}$$

Here, let us introduce a new set of scaling parameters considering a finite population with any of reciprocity mechanisms by defining a new set of GID and RAD as $D_g{}'$ and $D_r{}'$, respectively.

$$D_g{}' = \frac{T-R}{R-P} = \frac{D_g}{R-P}, \quad D_r{}' = \frac{P-S}{R-P} = \frac{D_r}{R-P} \tag{2.39}$$

This is what we call the new universal scaling for dilemma strength. Based on this definition, the payoff matrix can be re-written again in following form:

$$\mathbf{A} = [a_{ij}] = \begin{matrix} \\ \mathrm{C} \\ \mathrm{D} \end{matrix} \begin{matrix} \begin{matrix} \mathrm{C} \end{matrix} & \begin{matrix} \mathrm{D} \end{matrix} \\ \begin{pmatrix} R & P-(R-P)D_r{}' \\ R+(R-P)D_g{}' & P \end{pmatrix} \end{matrix}. \tag{2.40}$$

2.7.2 *Analytical Approach*

Taylor and Nowak (2007) successfully deduced that any of the five reciprocity mechanisms by Nowak can be expressed by each transformation that is applied to an original 2 × 2 game payoff; Eq. (2.34). This allows us to derive the equilibriums of each of the five mechanisms when applying the replicator dynamics on the basis of the transformed matrix.

In this sub-section, following the analytical approach presented by their work, we determine whether $D_g{}'$ and $D_r{}'$ are theoretically consistent as scaling parameters for evaluating each of the five reciprocity mechanisms. After confirming this theoretical consistency, we demonstrate that the set of these new scaling parameters works well in a finite and well-mixed population. Finally, we demonstrate that $D_g{}'$ and $D_r{}'$ can prove that the "paradox of cooperation" reported by Németh and Takács (2010) is not paradox at all.

Theoretical Consistency for Nowak's Five Reciprocity Mechanisms

Following Taylor and Nowak (2007), let us describe how the Nowak's five reciprocity mechanisms can be expressed by applying their respective transformed game matrices.

Direct Reciprocity

In repeated games by a pair composed with same two agents, or when the same agents play a different game in another round, direct reciprocity stimulates

cooperation (Trivers 1971, 1985). In each round, the two agents must choose either cooperation or defection. With probability, w, the same two agents play another round. We assume that defectors, denoted by D, always choose defection and cooperators, C, play tit-for-tat (TFT): they start with cooperation and then follow what the other player has done in the previous move.

Indirect Reciprocity

Indirect reciprocity is based on reputation (Alexander 1987; Nowak and Sigmund 1998). Unlike the direct reciprocity, where the focal player's decision is based on whether cooperation or defection her opponent has offered to her in the previous encounter; in the indirect reciprocity, the focal agent's decision is determined on whether cooperation or defection her opponent has offered to another agent in the previous round. In fact, the focal agent chooses her strategy (offering C or D) based on her opponent's reputation; called Image Score (IS). The parameter q denotes the probability of knowing the IS of another individual, in short knowing whether another individual is a cooperator or defector. Let us assume, a defector, D, always defects, whereas a cooperator, C, only defects when she knows her opponent is a defector, and cooperates otherwise. Thus, C cooperates with D with probability $1 - q$.

Kin Selection

The concept of kin selection arose from the idea that evolutionary games are often played between individuals who are genetic relatives (Hamilton 1964). Consider a population in which the average relatedness between interacting individuals is given by r, which is a real number between 0 and 1. In such a population, the opponent's contribution that equals the r of the opponent's payoff can be joined to the focal agent's payoff.

Group Selection

Group selection is based on the idea that competition occurs not only between individuals but also between groups.[14] Here, we use the approach described by Traulsen and Nowak (2006). A population is subdivided into m groups. The maximum group size is n. Individuals interact with others in the same group according to a 2×2 game. The fitness of an individual is $1 - \omega - \omega F$, where F is

[14] There are so many literatures concerning this point. Because of space limitation, we cite only five of those; Wynne-Edwards (1962), Williams (1996), Wilson (1975), Maynard Smith (1976), Slatkin and Wade (1978).

the payoff and ω is the intensity of selection. At each round, an individual from the entire population is chosen for reproduction proportional to fitness. The offspring is added to the same group. If the group reaches the maximum size, it can split into two groups with a certain probability, p. In this procedure, a randomly selected group dies to prevent the population from exploding. The maximum population size is defined as mn. With probability $1-p$, however, the group does not divide, but a random individual of that group is chosen to die. We assume weak selection ($\omega << 1$) and rare group splitting ($p << 1$) large n and m.

Network Reciprocity

Network reciprocity relies on two effects: (1) limiting the number of game opponents (diminishing anonymity), leading to increased mutual cooperation; and (2) a local adaptation mechanism wherein a player copies a strategy from a neighbor linked to the player through a network. These two effects explain how cooperators survive in a network game of PD, even though players are required to use only the simplest strategy—either cooperation or defection (requiring only 1 bit memory) (Nowak and May 1992). Therefore, hundreds of studies have reported on network reciprocity, primarily in the fields of theoretical biology and statistical physics.[15] The individuals of a population occupy the vertices of a graph. The edges denote who interacts with whom. Each individual interacts with all of its neighbors according to the standard payoff matrix, as in Eq. (2.34). The payoff of each agent is totaled over all games with her neighbors. An individual's fitness is given by $1-\omega-\omega F$ where F is the payoff for the individual and ω ($\omega \in [0,1]$) is the intensity of selection. Here, we consider evolutionary dynamics according to Death-Birth updating (DB) (Ohtsuki et al. 2006), where in each round a random individual is chosen to die; then the neighbors compete for the empty site proportional to their fitness.

A calculation using pair approximation on regular graphs (where each vertex has k edges) leads to a deterministic differential equation that describes how the expected frequency of cooperation (defection) changes over time. This differential equation is actually a standard replicator equation with a modified payoff matrix (Ohtsuki and Nowak 2006).

From the above-mentioned discussion, now we are able to describe the five reciprocity mechanisms in the following transformed 2 × 2 matrix from the original game payoff matrix, as in Eq. (2.34) (Taylor and Nowak 2007).

[15] Because of space limitation, we can cite here only five of those; Hassell et al. (1994), Ebel and Bornholdts (2002), Santos and Pacheco (2005), Santos et al. (2006), Yamauchi et al. (2010).

$$\text{Direct Reciprocity} \quad \begin{matrix} \\ \text{C} \\ \text{D} \end{matrix} \begin{matrix} \begin{matrix} \text{C} & \text{D} \end{matrix} \\ \begin{pmatrix} \dfrac{R}{1-w} & S+\dfrac{wP}{1-w} \\ T+\dfrac{wP}{1-w} & \dfrac{P}{1-w} \end{pmatrix} \end{matrix}, \tag{2.41}$$

$$\text{Indirect Reciprocity} \quad \begin{matrix} \\ \text{C} \\ \text{D} \end{matrix} \begin{matrix} \begin{matrix} \text{C} & \text{D} \end{matrix} \\ \begin{pmatrix} R & (1-q)S+qP \\ (1-q)T+qP & P \end{pmatrix} \end{matrix}, \tag{2.42}$$

$$\text{Kin Selection} \quad \begin{matrix} \\ \text{C} \\ \text{D} \end{matrix} \begin{matrix} \begin{matrix} \text{C} & \text{D} \end{matrix} \\ \begin{pmatrix} R & \dfrac{S+rT}{1+r} \\ \dfrac{T+rS}{1+r} & P \end{pmatrix} \end{matrix}, \tag{2.43}$$

$$\text{Group Selection} \quad \begin{matrix} \\ \text{C} \\ \text{D} \end{matrix} \begin{matrix} \begin{matrix} \text{C} & \text{D} \end{matrix} \\ \begin{pmatrix} (n+m)R & nS+mR \\ nT+mP & (n+m)P \end{pmatrix} \end{matrix}, \tag{2.44}$$

$$\text{Network Reciprocity} \quad \begin{matrix} \\ \text{C} \\ \text{D} \end{matrix} \begin{matrix} \begin{matrix} \text{C} & \text{D} \end{matrix} \\ \begin{pmatrix} R & S+H \\ T-H & P \end{pmatrix} \end{matrix}. \tag{2.45}$$

Here, H in Eq. (2.45) is defined as follows:

$$H = \frac{(k+1)(R-P)-T+S}{(k+1)(k-2)}. \tag{2.46}$$

We assume $k > 2$.

It is worth noting that, in Eq. (2.43), summations of two players, $R+R$, $P+P$, and $(S+rT)/(1+r)+(T+rS)/(1+r)$ are consistent with those of Eq. (2.34), $R+R$, $P+P$, and $S+T$.

From these equations, we can draw each set of conditions, wherein C and D become evolutionarily stable strategies (ESS), and the internal equilibrium, as shown in Table 2.2. One important point to be addressed is that all these conditions and the internal equilibrium can be described only by $D_g{}'$ and $D_r{}'$ with the defined model parameters.

Assuming the parameters $w = 0.1$, $q = 0.1$, $r = 0.1$, $m = 50$, $n = 500$, and $k = 12$, we obtain Figs. 2.17, 2.18, 2.19, 2.20, and 2.21, (Fig. 2.17; direct reciprocity; Fig. 2.18; indirect reciprocity; Fig. 2.19; kin selection; Fig. 2.20; group selection; Fig. 2.21; network reciprocity), wherein the $D_g - D_r$ diagrams (upper panels) as well as the $D_g{}' - D_r{}'$ diagrams (lower panels) of equilibria for different $R-P$ are shown. Those results come from Eqs. (2.41, 2.42, 2.43, 2.44, 2.45, and 2.46), assuming that the initial cooperation fraction is 0.5. In these figures, each of white circles indicates the boundary point of four games classes; D-dominant, C-dominant, polymorphic and bi-stable (hereafter "four-corners"). Each horizontal

Table 2.2 Conditions of cooperation being ESS, defection being ESS, and interior equilibrium for each of the five mechanisms: direct reciprocity, indirect reciprocity, kin selection, group selection, and network reciprocity

	Cooperation is ESS	Defection is ESS	Internal equilibrium
Direct reciprocity	$\frac{w}{1-w} > D_g{}'$	$D_r{}' > 0$	$x^* = \frac{(1-w)D_r{}'}{(1-w)\left(D_r{}'-D_g{}'\right)+w}$
Indirect reciprocity	$\frac{q}{1-q} > D_g{}'$	$D_r{}' > 0$	$x^* = \frac{(1-q)D_r{}'}{(1-q)\left(D_r{}'-D_g{}'\right)+q}$
Kin selection	$r(1+D_r{}') > D_g{}'$	$r\left(1+D_g{}'\right) < D_r{}'$	$x^* = \frac{-r\left(D_g{}'+1\right)+D_r{}'}{(1+r)\left(D_r{}'-D_g{}'\right)}$
Group selection	$\frac{m}{n} > D_g{}'$	$\frac{m}{n} < D_r{}'$	$x^* = \frac{nD_r{}'-m}{n\left(D_r{}'-D_g{}'\right)}$
Network reciprocity	$k^2D_g{}' - k\left(D_g{}'+1\right) + \left(D_r{}'-D_g{}'\right) < 0$	$k^2D_r{}' - k(D_r{}'+1) + \left(D_g{}'-D_r{}'\right) > 0$	$x^* = \frac{\left(k^2-k-1\right)D_r{}'+D_g{}'-k}{\left(k^2-k-2\right)\left(D_r{}'-D_g{}'\right)}$

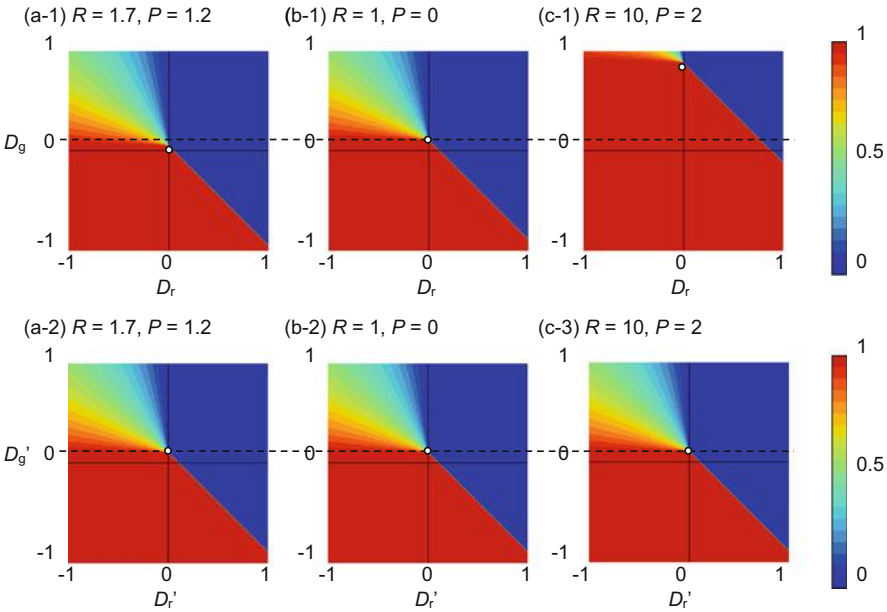

Fig. 2.17 Equilibrium cooperation fraction-$D_r - D_g$ (in the *upper line*) and $D_r{}' - D_g{}'$ (in the *lower line*) diagrams of direct reciprocity for (**a**) $R = 1.7$, $P = 1.2$, (**b**) $R = 1$, $P = 0$, and (**c**) $R = 10$, $P = 2$ with probability of another round $w = 0.1$

black broken-line in Figs. 2.17 and 2.18 means the difference between the four-corners in case of $R = 1$ and $P = 0$ and that of $D_g{}' = D_r{}' = 0$. Whereas, each white broken-line in Figs. 2.19, 2.20, and 2.21 shows that the four-corners shifting from the point of $D_g{}' = D_r{}' = 0$ along $D_g{}' = D_r{}'$ line (45 degree line).

Let us confirm that by the effect of direct and indirect reciprocity, the original four game-classes (PD in the first quadrant, Chicken in the second quadrant, Trivial

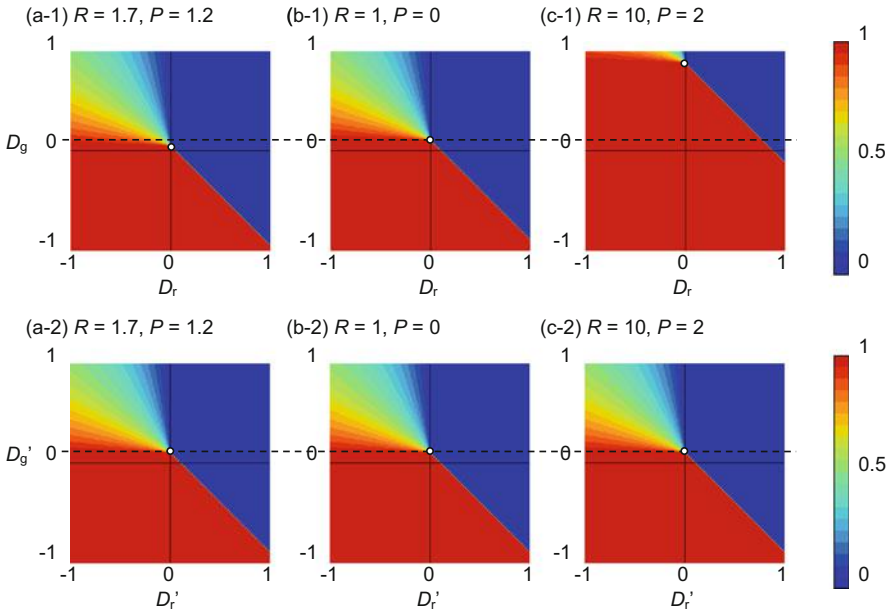

Fig. 2.18 Equilibrium cooperation fraction-$D_r - D_g$ (in the *upper line*) and $D_r' - D_g'$ (in the *lower line*) diagrams of indirect reciprocity for (**a**) $R = 1.7$, $P = 1.2$, (**b**) $R = 1$, $P = 0$, and (**c**) $R = 10$, $P = 2$ with probability of knowing the reputation of another individual $q = 0.1$

in the third quadrant, and SH in the fourth quadrant) shift to the positive side of the D_g-axis (D_g'-axis) (depicted by the black dotted line). Shifting upward implies that the weaker region of PD changes to SH, which has a bi-stable equilibrium. In short, direct and indirect reciprocities can weaken GID ($D_g = T - R$ or $D_g' = (T - R)/(R - P)$). Further, through the effects of kin selection, group selection, and network reciprocity, the four original game-classes simultaneously shift to the positive side of both the D_g-axis (D_g'-axis) and D_r-axis (D_r'-axis). Shifting upper-right along the $D_g' = D_r'$ line means that a weaker region of PD changes to either Chicken SH, or even Trivial, as confirmed on the $D_g' - D_r'$ diagram. Thus, kin selection, group selection, and network reciprocity can weaken both GID and RAD.

In the $D_g - D_r$ diagrams of Figs. 2.17, 2.18, 2.19, 2.20, and 2.21, (upper panels), the larger $R - P$ becomes, the larger upward shifting can be observed. In the $D_g' - D_r'$ diagrams of Figs. 2.17, 2.18, 2.19, 2.20, and 2.21, (lower panels), however, the upward shifting is irrespective to $R - P$. Surprisingly, respective equilibriums on the $D_g' - D_r'$ diagrams are completely consistent with each other, despite different $R - P$. Therefore a set of parameters, D_g' and D_r', that considers D_g and D_r as well as $R - P$, can be universally appropriate for evaluating dilemma strength in a population with any reciprocity mechanisms.

Concerning kin selection (Fig. 2.19), we can observe the interesting phenomenon of where the cooperation fraction increases with the increase of both D_g' and D_r' (see the dotted box in Fig. 2.22(a)). Figure 2.22 shows equilibrium cooperation

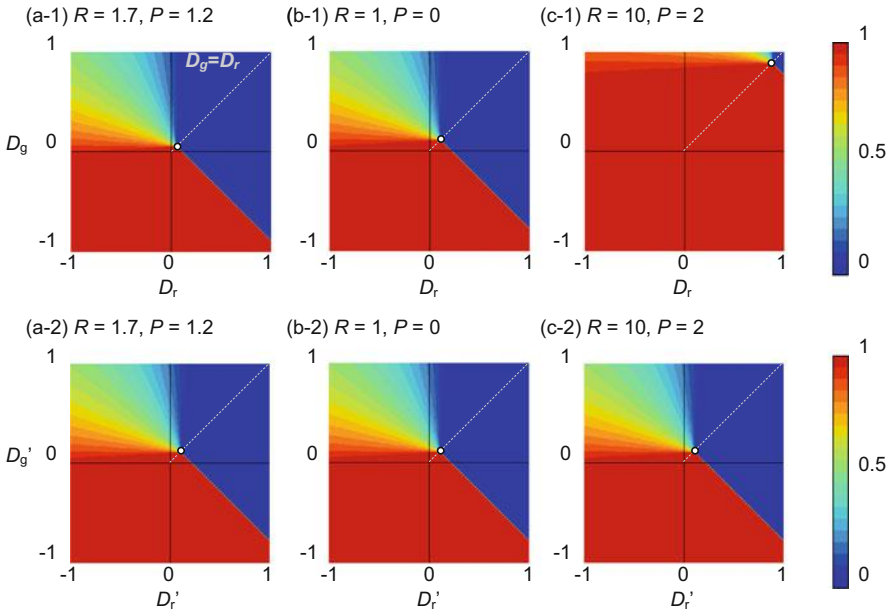

Fig. 2.19 Equilibrium cooperation fraction-$D_r - D_g$ (in the *upper line*) and $D_r' - D_g'$ (in the *lower line*) diagrams of kin selection for (**a**) $R = 1.7, P = 1.2$, (**b**) $R = 1, P = 0$, and (**c**) $R = 10, P = 2$ with the average relatedness between interacting individuals $r = 0.1$

when assuming $r = 0.3$. Figure 2.22(a) shows the $D_g' - D_r'$ diagram, and (b) shows the relationship between D_g' and the cooperation fraction when $D_r' = 0.46$. In a population with kin selection, the payoff of a focal agent is determined by a part of the opponent agent's payoff as described in Eq. (2.43). This creates evolutionary dynamics attracted by an internal (polymorphic) equilibrium in which both C and D agents co-exist, rather than an equilibrium consisting of only D agents, because the mutual dependency on payoff enables an agent to offer C instead of D even if increasing a risk to be exploited by opponent. It is possible in this situation that the total of S and the contribution from the opponent (i.e. rT) is much greater than $(1 + r)P$, and this possibility increases as r and T (D_g') become larger. The behavior explains the paradoxical situation, wherein more cooperative equilibrium can be attained under a larger D_g'. We can observe lots of proofs to back this interesting thing in real human societies. A parent is willing to support his/ her child, sometimes giving more and more to the child even if the parent eating nothing caused by a bleaker social dilemma situation than usual time, isn't he/ she? This phenomenon causes another paradoxical situation, wherein less cooperative equilibrium can be attained under smaller D_r'. We must note that this particular phenomenon has no relevance to what Németh and Takács (2010) reported about the possibility of the paradox of cooperation benefits when a population is featured with positive assortment. As we discuss in the text below, our new scaling parameters, D_g' and D_r', demonstrate that their finding is not paradoxical whatsoever.

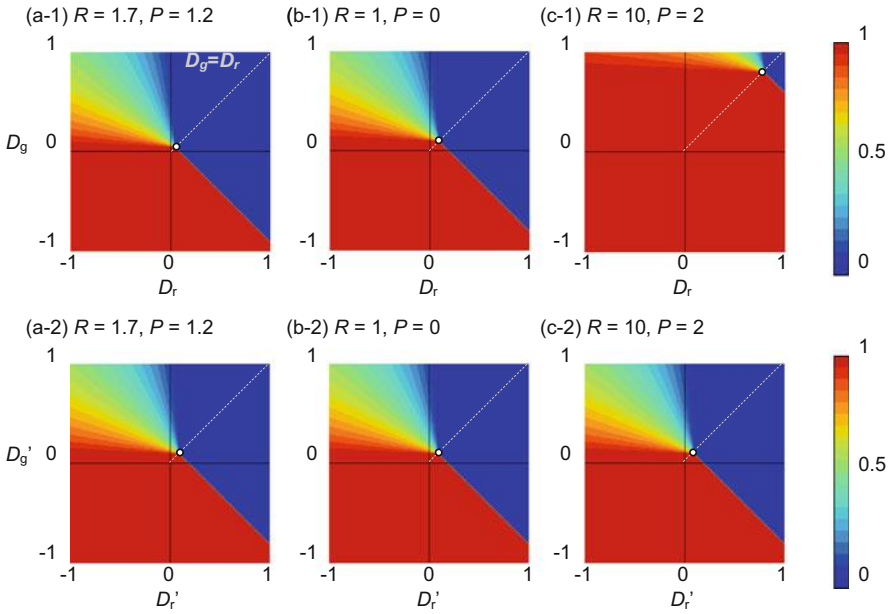

Fig. 2.20 Equilibrium cooperation fraction-$D_r - D_g$ (in the *upper line*) and $D_r' - D_g'$ (in the *lower line*) diagrams of group selection for (**a**) $R = 1.7$, $P = 1.2$, (**b**) $R = 1$, $P = 0$, and (**c**) $R = 10$, $P = 2$ with the number of groups $m = 50$ and maximum size of group $n = 500$

Theoretical Consistency for Finite Well-Mixed Population

Even a well-mixed population should be considered for the influence of social viscosity when the population in not infinite but finite. Although being a finite, well-mixed population is not one of Nowak's five reciprocity mechanisms, "finiteness" allows the possibility of repeated encounters between two agents. Because of a finite population, we cannot apply replicator dynamics. In this situation, we should discuss the so-called fixation probability, i.e., whether a selection favors the mutant's strategy over the resident's strategy (Nowak et al. 2004). Let us denote finite population size as N. If the fixation probability of C (D) is greater than $1/N$, then the selection favors C (D), which implies that the resident D (C) population would be replaced by a single mutant C (D) in the long term. Let us consider a Moran process with frequency dependent fitness. At each round, an individual is chosen for reproduction proportional to its fitness. One identical offspring is produced that replaces another randomly chosen individual. The fixation probability of C (D), ρ_C (ρ_D), is given by the probability that a single C (D) player in a population of $N-1$ D (C) agents generates a lineage of C (D) that does not become extinct, but rather takes over the entire population. When assuming weak selection ($\omega << 1$) both ρ_C and ρ_D are given as follows.

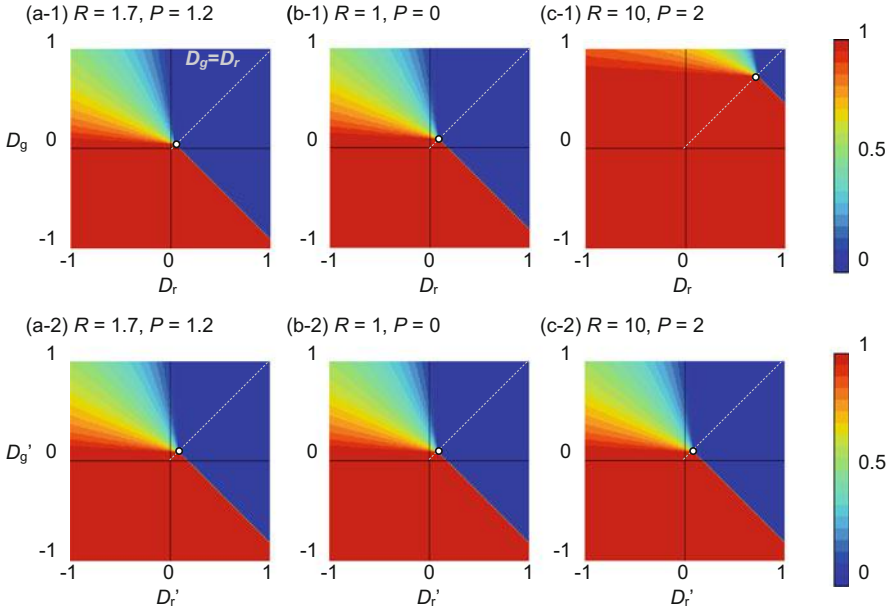

Fig. 2.21 Equilibrium cooperation fraction-$D_r - D_g$ (in the *upper line*) and $D_r' - D_g'$ (in the *lower line*) diagrams of network reciprocity for (**a**) $R = 1.7$, $P = 1.2$, (**b**) $R = 1$, $P = 0$, and (**c**) $R = 10$, $P = 2$ with the number of neighbors $k = 12$

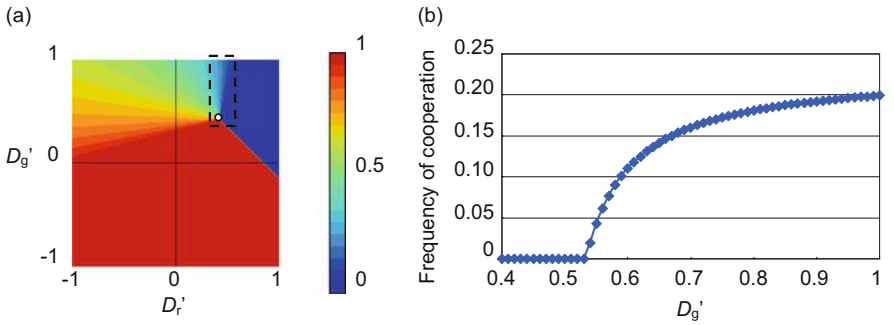

Fig. 2.22 Equilibrium cooperation fraction within the limits of (**a**) $-1 \leq D_g' \leq 1$ and $-1 \leq D_r' \leq 1$ and (**b**) $0.4 \leq D_g' \leq 1$ and $D_r' = 0.46$ (highlighted areas within *dashed-line boxes*) with the average relatedness between interacting individuals $r = 0.3$

$$\rho_C \approx \frac{1}{NN - (\alpha_C N - \beta_C)w/6}, \quad \rho_D \approx \frac{1}{NN - (\alpha_D N - \beta_D)w/6}. \tag{2.47}$$

Here, $\alpha_C = R + 2S - T - 2P$, $\alpha_D = P + 2T - S - 2R$, $\beta_C = 2R + S + T - 4P$, and $\beta_D = 2P + T + S - 4R$. If $\rho_C > 1/N$ ($\rho_D > 1/N$) is satisfied, then the selection favors C (D) replacing D (C). These conditions are as follows:

$$\rho_{\mathrm{C}} > 1/N \Leftrightarrow D_g(N+1) + D_r(2N-1) + 3(R-P) < 0, \tag{2.48-1}$$

$$\rho_{\mathrm{D}} > 1/N \Leftrightarrow D_r(N+1) + D_g(2N-1) + 3(R-P) > 0. \tag{2.48-2}$$

To describe this condition in relation with the game structure, say the dilemma strength, one needs not only D_g and D_r, but also R and P. This indicates that the set of parameters, D_g and D_r is not appropriate for evaluating the process. However, adopting $D_g{}'$ and $D_r{}'$ instead of D_g and D_r, we can transform inequalities (2.48-1) and (2.48-2) into the following:

$$\rho_{\mathrm{C}} > 1/N \Leftrightarrow D_g{}'(N+1) + D_r{}'(2N-1) + 3 < 0, \tag{2.49-1}$$

$$\rho_{\mathrm{D}} > 1/N \Leftrightarrow D_r{}'(N+1) + D_g{}'(2N-1) + 3 > 0. \tag{2.49-2}$$

Now, we can say that the fixation probabilities can be described by only $D_g{}'$ and $D_r{}'$ as inequality (2.49-1), (2.49-2).

When dilemma strength becomes weaker by increasing $R-P$, the selection favors D rather than C strategy because inequality (2.48-2) tends to be easily satisfied, but the opposite is true for inequality (2.48-1). Although this fact seems paradoxical at the first glance, it can be justified when we recall that the fixation probability intrinsically means the probability that a mutant can take over the entire population. In an Avatamasaka game (Akiyama and Aruka 2004), wherein $R-P$ is very large, a focal player's gain becomes irrelevant to his own offer. Instead, it is affected more by whether her opponent offers C or D. Thus, as $R-P$ becomes greater, it is more difficult for a single C player, in a population of $N-1$, and D agents to take over the entire population, and the reverse situation becomes more easily achieved.

Is There a Real Paradox?

In this sub-ion, we discuss the paradox reported by Németh and Takács (2010). We introduce their model and discuss why they call it a paradox. Further, we prove that the paradox is not paradoxical by applying the scaling parameters, $D_g{}'$ and $D_r{}'$.

Populations with a Positive Assortment Model

Let us consider a population wherein the interaction probability of an individual playing a game with another individual having the same strategy is greater than the focal agent's strategy fraction, which is called an assortative population (Németh and Takács 2010). The interaction probability of two individuals of the same strategy is denoted by α (If $\alpha = 1$, then an individual interacts with only same strategy opponents, and if $\alpha = 0$, then an individual interacts with randomly chosen individuals.) The average fitness of Cooperators, f_{C}, and Defectors, f_{D}, are given as follows:

$$f_{\mathrm{C}} = \alpha R + (1-\alpha)[xR + (1-x)S], \tag{2.50-1}$$
$$f_{\mathrm{D}} = \alpha P + (1-\alpha)[xT + (1-x)P]. \tag{2.50-2}$$

From the Price equation (Price 1970), the conditions in which C (D) becomes ESS, the internal equilibrium can be given as

$$\alpha(T-P) > T-R. \tag{2.51-1}$$
$$\alpha(R-S) < P-S. \tag{2.52-1}$$
$$x^* = \frac{P-\alpha R-(1-\alpha)S}{(1-\alpha)(R+P-S-T)}. \tag{2.53-1}$$

The internal equilibrium x^* is stable (sinks) and exists in the region [0, 1], if $R-S<T-P$ and $(P-S)/(R-S)<(T-R)/(T-P)$. It is unstable (source) and exists in the region [0, 1], if $R-S>T-P$ and $(P-S)/(R-S)>(T-R)/(T-P)$. Inequalities (2.51-1) and (2.52-1) and Eq. (2.53-1) can be described as follows by applying $D_g{}'$ and $D_r{}'$:

$$\alpha\left(1+D_g{}'\right) > D_g{}', \tag{2.51-2}$$
$$\alpha(1+D_r{}') < D_r{}', \tag{2.52-2}$$
$$x^* = \frac{(1-\alpha)D_r{}'-\alpha}{(1-\alpha)\left(D_r{}'-D_g{}'\right)}. \tag{2.53-2}$$

The internal equilibrium x^* is stable and exists in the region [0, 1], if $D_r{}' < D_g{}'$ and $D_r{}' < \alpha/(1-\alpha) < D_g{}'$. It is unstable and exists in the region [0, 1], if $D_r{}' > D_g{}'$ and $D_r{}' > \alpha/(1-\alpha) > D_g{}'$. Thus, the condition of ESS (inequalities (2.51-1) and (2.52-1)) and the internal equilibrium (Eq. (2.53-1)) can be described by only $D_g{}'$, $D_r{}'$, and α.

The Paradox of Cooperation Benefits by Németh and Takács

In the model, mentioned above, Németh and Takács (2010) insisted that a paradox may occur when two or more payoff elements among P, R, S, and T are modified.

Let us consider PD in which $T>R>P>S$ is satisfied. When assuming two equations derived from inequality (2.51-1) and (2.52-1), i.e.,

$$\alpha_{\mathrm{L}} = (P-S)/(R-S) \text{ and} \tag{2.54-1}$$
$$\alpha_{\mathrm{H}} = (T-R)/(T-P), \tag{2.55-1}$$

we note that the conditions in which C and D become ESS are $\alpha_{\mathrm{H}} < \alpha$ and $\alpha_{\mathrm{L}} > \alpha$, respectively. Figure 2.23 shows equilibrium curves (1) with keeping payoff structure and increasing α from 0 to 1. When $R-S<T-P$, the equilibrium point is

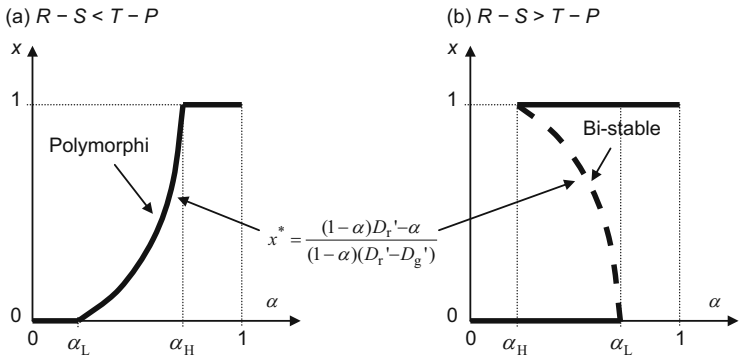

Fig. 2.23 Equilibrium cooperation fraction as a function of α in PD with positive assortment, if (**a**) $R-S<T-P$ and (**b**) $R-S>T-P$. The *dashed line* indicates the unstable internal equilibrium point x^*

$x=0$ for $0<\alpha<\alpha_L$; internal equilibrium x^* (Eqs. (2.53-1 and 2.53-2)) for $\alpha_L<\alpha<\alpha_H$; and $x=1$ for $\alpha_L<\alpha<1$ (Fig. 2.23(a)). However, when $R-S>T-P$, the equilibrium point is $x=0$ for $0<\alpha<\alpha_H$; $x=0$ or $x=1$ for $\alpha_H<\alpha<\alpha_L$ and $x=1$ for $\alpha_L<\alpha<1$ (Fig. 2.23(b)).

Here, let us consider *Game A1*, wherein $T=7$, $R=3$, $P=1$, and $S=0$, and *Game B1*, where $T=21$, $R=5$, $P=1$, and $S=0$ for the sake of discussion. Comparing those two examples, we should note that $\Delta R=2$ and $\Delta T=14$. Both games have stable internal equilibria x^* as shown in Fig. 2.23(a) because they satisfy $R-S<T-P$. When we apply D_g and D_r as scaling parameters (not D_g' and D_r'), $0<\Delta R<\Delta T$ means that the incentive for offering D in *Game B1* is larger than that in *Game A1* because D_g increases. Thus, the equilibrium point of *Game B1* seems to be lower than that of *Game A1*. However, within a certain range of positive assortment, α, the paradox can occur, i.e., cooperation growing despite D_g increasing ($0<\Delta R<\Delta T$). Noting that $\alpha_{H\_GameA1}<\alpha_{H\_GameB1}$ and $\alpha_{L\_GameA1}>\alpha_{L\_GameB1}$ are satisfied, we can draw equilibria of these two games as shown in Fig. 2.24. From Fig. 2.24, one could say that a paradox exists because there is the region where the cooperation fraction of *Game B1* is greater than that of *Game A1*. This phenomenon can occur in each combination of any two parameters among P, R, S, and T. Németh and Takács see this phenomenon as paradoxical.

In the next sub-section, we demonstrate that their paradox is, in fact, never a paradox by applying the proposed scaling parameters, D_g' and D_r'.

Explanation of the Paradox of Cooperation Benefits by Applying D_g' and D_r'

If $0<\Delta R<\Delta T$, D_g increases. In contrast, there exists the possibility that D_g' decreases. In addition, D_r' must always decrease. In fact, differences in D_g, D_r, D_g', and D_r' between *Game A1* and *Game B1* are $\Delta D_g=12$, $\Delta D_r=0$, $\Delta D_g'=2$, and $\Delta D_r'=-1/4$, respectively. Because D_g' is defined by GID divided (scaled) with

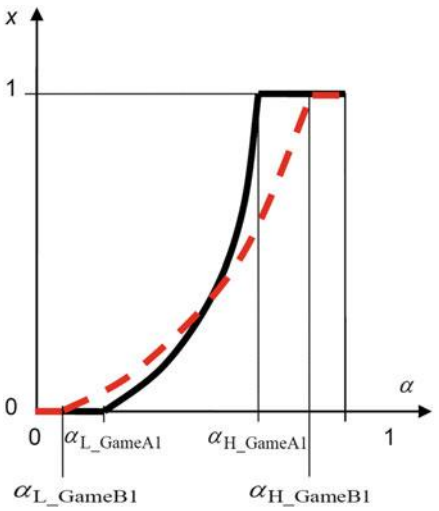

Fig. 2.24 The paradox of cooperation benefits in PD with positive assortment reported by Németh and Takács (2010) in *Game A1*, in which $T = 7$, $R = 3$, $P = 1$, $S = 0$ (*black solid line*) and *Game B1*, in which $T = 21$, $R = 5$, $P = 1$, $S = 0$ (*red dashed line*)

$R - P$ and D_r' is defined by RAD scaled with $R - P$, those two intrinsically imply different dilemma strengths. Therefore, it makes no sense to compare ΔD_g with $\Delta D_r'$. Thus, $\Delta D_g' > 0 > \Delta D_r'$ and $|\Delta D_g'| > |\Delta D_r'|$ does not imply that the cooperation fraction at an equilibrium decreases. Finally, we cannot say that dilemma strength always increases when $0 < \Delta R < \Delta T$, as Németh and Takács assert. Therefore, increasing the equilibrium cooperation fraction in such a case is not paradoxical. This argument is true for any combinations of two payoff elements other than R and T.

Let us confirm that a paradox never occurs when applying the proposed scaling parameters. First, we discuss the equilibrium on the basis of Eqs. (2.51-2), (2.52-2) and (2.53-2). Equations (2.54-1) and (2.55-1) can be described as follows by applying D_g' and D_r', respectively:

$$\alpha_{\mathrm{L}} = D_r'/(1 + D_r'), \tag{2.54-2}$$

$$\alpha_{\mathrm{H}} = D_g'/(1 + D_g'). \tag{2.55-2}$$

Here, we limit our discussion comparing *Game A2* and *Game B2*, wherein D_g' and D_r' of *Game B2* are simultaneously larger than those of *Game A2*; i.e., $D_{g\_\mathrm{GameA2}}' \leq D_{g\_\mathrm{GameB2}}'$ and $D_{r\_\mathrm{GameA2}}' \leq D_{r\_\mathrm{GameB2}}'$. Unlike *Game A1* and *Game B1*, we can argue the following without presuming concrete T, R, P, and S. From Eqs. (2.54-2) and (2.55-2), whenever $D_r' > -1$ and $D_g' > -1$, it is obvious that $\alpha_{\mathrm{L\_GameA2}} \leq \alpha_{\mathrm{L\_GameB2}}$ and $\alpha_{\mathrm{H\_GameA2}} \leq \alpha_{\mathrm{H\_GameB2}}$. Figure 2.25 shows equilibrium curves when (a) $D_r' < D_g'$, wherein internal equilibrium x^* is stable (polymorphic) and (b) $D_r' > D_g'$, wherein x^* is unstable (bi-stable). It is notable that the equilibrium cooperation fraction in games having greater dilemma strength (*Game B2*; red dashed line) is always lower than the black line (*Game A2*) whenever the same α is

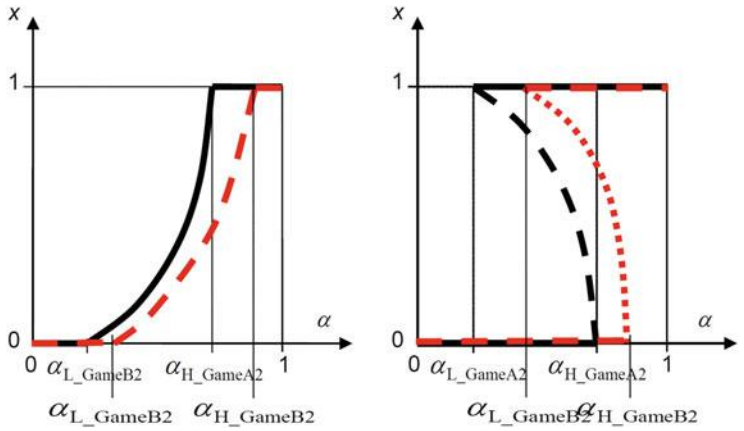

Fig. 2.25 Equilibrium cooperation fraction as a function of α in PD with positive assortment in (**a**) $D_r' < D_g'$ and (**b**) $D_r' > D_g'$ for comparison between *Games A2 and B2*. The strength for *Game B2's* dilemma is higher than that of *Game A2*. The *black solid line* and the *black dashed line* indicate stable equilibrium points and unstable equilibrium points, respectively, for *Game A2*. The *red dashed line* and the *red dotted line* indicate stable equilibrium points and unstable equilibrium points, respectively, for *Game B2*. The paradox of cooperation benefits never occurs

assumed. Thus, no paradox ever occurs. Even if $D_g' \leq -1$ or $D_r' \leq -1$, we deduce that no paradox ever occurs.

In summary, from the viewpoint of Németh and Takács's paradox, we can prove that the proposed parameters, D_g' and D_r', are appropriate as universal scaling parameters to evaluate dilemma strength.

2.7.3 Simulation Approach

Although we will elaborate network reciprocity in the next Chapter, it is one of the Nowak's five social viscosity mechanisms, which has been already discussed around Eq. (2.45). To this point the discussion concerning network reciprocity assumes that an underlying network must be regular and strategy updating must follow the Death-Birth (DB)[31] process, as required by the analytic approach. In this section, we discuss whether the set of D_g' and D_r' is appropriate as universal scaling parameters for various situations through a series of numerical simulations.

Simulation Setting

In this discussion, we limit the game class to be observed to PD, wherein $0 \leq D_g \leq 1$ and $0 \leq D_r \leq 1$ or $0 \leq D_g' \leq 1$ and $0 \leq D_r' \leq 1$ for various $R - P$. We assume

specially structured agents on a network. Because we confirmed that the equilibrium has no sensitivity to the number of agents when considering a sufficiently large number ($N > 1600$) (Yamauchi et al. 2011), we assumed $N = 4900$. The average degree $< k >$ is assumed to be 8. We investigate four types of network structures: (i) lattice; (ii) homogeneous small world network, (hereafter Ho-SW), generated from a cycle graph by replacing several links with random shortcuts (a shortcut probability of 0.2) strictly enforcing the condition that every vertex has the same degree; (iii) Watts–Strogatz's (1998) heterogeneous small world network (hereafter He-SW), which is generated from a cycle graph with swapping probability 0.2 (Ren et al. 2007) such that every vertex may have different degrees; (iv) scale-free network (hereafter SF) based on the Barabasi–Albert algorithm (Barabasi and Albert 1999) In every round, an agent plays with her neighbors and accumulates payoffs resulting from games played with all neighbors in that round.

An agent synchronously updates her strategy in every round on the basis of the accumulated payoffs with all neighbors during each round. In this study, we adopt four strategy updating rules.

(i) Imitation Max (hereafter IM): A focal player imitates the strategy having the largest payoff among all the strategies adopted by the focal player and her immediate neighbors.

(ii) Fermi-PW (hereafter F-PW): A focal player i adopts a randomly chosen player j's strategy with the probability calculated using the Fermi function. A F-PW process determines the probability of her imitating the strategy, depending on differences in payoff:

$$W_{s_i \leftarrow s_j} = \frac{1}{1 + \exp\left[\left(\Pi_i - \Pi_j\right)/\kappa\right]}. \tag{2.56}$$

Here, Π_i and s_i indicate the accumulated payoff and strategy, respectively, of the ith (focal) agent. The parameter κ in the Fermi function is set to 0.2.

(iii) Linear-PW (hereafter L-PW): The strategy of a player j is chosen as in Fermi-PW, but the probability is given by a linear function and operates as follows:

$$W_{s_i \leftarrow s_j} = \frac{\Pi_j - \Pi_i}{\max\left(k_i, k_j\right)\left[\max(R, T, S, P) - \min(R, T, S, P)\right]}. \tag{2.57}$$

Here, k_i indicates the degree of the ith (focal) agent.

(iv) Roulette (hereafter RS): A focal player chooses one among the strategies adopted by the focal player and her immediate neighbors with a probability proportional to the payoff and operates as follows:

$$W_{S_j \leftarrow S_i} = \frac{\Pi_j - \min_{k \in N_i} [\Pi_k]}{\sum_{j \in \{N_i\}} \left(\Pi_j - \min_{k \in N_i} [\Pi_k] \right)}, \tag{2.58}$$

where $\{N_i\}$ indicates the set of neighbors for the focal agent i and himself. When all agents of $\{N_i\}$ happen to have an exactly same payoff, a focal player randomly chooses one of agents of $\{N_i\}$ to copy with a probability as follows:

$$W_{S_j \leftarrow S_i} = \frac{1}{k_i + 1}. \tag{2.59}$$

The initial fraction of C, imposed at the beginning of every simulation round, is assumed to be 0.5. A single simulation round continues until the time variations of the average social cooperation fraction and the payoff are sufficiently small to equal an asymptotic equilibrium. If the frequency of cooperation continues to fluctuate, we calculate the average cooperation for the last 100 generations over a 10,000-generation run. We conduct this procedure at 11×11 points on the PD area ($0 \leq D_g \leq 1,\ 0 \leq D_r \leq 1$ or $0 \leq D_g{}' \leq 1,\ 0 \leq D_r \leq 1$) 100 times to draw an ensemble average at each point.

Results

Figures 2.26, 2.27, 2.28, and 2.29 show results on lattice and Ho-SW, which are regular networks and the equilibrium cooperation fraction on $D_g - D_r$ diagrams and $D_g{}' - D_r{}'$ diagrams. Although we can see $D_g - D_r$ diagrams for the IM in Fig. 2.15, we describe these again in Fig. 2.26(a) to make it easier to compare. As mentioned in the previous section, although results on the $D_g - D_r$ diagram are significantly affected by the value of $R - P$, those on the $D_g{}'$ and $D_r{}'$ diagram never depend on $R - P$, with the exception of the result for F-PW. Thus, the set of D_g and D_r does not provide appropriate scaling parameters, whereas $D_g{}'$ and $D_r{}'$ perform much better.

Again, for F-PW, we cannot see universal contour areas consistent with each other for different $R - P$ even when applying $D_g{}'$ and $D_r{}'$ as scaling parameters. This occurs because, unlike other rules, F-PW uses the parameter κ, indicating intensity of selection. Increasing $R - P$ leads to larger payoff differences among agents, which inevitably entails increased intensity of selection. Therefore, the set of $D_g{}'$ and $D_r{}'$ seems insufficient as universal scaling parameters. To compensate for this shortcoming, one reasonable solution is to scale the intensity of selection in F-PW with $R - P$; i.e., we should apply $\kappa' = \kappa(R - P)$ instead of κ; Fig. 2.30 shows the result. We obtained a universal equilibrium cooperation fraction, irrespective of $R - P$. A plausible question might arise here: why does the scaling by $D_g{}'$ and $D_r{}'$ look good for L-PW and RS, even though the copying probabilities of L-PW and RS depend on payoff differences as does F-PW? As shown in Eqs. (2.57) and (2.58) contain terms to scale the payoff difference, $[\max(R, T, S, P) - \min(R, T, S, P)]$ for

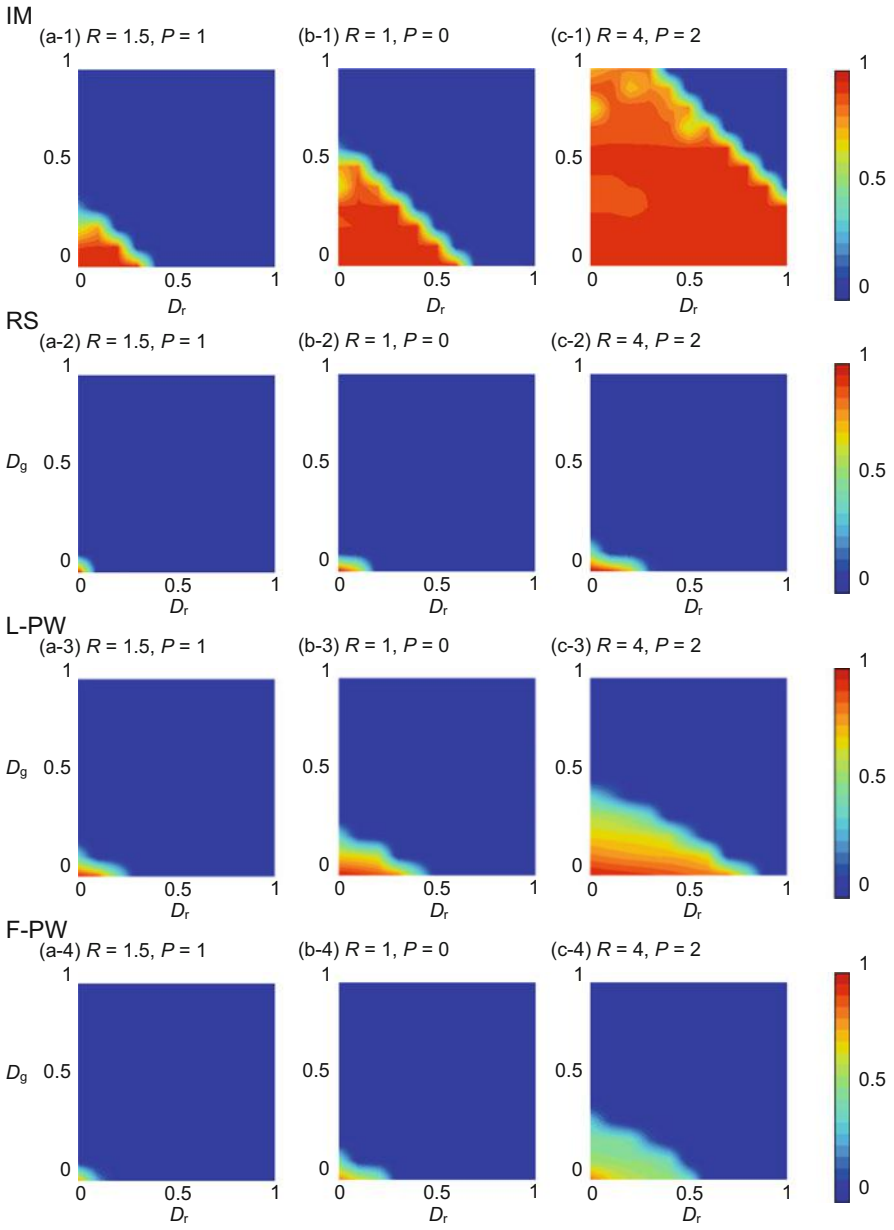

Fig. 2.26 Averaged cooperation fraction-$D_r - D_g$ diagrams for (**a**) $R = 1.5$, $P = 1$, (**b**) $R = 1$, $P = 0$, and (**c**) $R = 4$, $P = 2$. Games are played on 8-neighbor lattice. IM (in the *first line*), RS (in the *second line*), L-PW (in the *third line*) and F-PW (in the *last line*) are adopted as the strategy update rule. For results in case of IM, see Fig. 2.15

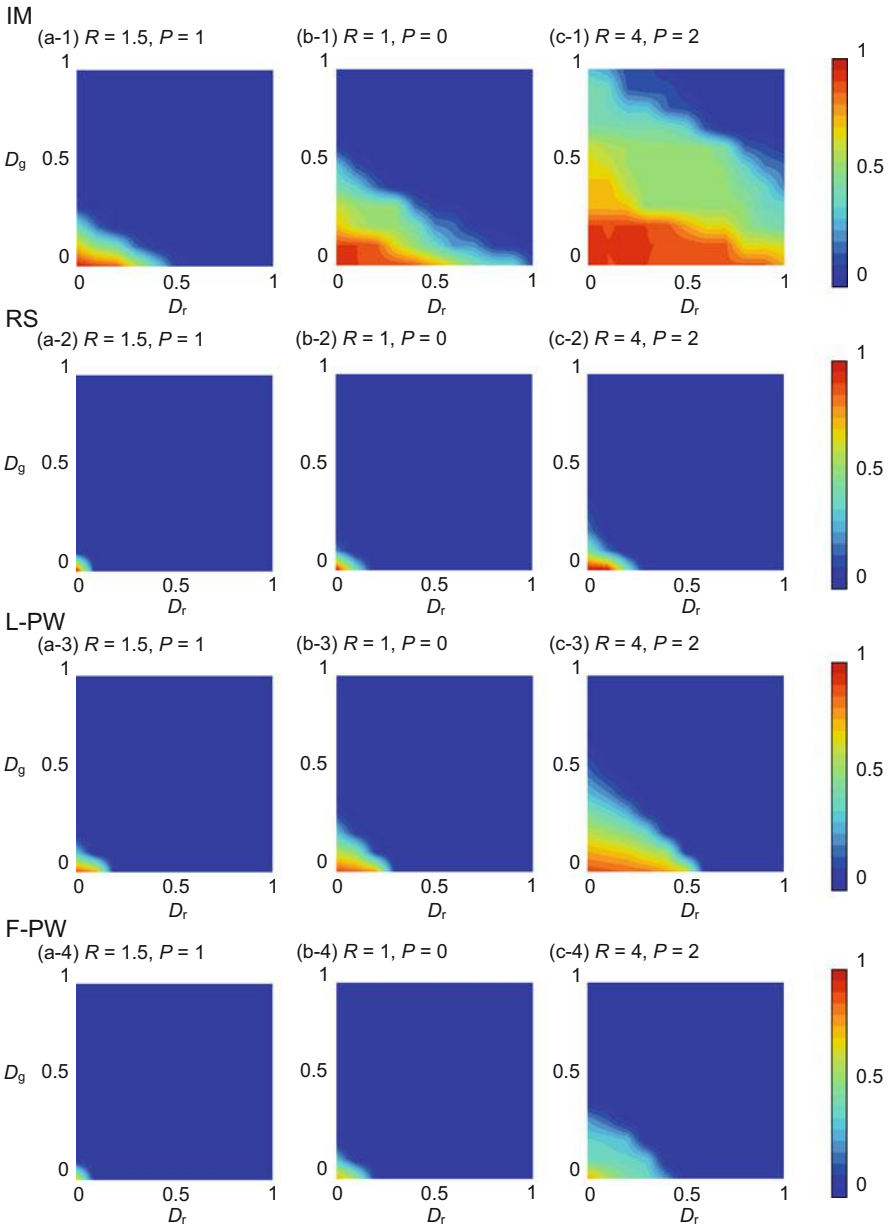

Fig. 2.27 Averaged cooperation fraction-$D_r - D_g$ diagrams for (**a**) $R = 1.5$, $P = 1$, (**b**) $R = 1$, $P = 0$, and (**c**) $R = 4$, $P = 2$. Games are played on 8-neighbor Ho-SW. IM (in the *first line*), RS (in the *second line*), L-PW (in the *third line*), and F-PW (in the *last line*) are adopted as the strategy update rule

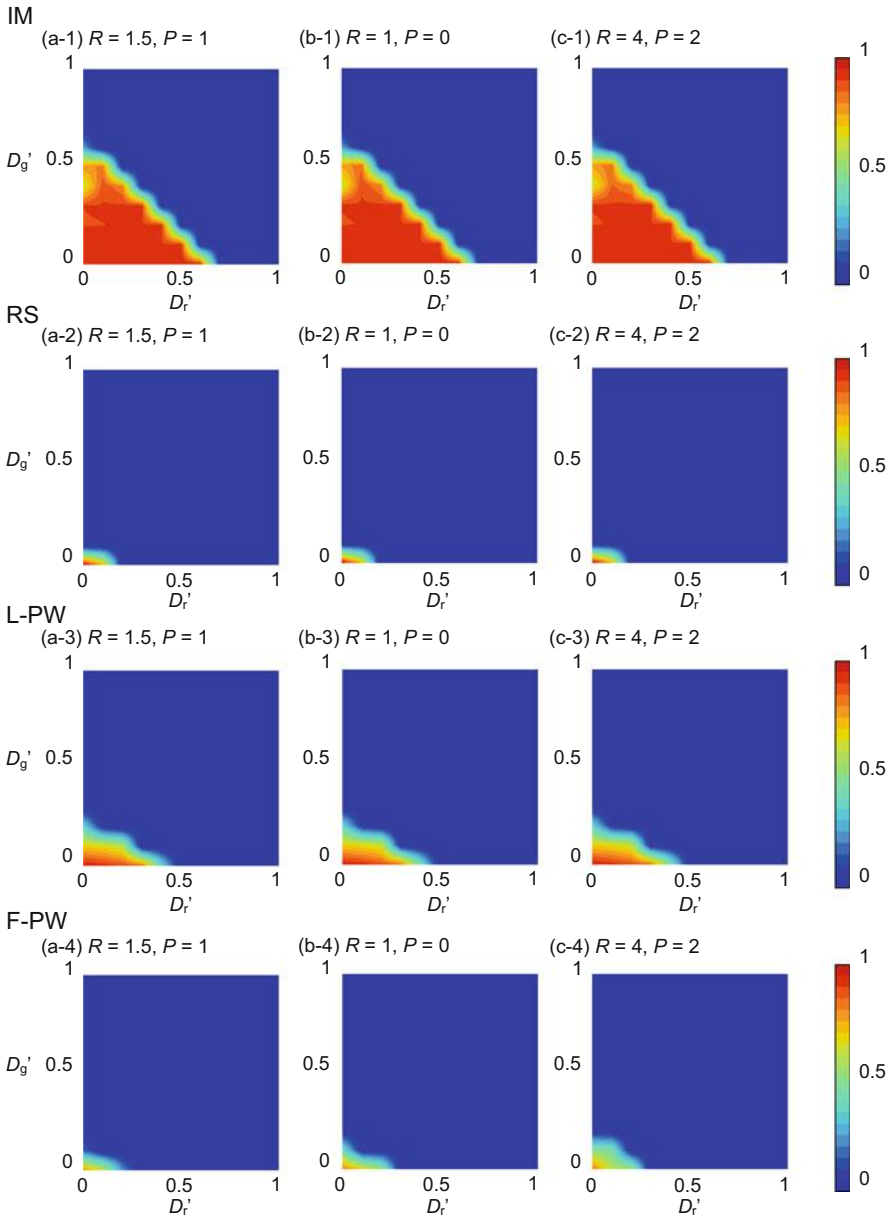

Fig. 2.28 Averaged cooperation fraction-$D_r' - D_g'$ diagrams for (**a**) $R = 1.5$, $P = 1$, (**b**) $R = 1$, $P = 0$, and (**c**) $R = 4$, $P = 2$. Games are played on 8-neighbor lattice. IM (in the *first line*), RS (in the *second line*), L-PW (in the *third line*), and F-PW (in the *last line*) are adopted as the strategy update rule

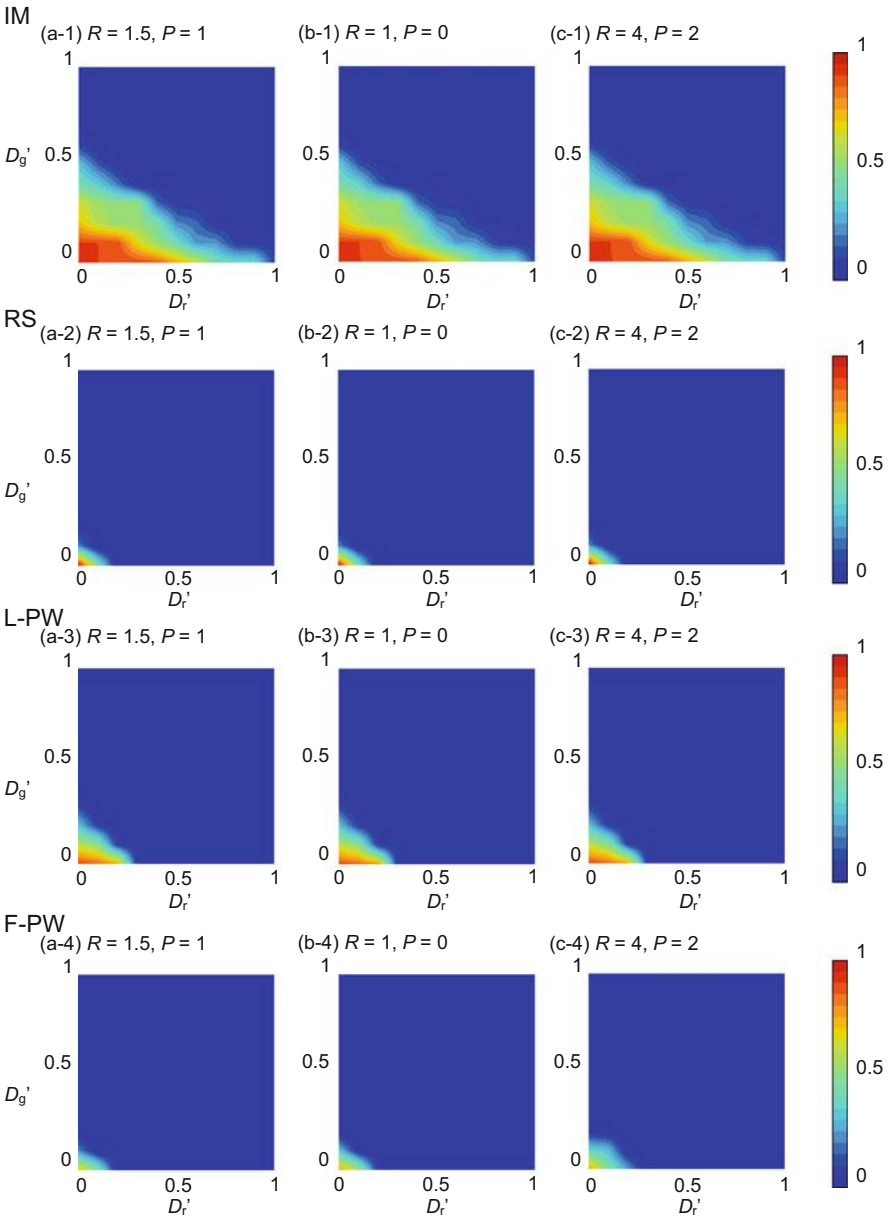

Fig. 2.29 Averaged cooperation fraction-$D_r' - D_g'$ diagrams for (**a**) $R = 1.5$, $P = 1$, (**b**) $R = 1$, $P = 0$, and (**c**) $R = 4$, $P = 2$. Games are played on 8-neighbor Ho-SW. IM (in the *first line*), RS (in the *second line*), L-PW (in the *third line*), and F-PW (in the *last line*) are adopted as the strategy update rule

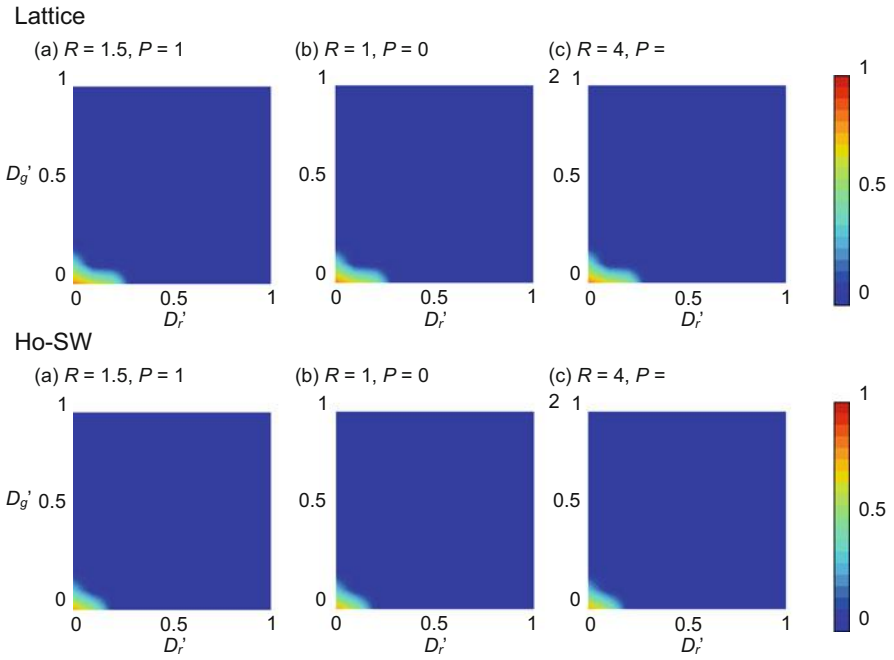

Fig. 2.30 Averaged cooperation fraction-$D_r' - D_g'$ diagrams for (**a**) $R = 1.5$, $P = 1$, (**b**) $R = 1$, $P = 0$, and (**c**) $R = 4$, $P = 2$. Games are played on 8-neighbor lattice (in the *upper line*) and Ho-SW (in the *lower line*). F-PW, of which intensity of selection is scaled by $R - P$, is adopted as the strategy update rule

L-PW and $\sum_{j \in N_i} \left(\Pi_j - \min_{k \in N_i} [\Pi_k] \right)$ for RS., those terms depend on value of $R - P$. As a result, it is possible to capture uniform contours irrespective of $R - P$ in the two update rules.

Next, let us discuss He-SW and SF, which are both degree-heterogeneous networks. Figures 2.31 and 2.32 show contours of the equilibrium cooperation fraction on the $D_g - D_r$ diagram and the $D_g' - D_r'$ diagram. For simplicity in this discussion, we limit IM as an updating rule (which we confirmed to draw qualitatively the same conclusion as below, even though other updating rules are assumed). Both the sets of D_g and D_r and those of D_g' and D_r' do not operate appropriately as scaling parameters. This failure is particularly noticeable when assuming SF. This shortcoming might be justified by the fact that "in a degree-heterogeneous network for underlying topology, there is significant influence on payoff caused by the difference of the number of games played by agents depending on their degrees," as reported by Masuda (2007) and Tanimoto and Yamauchi (2010). Obviously, when the number of games differs depending on the degree of distribution, the dilemma strength affecting each agent must also differ. Therefore,

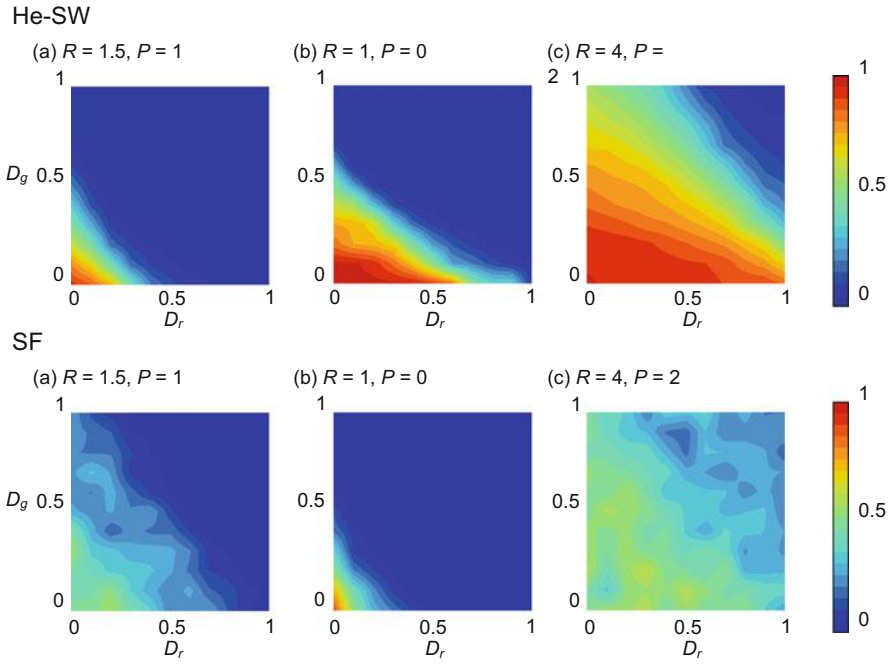

Fig. 2.31 Averaged cooperation fraction-$D_r - D_g$ diagrams for (**a**) $R = 1.5$, $P = 1$, (**b**) $R = 1$, $P = 0$, and (**c**) $R = 4$, $P = 2$. Games are played on He-SW (in the *upper line*) and SF (in the *lower line*) with the average degree $< k > = 8$. IM is adopted as the strategy update rule

scaling by $D_g{}'$ and $D_r{}'$, i.e., considering only the effect of dilemma per one game, is insufficient.

In summary, we have confirmed that the universal scaling concept by $D_g{}'$ and $D_r{}'$ reasonably works well even if various strategy update rules are assumed. In assuming degree-heterogeneous networks instead of regular topology, the scaling concept malfunctions, because different number of playing games among agents that a degree-heterogeneous networks intrinsically allows significantly affects on its evolutionary process. Thus, underlying topology sometimes becomes more significant than influence resulting from game structure.

2.8 *R*-Reciprocity and *ST*-Reciprocity

Unequivocally, Prisoner's Dilemma (PD) is the most well-known archetype for dilemma games. From a biological viewpoint, the Chicken game is sometimes called a Hawk–Dove game (Maynard Smith 1982), which revolves around a pair of organisms competing for a resource and engaging in moderate fighting (C) or

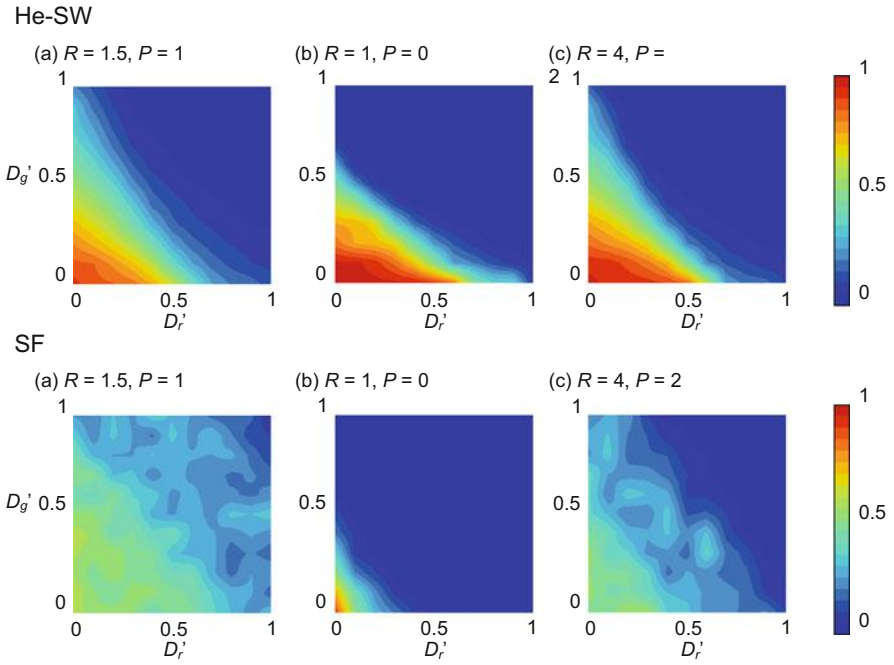

Fig. 2.32 Averaged cooperation fraction-$D_r' - D_g'$ diagrams for (**a**) $R = 1.5$, $P = 1$, (**b**) $R = 1$, $P = 0$, and (**c**) $R = 4$, $P = 2$. Games are played on He-SW (in the *upper line*) and SF (in the *lower line*) with the average degree $< k > = 8$. IM is adopted as the strategy update rule

defecting through escalated fighting (D).[16] The Leader game may occur in nature when two organisms need to escape from a predator via an escape route through which only one can pass at a time. Each player can choose either to escape before the other player (D) or wait for the other player to escape with the intention of following immediately after (C). The Hero game, sometimes called Battle of Sexes, was introduced by Luce and Raiffa (1957). A typical biological application might occur if two predators feeding on a kill are being harassed by scavengers (Browning and Colman 2004). Obviously, although we continue to use the symbols C and D for convenience, the terms cooperation and defection are hardly applicable to this game. Each predator can either ignore the scavengers (C), or temporarily abandon the prey to chase the scavengers (D). The best payoff for a player results from ignoring the scavengers and continuing to feed while the co-player chases the scavengers (S). The second best option is for a player to stop feeding in order to chase the scavengers, losing a little feeding time (T). The third best for each player is that both ignore the scavengers and therefore lose some of the prey (R). The worst

[16] Also, multi-player Chicken game is sometimes used as a template for the discussion on environmental problems like Hardin's tragedy of commons (Hardin 1968) as mentioned before.

option is that both players simultaneously abandon the prey to chase the scavengers, since they run the risk of losing the whole prey (P).

A set of Chicken-type games satisfying $T+S>2R$, such as Leader and Hero, have a feature that is different from PD, where the mixing of S and T shared by focal and opposing players can get more payoff than mutual Cs (or R), which is the best cooperative solution in PD (***R* reciprocity**). This quite unique feature of getting a high payoff by sharing S and T is called Alternating Reciprocity (Browning and Colman 2004) or ***ST*-reciprocity**. In terms of direct reciprocity, *ST*-reciprocity seems to be as important as mutual cooperation in PD.

Crowley (2001) investigated *ST*-reciprocity in a series of numerical experiments, where agents possessing a 2-length memory (capable of memorizing previous focal and opposing actions) classifier system play generalized Hawk–Dove games. He assumes four fundamental strategies for the classifier system: (1) AllC, always offering C, (2) AllD, always offering D, (3) CAD, random responses initially, followed by coordinated alternating responses (S and T), and (4) DorC, random responses initially, followed by repeated responses of S or T. He confirmed that *ST*-reciprocity can be established by CAD or DorC classifiers in usual Hawk–Dove games. However, in games having strong dilemmas, the AllD classifier dominates the strategy space, eliminating CAD and DorC.

Browning and Colman (2004) also investigated *ST*-reciprocity by assuming 2×2 games with a 6-length memory strategy (memorizing three previous iterations of focal and opponent actions), where more effective *ST*-reciprocity can be observed in Leader and Hero games satisfying $T+S>2R$ than in Chicken games (which we should call pure Chicken to distinguish it from general Chicken games, which include Leader and Hero) not satisfying $T+S>2R$.

An important condition is that organized *ST*-reciprocity needs some asymmetric cooperation, because the two players must offer C or D differently, and this differs substantially from the PD situation. In fact, in the PD game, TFT (tit-for-tat) can create stable cooperation (R reciprocity) under certain conditions (e.g., disregarding error and noise effects). The TFT requires a 1-length memory that can only remember the previous action of his opponent. It seems, however, that 1-length memory cannot successfully produce *ST* reciprocity, since "alternating" reciprocity inevitably requires information on the previous actions of both the focal player and the opponent. Therefore, *ST* reciprocity requires 2-length memory, and 1-length memory is insufficient. Therefore, it is necessary to embed an agent's memory into a model to obtain efficient *ST* reciprocity. Of course, assuming a memory-free scenario, we could observe *ST* reciprocity to some extent, determined by the interior stationary equilibrium with co-existing C and D. However, this *ST* reciprocity is less efficient (and also, less intentional) than the memory entailing case discussed in the present paper.

The most important goal of this section is to decide whether there is a relationship between game structure (characterized by both the dilemma strength and the extent of $T+\mathrm{S}>2R$) and the emerging *ST* reciprocity phase. In other words, *ST* reciprocity has different phases depending upon a game's structure.

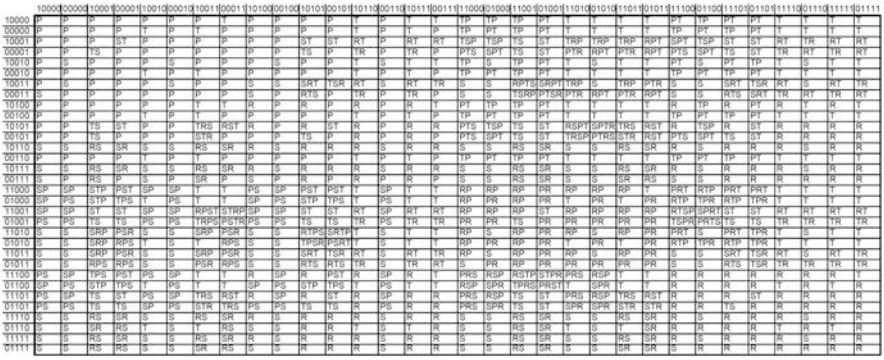

Fig. 2.33 *P*, *R*, *S*, *T* sequences of any two of 32 strategies

For our example, we made two assumptions: (1) a player has a 2-length memory strategy, and (2) the game has an infinite number of iterations. Due to the latter assumption, we can explicitly determine a 32×32 game structure matrix that expresses respective payoffs for any gaming pairs among $2^5 = 32$ strategies. Thus, an analytical approach is made possible by means of replicator dynamics.

We assumed that a player's strategy is defined by a 5-bit string like "11010". The first bit indicates the player's decision in favor of C (1) or D (0) at the beginning of a game sequence. Each subsequent bit indicates the player's decision in favor of C (1) or D (0) when the previous consequence is *P* (mutual defection), *R* (mutual cooperation), *S* (a focal and opponent offering C and D) or *T* (a focal and opponent offering D and C), respectively. According to the strategy description, TFT and PAVLOV are defined as "10101" and "11100," respectively. The total number of strategies is $2^5 = 32$. The idea of strategy depiction of the present model is basically the same as the Look-up Table, Finite State Machine (FSM).

Assuming that a game is infinitely iterated, we can predict a periodic steady state of game consequences for any pairs of 32 strategies, as shown in Fig. 2.33. Thus, the game structure matrix **M** must be defined by an element value divided by the period (for *RST* in Fig. 2.33, the element value is $(R+S+T)/3$). This particular simplification inevitably entails a certain error derived from transient influence. For example, in a game played with AllD and TFT, the assumed method indicates that both AllD and TFT get the same *P* on the ground of infinite mutual defection. And yet, the exact reality is that TFT can never defeat AllD, because TFT is exploited by AllD at the beginning of the session. In that sense, our assumption seems to be for a hypothetical game only. However, we thought the advantage coming from this particular assumption, allowing us to see an analytical picture by replicator dynamics, was much more important than this drawback.

Assuming the number of game players is sufficiently large (namely, infinite and well-mixed population), we can apply replicator dynamics to the game evolution as described in Eq. (2.35):

$$\frac{\dot{s}_i}{s_i} = \left[{}^T\mathbf{s_i} \cdot \mathbf{M}\,\mathbf{s} - {}^T\mathbf{s} \cdot \mathbf{M}\,\mathbf{s} \right]. \tag{2.60}$$

Both $\mathbf{s}_i$ and $\mathbf{s}$ indicate 32-row vectors. The former indicates the i-th strategy expressed as $\mathbf{s}_i \in S = \{(1\ \ 0\ \ \cdots\ \ 0), \cdots, (0\ \ \cdots\ \ 0\ \ 1)\}$. The latter is a strategy distribution at a certain time-step expressed by $\mathbf{s} = (s_1\ \ s_2\ \ \cdots\ \ s_{32})$. The superscript T indicates a transposition.

In general, the number of equilibriums of Eq. (2.60) is $\sum_{k=1}^{n} {}_nCk$, where n is the number of strategies. There are about 4.29×10^9 equilibria in this case ($n = 32$). Hence, a perfect analytical approach based on replicator dynamics is almost impossible.

Because of the difficulties of the perfectly analytical approach, we numerically obtain an equilibrium strategy distribution by means of a recurrence formula calculation for Eq. (2.60) and assuming initial distribution as $\mathbf{s} = (1/32\ \ \cdots\ \ 1/32)$. We confirm that the result is not very sensitive to the initial distribution, although the influence surely exists. The equilibrium strategy distribution based on the random initial distribution is almost consistent with the uniform case.

We varied the universal scaling parameters with $-5 \le D_g' \le 5$ and $-5 \le D_r' \le 5$. Although we take overview on the result we obtained as following, you can consult with Tanimoto and Sagara (2007b) if you are interested in more detailed result.

The result expressed in a for of $D_g' - D_r'$diagram is shown in Fig. 2.34, (b) relative payoff, defined by $([\text{payoff}] - R)/(R - P)$; (c) – (d) showing frequencies of mutual defection, R-reciprocity and ST-reciprocity, respectively. For comparison, (a) shows the relative payoff derived from the analytic solution where no-memory (only 1 bit; C or D) agents playing games in an infinite and well-mixed population, which is derived from the procedure explained in the previous sections.

What we have to address here, first of all after comparing Fig. 2.34(b) and (a), is that the social averaged payoff is never less than R in any games even with strong dilemmas composed of GID and RAD. This is because the 2-length memory acts to support mutual cooperation; R-reciprocity, which is consistent with the fair Pareto Optimum, at least. In other words, agents equipped with 2-length memory under direct reciprocity situation (because they play infinite times with a same opponent[17]) can establish cooperative state where they obtain R at least in any dilemma strength, or say, can establish R-reciprocity under any stronger dilemma is imposed to the agents.

[17] It is worthwhile to note that an individual agent in the assumed model is exposed to direct reciprocity situation because the number of games played with a same opponent is presumed infinite. But, viewing each of 32 strategies (not viewing each of agents), we can say this society is well-mixed because we applied replicator dynamics to solve the equilibrium distribution of strategies.

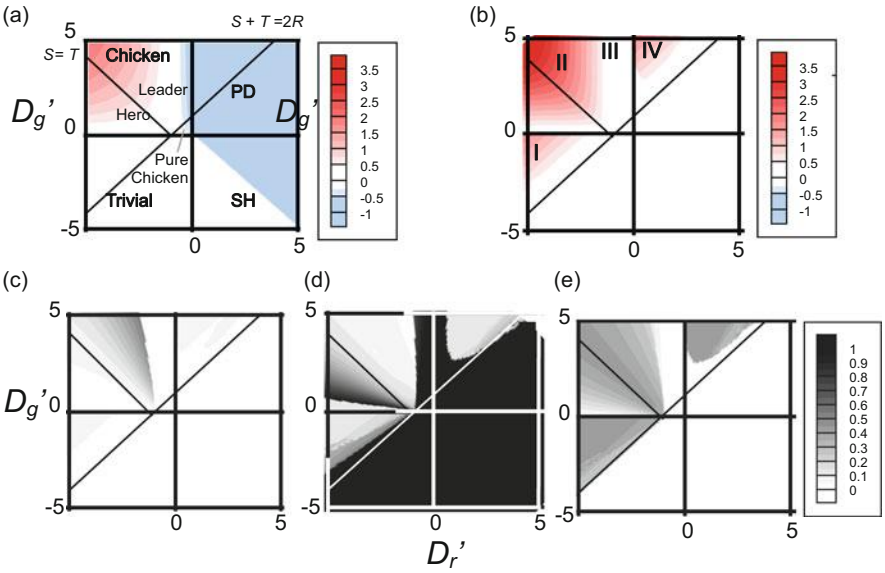

Fig. 2.34 Numerical result described on a $D_g' - D_r'$diagram; (**b**) relative payoff, defined by ([payoff] $- R$) / $(R - P)$; (**c**) – (**d**) showing frequencies of mutual defection, *R*-reciprocity and *ST*-reciprocity, respectively. For comparison, (**a**) shows the relative payoff derived from the analytic solution where no-memory (only 1 bit; C or D) agents playing games in a infinite and well-mixed population. (**a**) Relative payoff of analytic solution, (**b**) Relative payoff, (**c**) *P* frequency, (**d**) *R* frequency, (**e**) *S* or *T* frequency

Let us discuss about what happens in the area on $D_g' - D_r'$diagram where *ST*-reciprocity is beneficial than *R*-reciprocity, which is the area upper than the line of $S + T = 2R$ drawn in Fig. 2.34. In the analytic solution, Chicken area shows gradual payoff increase/ decrease, which is basically consistent with what we observed in the sub-panel in Fig. 2.10.[18] In region far from the line of $S + T = 2R$, *ST*-reciprocity, where social average payoff is larger than *R*, is realized. However, this is a product of incidence. Since cooperators and defectors co-exist in a population, happening C – D and D – C is inevitable. Thus, we should call this unintentional *ST*-reciprocity. So our question should be how much more effective the current *ST*-reciprocity works than this. Obviously, Fig. 2.34(b) shows more effective *ST*-reciprocity than the analytic solution. Careful observation on the area upper than the line of $S + T = 2R$ makes us perceive that there are distinctly four phases; denoted by (I), (II), (III) and (IV). Figure 2.35 shows time evolution of structure distribution at each of representative game structures of Phase (I), (I) and (III), denoted by Point 1, 2 and 3 (as shown in panel (d)).

[18] That is just part of the Chicken area in Fig. 2.34 (a), because, in Fig. 2.10, we assumed $R = 1$ & $P = 1$, and $-1 \leq D_g \leq 1$ & $-1 \leq D_r \leq 1$.

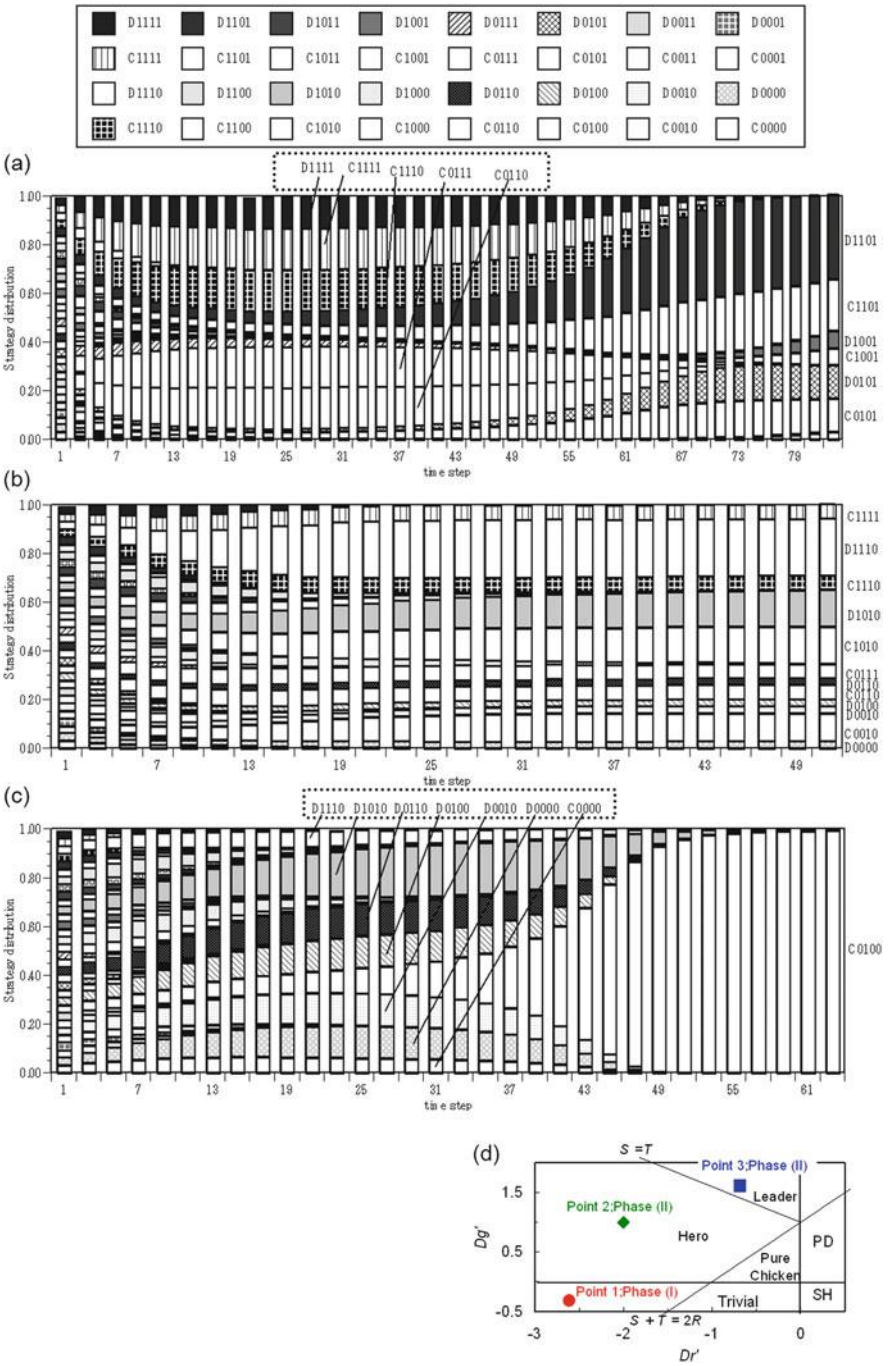

Fig. 2.35 Strategy distribution in each evolution process; (**a**) Point 1 (representing Phase I), (**b**) Point 2 (Phase II), and (**c**) Point 3 (Phase III). Panel (**d**) indicates game structures; $D_g{}'$ and $D_r{}'$. Legends of D(C)**** mean 0(1)**** implying respective 5 bit strategies

By a series of deliberate investigations on strategy distribution at equilibrium, detailed time evolution etc., the following facts are elucidated (Tanimoto and Sagara 2007b).

2.8.1 ST-*Reciprocity in Phase (I)*

As shown in Fig. 2.34(b), Phase (I) extends to a dilemma-free Trivial game area. In Fig 2.25(a), it turns out that "***01" occupies most of the strategy distribution. If two players having "***01" strategy play iterated games, it is possible that *T* and *S* appear alternately, which result in 2-periodic *ST* or *TS*. Hence, in Phase (I), coordinated alternating games just like an effective role-play bringing *S* and *T* are performed; this can be said to be the same phase of *ST*-reciprocity that Crowley (2001) called *ST*-reciprocity established by a CAD classifier. Then, we call this particular *ST*-reciprocity emerging in Phase (I) as a "CAD-type *ST*-reciprocity". In the same manner, if two players, one having "**011" and another having "**101", play iterated games, 3-periodic *RST* can be possible. This is, however, proved unlikely, since we could find very few "**011" strategies in Phase (I), which is also confirmed by Fig. 2.25(a).

Let us carefully observe the evolutionary process shown in Fig. 2.35(a). We can see the main remnant strategies on the equilibrium at the right margin of the graph (e.g. "D1101 (01101)"), while temporarily prosperous strategies on the evolution process at the upper margin are enclosed by a break line rectangle (e.g. "D1111 (01111)"). At the early stage of the evolution, strategies trying to exploit others perish. At this moment, the final remnant strategies are minorities beside the temporarily prosperous strategies aiming at obtaining *R* at least. The remnants, however, gradually have grown over temporary strategies, because they can obtain higher payoff by means of CAD-type *ST*-reciprocity than *R*-reciprocity. Finally, they can overwhelm the temporary strategies.

Summing up so far, the major cause for CAD-type *ST*-reciprocity observed in Phase (I) is that the strategy "***01" has evolved as the major strategy in order to benefit the game's structural feature characterized by $T+S>2R$.

2.8.2 ST-*Reciprocity in Phase (II)*

In Phase (II) where a Chicken-type dilemma exists, strategy "***01" cannot survive, which inevitably leads to another *ST*-reciprocity phase. As shown in Fig. 2.35(b), there are three major strategies on the equilibrium: "*1010"; "*1110" and "*0010". These three strategies prompt players to offer C after *S* or D after *T*. So we could say from a figurative point of view that these strategies are ordered to play in the same manner as at the previous step irrespective of being exploited or exploiting the opponent. This implies that *ST*-reciprocity occurring in

Phase (II) seems to be the same phase that Crowley (2001) called an *ST*-reciprocity established by DorC classifier. Thus, we call this particular *ST*-reciprocity emerging in Phase (II) "DorC-type *ST*-reciprocity". This particular system makes sense for a certain player who can obtain not only *S* but also *T* at a flat-rate base: Even if he has been exploited by someone for some time, he has another chance to exploit someone in return by changing his opponent. In short, a player never changes his role for a single session playing with a certain opponent, but he does change his role in cases of shuffling his opponent.

One plausible explanation for this emergence of DorC-type *ST*-reciprocity instead of CAD-type *ST*-reciprocity in Phase (II) is that strategy "***01" (playing an efficient role within a single playing session) is inevitably culled out in the path of evolutionary process due to the dilemma stress brought on by GID. This is confirmed by comparing Fig. 2.35(b) with Fig. 2.35(a) and (c). Namely, at the early stage of the evolution, strategies for CAD-type *ST*-reciprocity perish; however, strategies for DorC-type *ST*-reciprocity can never be dominated by initially-defective strategies "D**** (0****)" (as in Point 3; Phase (III)). Eventually, Strategies for DorC-type *ST*-reciprocity stably survive.

2.8.3 ST-*Reciprocity in Phase (III)*

It might be interesting to raise the question of why *ST*-reciprocity cannot be observed in Phase (III) even though satisfying $T+S>2R$. With increasing dilemma stress expressed by $D_g{}'$, the evolutionary process cannot maintain DorC-type *ST*-reciprocity, then gives up *ST*-reciprocity itself and selects the second-best solution, which is simple mutual cooperation to gain *R* by *R*-reciprocity. In the course of the evolution process (Fig. 2.35(c)), a group of initially-defective strategies "D**** (0****)" that are likely trapped by consecutive *P*s or periodic *P*s are dominant. Under this particular circumstance, "C0100 (10100)" is a minority that gradually overwhelms others, because "C0100 (10100)"s can obtain *R*s for each other. Finally, this strategy monopolizes.

Let us analyze the phase transition from (II) to (III).

Observing the equilibrium, we can notice a monopoly by strategy "C0100 (10100)" that can be named #9 in the right column of Fig. 2.33. This fact implies that $\mathbf{s_9}$ is one of the equilibriums of Eq. (2.60). Eigenvalues of Jacobi matrix $\mathbf{J}$ can be solved in an analytical way that leads to 32 eigenvalues for the equilibrium. Namely, 0 (7th repeated), $-\frac{1}{\sqrt{2}}$ (9th repeated), $-2-\frac{1}{2\sqrt{2}}$ (single), $-\frac{1}{2\sqrt{2}}+r\cdot\cos\left(\frac{\pi}{4}+\theta\right)$ (9th repeated), $-2-\frac{1}{2\sqrt{2}}+\frac{1}{2}\cdot\left(4-\frac{1}{2\sqrt{2}}+r\cdot\cos\left(\frac{\pi}{4}+\theta\right)\right)$ (6th repeated), where $D_g^{'}=-0.5+r(\cos\theta+\sin\theta)$ and $D_r^{'}=-0.5-r(\cos\theta-\sin\theta)$. The necessary and sufficient condition to avoid negative signs for these 32 eigenvalues is; $\cos\left(\frac{\pi}{4}+\theta\right)<\frac{1}{r}\cdot\frac{1}{2\sqrt{2}}$.

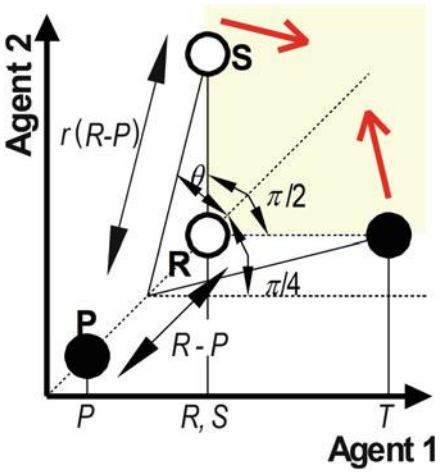

Fig. 2.36 The critical situation if all the eigenvalues are negative

The relationship on the critical situation between θ and r can be drawn in Fig. 2.36 that shows the feasible solutions region. The threshold is in the Leader game region. This schematic expression makes us understand that all 32 eigenvalues become non-positive unless the angle composed by linking the plots of S, R and T would be less than $\pi/2$ rad, which means that $\mathbf{s_9}$ becomes a stable equilibrium. That is to say, if θ becomes large, so that the S-R-T angle exceeds $\pi/2$ rad, only "10100", a very stiff and intransigent strategy that can endure strong dilemma stress for maintaining mutual cooperation (R-reciprocity), can survive. Inversely, if θ is less than the threshold, meaning less dilemma stress relatively compared with the extent of $S+T$-$2R$ (meaning a benefit of ST-reciprocity) strategies to attain DorC-type ST-reciprocity such as "*1010", "*1110" and "*0010" can survive.

2.8.4 ST-*Reciprocity in Phase (IV)*

By observing detailed strategy distribution carefully, it turns out that in Phase (IV), appeared in region of $S+T>>2R$ of PD area, both CAD-type and CorD-type ST-reciprocities simultaneously happen only when $S+T>>2R$ is satisfied.

Let us summarize the discussion so far. What we have to mention, first of all, is that the effect of 2-length memory indeed helps cooperation to avoid mutual defection. In this sense, the dilemma has completely suppressed by the assistance of memory strategy.

1. If $T+S>2R$ and the game is dilemma free, CAD-type ST-reciprocity where S and T are alternating within a single game session can evolve.
2. If $T+S>2R$ and the game contains a dilemma, DorC-type ST-reciprocity where S and T are alternating in several game sessions can evolve.

3. If $T+S>2R$ but the game contains a strong dilemma crossing over the critical condition, *ST*-reciprocity cannot evolve; thus, only the mutual cooperation backed by *R*-reciprocity emerges.

References

Akiyama, E., and Y. Aruka. 2004. The effect of agents memory on evolutionary phenomena—The Avatamsaka game and four types 2×2 dilemma games. *Proceedings of 9th Workshop on Economics and Heterogeneous Interacting Agents*, CD-ROM.

Alexander, R. 1987. *The biology of moral systems*. New York: Aldine De Gruyter.

Barabasi, A.L., and R. Albert. 1999. Emergence of scaling in random networks. *Science* 286: 509–512.

Browning, L., and A. Colman. 2004. Evolution of coordinated alternating reciprocity in repeated dynamic games. *Journal of Theoretical Biology* 229: 549–557.

Crowley, P. 2001. Dangerous games and the emergence of social structure: evolving memory-based strategies for the generalized hawk-dove game. *Behavioral Ecology* 12(6): 753–760.

Ebel, H., and S. Bornholdt. 2002. Coevolutionary games on networks. *Physical Review E* 66: 056118.

Hamilton, W.D. 1963. The evolution of altruistic behavior. *American Naturalist* 97: 354–356.

Hamilton, W.D. 1964. The genetical evolution of social behavior. *Journal of Theoretical Biology* 7: 1–16.

Hardin, G. 1968. Tragedy of the commons. *Science* 162(3859): 1243–1248.

Hassell, M.P., H.N. Comins, and R.M. May. 1994. Species coexistence and self-organizing spatial dynamics. *Nature* 313: 10–11.

Luce, R.D., and H. Raiffa. 1957. *Game and decisions: Introduction and critical survey*. New York: Wiley.

Masuda, N. 2007. Participation costs dismiss the advantage of heterogeneous networks in evolution of cooperation. *Proceedings of the Royal Society B* 274: 1815–1821.

Maynard Smith, J. 1976. Group selection. *Quarterly Review of Biology* 51: 277–283.

Maynard Smith, J. 1982. *Evolution and the theory of games*. Cambridge: Cambridge University Press.

Németh, A., and K. Takács. 2010. The paradox of cooperation benefits. *Journal of Theoretical Biology* 264: 301–311.

Nowak, M.A. 2006a. *Evolutionary dynamics*. Cambridge, MA: Belknap Press of Harvard University Press.

Nowak, M.A. 2006b. Five rules for the evolution of cooperation. *Science* 314: 1560–1563.

Nowak, M.A., and R.M. May. 1992. Evolutionary games and spatial chaos. *Nature* 359: 826–829.

Nowak, M.A., A. Sasaki, C. Taylor, and D. Fundenberg. 2004. Emergence of cooperation and evolutionary stability in finite populations. *Nature* 428: 646–650.

Nowak, M.A., and K. Sigmund. 1998. Evolution of indirect reciprocity by image scoring. *Nature* 393: 573–577.

Ohtsuki, H., C. Hauert, E. Lieberman, and M.A. Nowak. 2006. A simple rule for the evolution of cooperation on graphs and social networks. *Nature* 441: 502–505.

Ohtsuki, H., and M.A. Nowak. 2006. The replicator equation on graphs. *Journal of Theoretical Biology* 243: 86–97.

Price, G.R. 1970. Selection and covariance. *Nature* 227: 520–521.

Ren, J., W.X. Wang, and F. Qi. 2007. Randomness enhances cooperation: a resonance-type phenomenon in evolutionary games. *Physical Review E* 75: 045101(R).

Santos, F.C., and J.M. Pacheco. 2005. Scale-free networks provide a unifying framework for the emergence of cooperation. *Physical Review Letter* 95: 098104.

Santos, F.C., J.M. Pacheco, and T. Lenaerts. 2006. Cooperation prevails when individuals adjust their social ties. *PLoS Computational Biology* 2: 1284–1291.

Slatkin, M., and M.J. Wade. 1978. Group selection on a quantitative character. *Proceedings of the National Academy of Science of the United States of America* 75: 3531–3534.

Tanimoto, J. 2005. Environmental dilemma game to establish a sustainable society dealing with an emergent value system. *Physica D* 200: 1–24.

Tanimoto, J. 2009. A simple scaling of the effectiveness of supporting mutual cooperation in donor-recipient games by various reciprocity mechanisms. *Biosystems* 96: 29–34.

Tanimoto, J. 2014. *Mathematical analysis of environmental system*. Tokyo: Springer.

Tanimoto, J., and H. Sagara. 2007a. Relationship between dilemma occurrence and the existence of a weakly dominant strategy in a two-player symmetric game. *Biosystems* 90(1): 105–114.

Tanimoto, J., and H. Sagara. 2007b. A study on emergence of coordinated alternating reciprocity in a 2x2 game with 2-memory length strategy. *Biosystems* 90(3): 728–737.

Tanimoto, J., and A. Yamauchi. 2010. Does "game participation cost" affect the advantage of heterogeneous networks for evolving cooperation? *Physica A* 389: 2284–2289.

Taylor, M., and M.A. Nowak. 2007. Transforming the dilemma. *Evolution* 61(10): 2281–2292.

Traulsen, A., and M.A. Nowak. 2006. Evolution of cooperation by multilevel selection. *Proceedings of the National Academy of Science of the United States of America* 103: 10952–10955.

Trivers, R. 1971. The evolution of reciprocal altruism. *Quarterly Review of Biology* 46: 35–37.

Trivers, R. 1985. *Social evolution*. Menlo Park: Benjamin/Cummings.

Watts, D.J., and S.H. Strogatz. 1998. Collective dynamics of "small-world" networks. *Nature* 393: 440–442.

Weibull, J.W. 1997. *Evolutionary game theory*. Cambridge, MA: MIT Press.

Williams, G.C. 1996. *Adaption and natural selection: A critique of some current evolutionary thought*. Princeton: Princeton University Press.

Wilson, D.S. 1975. A theory of group selection. *Proceedings of the National Academy of Science of the United States of America* 72: 143–146.

Wynne-Edwards, V.C. 1962. *Animal dispersion in relation to social behavior*. Edinburg: Oliver and Boyd.

Yamauchi, A., J. Tanimoto, and A. Hagishima. 2010. What controls network reciprocity in the prisoner's dilemma game? *Biosystems* 102(2–3): 82–87.

Yamauchi, A., J. Tanimoto, and A. Hagishima. 2011. An analysis of network reciprocity in Prisoner's Dilemma games using full factorial designs of experiment. *Biosystems* 103: 85–92.

Chapter 3
Network Reciprocity

Abstract In the previous chapter, we discussed Nowak's five fundamental reciprocity mechanisms for adding social viscosity: kin selection, direct reciprocity, indirect reciprocity, network reciprocity, and group selection. In this chapter, we focus specifically on network reciprocity, as this mechanism has received the most attention in communities of statistical physicists and theoretical biologists who specialize in evolutionary game theory. Since 1992, when the first study of the spatial prisoner's dilemma (SPD) was conducted by Nowak and May (1992), the number of papers dealing with network reciprocity has increased to several thousand. The main reason for this is that network reciprocity is regarded as the most important and interesting of the mechanisms from an application point of view. In fact, we can observe a lot of evidence in real life of network reciprocity working to establish mutual cooperation not only in human social systems but also in those of other animal species. The network reciprocity mechanism relies on two effects. The first is limiting the number of game opponents (that is, "depressing anonymity," rather than having an infinite and well-mixed population), and the second is a local adaptation mechanism, in which an agent copies a strategy from a neighbor linked by a network. These two effects explain how cooperators survive in a social dilemma system, even though it requires agents to use only the simplest strategy—either cooperation (C) or defection (D), and this has attracted biologists who guess that network reciprocity may explain the evolution of cooperation even among primitive organisms without any sophisticated intelligence.

In this chapter, we begin to discuss the factors that influence network reciprocity, e.g., the underlying network topology, the update rule, and whether synchronous or asynchronous update are more influential in enhancing network reciprocity.

We also discuss how the initial cooperation fraction influences the equilibrium when we are concerned with network reciprocity.

After this, we discuss several new mechanisms relevant to network reciprocity, like coevolution, where not only strategy but also network topology can evolve. Also, we discuss how the definition of strategy, either discrete (binary – C or D), mixed, or continuous strategy, influences the features of network reciprocity.

Finally, we try to draw a holistic picture to understand the network reciprocity from a dynamics point of view, which may end the bells-and-whistles situation in

J. Tanimoto, *Fundamentals of Evolutionary Game Theory and its Applications*,
Evolutionary Economics and Social Complexity Science 6,
DOI 10.1007/978-4-431-54962-8_3

the field, with one paper after another claiming a new model for enhancing network reciprocity, but none providing an explanation for a substantial mechanism working behind the network reciprocity.

3.1 What Is Most Influential to Enhance Network Reciprocity? Is Topology So Critically Influential on Network Reciprocity?

As mentioned just above, in the last decades, many studies have dealt with network reciprocity. From the network topology viewpoint, previous works have assumed evolutionary games to be played not only on regular graphs where respective vertices have identical degrees (e.g., a ring or square lattice, which we refer to as regular networks), but also on complex networks where vertices have different degrees, which we call degree-heterogeneous networks. Figure 3.1 shows several representative networks (e.g., Tang et al. 2006). Examples of degree-heterogeneous

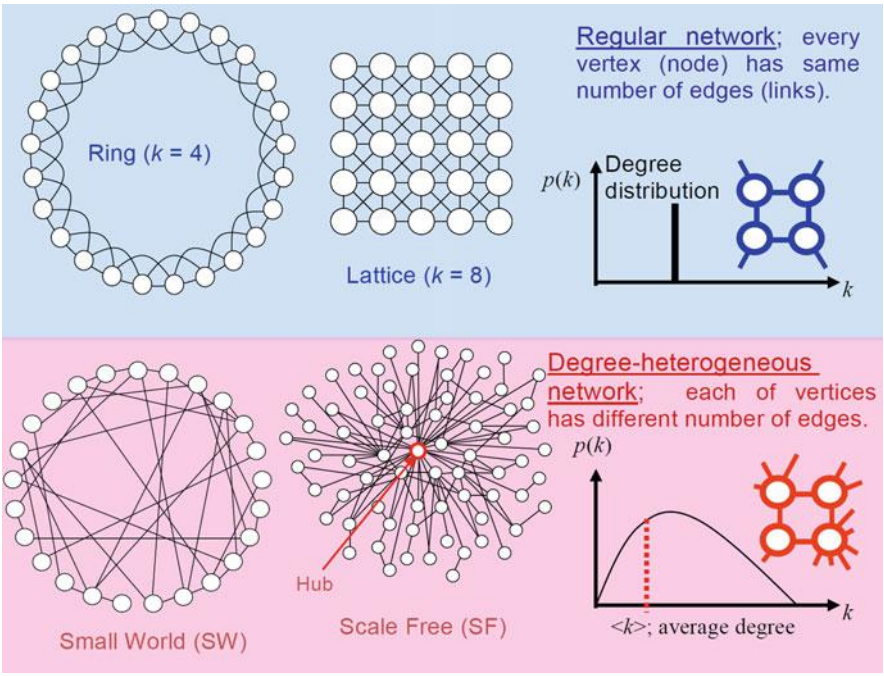

Fig. 3.1 Regular and degree-heterogeneous networks. Ring and Lattice are representative regular networks, while Small World (SW) and Scale Free (SF) are degree-heterogeneous ones. A SW can be generated from a regular network like Ring and Lattice by replacing (or adding) random short cuts

networks include the small-world (SW) network (e.g., Tomochi 2004) and the scale-free (SF) network (e.g., Gomez-Gardenes et al. 2007). In particular, it has been shown that an SF network enhances cooperation more easily than any other networks, since it allows the existence of hub C-agents, which compel cooperation among their neighbors, leading to strong and stable cooperation. Moreover, some reports have found that a difference in the assortativity coefficient (Newman 2002) in degree-heterogeneous networks (Rong et al. 2007; Roca et al. 2009; Tanimoto 2010) changes the robustness of the dilemma. Thus, it is reasonable to say that most previous works have focused on network reciprocity with respect to the network topology. A simple question comes our mind is whether network topology really dominates the network reciprocity as we have imagined, when we note there are other factors affecting on the network reciprocity other than topology; such as strategy update method and so forth. One problem is that factors other than network topology are assumed to have different properties respectively in different respective studies, which implies that we can not compare the previous works on a same ground despite huge number of papers have been reported. If the factors such as update rules, update dynamics, average degree, and population size influence network reciprocity, we cannot compare previous results with each other.

In the case of update rules, four particular rules have been studied widely. The simplest of them is the so-called Best Imitation (IM), where a focal player copies the strategy of the neighbor getting the largest payoff in the current time step. Two others can be classified as pairwise stochastic updating, in which a player compares his or her payoff with that of a randomly selected neighbor and copies the neighbor's strategy according to a certain function. In the second rule, the so-called Fermi function (Fermi-PW or F-PW) and in the third rule, the linear function of the payoff difference is adopted (Linear-PW or L-PW). The fourth rule is also stochastic, each focal player chooses either to repeat his or her strategy or to take on a neighbor's strategy with a probability proportional to the payoffs in the previous step (Roulette).

Also, there are two update dynamics, synchronous update and asynchronous update, which are known to influence the results, according to work reported by Grilo and Correia (2007).

Reviewing previous studies on network reciprocity, we notice that each study draws a different conclusion based on its own particular assumptions relating to the various choices we have described, although several comprehensive review papers have been shown (Szabo and Fath 2007; Perc and Szolnoki 2010). Thus, we cannot generally answer in a quantitative manner such questions as whether network topology is more influential than the update rule or; whether the factorial effect of degree-heterogeneous vis-à-vis regular networks is larger than that of synchronous vis-à-vis asynchronous updates. Although there have been several earlier studies suggesting that the substance of network reciprocity might be relevant to the time scale of strategy adaptation on the network (e.g., Santos et al. 2006b), and also suggesting that the co-evolution model could explain the network reciprocity (e.g., Szolnoki and Perc 2009a, b), it seems difficult to generalize which factors determine network reciprocity as a whole.

On this point, the studies of Nowak (2006) and Ohtsuki et al. (2006) seem important. They deduced that, in general, a smaller average degree $< k >$ of the network implies more robust dynamics in playing the dilemma regardless of network topology. However, their deductive approach was premised on the death-birth update rule, which is similar to the roulette selection described above (specifically, it does not consider the focal player's contribution). They also postulated weak selection and a Donor & Recipient games (descried in the previous chapter), a special case of PD. Therefore, it is still not clear whether their results are universal and will hold in the face of changes in the other assumptions (update rules, for example).

We also point out that most of the previous work has focused only on the network effect, ignoring the effects from assumptions made about other conditions, which is more significant than the network topology. Studies by Roca et al. (2006) and Tomassini et al. (2007) are exceptions, as they considered other effects extensively and also acknowledged that the point is open to further discussion. Grilo and Correia (2008) examined network reciprocity mainly for SW networks with simultaneous consideration of various update rules and synchronism, but there has not yet been a comprehensive look at what is important in terms of the network reciprocity.

Regarding the technical question of how to develop a comprehensive perspective that considers various independent factors and several different levels, we suggest applying the so-called FFDOE (Full Factorial Design of Experiments), which is a well-established statistical approach used in various engineering fields. Let us suppose, for example, that there are three factors ($A \times B \times C$) with respective levels (a_1,a_2 / b_1, b_2, b_3, b_4 / c_1, c_2, c_3). Considering all combinations; $2 \times 4 \times 3 = 24$ cases, we can obtain each factorial effect. For example, the factorial effect of A is expressed by the two averages derived from the 12 cases of $a_1 \times b^* \times c^*$ and $a_2 \times b^* \times c^*$ (where * indicates wildcard). We can also evaluate which factors are more influential than others by comparing the F-value of each, derived from an ANOVA (Analysis of Variance) process. F-value is regarded as a guidepost to evaluate whether a certain factor is significant or not, which is coming from F-test theory. In general, the larger F-value means that the factorial effect is more influential.

In this section, we discuss how various factors influence network reciprocity in order to obtain a holistic picture of what is significant in an evolutionary game on a network. Our approach is to apply a series of systematic numerical experiments, or say a series of systematic simulations based on FFDOE, which will enable us to compare the quantitative factorial effects comprehensively.

3.1.1 Model Description

Game Setting

According to the discussion expanded in the previous chapter, by assuming $R = 1$ and $P = 0$, we define the dilemma from a stag-hunt type of game as $D_r = P - S$ and

from a chicken type of game as $D_g = T - R$,[1] and in this case the payoff matrix can be given as

$$\begin{pmatrix} R & S \\ T & P \end{pmatrix} = \begin{pmatrix} 1 & -D_r \\ 1 + D_g & 0 \end{pmatrix} \quad . \tag{3.1}$$

In this section, we limit the PD game class by assuming that $0 \leq D_g \leq 1$ and $0 \leq D_r \leq 1$. Each agent plays 2×2 games with all other neighboring agents connected via his or her links that will be explained in the next section. The total payoff is evaluated by summing all games played by a certain agent at a certain time step.

Networks

We assume three levels for the number of players, $N = \{1600, 2500, 3600\}$, and four levels for average degree, $< k > = \{4, 6, 8, 12\}$.

We investigate eight types of network structures: (i) lattice, (ii) cycle, (iii) homogeneous SW (made from a cycle graph by replacing several links with random shortcuts, with a shortcut probability of 0.2, so that every vertex has the same degree), and (iv) heterogeneous SW (hetero-SW) which is the same as Watts–Strogatz SW (1998), which is generated from a cycle graph with swapping probability 0.2, (v) a regular random network (RR), and three SF networks based on the BA algorithm (SF) (Barabasi and Albert 1999). In the SF networks, we limit the assortativity coefficient to 0.15, 0, or −0.15 by the algorithm proposed by Xulvi–Brunet and Sokolov (2004); those three networks will be indicated by (vi) SF(0.15), (vii) SF(0), and (viii) SF(−0.15), respectively. Thus, the factor for network structure has eight levels. In preliminary experiments, we added (ix) a Erdős–Rényi random network (E-R) (Bollobás 1985). In this case, we cannot help excluding $< k > = 4$ from the average degree levels to meet the inequality $< k > \geq \ln N$ (Tomochi 2004), which is necessary to obtain a single clumpy random network. However, considering that a small average degree is important for comparison with previous works, and having confirmed that the general tendency of the result with (ix) E-R (and without $< k > = 4$) is similar to the result without E-R (and with $< k > = 4$),[2] we decided to exclude the E-R random network in order to keep four levels for the average degree factor.

[1] For a more precise discussion, we should use D_g' and D_r' by varying R while keeping $P = 0$ for example, instead of relying on D_g and D_r. Although we can go along that, hereafter, throughout the following text in the book, we assume assuming $R = 1$ and $P = 0$, and apply D_g' $(= D_g')$ and D_r $(= D_r')$ as a set of scaling parameters for simplicity and transparency for the discussion.

[2] Not only this point but also all the detailed result provided in this section can be referenced to Yamauchi et al. (2010, 2011).

Strategy Update and Its Dynamics

Concerning the update rule, we assume, as mentioned before, the four levels shown in Table 3.1. Those four are commonly used in previous studies. In the first case of Fermi-PW, a focal player i adopts a randomly chosen player j's strategy with probability calculated by a Fermi function. Although we recognize that the noise effect influences the cooperation level to some extent (Vukov et al. 2006), the parameter τ in the Fermi function is set to 0.2. The second level is Linear-PW, in which the strategy of a player j is chosen as in Fermi-PW, but the probability is given by a linear function. One important difference between Fermi-PW and Linear-PW is that the former might allow copying an opponent's strategy even if the opponent's strategy has a far smaller payoff than that of the focal player. In a sense, this allows the adoption of a worse strategy, which may help to avoid local maxima during evolution. The third level is IM, in which the focal player i imitates the strategy with the maximum payoff among all the strategies taken by the focal player and his or her immediate neighbors. The last level is roulette, in which a focal player chooses from among all the strategies taken by the focal player and his /her immediate neighbors with a probability proportional to the payoff (or, strictly speaking, to the payoff difference with the minimum of the neighbors' payoffs; see Table 3.1).

For update dynamics, we use two levels. In synchronous updating, after playing all games, all players update their strategy simultaneously. In asynchronous updating, a randomly chosen player plays the game immediately followed by his/her strategy update; following that, another randomly chosen player plays and updates.

Mutation

We assume that an agent is infected with a mutation in the strategy update process where he or she takes C or D randomly with probability ε. We assume two level of the mutations; $\varepsilon = \{0, 0.01\}$.

Table 3.1 Update rules. We assumed the following four rules in the experiment

Update rules	Procedures
Fermi-PW	$W_{S_i \leftarrow S_j} = \frac{1}{1+\exp\left[\left(\Pi_i - \Pi_j\right)/\tau\right]}$
Linear-PW	$W_{S_i \leftarrow S_j} = \frac{\Pi_j - \Pi_i}{\max\left(k_i, k_j\right)\left[\max(T,1) - \min(S,0)\right]}$
IM	$S_i = \begin{cases} S_i & \text{if } \Pi_i > \max\{\Pi \in N_i\} \\ S_j & \text{if } \Pi_j = \max\{\Pi \in N_i\} \end{cases}$
Roulette	$W_{S_j \leftarrow S_i} = \frac{\Pi_j - \min\limits_{k \in N_i}[\Pi_k]}{\sum\limits_{j \in N_i}\left(\Pi_j - \min\limits_{k \in N_i}[\Pi_k]\right)}$

S_i is the strategy of the ith agent, k_i is the degree of i, Π_i is the payoff of i, N_i is the neighbor agents of i (in the case of Roulette selection, N_i includes i), τ is an assumed constant, and $W\,S_i \leftarrow S_j$ is the probability of i's strategy being overwritten by j's

Experimental Setting

We simulate a series of perfect factorial experiments consisting of $3 \times 4 \times 4 \times 2 \times 2 \times 8 = 1536$ combination cases, reflecting the above-described choices: (a) the number of players has three levels, (b) the average degree has four levels, (c) the update rule has four levels, (d) the update dynamics has two levels, (e) the mutation has two levels, and (f) the network has eight levels, Each simulation runs as follows. Initially, an equal percentage of strategies are distributed randomly to the players allocated on different vertices of the network. Then, several generations are run until the frequency of cooperation arrives at a certain quasi-equilibrium. If the frequency of cooperation continues fluctuating, we obtain the frequency of cooperation for the last 100 generations over a 3000-generation run. We conduct this procedure at 11×11 points of the PD area ($0 \leq D_g \leq 1$, $0 \leq D_r \leq 1$) 20 times to draw 121 ensemble averages.

As the characteristic values used to evaluate cooperation, we defined three sub-classes of PD. The first one is a single algebraic average of those 121 ensemble averages covering all PD areas (hereafter All). The second is another average of 11 points featured by $D_g = D_r$, which is the so-called Donor & Recipient Game (hereafter D&R). The last is another 11-points average collected from the region of $D_r = 0$, which consists of boundary games between the PD and Chicken games featured without stag-hunt type dilemma (hereafter PDCH). Many previous works prefer to postulate PDCH for representing PD, because it can be characterized by a single dilemma parameter D_g.

3.1.2 Results and Discussion

Which Main Effect Is Significant?

Figure 3.2 shows the F-value for each factor normalized by the largest one, which is the factorial effect of the update rule. F-values are derived from an analysis of variance (ANOVA) based on the result obtained by FFDOE. In ANOVA, a larger F-value implies a greater factorial effect, which significantly influences the equilibrium frequency of cooperation.

Examining the differences that arise in choosing which game area is evaluated, we found that All and D&R had similar tendencies in general but PDCH appeared different. In PDCH, the all factorial effects except for the number of players were observed to be stronger than those for All and D&R. In particular, the effect of the network structure is remarkably stronger than the case for All and D&R. This implies that one might overestimate the network reciprocity that results from network topology when using the boundary games (PDCH) to evaluate the cooperation level, as the results are not consistent with the network reciprocity obtained

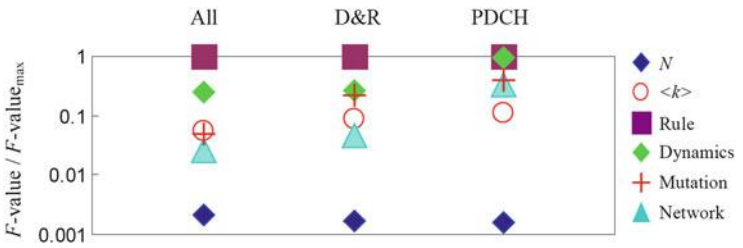

Fig. 3.2 Result of ANOVA for the main effect analyzed on different dilemma areas. Values along the *Y*-axis indicate the normalized *F*-value. Plot legend is as follows: *Closed blue diamonds* represent the number of agents; *circles*, the average degree; *squares*, the strategy update rule; *closed green diamonds*, the update dynamics; *plus signs*, the mutation rate; and *closed triangles*, the network structure. All means averages over all PD area. D & R and PDCH indicate averages of Donor and Recipient games and boundary games between PD and Chicken (see text)

for the all-PD-game area. The D&R set is much better as a representing archetype for all PD games.

As for the fundamental question of which factor is more important than the others, our results show that the factorial effects from the update rule and its dynamics are the most and the second-most significant; they are more significant than network topology. The factorial effect of network topology (meaning the influence caused by network structural differences), with which most of the previous studies have been concerned, is not so significant, being similar to the effects due to average degree and mutation.

Main Factorial Effects

Figure 3.3 shows the main factorial effects except for the effects of the network structure. The bold lines indicate level average values and distributions mean frequency of all combination cases that are scattering from entire defective situation to reasonable cooperation level in *X*-axis. For example, in the case of (a) the number of agents, *Y*-axis values of three bar lines are the average cooperation fractions of the respective experimental levels, which are based on $1536/3 = 512$ combination cases. In the following text, we will restrict our discussion to the results for All unless otherwise noted, because no significant differences among the results of All, D&R, and PDCH were found.

Figure 3.3(a) shows no sensitivity to the number of agents this implies that a social size of $N = 1600$ is sufficient for this simulation study.

Remarkably, we can see an irregular behavior in which $< k > = 6$ is observed to be slightly more cooperative than $< k > = 4$ (Fig. 3.3(b)). This is inconsistent with the report by Nowak (2006) and Ohtsuki et al. (2006), who found that a lower average degree tends to enhance cooperation. This contrasting result might be

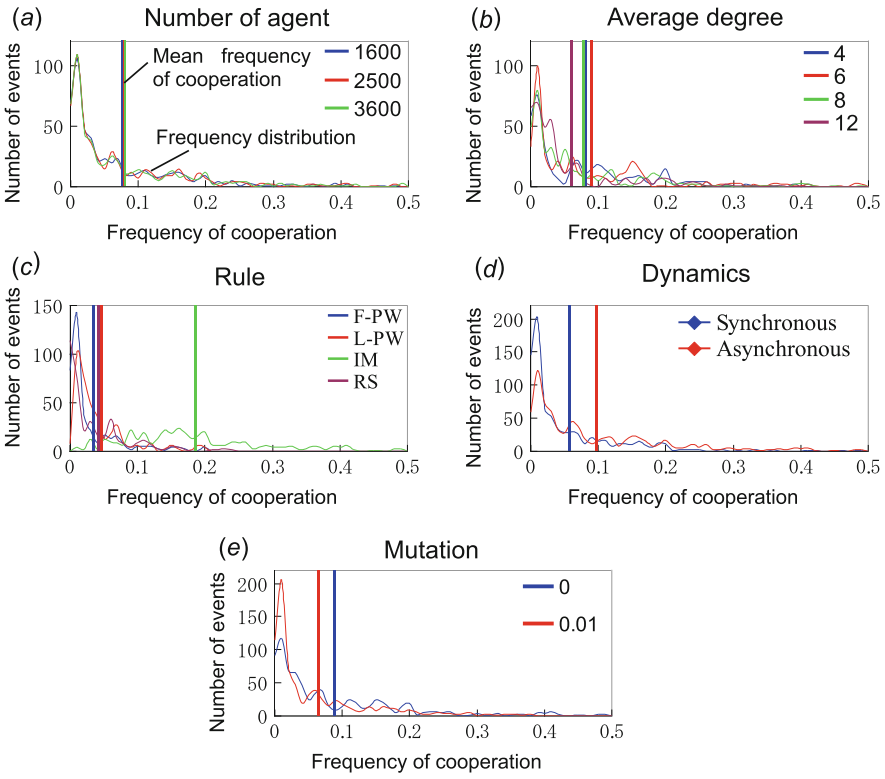

Fig. 3.3 Frequency distribution of average cooperation fraction and mean frequency of cooperation of each level for (**a**) number of agents, (**b**) average degree, (**c**) strategy update rule, (**d**) update dynamics, and (**e**) mutation rate. The *bold lines* indicate level average values and distributions mean frequency of all combination cases that are scattering from entire defective situation to reasonable cooperation level in *X*-axis

drawn if we are concerned on the average effect considered by every network structure, number of agents, up date rules, synchronism, and others on average. In fact, we can see results that are consistent with Nowak and Ohtsuki when considering certain interaction effects, as will be discussed later. One important thing to note is that the statement "a lower average degree tends to enhance cooperation" is true under certain conditions, but we cannot say the average degree dominates (or can explain for) network reciprocity, because its factorial effects are subtle (Fig. 3.3(b)) and less than the factorial effects due to the update rule and dynamics (Fig. 3.2).

Observing Fig. 3.3(c), we see that IM is the only deterministic update rule that shows a much stronger cooperation-enhancing effect than others. Concerning the update dynamics illustrated in Fig. 3.3(d), Asynchronous is more significant than Synchronous in supporting cooperation, which is consistent with previous studies

(e.g., Roca et al. 2006). The results of Fig. 3.3(e) seem plausible, since mutation damages cooperation by destroying C clusters.

Main Factorial Effect of Network Structure

Figure 3.4 shows the factorial effects of the network structure for both All and PDCH. The results for D&R were similar to those for All. Observing PDCH in Fig. 3.4(b), we can see that the more degree-heterogeneous network lead to more cooperative situations, this is consistent with what Santos et al. (2006a) found. However, in All there is a different tendency, as can be seen in Fig. 3.4(a). Amazingly, aside from the SF networks with neutral and negative assortative mixing, that is, SF(0) and SF(−0.15), the degree-heterogeneous networks, such as He-SW, RR, and SF(0.15) show less cooperation than the regular networks, i.e., the high spatial regularity graphs, cycle and lattice. Usually, the fact that degree-heterogeneous networks such as FS enhance cooperation is explained by the generally accepted suggestion that a hub C agent (that is, a hub vertex occupied by a C strategy) makes its neighbors maintain a C strategy because of its large accumulated payoff. In this sense, high heterogeneity, that is, a broad degree distribution allows high degree (hub) agents to exist. Although it might seem that the observations in Fig. 3.3 are opposed to this general consensus, that is not necessarily so. When $D_r > 0$, a hub C agent is more difficult to keep C than when $D_r = 0$ because for a hub C agent in a degree-heterogeneous network being exploited by D neighbors (obtaining S, in other words) when $P > S$ ($D_r > 0$) is more serious than being exploited by D neighbors when $P = S$ ($D_r = 0$). Thus, we can predict that if all PD game area is considered, regular networks are not as much weaker than degree-heterogeneous networks as the general consensus based on the previous studies. It should be noted that just observing PDCH game area investigation is dangerous, although it is easier due to a single dilemma parameter; D_g. If you prefer a single dilemma parameter system like PDCH and still try to evaluate all PD games, D&R ($D_g = D_r$) is better than PDCH, which is already insisted in the earlier section.

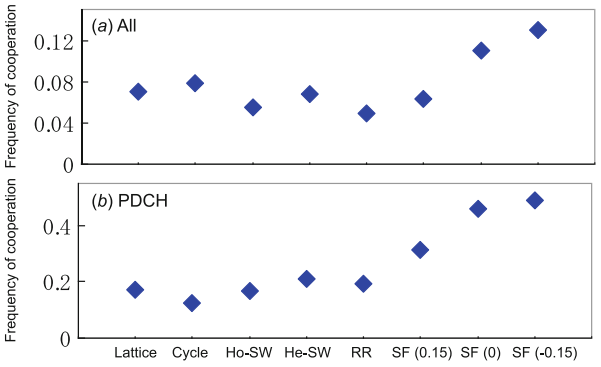

Fig. 3.4 Frequency of cooperation for each network. (**a**) shows the results analyzed on All PD game area and (**b**) shows results for PDCH area

Second Interaction of Update Rule × Update Dynamics

Figure 3.5 shows the second interactions normalized by the update rule × update dynamics for different PD areas in a manner similar to that used for Fig. 3.2. The interactions relating to the number of agents are not shown because they are negligible. The interaction of the update rule × update dynamics is particularly significant, whereas the other interactions are stronger or weaker depending on PD area.

Let us confirm the details of the interaction of update rule × update dynamics in Fig. 3.6, which displays not only average values but also maximum and minimum values. Obviously, the cooperation level when adopting either Fermi-PW or Linear-PW is independent of whether Synchronous or Asynchronous is chosen, which is consistent with the report by Grilo and Correia (2008). They suggest that this

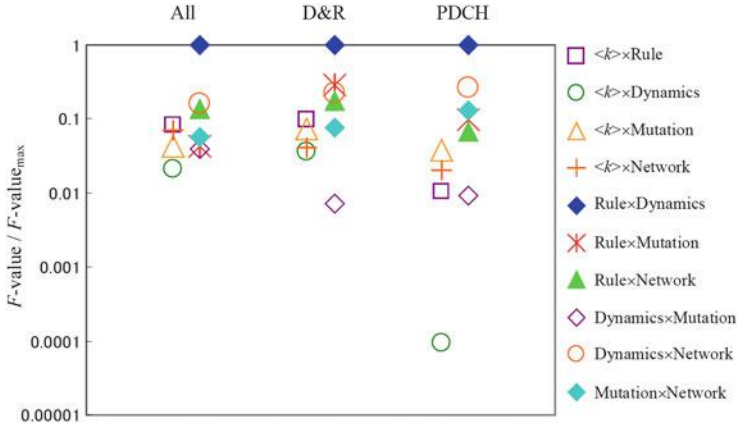

Fig. 3.5 Result of ANOVA for the second interaction analyzed on various dilemma areas. *Y*-axis shows the normalized *F*-value. Legends are shown at *right side* of the figure. The second interactions normalized by the update rule × update dynamics for different PD areas in a manner similar to that used for Fig. 3.2

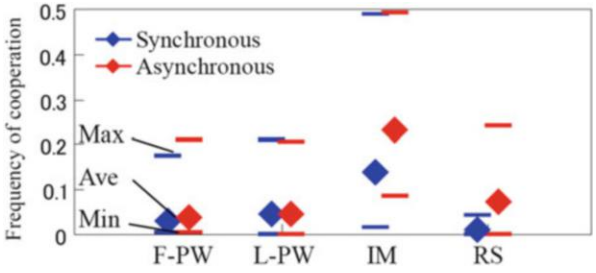

Fig. 3.6 The second interaction of update rule × update dynamics. Maximum value, minimum value, and average value under the condition of each update rule. *Blue plots* show the results of synchronous update, and *red plots* show that of asynchronous update

phenomenon is explained by a situation in which a certain agent tends not to copy an opponent's strategy when the opponent has fewer payoff, which they call Payoff Monotonicity. From a microscopic view, there are many agents who do not change their own strategy due to Payoff Monotonicity when a pairwise update is imposed. It is as if the agents' strategy updates are taking place in sequential manner even though the Synchronous update is imposed. This explains why there is no significant difference between Synchronous and Asynchronous in Fig. 3.6. Furthermore, this particular process, which entails gradual updating in a single time step, that is, as if there is asynchronous updating even if Synchronous was selected, prevents D agents from amplifying (see Fig. 3.10). Thus in IM and RS, which do not contain this function, the Asynchronous update enhances cooperation more than Synchronous, since the cooperation diffusion effect occurs more effectively for the Asynchronous update than for Synchronous.

Second Interaction Relating to Mutations

Figure 3.7 shows the interactions of mutations with update rule (a) as well as with network structure (b) expressed in the same manner as in Fig. 3.6.

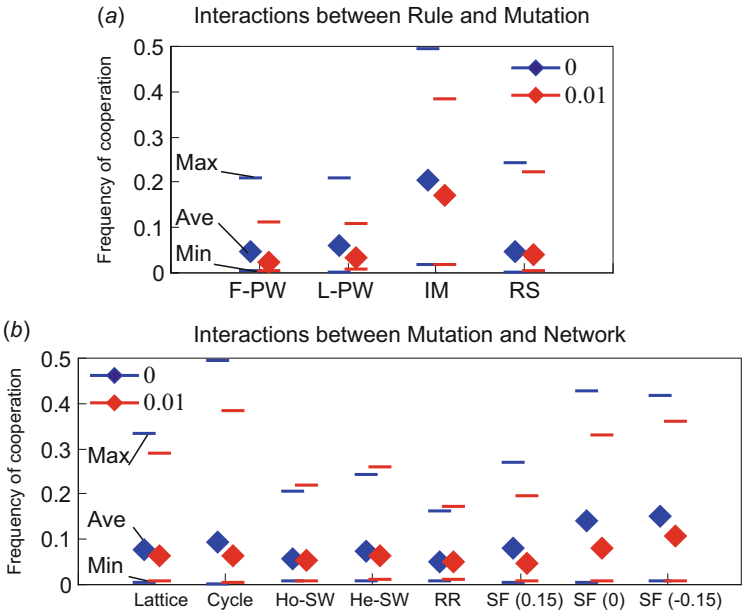

Fig. 3.7 The second interactions of mutations with update rule (**a**) as well as with network structure (**b**). Maximum value, minimum value, and average value under the condition of (**a**) each update rule and (**b**) each network structure. *Blue plots* show the results of no update error, and *red plots* show the results with error rate $\varepsilon = 0.01$

Concerning the update rule illustrated in Fig. 3.7(a), we note that RS has no significant difference between the cases with and without mutations. This results from the fact that RS contains a probabilistic element in its copying process. In contrast, for other update rules, including pairwise rules that contain some probabilistic facet not in the update rule itself but in the random process used to select an opponent, mutation evidently devastates cooperation. This can be explained by the fact that, for update rules other than RS, it is difficult to expel D agents once they have successfully invaded a C cluster, which inevitably makes it difficult to rebuild the C cluster once it has been impaired. This is consistent with what Tomassini et al. (2007) reported.

Observing the interaction with the network structure illustrated in Fig. 3.7(b), we can see SF is significantly affected by the consideration of a mutation. This can be explained by the fact that hub C agents that can take charge of diffusing a C strategy are going to spread a D strategy when mutated from C to D, which is consistent with the well-known observation that SF free networks such as the Internet are fragile in the face of attacks concentrated on hub nodes.

Second Interaction Relating to Average Degree

Figure 3.8 shows the interactions between the average degree and the update rule. As mentioned before, the statement by Ohtsuki et al. (2006) that "a smaller average degree $< k >$ of the network implies more robust dynamics against the dilemma irrespective of network topology" (Ohtsuki et al. 2006) is premised on the death-birth update rule, that is, more or less, similar to the RS. Certainly, we can confirm here that their statement is true when RS is assumed (Fig. 3.8(d)) as well as for pairwise rules (Fig. 3.8(a), (b)) despite a feeble tendency in these cases. However,

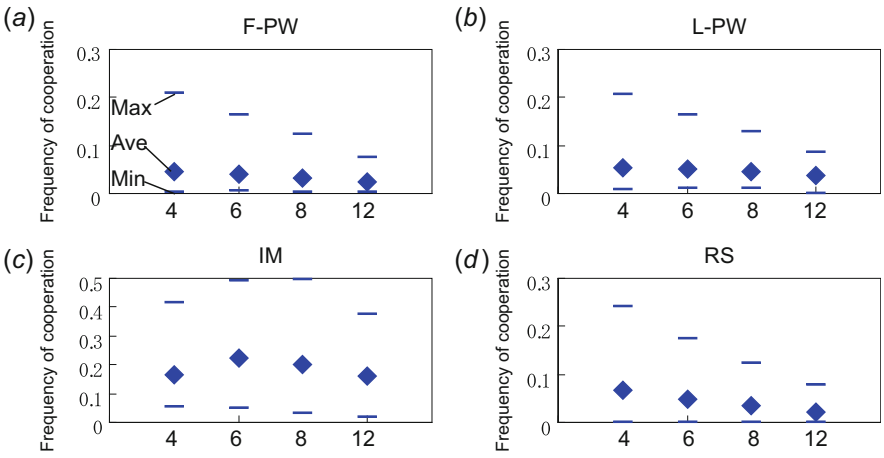

Fig. 3.8 The second interactions between the average degree and the update rule. Maximum value, minimum value, and average value on respective average degree under the condition of (**a**) F-PW, (**b**) L-PW, (**c**) IM, and (**d**) RS

the IM case is obviously different, as an irregular peak at $< k > = 6$ is observed. This is why we cannot see the consistent tendency with the Ohtsuki's statement as the whole main factorial effect for average degree in Fig. 3.3(b). It is important to address that the Ohtsuki's statement cannot be permissively interpreted by "average degree on networks determines network reciprocity in PD games," although their deductive work is possibly perfect on the ground of analogy or consistency to the so-called Hamilton principle (Hamilton 1964) expressed by a simple inequality equation explaining for a question when collective cooperation can be evolved under dilemma situations.

Third Interaction

Figure 3.9 shows the third interaction effect in the update rule × update dynamics × network structure, which has the largest F-value among all the third interactions. Figure 3.9 is a breakdown of Fig. 3.6 into their respective network structures. When pairwise update is used, there is none of significant difference between Synchronous and Asynchronous update among all networks structures. If IM is used, however, Asynchronous operation enhances more cooperation than Synchronous, this tendency is evident for SF, especially for SF with negative assortative mixing. Surprisingly, if IM and Synchronous update are chosen, SF (0) and SF (0.15) become the worst and second worst networks for cooperation.

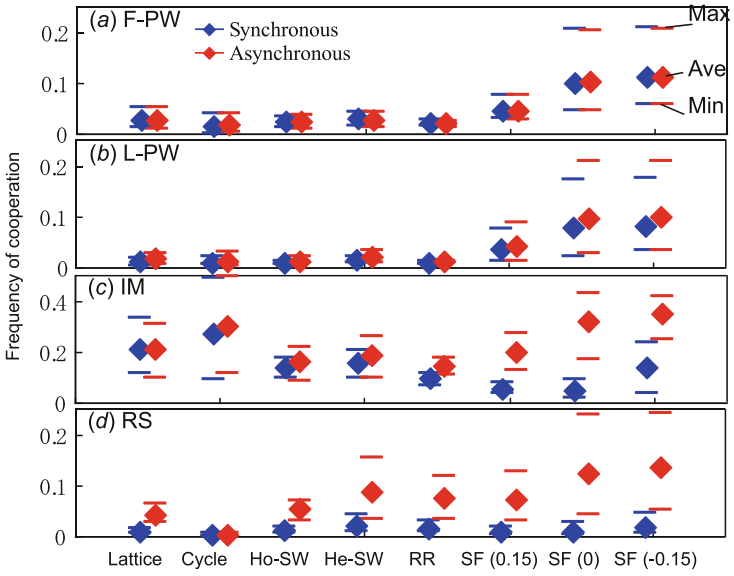

Fig. 3.9 The third interaction effect in the update rule × update dynamics × network structure. Maximum value, minimum value, and average value of (**a**) Fermi-PW, (**b**) Linear-PW, (**c**) IM, (**d**) Roulette selection update rules on each network. *Blue plots* show the results of synchronous update, and *red plots* show results of asynchronous update

This indicates that degree-heterogeneous networks are not always the most effective in enhancing cooperation. This disagrees with the existing consensus, but it can be explained as follows. Under the condition of both IM and Synchronous, D agents that are initially allocated on high-degree vertices (say, hub D agents) can diffuse the D strategy quickly and efficiently through a degree-heterogeneous network structure, which is counterproductive to the generally recognized hub effect of SF networks to support cooperation. In contrast, if Asynchronous update dynamics are put into effect, the strategy diffusion during a single time step (i.e., the discrete time step at which point all agents have finished strategy refreshing) is gradual so that a hub D agent can be taken over by a C strategy copied from a neighboring hub C. Figure 3.10 illustrates those two different scenarios for Synchronous and Asynchronous updating, which was presented in our previous report (Yamauchi et al. 2010). In RS, Asynchronous is superior to Synchronous at enhancing cooperation for every network except Cycle, where network reciprocity is so weak that it is not possible to attain any cooperative germs.

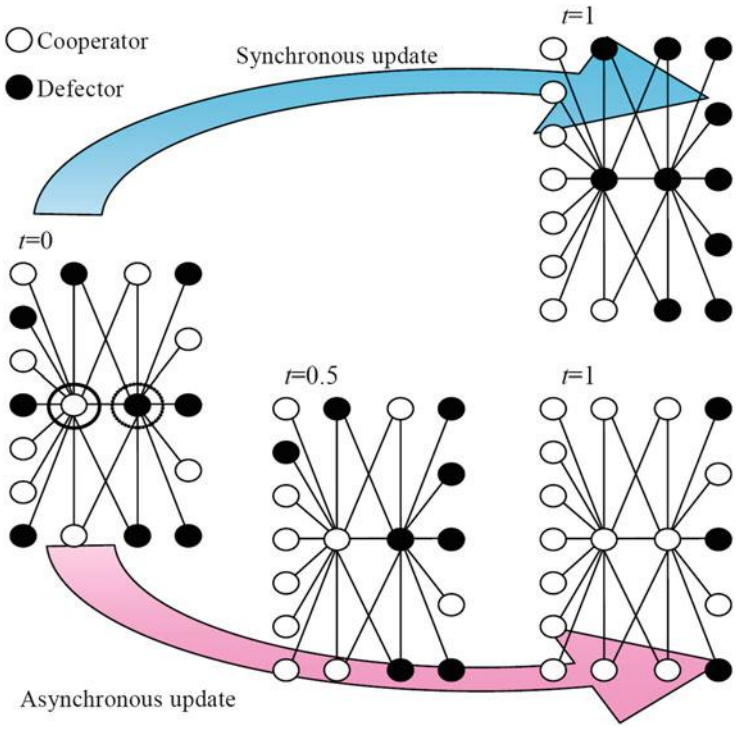

Fig. 3.10 Intuition of SF with synchronous and asynchronous updating. In synchronous updating, hub C player refers to neighbor hub D's strategy easily, while in asynchronous updating, players surrounding hub C change to C, but players surrounding hub D change to D in the middle of a generation, which causes a reversal of the hubs' payoff. Subsequently, the hub D player refers to hub C's strategy

Summary

We have conducted a series of systematic FFDOE considering all factors related to network reciprocity, such as the number of agents, average degree, update rule, update dynamics, network structure, and mutation (noise of strategy) in order to clarify which effects dominate network reciprocity and what is network reciprocity. For the experimental evaluation, we considered three PD game areas: All, PDCH, and D&R. To supplement our previous work, we added a new factor (mutation), and revised some levels, which seems meaningful to draw more robust results,

Our first result, which is consistent with what we saw in our previous work, is that strategy update rules and update dynamics are much more significant than network topology. Whether the mutation is considered or not is more influential than the average degree, which has been accepted as the primary factor explaining the network reciprocity originally reported by Ohtsuki et al. (2006).

Our analysis of the interactions indicates that Ohtsuki's statement, "the effect of average degree, where a smaller degree network can be more robust for cooperation," is questionable and not universal. If Imitation Max is assumed to be the update rule, this statement is invalid.

Furthermore, if Imitation Max and Synchronous are used for updating, the SF network, one of the representative degree-heterogeneous topologies, shows only meager enhancing of cooperation compared with regular graphs. In this condition, the cycle graph offers the most favorable conditions for supporting cooperation.

These findings can be explained by the relationship between the network topology and the stochastic characteristics of strategy updating, in other words, which network structure is suitable to a certain updating (rule and dynamics) is the most dominant for supporting cooperation.

Finally, we find that the PD game type chosen for evaluation is very important and has great influence on the consequence. Boundary games between PD and Chicken, commonly used as an archetype for PD, tend to overestimate the network reciprocity of Scale Free networks.

3.2 Effect of the Initial Fraction of Cooperators on Cooperative Behavior in the Evolutionary Prisoner's Dilemma Game

Concerning the detailed content discussed in this section, one should consult with Shigaki et al. (2013). In spite of the relatively large body of work concerning network reciprocity that has accumulated, there is one situation of particular relevance that has received little attention until now. That is the impact of the initial fraction of cooperators on the final equilibrium state.

Most previous works offering simulation results have assumed an initial population of half cooperators and half defectors, randomly assigned on the vertices of a

network grid, as the initial condition. This has been the de facto standard, accepted without any doubt, for a long time. It might be acceptable and plausible if one relies on a standpoint that the evolutionary trail reproduced by their particular model should be regarded as one of the general dynamical systems, because the assumption of 50 % initial cooperators fraction implies neutrality and fairness, in not particularly favoring the success of cooperators or defectors. However, it seems rather specific from a biological scenario point of view. What biologists are primarily interested in is whether a mutant cooperator can invade a resident population of non-cooperators (defectors) and fix it, or whether a mutant defector can invade a cooperative population and dominate. This kind of discussion can imply that the system features a stable cooperative phase, or that the system is vulnerable against the invasion of defectors, which is crucially important in the context of biological applications. Thus, an allegation that the automatic assumption of 50 % initial cooperators might be questionable seems persuasive. At the very least, it is important that we discuss whether network reciprocity has a significant sensitivity to the initial cooperation fraction or not.

We will focus on this point in this section.

In a recent research by Poncela et al. (2007), where the stochastic updating rule and degree-heterogeneous networks were implemented, it was demonstrated that the characterization of the asymptotic states of the evolutionary dynamics was largely independent of the initial concentration of cooperators. However, it was obvious that the stochastic influence coming from updating rule and degree-heterogeneous topology always existed within such a framework. Based on the achievement, one question poses itself, which we aim to address in what follows. Namely, if we remove these stochastic factors, how does the initial concentration of cooperators affects the final equilibrium states?

In the following discussion, we refer to the result of a series of simulations we did, where a PD game of $0 \leq D_g \leq 1$ and $0 \leq D_r \leq 1$ with synchronous updating based on Imitation Max (IM) is assumed. As the interaction network, we use a cycle, a square lattice with periodic boundary condition having 4 or 8 nearest neighbors, the regular random graph (RR) or the scale-free (SF) network with average degree of 4 or 8 (i.e., $<k>=$ 4, 8) generated via the Barabási-Albert algorithm (Barabasi and Albert 1999). The total number of agents is $N = 10{,}000$.

3.2.1 *Enduring and Expanding Periods*

For the sake of the following discussion, we define the terminology as the enduring (END) period and the expanding (EXP) period as shown in Fig. 3.11. In a typical evolution course, where the initial value of the cooperation fraction is 0.5, there are usually two evident processes: the former period features the rapid downfall of cooperation, while the following one is along with the increase of cooperation level unless the evolutionary trail is absorbed by all-defectors state during the foregoing

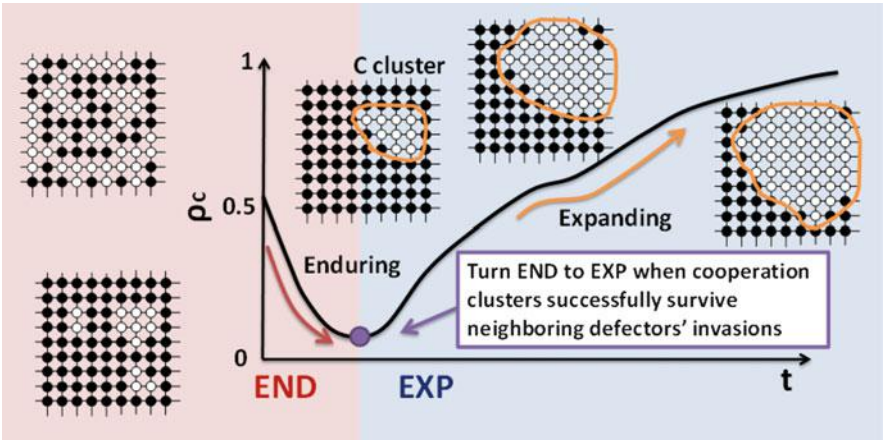

Fig. 3.11 Schematic view for the evolution of cooperation in spatial prisoner's dilemma game with concept of END and EXP. Enduring (END) period: Initial cooperators will be rapidly plundered by defectors, which cause only few cooperators left through forming compact C-clusters. *Expanding* (*EXP*) *period*: C-clusters start to expand, since a cooperator on the clusters' border can attract a neighboring defector into the cluster

period. In our study the first is the so-called enduring (END) period because cooperators try to endure defectors' invasion (or cooperators avoid learning defection from neighbors). Correspondingly, we call the other the expanding (EXP) period, since cooperators, who successfully survive in the END period by forming cooperative clusters (C-clusters), expand their area by converting defectors into cooperators. In some particular cases (such as, weak dilemma), when the initial fraction of cooperation is low, the evolutionary trail may start from EXP period.

One thing to be confirmed is the discussion above, about Fig. 3.11 presumes that an underlying network is regular like a lattice, and strategy update rule is deterministic like IM. For the sake of a substantial discussion, it seems more transparent to assume entirely deterministic processes for topology, update rule, whether synchronous (deterministic) or asynchronous (stochastic), and others than stochastic ones. Although we know some regular networks enable to enhance network reciprocity and asynchronous and stochastic updates seem plausible if one observes what happening in real world, adding noise makes hard to be observed the substantial effect caused by network reciprocity. Noise masks the substance, which makes ambiguous our following discussion, even though it can somehow foster the instinct network reciprocity.

3.2.2 Cluster Characteristics

To feature how emerging spatial patterns qualitatively affect the evolution of cooperation, three cluster characteristics: cluster number N_C, cluster size S_C and

cluster shape SH_C of cooperator aggregations are employed (Fu et al. 2010). In particular, we need to give the detailed definition of the third term. For each cluster i, we can derive SH_{Ci} based on the number of C-C links, l_{CC}, within cluster i and the number of C-D links, O_{CD}, that connect cluster i with the surrounding defectors:

$$SH_{Ci} = \frac{2l_{CC} - O_{CD}}{2l_{CC} + O_{CD}} \tag{3.2}$$

The value of SH_{Ci} is constrained to the interval $[-1, 1]$. Obviously, compact C-cluster has more links within the cluster rather than to the surrounding defectors. The value of SH_{Ci} is positive, which indicates positive assortment of cooperators. While for the sparse cluster there are fewer links within the cluster but more links connecting to surrounding defectors. Thus, $SH_{Ci} < 0$ and negative assortment among cooperators takes place (or positive assortment between cooperators and defectors). Moreover, in order to eliminate the influence of isolated cooperators, the cluster size S_C and cluster shape SH_C are weighed such that the weight of each cluster corresponds to its size.

3.2.3 Results and Discussion

We have performed extensive numerical simulations under different interaction networks. The equilibrium fraction of cooperation ρ_C^{eq} is determined within the last 5000 generations out of the total 10^5 iteration steps. Moreover, to guarantee validity and statistical robustness of data, the final results are averaged over up to 100 independent runs for each set of parameter values. During one time step, the agents update their strategies synchronously. In all the figs, we use ρ_C^{ini} to denote the initial fraction of cooperators.

Effect of Initial Fraction of Cooperators

We start by presenting the color map encoding the equilibrium fraction of cooperators ρ_C^{eq} on the $\rho_C^{ini} - r$ parameter plane for different interaction topology networks and degree in Fig. 3.12. It is noteworthy that, on regular network, higher initial fraction of cooperators ρ_C^{ini} does not necessarily lead to the high equilibrium fraction of cooperation ρ_C^{eq} in weaker dilemma region ($r < 0.3$), especially on the square lattice with low degree (see Fig. 3.12(b)). On the contrary, a relatively low initial fraction of cooperators can induce the undisputed dominance of cooperation. While for the degree-heterogeneous networks, a higher initial fraction of cooperators usually provides better environment for the evolution of cooperation. This can be easily explained by the fact that enhanced initial fraction of cooperators increases the possibility of cooperators holding the highly connected nodes (such as, hub

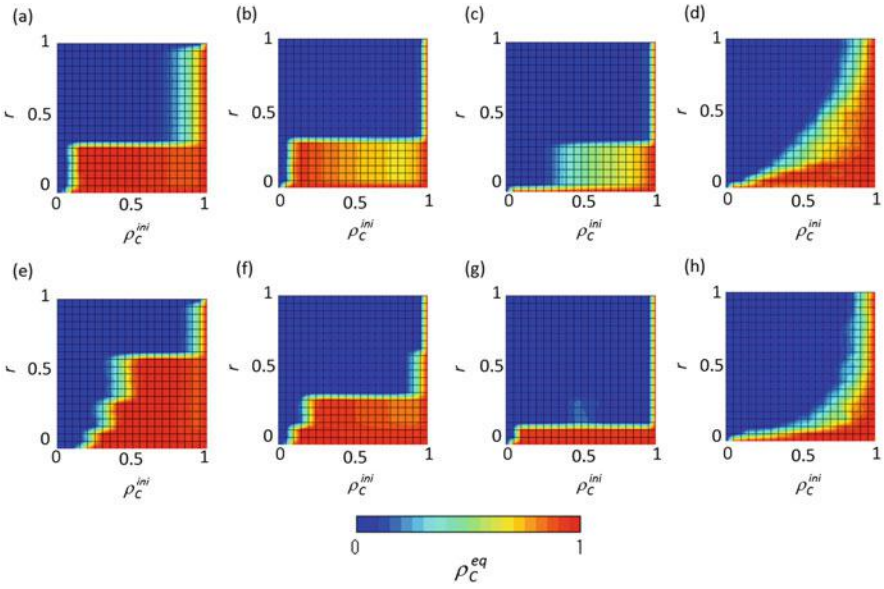

Fig. 3.12 Equilibrium fraction of cooperators ρ_C^{eq} on the ρ_C^{ini} -r parameter plane on various topologies. From left to right ((**a**–**d**) and (**e**–**h**)), the interaction networks are cycle network, square lattice network, RR and the scale-free network, respectively. For *top panel*, the average degree is $< k > = 4$, for *bottom panel* it is $< k > = 8$

nodes), which in turn attract their neighbors into cooperators and guarantee in this way their long-time success (Poncela et al. 2007). Thus, these results suggest that when the stochastic factor is removed (namely, the combination of deterministic updating rule and regular interaction topology), a relatively low initial fraction of cooperators can create better environment for the sustenance of cooperation. To simplify the discussion, we mainly focus on the case of square lattice with $k = 4$.

Square Lattice Network ($k = 4$, IM)

Figure 3.13 shows how ρ_C^{eq} varies as a function of the initial fraction of cooperators ρ_C^{ini} on a square lattice with $k = 4$ and IM rule. It is clear that the region of $\rho_C^{ini} \approx 0.15$ exhibits higher cooperation level than the other regions with a relatively low or high initial fraction of cooperators, which, to some extent, is similar to phenomenon of evolutionary resonance (Perc and Marhl 2006). For lower initial fraction of cooperators ($\rho_C^{ini} < 0.15$), though few cases can reach the coexistence phase of cooperators and defectors, majority of the realizations is absorbed by the phase of pure defectors. On the other hand, a relatively high initial fraction of cooperators ($\rho_C^{ini} > 0.15$) shows that its dynamics always ends up with the coexisting equilibrium in which cooperators and defectors simultaneously survive. To explain these

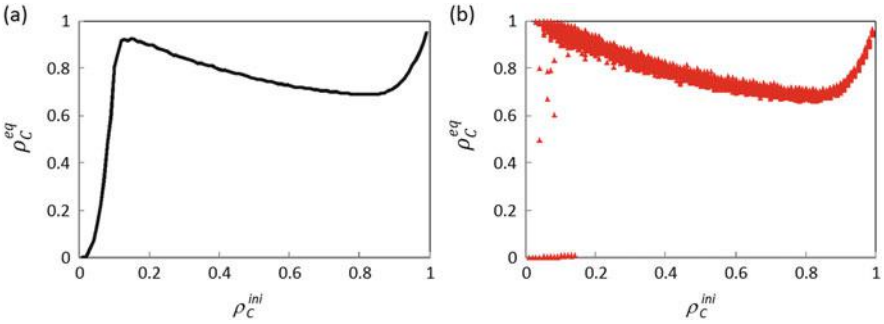

Fig. 3.13 Equilibrium fraction of cooperators ρ_C^{eq} in dependence on the density of initial cooperators ρ_C^{ini} on the square lattice network with $k = 4$ and IM rule. Panel (**a**) illustrates the average fraction of cooperators, while (**b**) corresponds to the level of cooperation reached in each of the 100 realizations. Depicted results are obtained for $r = 0.2$

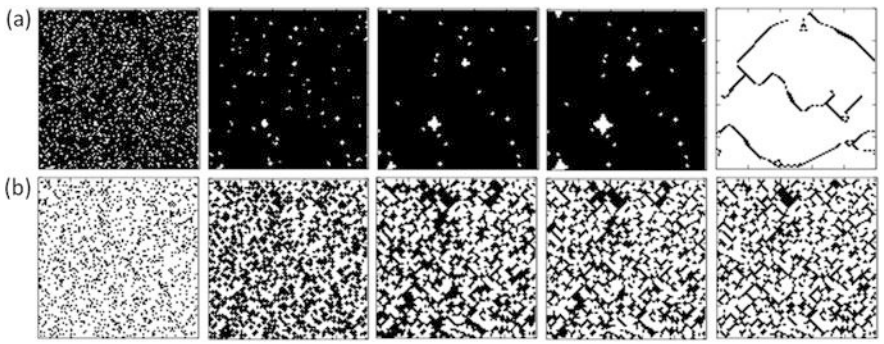

Fig. 3.14 Evolutionary snapshots for cooperators (*white*) and defectors (*black*) under different initial fraction of cooperators: (**a**) $\rho_C^{ini} = 0.15$ and (**b**) $\rho_C^{ini} = 0.85$. From left to right, the snapshots are given at $t = 0$, 1, 3, 5, 100 steps for all panels. Depicted results are obtained for $r = 0.2$

phenomena, we quantitatively explore the characters of microscopic evolution dynamics.

Figure 3.14 presents characteristic evolution snapshots of cooperators and defectors for different initial fractions of cooperators; (a) $\rho_C^{ini} = 0.15$ and (b) $\rho_C^{ini} = 0.85$, respectively. In the case of low initial cooperation fraction, the system rapidly falls into the state of numerous defectors. However, at the end of EXP period, a few C-clusters can successfully survive under the exploitation of free-riders, and then these remaining C-clusters start recovering lost ground against weakened defectors. During the END period, a defector is always ready to change its status and tries to penetrate into the C-clusters, which finally yields the exclusive dominance of cooperators. On the other hand, for large initial value of ρ_C^{ini}, a great number of C-clusters can survive during the END period. But these C-clusters mutually hinder the expansion of others in EXP period (namely, can not expand

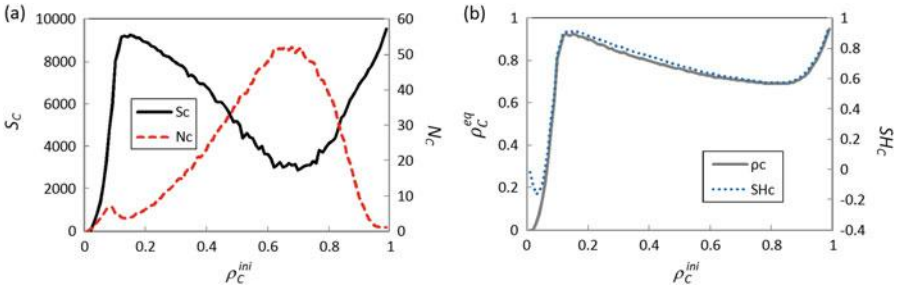

Fig. 3.15 Macroscopic features for the cluster characteristics and the equilibrium fraction of cooperators. Panel (**a**): cluster size S_C and cluster number N_C as well as (**b**): equilibrium fraction of cooperators ρ_C^{eq} and cluster shape SH_C in dependence on the initial fraction of cooperators ρ_C^{ini}. Depicted results are obtained for $r = 0.2$

enough smoothly), which thus induces many remaining defectors surrounding the C-clusters.

Furthermore, we quantify the effect of ρ_C^{ini} from the viewpoint of cluster characteristics. Figure 3.15 features how three C-cluster characteristics and the equilibrium fraction of cooperators change versus initial fraction of cooperators. In the region of $\rho_C^{ini} \approx 0.15$, where the cooperation reaches the optimal state, both cluster size S_C and cluster shape SH_C also obtain their maximum values. On the contrary, cluster number N_C shows its minimum value. This means that the formed C-clusters in the END period can most effectively expand and even dominate the whole system. In order to further support our results, we examine the time course for fraction of cooperators and three cluster characteristics under different initial fractions of cooperators in Fig. 3.16. For $\rho_C^{ini} = 0.15$, during both END and EXP periods, the cluster size S_C and the cluster shape SH_C monotonically increase, while the cluster number N_C decreases (see Fig. 3.16(a), (b)). Correspondingly, in the case of $\rho_C^{ini} = 0.85$, the cluster size S_C and the cluster shape SH_C decrease, while the cluster number N_C increases during the END period, However, concerned with the EXP period, the cluster size S_C and the cluster shape SH_C start to increase, the cluster number N_C decreases (see Table 3.2). It is interesting that the change of evolution trend for cluster characteristics prevents the smooth expansion of C-clusters in EXP period. Thus, the consistency of trend for three cluster characteristics during END and EXP periods may be seen as an effective index to estimate whether the initial state is able to bring a highly cooperation equilibrium.

3.2.4 Summary

We have investigated the effect of initial fraction of cooperators on the equilibrium level of cooperation. Our results show that when regular network is assumed as the underling topology, an interesting phenomenon takes place: relatively low initial fraction of cooperators can lead to a higher level of cooperation at equilibrium. To

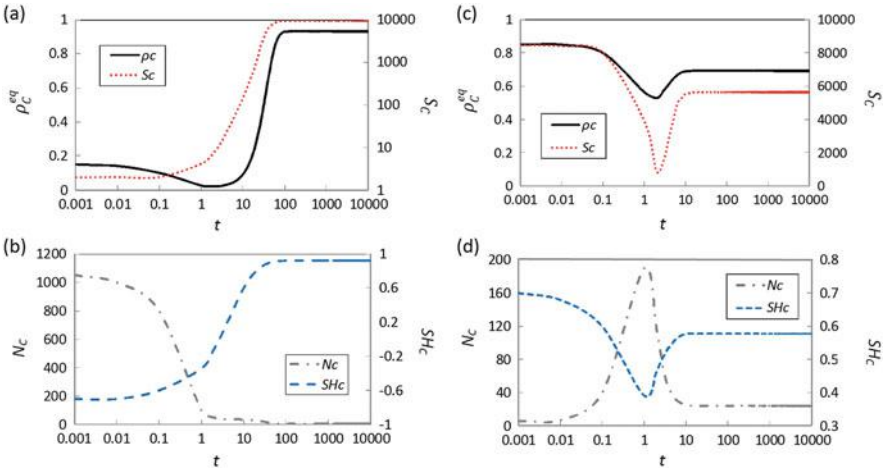

Fig. 3.16 Time evolution of the fraction of cooperators (*top row*, *black solid line*), cluster size (*top row*, *red dotted line*), cluster number (*bottom row*, *gray dashed-dotted line*) and cluster shape (*bottom row*, *blue dashed line*) for $\rho_C^{ini} = 0.15$ (*left*) and $\rho_C^{ini} = 0.85$ (*right*) when assuming $r = 0.2$. Each of the time evolution curves indicates an ensemble average of 100 realizations

Table 3.2 Cluster characteristics (cluster size, cluster number and cluster shape) for two different initial fractions of cooperators $\rho_C^{ini} = 0.15,\ 0.85$

$\rho_C^{ini} = 0.15$	END	EXP
S_C	Increase	Increase
N_C	Decrease	Decrease
SH_C	Increase	Increase
$\rho_C^{ini} = 0.85$	END	EXP
S_C	Decrease	Increase
N_C	Increase	Decrease
SH_C	Decrease	Increase

Note that in the case of $\rho_C^{ini} = 0.15$, the tendency of three cluster characteristics is same from END to EXP period, on the other hand, in the case of $\rho_C^{ini} = 0.85$, the tendency of three cluster characteristics is different with END from EXP period

support this, we examine the time courses. We find that for low initial fraction of cooperators, a few C-clusters can survive during the END period. And, in the following EXP period, these C-clusters expand smoothly till they dominate nearly the whole system. On the other hand, when one starts from a high initial fraction of cooperators, a great number of C-clusters survive during END period. But these C-clusters can not guarantee the prosperity of cooperation because they mutually hinder the expansion of other clusters in the EXP period. Moreover, we study the performance of three cluster characteristics: cluster size, cluster number and cluster shape under different initial cooperation setup. If one observes coherent tendency of those three cluster characteristics in both END and EXP periods, the scope of cooperation could be extended.

3.3 Several Applications of Stronger Network Reciprocity

As mentioned previously, there has been huge number of papers dealing with network reciprocity for last several years. Due to our space limitation, this book does not touch each of those respectively, but a reader who is interested can consult with the affluent stock of those papers that can be reached by a retrieval termed with "network reciprocity & games" at Web of Science for example. Each of them insists that a new model enhanced network reciprocity is found, which might be likened a situation of "bells-and-whistles", in which one new attractive and interesting model is reported after another, while no holistic picture to persuade what network reciprocity is. On this point, as profoundly declared at the ground summary provided at the beginning of this chapter, we discuss in the next section. Before entering the "main-event", I think it would be a good idea that we discuss several models to strongly enhance network reciprocity reported by recent works.

3.3.1 Co-evolutionary Model

One important model is the so-called co-evolutional model (e.g., Szolnoki and Perc 2009a, b). Although we do not note detail, let me give an overview about co-evolutionary models.

As mentioned in the Sect. 2.1, many previous studies have insisted that degree-heterogeneous networks, such as scale-free (SF) networks, generate more robust cooperation than regular networks, because the degree-heterogeneous networks can bring hub cooperators (hub C agents) which compel cooperation among their neighbors, leading to strong and stable cooperation.

Those previous studies were based on a framework, where agents are initially allocated to a fixed network. Zimmermann and Eguiluz (2005), who is a precursor with respect to co-evolutionary games, demonstrated a variant of a co-evolutionary system in a networking game considering simultaneous evolution of networks and strategies. The co-evolution model might enable more robust cooperation than fixed network games and shed light on what network type is adaptively appropriate for cooperation to emerge. In fact, by applying this model to several PDs, they observed a stable cooperation phase when a cooperative hub agent (the C Leader) emerged, resulting in a SF degree-heterogeneous network, even though starting from a random network.

Following Zimmerman's milestone study, many studies on co-evolution models have been undertaken,[3] mainly in the field of physics. Poncela and her colleagues (2008) assume dynamic networks with growing degrees (i.e., those growing network models involving an increase in the social size). However, most previous

[3] A reader can find many literatures. Among those, we only cite, here, only four works as below: Tanimoto (2007a), Li et al. (2007), Fu et al. (2009), Chen et al. (2009).

works including that of Zimmermann, presume dynamic networks with the total number of links frozen, which signifies that the number of agents and links are preserved. Tanimoto (2009, 2010) discovered that with a relatively weak dilemma, the adaptation process favors non-deviated (relatively regular) networks with positive assortative mixing[5]; however, in a relatively strong dilemma, network adaptation favors degree-heterogeneous topology with negative assortative mixing. Pacheco et al. (2006) and Santos et al. (2006a, b) found that robust cooperation can be observed when the speed of network adaptation is greater than the speed of strategy adaptation. This can be explained by the fact that network adaptation can expel neighboring D agents effectively and quickly by severing links with them, which serves the same function as the Game Exiting Option (e.g., Schuessler 1989). Namely, for defending a C cluster from D agents' attacks, immediately severing links with D agents is more effective than instigating D against D agents as retaliation. Van Segbroeck et al. (2009) and Szolnoki and Perc (2009a, b) are concerned with link-severing procedures of the network dynamics and with procedures to build new links after severing by means of deductive and numerical approaches. Their approach illuminates how significantly the network dynamics affects network reciprocity. Moreover, Pestelacci et al. (2008) study an endogenous criterion for severing and rewiring links.

Meanwhile, a relevant novel study was reported by Moyano and Sanchez (2009), who introduced a different type of co-evolution model. Their model permits strategy plus strategy updating rules (not for network) to evolve. An agent copies a strategy from her neighbors' sets (including the focal player) based on a selected updating rule. At the same time, the agent copies the update rule itself from the selected neighbor to copy the strategy. Moyano and Sanchez presume three different variants of updating rules: Imitation Max (IM), in which a focal player copies the strategy of the neighbor receiving the largest payoff in the current time step; Pairwise (PW), in which a player compares his or her payoff with that of a randomly selected neighbor and copies that neighbor's strategy according to a certain function; and pairwise comparison with all neighbors, which is analogous to Roulette Selection (RS). There are differences in how these three rules contain stochastic characteristics in the process of selecting opponents. Needless to say, IM is defined as deterministic in selecting opponents (there is no choice of copying from the best-payoff neighbor), whereas PW is entirely stochastic.

If we suppose a situation in which there is a spatial distribution of updating rules adopted by respective agents in a network, then we may consider that the strategy adaptation speed is also spatially distributed. This is because a stochastic updating rule implies lower strategy adaptation speed vis-à-vis a deterministic updating rule. This particular spatial distribution of strategy adaptation speed might help a C cluster grow, since a lower strategy adaptation speed avoids D diffusion among C agents (although it also prevents C dissemination among D agents). In the initial stage of an evolutionary trail, the question of how the network can prevent D diffusion rather than propel C diffusion is crucially important for sustainable cooperation, because the former determines whether C clusters can survive by

enduring initial D agents' attacks. Moyano and Sanchez (2009) assume time-constant networks. In that respect, their model differs from the co-evolutionary model for both strategy and network by Pacheco et al. (2006) and Santos et al. (2006a, b), but the principle underlying those two different models seem analogous. This is because quick-severing links with D agents prevents D diffusion, allowing C clusters to survive by avoiding D attacks in the early stage of evolution. According to the discussion above, like network adaptation, update rule adaptation might be an important factor for exploring network reciprocity.

Returning to co-evolution models, Van Segbroeck et al. (2009) and Szolnoki and Perc (2009a, b) decompose network adaptation into a severing process and a link re-building process, and they investigate network reciprocity by changing sub-rules for severing links for respective agents. Taking their work a step forward, we investigate another adaptation. Namely, if we define severing probability in network adaptation as one of the adaptation variables, each agent can control network adaptation speed against strategy adaptation speed to adapt more appropriately to circumstances. Among other pioneering works, in Kirchkamp's model (Kirchkamp 1999) both strategy and strategy adaptation mechanisms can evolve.

To that end, Tanimoto investigated what happens if the degree of freedom in an evolutionary trail would be enhanced by adopting adaptation variables other than agents' strategy and network topology, where a quadruple co-evolution model was established that makes an agent's four attributes evolve: strategy, network, update rule, and link-severing probability (Tanimoto 2011). He elucidated that the impact of network adaptation is dominant in enhancing cooperation. The impact of severing probability adaptation is secondary and that of update rule adaptation is negative. Thus, the double co-evolution framework that allows both strategy and topology to evolve is most important in terms of co-evolution.

3.3.2 *Selecting Appropriate Partners for Gaming and Strategy Update Enhances Network Reciprocity*

Concerning the detailed content discussed in this section, one should consult with Tanimoto (2014). Recently, researchers have been heavily concerned with identifying frameworks that can be added to the baseline model and that can realize the heightened levels of cooperation brought about by network reciprocity.

Reminding what we discussed in Fig. 3.11, this enhancement can be substantially understood by how the new model framework (a) can—at the beginning of a simulation episode—reduce defector invasions into cooperator clusters constructed by random allocation and (b) can encourage prosperous expansion of the surviving cooperator clusters in the neighboring sea of defectors as the global cooperation fraction (P_c) increases. The termed the initial period in which P_c decreases as the

enduring (END) period and the following period in which P_c increases as the expanding (EXP) period.

Among the many previous papers, it seems worthwhile to note two outstanding ideas to foster network reciprocity.

One is stochastically skewed selection of a pairwise opponent in the strategy adaptation process by using Fermi functions (Wang and Perc 2010; Perc and Wang 2010; Tanimoto et al. 2011). In this approach, more significant cooperation occurs if a pairwise opponent, chosen as a reference for comparison, is selected, not by random selection from all neighbors, but by a nonlinear proportional procedure applied to the payoff of each neighbor. Wang & Perc and also Tanimoto et al. confirmed that more significant cooperation can be attained if a high-payoff neighbor is selected as a pairwise opponent. For the second idea, perhaps inspired by these results, Brede (2011) investigated what happens if the focal player stochastically selects a gaming opponent at every game, instead of gaming with each neighbor; the number of neighbors is consistent with the degree of the focal player. He found outstanding enhancement of cooperation when a neighbor with a positively large payoff difference over the focal player was chosen more frequently. At a glance, these two ideas seem completely different but are analogous if we notice that the former idea addresses what happens when a stochastically skewed selection of an adaptation reference is presumed instead of random selection, and that the latter addresses what happens when a stochastically skewed selection of a gaming opponent is implemented.

The basic purpose of the discussion in this section is to determine what happens and how cooperative equilibrium comes about if both stochastic skewed processes, one for strategy adaptation and the other for gaming, are implemented simultaneously, potentially expecting to find a significant enhanced network reciprocity than usual one. This might be a plausible scenario in real human societies, considering that a human tends to select, among several potential neighbors, one or two (or a few, anyway) favorable neighbors as friend(s); further, her/his manner is more likely to be influenced by those few particular friends than by the other neighbors.

3.3.2.1 Model Setup

At every timestep, an agent on a network plays prisoner's dilemma (PD) games with neighbors varying $0 \leq D_g \leq 1$ and $0 \leq D_r \leq 1$ at Eq. (3.1) and obtains payoffs from all games. As the underlying topology, we use a two-dimensional lattice graph of degree $k = 8$, which means Moore neighborhood. The total number of agents is set to $N = 10^4$, confirmed as sufficiently large to yield simulation results that are insensitive to system size. After gaming, each agent updates his/her strategy synchronously. The boundaries of the system are looped, which implies all agents have 8 neighbors.

3.3.2.2 Selection of a Game Opponent and an Adaptation Reference

We presume two methods to implement stochastically skewed selection of a gaming partner and an adaptation reference. Namely, following Eqs. (3.3) and (3.4) are used alternatively for game/ reference partner selection.

The first one is what Brede (2011) did in his model, which we hereafter call "*B*" Brede assumed that an agent x selects agent y as a partner with probability P_y^B proportional to the payoff difference between agent x and each of k neighbors,

$$P_y^B = \frac{1/\left[1+\exp\left(w^B \cdot \left(\pi_y - \pi_x\right)\right)\right]}{\sum_{j\in\{N_x\}} 1/\left[1+\exp\left(w^B \cdot \left(\pi_j - \pi_x\right)\right)\right]}. \tag{3.3}$$

Here, π is the accumulated payoff, $\{N_x\}$ is the set of neighbors for agent x, and w^B is the skewed weight. If w^B is negative (positive), a neighbor who has a larger (smaller) payoff difference with agent x is more likely to be selected.

The second method is originally implemented by Wang & Perc (2010), hereafter referred to as "*W-P*" They assumed that an agent x selects agent y as a partner with probability P_y^{W-P} proportional to the payoff of each of k neighbors,

$$P_y^{W-P} = \frac{\exp\left(w^{W-P} \cdot \pi_y\right)}{\sum_{j\in\{N_x\}} \exp\left(w^{W-P} \cdot \pi_j\right)}, \tag{3.4}$$

where w^{W-P} is the skewed weight. If w^{W-P} is positive (negative), a neighbor who has a larger (smaller) payoff is more likely to be selected.

At every timestep, an agent plays a PD game k times. Unlike a conventional SPD game in which each agent plays a PD with one neighbor after another, our model lets each agent select a game partner at every time based on either *B* or *W-P*. When the weight ($w_{int}^B = 0$ or $w_{int}^{W-P} = 0$) is assumed 0, a game partner is randomly chosen among all neighbors every time; this would almost recover the conventional SPD.

After gaming, agents accumulate all payoffs and synchronously update their strategies. Based on either *B* or *W-P*, each agent first selects an opponent to compare mutually accumulated payoffs; this identifies the adaptation reference (*W-P*) or adaptation partner (*B*). Then, the focal agent x may or may not copy the strategy of pairwise opponent y based on a pairwise Fermi function (Fermi-PW). This decision is based on the difference in payoff between x and y, $p_{copy}^{x\leftarrow y} = 1/\left[1+\exp\left(\frac{\pi_x - \pi_y}{\kappa}\right)\right]$. When the weight ($w_{ad\,p}^B = 0$ or $w_{ad\,p}^{W-P} = 0$) is assumed 0, the model exactly recovers the conventional Fermi-PW process. In this study, we assumed $\kappa = 0.1$.

Let us confirm one important point. That is, our model is run such that each agent selects k gaming partners in a row before selecting an individual reference partner.

3.3.2.3 Simulation Procedure

Each simulation was performed as follows. Initially, an equal percentage of strategies was randomly distributed to the agents allocated on different vertices of the network. Several simulation timesteps, or generations, were run until the frequency of cooperation reached quasi-equilibrium. If the cooperation frequency continued to fluctuate, we used the average frequency of cooperation over the last 250 generations of a 10,000-generation run. We varied the dilemma strength to cover PD, $0 \leq D_g \leq 1$ and $0 \leq D_r \leq 1$. The results shown below were drawn from 100 runs; that is, each ensemble average was formed from 100 independent simulations.

3.3.2.4 Results and Discussion

Let us use the notation for the presumed weights; w_{int}^{B} (w_{int}^{W-P}) and $w_{ad\,p}^{W-P}$ ($w_{ad\,p}^{B}$) to imply selecting a game interaction partner and an adaptation reference, respectively. Figure 3.17 shows social average cooperation fractions for four cases: (a) conventional SPD, (b) $w_{int}^{B} = 1000$ and $w_{ad\,p}^{B} = -1000$, (c) $w_{int}^{B} = -1000$ and $w_{ad\,p}^{W-P} = 3$, and (d) $w_{int}^{W-P} = 3$ and $w_{ad\,p}^{W-P} = 3$. Regions where cooperation fraction is almost 1 and 0 indicate C-dominate and D-dominate respectively, while other area implies co-existence phase, in which both cooperators and defectors survive at equilibrium. In the work by Wang & Perc, $w_{ad\,p}^{W-P} = 3$ showed significantly strong enhancement of the cooperation fraction. In contrast, Brede used $w_{int}^{B} = -1000$ to enhance cooperation. The result for the conventional SPD in Fig. 3.17(a) represents the baseline of network reciprocity for a $k = 8$ lattice with synchronous strategy adaptation based on the Fermi-PW function. Figure 3.17 (b) shows that inappropriate assumptions for both weights devastate the original network reciprocity. Figure 3.17(c) and (d) show that, although $w_{int}^{B} = -1000$ enhances cooperation when B is used as the model for selecting a game partner, W-P with $w_{int}^{W-P} = 3$ shows somewhat better performance. This might be interpreted that stochastically choosing a game partner based on payoff enhances cooperation more than choosing a partner based on payoff differences with the focal agent. However, combining both stochastically skewed selection processes ((c) and (d)) shows much better cooperation than applying either of the two strategies independently.

As described before, one obvious difference in terms of basic concept is that B relies on payoff difference of a focal agent and neighboring agents while W-P refers to agents' payoff. Relating to this, because of their different mathematical definitions, W-P approach more exclusively favors the dominating agent than B approach does. Those points, to some extent, can explain the difference of Fig. 3.17(c) and (d). But, one point we would like to address is that combining both stochastically skewed selection processes may be able to thrust up further cooperation than applying either of the two independently, irrespective to whether W-P or B is presumed.

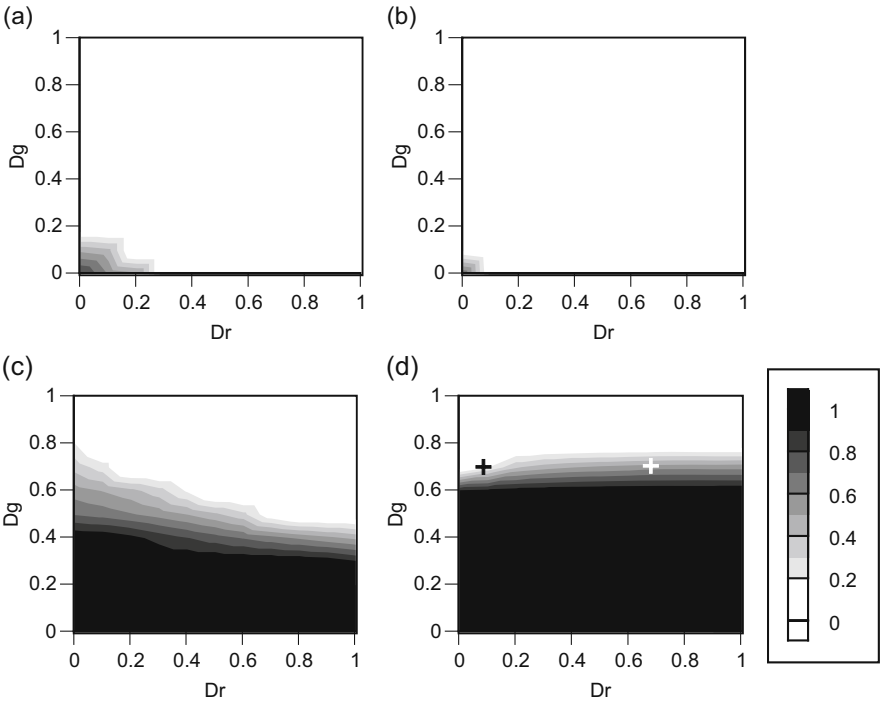

Fig. 3.17 Cooperation fractions ensemble-averaged over 100 realizations of PD with $0 \leq D_g \leq 1$ and $0 \leq D_r \leq 1$. (**a**) Conventional SPD, (**b**) using weights $= 1000$ and $= -1000$, (**c**) using weights $= -1000$ and $= 3$, (**d**) using weights $= 3$ and $= 3$. In panel (**d**), black cross is for $D_g = 0.7$ and $D_r = 0.1$, which is the subject of Figs. 3.21 and 3.23; white cross is for $D_g = D_r = 0.7$, which is the subject of Figs. 3.19 and 3.22

3.3.2.5 Effective Degree

To understand more precisely what is happening in our model, let us define a new characteristic value to measure the effectiveness brought about by network reciprocity. Although each agent has k links, because of the stochastically skewed selection, the number of active links is likely to be less than the nominal degree. By active links, we mean those that are heavily involved in gaming and strategy adaptation. Therefore, we define $S(j)$ to be the frequency with which the average agent chooses link j as a gaming/adaptation partner. Let us suppose a time-step. Each of N agents plays k games with her neighbors selected by the game partner selection process. Define *Agent j* as the j-th largest payoff neighbor among k neighbors, which globally means not indicating a particular neighbor of a particular agent among N agents. Taking the statistics over all N agents, we can evaluate how frequently *Agent j* is nominated as a game partner, which is the definition of $S(j)$ for the game partner selection process. Meanwhile, each agent selects one of her neighbors selected by the adaptation partner selection process. Thus, we can

also evaluate how frequently *Agent j*, who means the *j*-th largest payoff neighbor among *k* neighbors of any arbitrary agent, is nominated as a reference partner. This is the definition of $S(j)$ for the adaptation partner selection process. Then, we define the effective degree (*ED*) by

$$ED = k - k \sum_{j \in \{N_i\}} \mathrm{Max}\left[S(j) - \frac{1}{k}, 0\right]. \tag{3.5}$$

The concept for *ED* is illustrated schematically in Fig. 3.18. A small value for *ED* implies a situation in which the active links actually used for gaming or strategy adaptation are limited; thus, the actual anonymity vis-à-vis a well-mixed situation among agents is smaller than the nominal degree *k*.

Time evolutions of representative episodes over 100 realizations are shown in Fig. 3.19 for $D_g = D_r = 0.7$ when $w_{int}^{W-P} = 3$ and $w_{adp}^{W-P} = 3$, in Fig. 3.20 for $D_g = 0.1$ and $D_r = 0$ when $w_{int}^{B} = 1000$ and $w_{adp}^{B} = -1000$, and in Fig. 3.21 for $D_g = 0.7$ and $D_r = 0.1$ when $w_{int}^{W-P} = 3$ and $w_{adp}^{W-P} = 3$. In these figures, each panel (a) gives the cooperation fraction up to timestep 1000, and (b) indicates $S(j)$ and *ED*s for both gaming and adaptation at timesteps 3, 10, 50, 100, 250, 500, 750, and 1000. Each panel (c) shows (i) conditional probabilities for a cooperator (defector) selecting a cooperator as a game partner f_{CC_int} (f_{DC_int}) and as an adaptation reference f_{CC_adp} (f_{DC_adp}) and (ii) conditional probabilities that a cooperator (defector) has cooperators (defectors) among neighbors f_{CC} (f_{DC}).

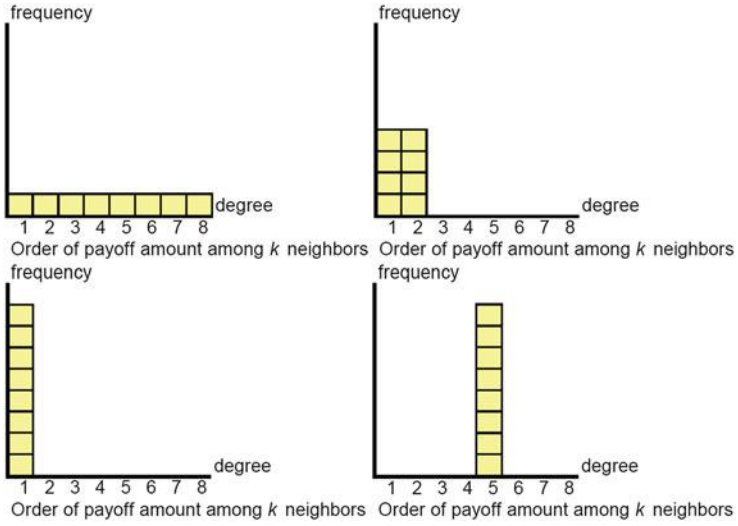

Fig. 3.18 Schematics illustrating effective degree (*ED*). Small values for *ED* represent situations in which only a limited number of active links are actually used for gaming or strategy adaptation

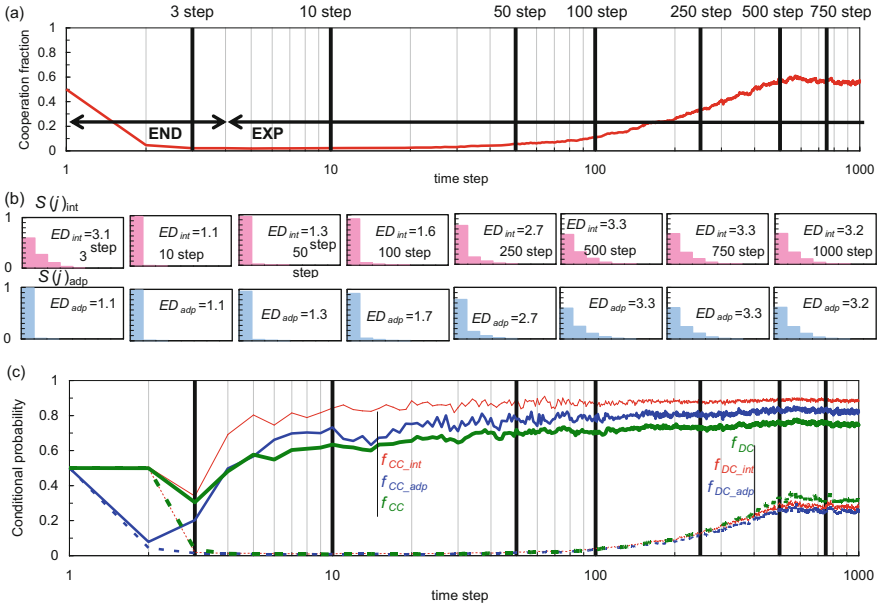

Fig. 3.19 Time evolution of representative episodes among 100 realizations for $D_g = D_r = 0.7$ when $= 3$ and $= 3$. Panel (**a**) shows cooperation fractions up to timestep 1000. Panel (**b**) gives $S(j)$ and ED for both gaming (*upper panels* with *red areas*) and adaptation (*lower panels* with *blue areas*) at timesteps 3, 10, 50, 100, 250, 500, 750, and 1000. Panel (**c**) shows conditional probabilities of a cooperator (defector) selecting a cooperator as a game partner f_{CC_int} (f_{DC_int}) (*red line* (*red dotted-line*)) and as an adaptation reference f_{CC_adp} (f_{DC_adp}) (*blue line* (*blue dotted-line*)). Also shown are conditional probabilities for cooperators among neighbors of a cooperator (defector) f_{CC} (f_{DC}) (*green line* (*green dotted-line*))

Figure 3.19(a) indicates that the model allows very small ED values near the end of the END period; this implies that agents successfully "endure" invasions of neighboring defectors by reducing the number of active links. More importantly, values of ED for both game partner and adaptation reference selections are almost unity, which is the minimum value; this means that the game partner chosen by a certain agent is also his/her adaptation reference at the same time. This complete correlation works much more positively to increase social viscosity than the nominal degree of the underlying network can provide as original network reciprocity. After this period (i.e., in the EXP period), ED tend to increase as the global cooperation fraction increases. This is because agents belonging to a C-cluster do not necessarily continue to limit game partners and adaptation references since there are fewer defectors around them. In Fig. 3.19(b), note that the model realizes $f_{CC} < f_{CC\_int}$ during the END period; this implies that cooperators in a C-cluster, i.e., agents who facing defectors in particular, tend to select cooperators for gaming. This helps them avoid being exploited by neighboring defectors. Also, during the EXP period, there occurs the rigid relation $f_{CC} < f_{CC\_adp}$; this means that

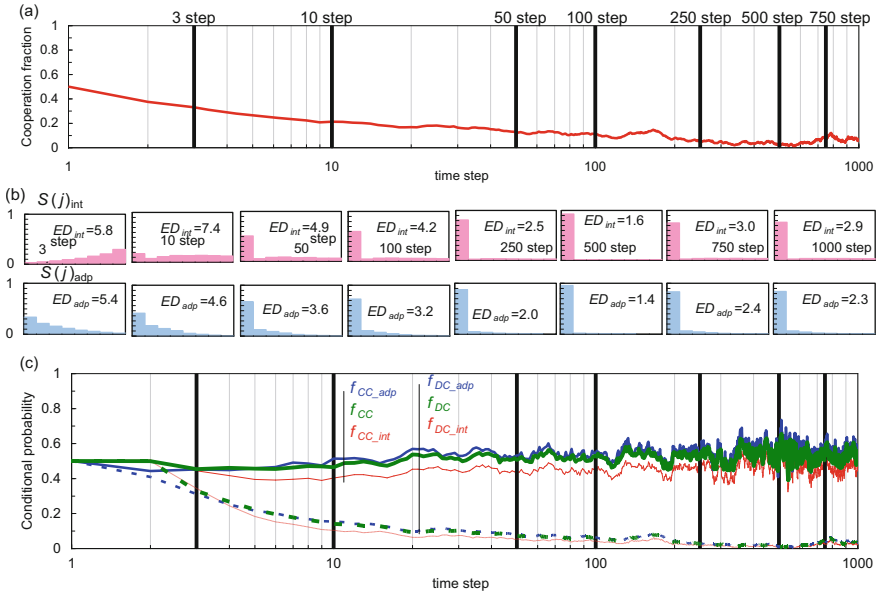

Fig. 3.20 Time evolution of representative episodes among 100 realizations for $D_g = 0.1$ and $D_r = 0$ when $= 1000$ and $= -1000$. Keys to panels and lines are the same as in Fig. 3.19

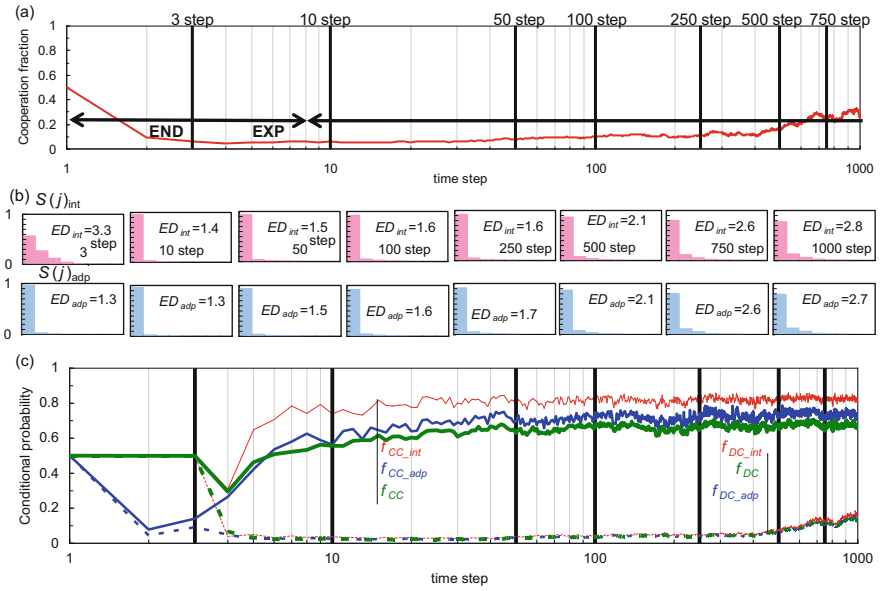

Fig. 3.21 Time evolution of representative episodes among 100 realizations for $D_g = 0.7$ and $D_r = 0.1$ when $= 3$ and $= 3$. Keys to panels and lines are the same as in Fig. 3.19

cooperators tend to select cooperators for pairwise opponents, leading to the situation in which a cooperator facing defectors can ignore the option of converting his/her strategy to defection.

In contrast to Fig. 3.19, for the situation in Fig. 3.20, agents fail to establish cooperation because of the large values for ED and because $f_{CC} > f_{CC\_int}$. One important point in this case is that distributions of $S(j)$ for both gaming and adaptation are inversely correlated with each other at early stages of the evolution (timestep 3); this occurs because the values assigned to w^B_{int} and $w^B_{ad\,p}$ were mutually conflicting. Namely, $w^B_{\text{int}} = 1000$ realizes that a neighbor of negative payoff difference over a focal agent; relatively small payoff neighbor in other words, is selected. Whereas, $w^B_{ad\,p} = -1000$ invites that a neighbor of positive payoff difference over a focal agent; relatively large payoff neighbor in other words, is selected.

3.3.2.6 Rather Bleak Environment During END Helps Cooperation?

Let us return to Fig. 3.17(d). Notice the curious fact that a critically severe dilemma ($D_g = D_r = 0.7$, highlighted with the white cross) shows rather higher cooperation than a relatively less severe dilemma ($D_g = 0.7$ and $D_r = 0.1$ highlighted with the black cross). Why is this possible? Figs. 3.19 and 3.21 show that the equilibrium cooperation fractions for D_g and D_r are 0.563 and 0.247, respectively, while the ensemble averages over 100 realizations for those two dilemma conditions, shown in Fig. 3.17(d), are 0.565 and 0.196, respectively. Let us also note that both timesteps 6 in Fig. 3.22 and 8 in Fig. 3.23 are the end of END period with 9 and 25 C-clusters surviving, of which instantaneous cooperation fractions are 0.02 and 0.05, respectively.

Figures 3.22 and 3.23 show snapshots of those two cases. Both panels (d) in Figs. 3.22 and 3.23 show the time evolutions of number of C-clusters and their averaged size with cooperation fraction. Figure 3.23 shows that the less-severe dilemma case ($D_g = 0.7$ and $D_r = 0.1$) allows more C-clusters to survive until the end of the END period than does the more-severe dilemma case (Fig. 3.22; $D_g = D_r = 0.7$). This is thought to be the crucially important point that explains the behaviors in those two cases. If a huge number of small-size C-clusters survive through the END period, then the following EXP period ends with a relatively low level of cooperation. This is perhaps because, as the C-clusters start expanding into the surrounding sea of defectors, the C-clusters inevitably interfere with each other; this allows many defectors to survive in the many chasms between C-clusters, allowing them to exploit different C-clusters. This illustrates one possible scenario by which strong network reciprocity comes about. Namely, a rather bleak situation during the END period may be able to bring about high cooperation at the end of an evolutionary process. However, if the environment is too bleak, the situation is counterproductive because no C-clusters survive the END period, which in turn

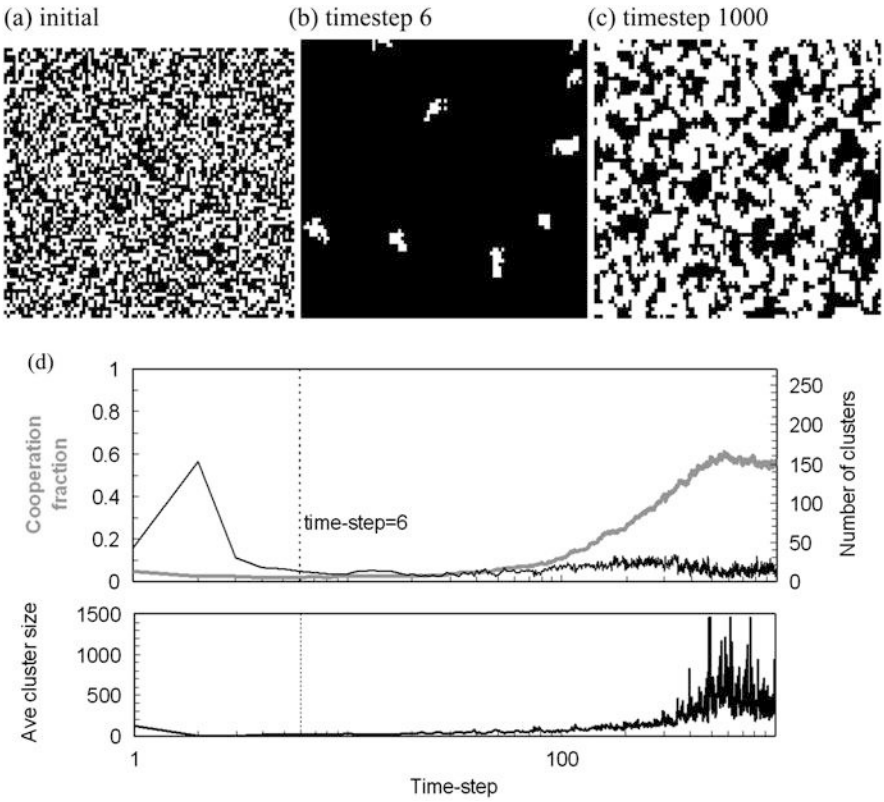

Fig. 3.22 Snapshot of representative episodes for $D_g = D_r = 0.7$ when $= 3$ and $= 3$, which is shown in Fig. 3.19. *Black* and *white* indicate cooperators and defectors, respectively. Timestep 6 is the end of the END period. Panel (**d**) shows time evolutions of cooperation fraction, number of clusters and averaged cluster size in this episode. (**a**) initial (**b**) timestep 6 (**c**) timestep 1000

leads to an undesirable equilibrium containing only defectors. Thus, a reasonably bleak environment in which a single C-cluster survives, ideally speaking, is most preferable for realizing high cooperation.

3.3.2.7 Summary

We established a new model for the spatial prisoner's dilemma game in which an agent selects a game partner and an adaptation reference independently using a stochastically skewed selection process based on the partner's payoff among her neighbors. This model can emulate relationships in a real human society because a human tends to select one or two favorable friend(s) from among the many potential acquaintances provided by a social network.

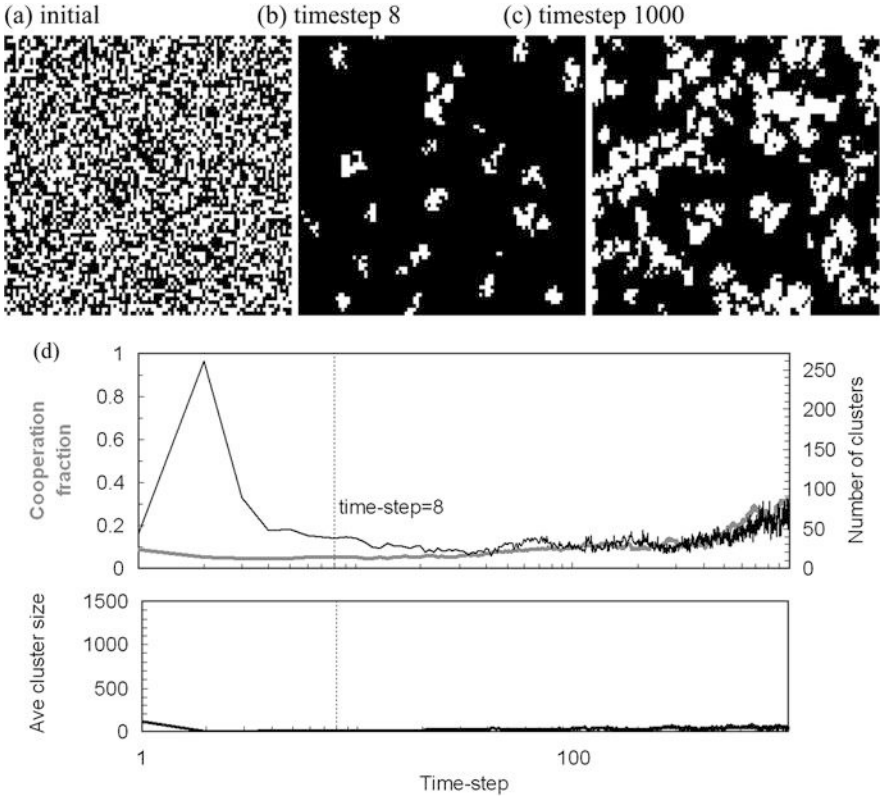

Fig. 3.23 Snapshot of representative episodes for $D_g = 0.7$ and $D_r = 0.1$ when $= 3$ and $= 3$, which is shown in Fig. 3.21. *Black* and *white* indicate cooperators and defectors, respectively. Timestep 8 is the end of the END period. Panel (**d**) shows time evolutions of cooperation fraction, number of clusters and averaged cluster size in this episode. (**a**) initial (**b**) timestep 8 (**c**) timestep 1000

We showed that the model can significantly enhance cooperation by implementing both stochastically skewed selection processes with appropriate parameters to ensure that high-payoff neighbors are more frequently selected as a partner. This claim is justified by our finding that agents reduce their degrees of real activity, which can be measured by *ED*. Generally speaking, small degrees of activity limit anonymity in interactions with neighbors, which in turn can lead to stronger network reciprocity.

By tuning our model, phenomenally enhanced cooperation can be realized in which only a small number of C-clusters survive the END period; this assures prosperous and smooth expansions of C-clusters into the sea of defectors in the following EXP period. This appears to be the most important factor that determines how network reciprocity can be bolstered in SPD models, and perhaps this factor captures the substance of how network reciprocity really works. Although this was drawn from our present result as a likely mechanism to highlight on how the

so-called network reciprocity really works, the idea still stays at hypothetic stage. Thus, further well- intrigued statistical analysis and even deductive approach should be expected in our future works.

3.4 Discrete, Mixed and Continuous Strategies Bring Different Pictures of Network Reciprocity

The discussion so far has assumed one central premise that the strategy of game players is defined by binary; namely either cooperation (C) or defection (D). A question everyone wonders is whether this central assumption is appropriate or not. In fact, we know lots of proofs indicating what happening in real world differs. In some situations, not only extreme two options either C/ D but also middle course offers like fairly cooperative, neutral, little bit defective etc. might be allowed, although the definition of binary strategy, let us call "discrete strategy" for the sake of following discussion, seems reasonable to start the discussion, and still meaningful for a first approximation to capture what happens in the assumed dynamical systems. Let us call this "continuous strategy", where a strategy is defined by a real number of [0,1] (0 and 1 meaning entire defection and cooperation respectively) and an actual offer is consistent with the strategy's real number. We there is another important strategy definition, which is the so-called mixed strategy, where a strategy is defined by a real number of [0,1] like continuous strategy but an actual offer is limited by binary C or D, that is determined with the strategy's real number in stochastic manner.

Recent works show that when the payoff of the continuous strategy model is a linear function, continuous setup poses the identical equilibrium with that of discrete protocol in the infinite well-mixed population (Vincent and Cressman 2000; Day and Taylor 2003). In addition, a recent investigation reports that a finite size of population can bring obvious different equilibria for continuous and discrete setups (Zhong et al. 2012). However, this is only suitable for the case of limited population. When the population size is sufficient large, the difference will become not so significant. Recalling that a finite population, instead of infinite, somehow adds Nowak's social viscosity even if the population is well-mixed, we can guess that network games, as another way of adding social viscosity, also brings different equilibria for continuous and discrete setups. If, moreover, more complex network is considered as the underlying interaction topology, what would happen? Inspired by these interesting questions, let us examine, in this section, how different strategy setups fare on complex networks, in particular, whether it promotes or hinders the evolution on cooperation (i.e., the development of network reciprocity).

3.4.1 Setting for Discrete, Continuous and Mixed Strategy Models

We consider the pairwise interaction game; 2×2 games as the archetype, that is described by Eq. (3.1) with $R = 1$, $P = 0$, chicken-type dilemma strength; D_g ($= P - S$), and stag hunt-type dilemma strength D_r ($= T - R$). When the discrete strategy is presumed, two players simultaneously have the choice between cooperation (C) and defection (D). If both cooperate (defect) they receive the reward R (the punishment P). If, however, one chooses cooperation while the other defects, the later gets the temptation T and the cooperator is left the sucker's payoff S.

With respect to continuous strategy, we assign each player i a random parameter s_i in the interval between zero to one to denote his strategy (the probability of cooperation). This setting is performed uniformly before the formal interaction. When player i plays the game with agent j, he can obtain the payoff;

$$\begin{aligned} \pi\left(s_i, s_j\right) \equiv & (S-P) s_i + (T-P) s_j + (P-S-T+R) s_i s_j + P \\ & = -D_r \cdot s_i + \left(1 + D_g\right) \cdot s_j + \left(-D_g + D_r\right) \cdot s_i \cdot s_j \ . \end{aligned} \tag{3.6}$$

This might be the simplest and most plausible setup, which expands the discrete strategy model but still uses the elementary payoff matrix.

When the mixed strategy is presummed, each agent i is still assigned with a real number $s_i \in [0, 1]$ as what to do in the continuous setup. But he can only offer either pure cooperation or defection as his strategy. That is, he chooses cooperation when $\mathrm{Rnd}[] < s_i$ otherwise he offers defection, where Rnd[] represents the random number obeying a uniform distribution.

3.4.2 Simulation Setting

Through this work we mainly study the spatial reciprocity in the prisoner's dilemma (PD) game, where $0 \leq D_r \leq 1$ and $0 \leq D_g \leq 1$ in Eq. (3.1) (See section "Supplemental discussion D"; latter, we discuss what happens in Chicken games). As the interaction networks, we use seven types of topology structure; (i) cycle; (ii) square lattice; (iii) homogeneous small world network (Ho-SW), which is made from a cycle graph by replacing several links with random shortcuts (a shortcut probability of 0.2); (iv) Watts–Strogatz's (1998) heterogeneous small world network (He-SW), which is generated from a cycle graph with swapping probability 0.2; (v) regular random network (RR); (vi) Erdos–Renyi random network (E-R) (Ballobas 1985); (vii) scale-free network (SF) constructed via the Barabasi–Albert algorithm (Barabashi and Albert 1999). For these networks, the total number of nodes N is 4900 and average degree $< k >$ is assumed to be 8 or 12. In particular, we do not consider the case of $< k > = 8$ on E-R, since the condition of a single clumpy network $< k > \geq \ln N$ is required.

The game is iterated forward in accordance with the sequential simulation procedure comprising the following elementary steps. In every time step, all the agents acquire their payoffs by playing the games with all their neighbors. Then, they synchronously update their strategy every τ step based on the accumulated payoffs during the last τ steps. Lastly, players mimic the strategy of agent who has the highest payoff among their neighborhoods (including themselves, this is the so-called Imitation Max rule, IM, as we mentioned before). We assume $\tau = 1$. We have approved that when $\tau \to \infty$ a mixed strategy model approaches to the continuous strategy setup, which might be acceptable for readers qualitatively (section "Supplemental discussion C").

Subsequently, we focus on the initial distribution of strategies in different models. For discrete setup, (without loss of generality) each player i is initially designated either as a cooperator ($s_i = 1$) or defector ($s_i = 0$) with equal probability, meaning initial cooperation fraction is 0.5. While for both continuous and mixed models, the uniform distribution of $s_i \in [0, 1]$ is performed in majority situations. But in certain cases, we use the prepared initial state: half of them are randomly chosen as the perfect cooperators (expressed by $s_i = 1$, similar to the pure cooperators in the discrete setup), others are perfect defectors (expressed by $s_i = 0$). The expected values of initial cooperation fraction for those two different ways are same as what the discrete setup assumes; 0.5. In order to make no practical difference with the above continuous and mixed models, we also consider the strategy mutation by adding a random number drawn from the Gaussian distribution (See section "Supplemental discussion A and B").

Results of simulations presented below were obtained by averaging out the final 5000 steps after the $2*10^4$ relaxation time, and the final results were averaged over up to 100 independent realizations for each set to guarantee the accuracy. We conduct this procedure at 11×11 points of the prisoner's dilemma (PD) area ($0 \leq D_g \leq 1$, $0 \leq D_r \leq 1$). As the characteristic values used to evaluate cooperation, we classify the prisoner's dilemma (PD) game into four subclasses. The first is a single algebraic average of the 121 ensemble averages covering all PD areas (AllPD). The second is an average of 11 points represented by $D_g = D_r$, which is so-called donor and recipient game (DRG). The third is another 11-point average collected from the region of $D_r = 0$, which consists of boundary game between the prisoner's dilemma game and chicken game without a stag-hunt-type dilemma (BCH). The last is another 11-point average collected from the region of $D_g = 0$, which consists of boundary game between the prisoner's dilemma and stag-hunt game without a chicken-type dilemma (BSH).

3.4.3 Main Results and Discussion

For comparison Fig. 3.24 features the average cooperation fraction under three types of setups: discrete, continuous, and mixed strategy model, remarkably, the

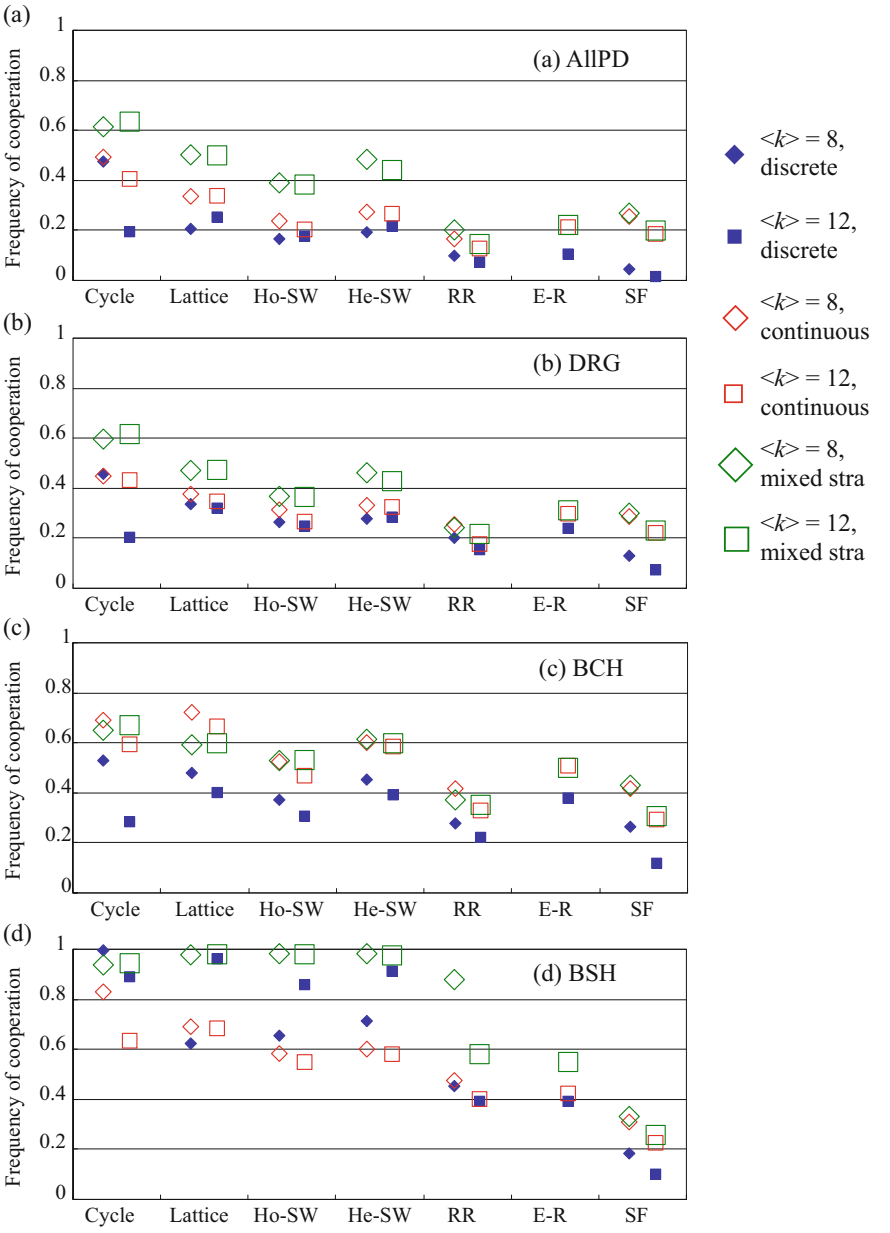

Fig. 3.24 Averaged cooperation proportion in different setups for (**a**) all PD games (AllPD), (**b**) Donor & Recipient Games (DRG), (**c**) boundary games between PD and Chicken (BCH), and (**d**) boundary games between PD and Stag-Hunt (BSH) within the limits of $0 \leq D_g \leq 1$ and $0 \leq D_r \leq 1$. The underlying interaction networks are cycle, lattice, Ho-SW, He-SW, RR, E-R and SF, respectively. Average degrees are 8 and 12 for these topologies. We adopt the Imitation Max (IM) as the strategy updating rule

equilibrium cooperation fraction varies widely. In the region of AllPD and DRG, the cooperation level of mixed model is highest, continuous model guarantees an intermediate level and discrete setup provides the least beneficial environment for the evolution of cooperation (Fig. 3.24(a) and (b)).

Cooperation among the three strategies is completely different depending on the dilemma subclass, BCH or BSH (Fig. 3.24(c) and (d)). Thus, in the following subsections, we discuss BCH and BSH separately. We restrict the almost all discussion to the lattice network with the degree $k = 8$, where the cooperation fraction is shown in Fig. 3.25 for each of the three strategies. Although not shown, what observed in the lattice seems general except for several cases.

Features in BCH

In BCH, equilibrium cooperation fractions of continuous and mixed strategy games are greater than those of discrete games (see lattice with $k = 8$ in Fig. 3.24(c)). In Fig. 3.25, we note that mid-level cooperation can be allowed for moderate strength dilemma games in continuous and mixed strategy systems (see highlighted areas within dashed-line boxes in Fig. 3.25(b) and (c)). In general, a situation with a relatively strong Chicken-type dilemma naturally tends to lead to what is considered internal equilibrium. In a discrete strategy game, players are not allowed to take a mid-cooperative strategy as in continuous and mixed strategy games but are forced to choose either C or D. Thus, a discrete strategy game rapidly declines from a state where all players offer C to a state where all offer D at a certain D_g, whereas continuous and mixed strategy games can maintain a moderate cooperation level even with a larger D_g. Relating to this, we note that continuous and mixed strategy games reveal lower cooperation levels than discrete games with a weak dilemma. This phenomenon has the following two causes. First, the proportion of perfect

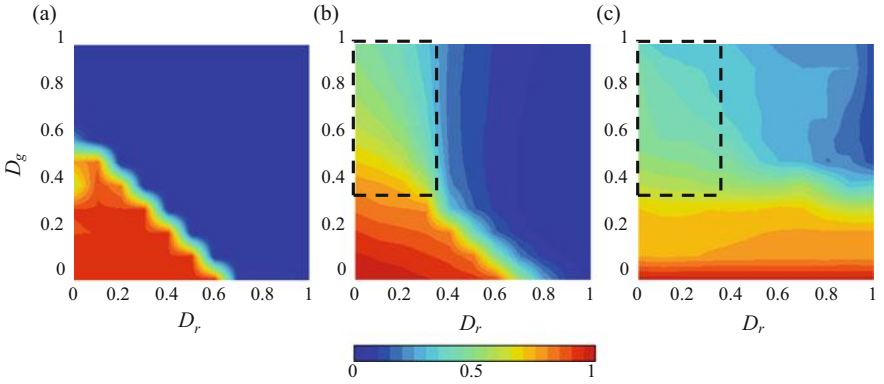

Fig. 3.25 Averaged cooperation proportion within the limits of $0 \leq D_g \leq 1$ and $0 \leq D_r \leq 1$ based on (**a**) discrete, (**b**) continuous, and (**c**) mixed strategy games. Games are played on 8-neighbor lattices ($k = 8$) with 4900 agents

cooperators in both continuous and mixed strategy games is lower than that of discrete games at the beginning of each simulation episode. If we provisionally define perfect cooperators as those who have $s_i > 0.9$, the proportion of perfect cooperators in continuous and mixed strategy games in the initial allocation is only 10 % (because we assumed uniform distribution within [0,1] for strategies in continuous and mixed strategy games). In contrast, the proportion of perfect cooperators in discrete strategy games at the beginning is 50 %. Second, at the beginning of an episode, neighbors of a perfect cooperator (defined by $s_i > 0.9$) possibly have lower strategy values than the focal perfect cooperator. Mean field approximation suggests that 90 % of neighbors of the perfect cooperator have more defective strategy than the perfect cooperator in continuous and mixed strategy games. In discrete strategy games, however, only 50 % of neighbors are more defective than the player. In summary, when assuming either continuous or mixed strategy, there are necessarily fewer perfect cooperators in the first place. In addition, these rare perfect cooperators might immediately copy a more defective strategy from relatively more defective neighbors. This fact inevitably causes scant cooperation even in weaker dilemma games than in a discrete strategy game.

Figure 3.26 shows the variance of equilibrium cooperation fraction among 100 episodes. The reason that we observe the moderately large variance close to BCH in a discrete strategy (the highlighted area in the dashed-line box in Fig. 3.26 (a)) indicates that bi-stable-like equilibrium occurs. In contrast, there is no larger variance area close to BCH in both continuous and mixed strategy games because a mid-cooperative strategy is allowed. Another highlighted area in the dashed-line box in Fig. 3.26(b) close to the BSH border in continuous strategy games also shows a large variance, which implies occurrence of bi-stable-like equilibrium.

Figure 3.27 shows equilibrium strategy distributions of continuous and mixed strategy games for BCH. It is worth noting that peak strategy gradually declines to the defective side with the increasing dilemma strength.

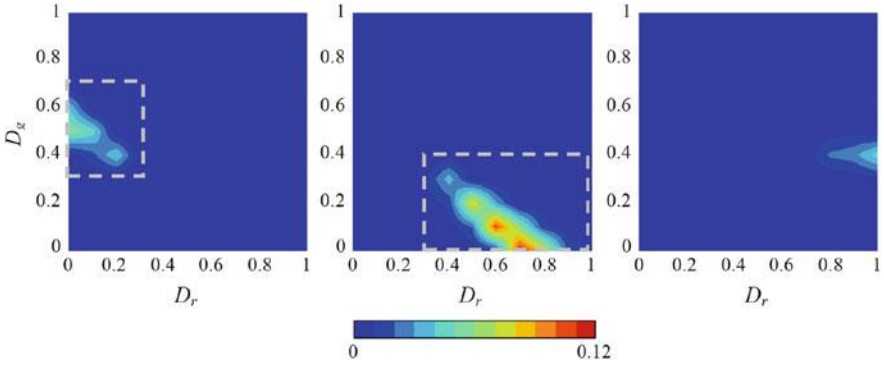

Fig. 3.26 Variance of equilibrium cooperation proportion among 100 trials within the limits of $0 \leq D_g \leq 1$ and $0 \leq D_r \leq 1$ based on (**a**) discrete, (**b**) continuous, and (**c**) mixed strategy games. Games are played on 8-neighbor lattices ($k = 8$) with 4900 agents

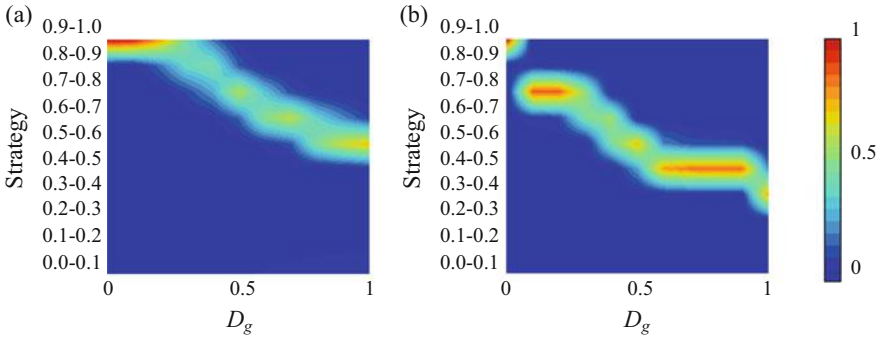

Fig. 3.27 Strategy distributions at equilibria for BCH based on (**a**) continuous and (**b**) mixed strategy games. Games are played on 8-neighbor lattices ($k = 8$) with 4900 agents

Therefore, one possible reason for the equilibrium cooperation proportion of continuous and mixed strategy games being greater than that of discrete games is that in continuous and mixed strategy games, agents are allowed to adopt mid-strategy values between perfect defection and perfect cooperation.

Summing up Figs. 3.26 and 3.27, we can infer that a PD game with a relatively larger Chicken-type dilemma naturally generates an internal equilibrium situation. Thus, a player, who is allowed to adopt mid-strategy values between perfect defection and perfect cooperation, as continuous and mixed strategy systems permit, can achieve the necessary internal equilibrium by having an appropriate real value strategy. By contrast, the discrete strategy inhibits the system from reaching that state because it provides only a binary option, either C or D. This situation can be explained as follows. In general, agents cannot establish a C-cluster in the Chicken dilemma games despite being able to in PD games. Thus, we observe not emerging C-clusters but strip-like C chunks in the Chicken games because building a C-cluster (the focal agent and all her neighbors offering C simultaneously) is less beneficial in solving a Chicken-type dilemma, where a player is forced to choose either C or D strategy. A player in continuous and mixed strategy games, however, can adopt a mid-cooperative (mid-defective) strategy, which might be consistent with internal equilibrium if a pure Chicken game is assumed. This encourages them to form mid-C clusters consisting of mid-cooperative strategies, which can establish reasonable cooperation (See section "Supplemental discussion D").

Features in BSH

Here, we compare three types of strategy games by focusing on BSH. Differences of equilibria between discrete and continuous strategy games are different from those between discrete and mixed strategy games (Fig. 3.24(d)). Thus, we divide the discussion of BSH into two parts, namely comparison between discrete and continuous strategy games and that between discrete and mixed games.

First, we compare discrete and continuous strategy game equilibria. The amounts of cooperation and degrees of difference in equilibrium cooperation levels vary between these two games according to the network topology. As opposed to the results for BCH, discrete strategy in BSH can be more cooperative than continuous strategy in major networks. One reason explaining this might be related to the fact that the Stag-Hunt-type dilemma leads a game to a particular bi-stable-like equilibrium. As mentioned in the previous sub-section, it is difficult for perfect cooperators in a continuous strategy game with several moderate cooperators to survive at the early stage of an episode. If a PD game with a relatively larger Chicken-type dilemma than a Stag-Hunt-type dilemma is assumed, players could maintain a certain level of cooperation by C-clusters formed by moderate cooperators who can endure the invasion of defectors. In contrast, when a PD with relatively larger Stag-Hunt-type dilemma than a Chicken-type dilemma is assumed, a player with mid-strategy value would be weeded out by perfect defectors, because the Stag-Hunt-type dilemma leads a game to a bi-stable-like equilibrium. Figure 3.28 shows equilibrium strategy distributions of continuous and mixed strategy games for BSH. It should be noted that a player holding mid-strategy value never exists at equilibrium. Consequently, for BSH, a continuous strategy game tends to attain an equilibrium composing only of more defectors than does a discrete strategy game. In short, existence of mid-strategy value players tends to encourage D-like behavior and prevent C-like behavior in BSH.

Next, we compare the equilibria of discrete and mixed strategy games. We can find a greater cooperation level in mixed strategy games than in discrete games in major networks. The following model scenario might occur. In a mixed strategy game, an agent probabilistically offers either C or D based on her real number strategy. As an example, let us assume that one Agent i whose strategy value is s_i plays with another agent j whose strategy value is s_j. When s_i is higher than s_j ($s_i > s_j$), agent j always achieves higher fitness than agent i in discrete and continuous strategy games. However, in mixed strategy games, agent i might be able to achieve higher fitness than agent j, because agent i might be able to exploit agent

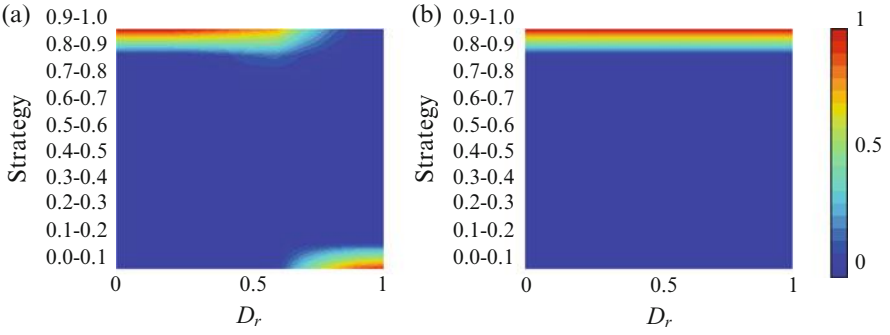

Fig. 3.28 Strategy distributions at equilibria for BSH based on (**a**) continuous and (**b**) mixed strategy games. Games are played on 8-neighbor lattices ($k = 8$) with 4900 agents

j by offering D against agent j's C, although that would occur less frequently. This "come-from-behind" victory for a more cooperative agent over a defective agent, occurring probabilistically, causes higher cooperation in the area close to BSH in a mixed strategy game because cooperative agents have the opportunity to survive by enduring invasion from neighboring defectors at the early stage in an episode. Figure 3.29 might prove this hypothesis, showing the survival of perfect cooperators (whose strategy values are higher than 0.9, $s_i > 0.9$) for initial second time steps.

However, we observe an exceptional result in BSH of an SF network, where the cooperation levels of continuous and mixed strategy games are almost consistent and larger than that of discrete games (Fig. 3.24(d)). Figure 3.30 shows the respective cooperation proportions within the limits of $0 \leq D_g \leq 1$ and $0 \leq D_r \leq 1$ based on discrete, continuous, and mixed strategy games, which are played on

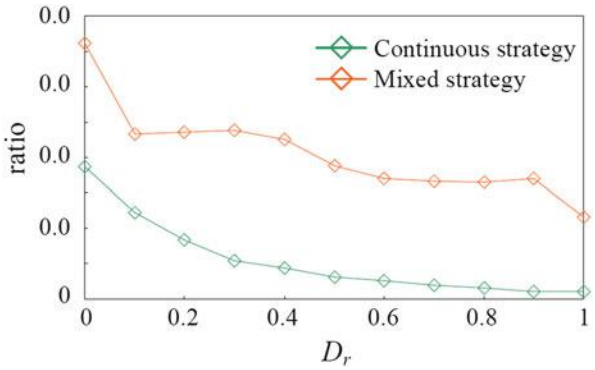

Fig. 3.29 Survival ratio of agents with cooperative strategy s_i, > 0.9 for BSH at the initial two time steps. Games are played on 8-neighbor lattices ($k = 8$) with 4900 agents

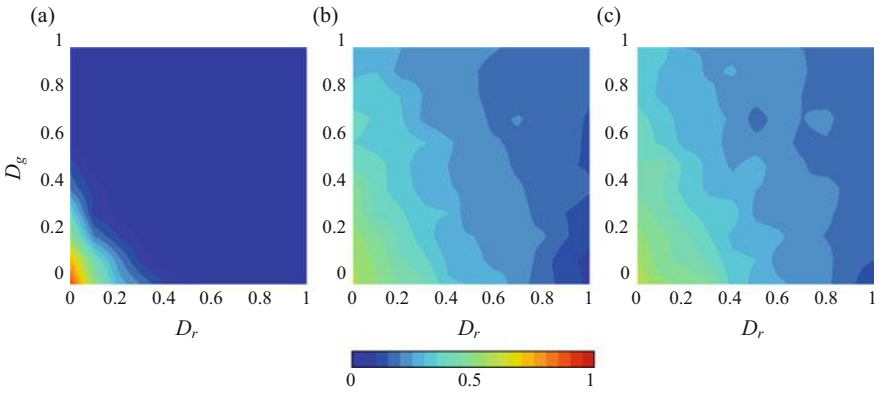

Fig. 3.30 Averaged cooperation proportion within the limit of $0 \leq D_g \leq 1$ and $0 \leq D_r \leq 1$ based on (**a**) discrete, (**b**) continuous and (**c**) mixed strategy games. Games are played on SF networks with the average degree $< k > = 8$

SF networks with the average degree $< k >= 8$. Compared with discrete strategy games, both continuous and mixed strategy games can maintain a moderate cooperation level even with larger D_g and D_r. By contrast, both continuous and mixed strategy games exhibit a cooperation level in a weak dilemma lower than that exhibited by discrete games. Following Figs. 3.30 and 3.31 shows the equilibrium cooperation proportion of each episode and the average cooperation proportion of 100 episodes for BSH. This completely differs from the result with a lattice (Fig. 3.28). Evidently, the equilibrium of each episode is not bi-stable but is various internal equilibria. Figure 3.32 shows the variance of the strategies of agents at the equilibrium. Except for strong Stag-Hunt-type dilemma games, we note that this internal equilibrium contains less deviated continuous strategy values (Fig. 3.32 (a) and (b)). From these results, we can infer the following. In general, hub agents

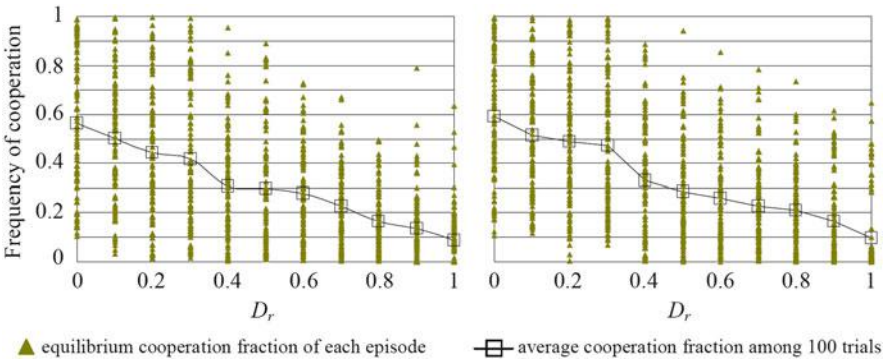

Fig. 3.31 Equilibrium cooperation proportion of each episode and average cooperation fraction of 100 trials based on (**a**) continuous and (**b**) mixed strategy games. Games are played on SF networks with the average degree $< k >= 8$

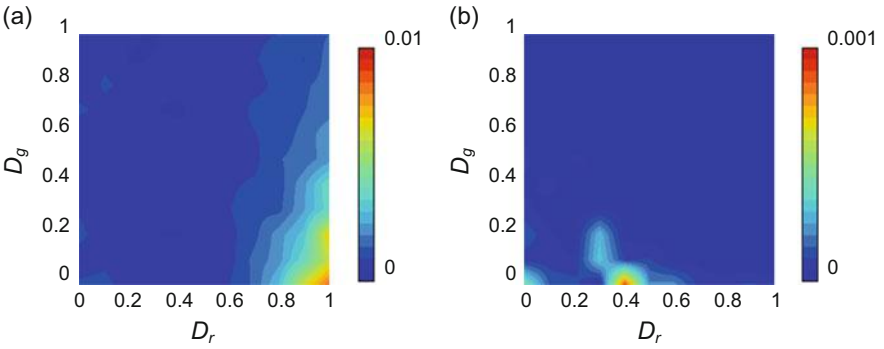

Fig. 3.32 Variance of strategy value at equilibrium within the limit of $0 \leq D_g \leq 1$ and $0 \leq D_r \leq 1$ based on (**a**) continuous and (**b**) mixed strategy games. These data are the average values of 100 trials. Games are played on SF networks with the average degree $< k >= 8$

having a very high degree (i.e. $k_i >> <k>$) in a degree-heterogeneous network such as an SF network play an important role in diffusing a strategy to the entire society, because they have a large number of neighbors. In both continuous and mixed strategy games, perfect cooperators ($s_i > 0.9$, for example) can rarely become hub agents at the beginning of an episode compared with discrete strategy games, because 90 % of their neighbors have a more defective strategy, and thus, they would be immediately replaced by defectors. In contrast, when a continuous or mixed strategy game is played, perfect defectors ($s_i < 0.1$, for example) can also rarely become hub agents at the beginning of an episode. Toward the games' end, hub agents in both continuous and mixed strategy games would become less cooperative and less defective than their initial strategies. This situation causes both continuous and mixed strategy games played on an SF network to attain more cooperative equilibrium than attained by discrete strategy games with a relatively stronger dilemma, whereas they exhibit less cooperation than discrete games with a relatively weaker dilemma.

Recalling Fig. 3.24(d), we can also note that the difference in equilibrium cooperation among the three strategy games in both RR and E-R networks is smaller than that in other networks. One plausible reason for this is that the substantial feature of these two topologies can be called a well-mixed population, especially if the average degree becomes large. As Zhong et al. (2012) revealed, in a large population of well-mixed situation with no special structure, there is almost no difference in terms of equilibria among discrete and continuous strategies, although there is little difference in terms of deductive point of view.

Insight into What Happens in the Early Stage of an Evolutionary Process

One simple question is why continuous strategy has a different equilibrium from discrete strategy. To seek an acceptable answer, let us examine what happens in the early stage of an episode. Roughly speaking, we can say that the most important core mechanism of network reciprocity is how initially allocated C clusters can survive over D invasions in the early stage of an evolutionary process. If C clusters, initially formed by random allocation of cooperators and defectors, would be eradicated by defectors' initial diffusion, cooperation can never expand, whereas if they survive, cooperation might increase in the long run to a level approaching either the co-existence of C and D or perfect cooperation. Thus, we have investigated what happens during the early stage of evolution in each of the three strategy games (played on 8-neighbor lattices).

Figures 3.33, 3.34, and 3.35 show $\psi_{D\to C}$, $\psi_{C\to D}$, Δp_C, and p_C at each initial fifth time step, where $\psi_{D\to C}$ ($\psi_{C\to D}$) denotes the sum of the strategy variations of players who convert D (C) to C (D) at each time step for discrete strategy games, and in both continuous and mixed strategy games, $\psi_{D\to C}$ ($\psi_{C\to D}$) denotes the sum of the strategy variations of players who convert to a more cooperative (defective)

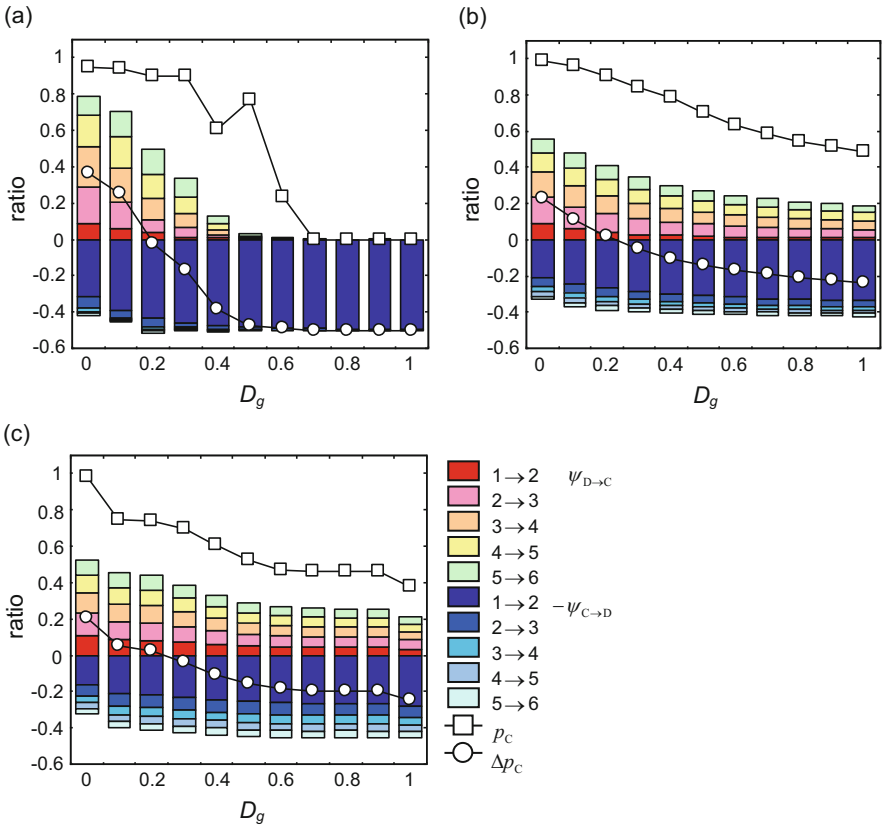

Fig. 3.33 Relationships between dilemma strength and $\psi_{D\to C}$, $\psi_{C\to D}$, Δp_C, and p_C at each initial fifth time step of (**a**) discrete, (**b**) continuous, and (**c**) mixed strategy games. Game structure is BCH. Games are played on 8-neighbor lattices ($k = 8$) with 4900 agents

strategy at each time step. Here p_C indicates cooperation proportion at each time step. Thus, $\Delta p_C = \psi_{D\to C} - \psi_{C\to D}$. Therefore, we can say that $\psi_{C\to D}$ denotes how quickly and strongly D (defective) attacks C (cooperative) agents, and $\psi_{D\to C}$ denotes how quickly and robustly C-clusters expand by overcoming D.

It is obvious that both continuous and mixed strategy games exhibit less D invasion and more steady C expansion than do discrete games even with increasing dilemma strength. Those two points are crucially important for cooperation to emerge, because they are related to how successfully the initially allocated C clusters can survive D invasions, and how significantly the C clusters can expand after the initial D attacking phase to attain a moderate cooperation level at the end of the evolution process. Adopting a real number strategy makes these outcomes possible.

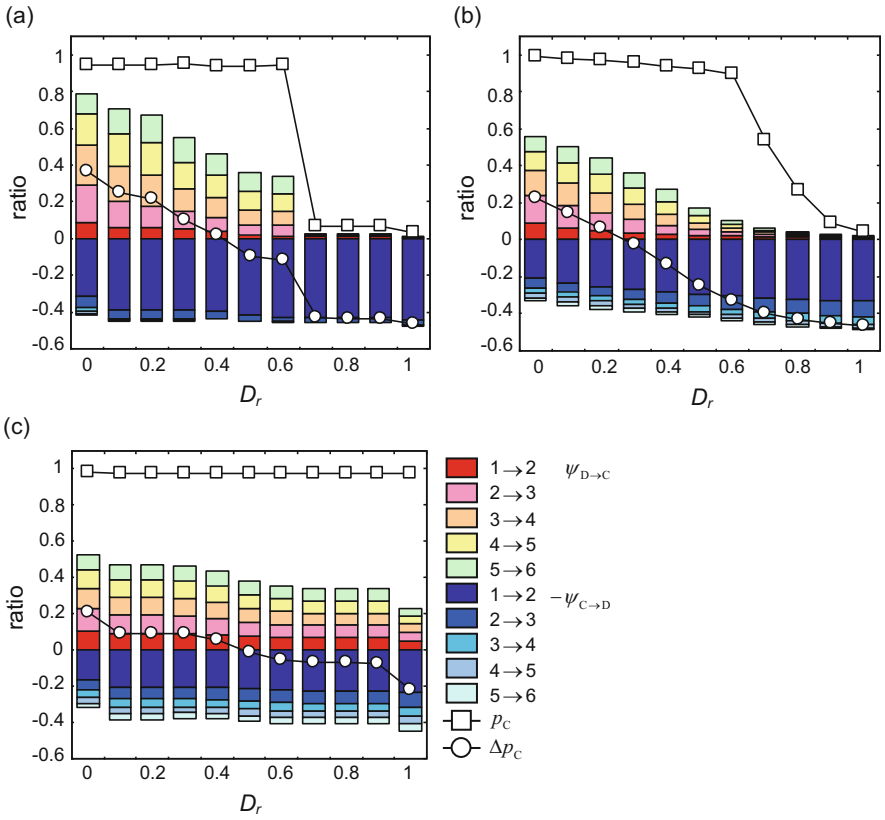

Fig. 3.34 Relationships between dilemma strength and $\psi_{D\to C}$, $\psi_{C\to D}$, Δp_C, and p_C at each initial fifth time step of (**a**) discrete, (**b**) continuous, and (**c**) mixed strategy games. The game structure is BSH. Games are played on 8-neighbor lattices ($k = 8$) with 4900 agents

Supplemental Discussion A

This appendix sub-section presents continuous or mixed strategy's influences on equilibrium, depending on the assumed initial strategy distribution and whether a mutation event is assumed. As explained in the main text, we have assumed that the initial distributions of both continuous and mixed strategy games are uniform distribution for $s_i \in [0, 1]$. Furthermore, we have not assumed strategy mutation. As another possible setting, we could assume the specific initial state, where half the agents are perfect cooperators (expressed by $s_i = 1$) and remaining half are perfect defectors (expressed by $s_i = 0$), rather than uniform distribution. This initial setting emulates the initial state in discrete strategy games. In this setting, we must assume strategy mutation by adding a random number drawn from a Gaussian distribution with a mean of 0 and an s.d. of 0.002 [5], otherwise agents having only either 1 or 0 can never develop their strategy to a real equilibrium. A mutation

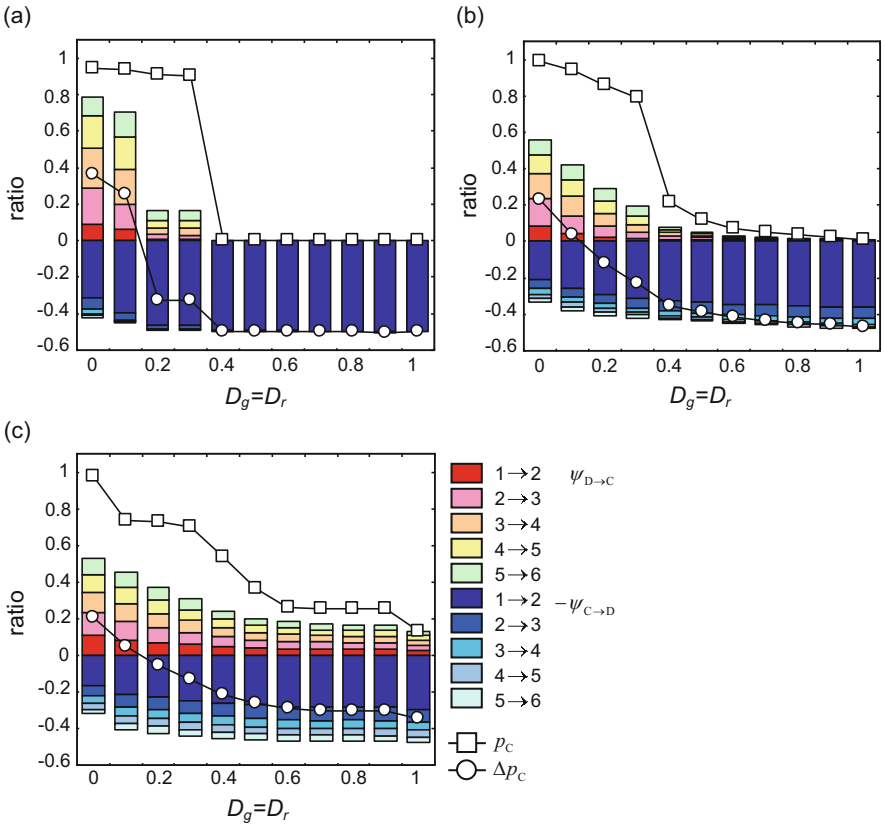

Fig. 3.35 Relationships between dilemma strength and $\psi_{D\to C}$, $\psi_{C\to D}$, Δp_C, and p_C at each initial fifth time step of (**a**) discrete, (**b**) continuous, and (**c**) mixed strategy games. Games are played on 8-neighbor lattices ($k = 8$) with 4900 agents

occurs with a small probability (0.1). Figure 3.36 summarizes average cooperation proportions for visual comparison among the three types of games: discrete, continuous, and mixed strategies. Note that the mutation procedure above is applied only to continuous and mixed strategies. Their equilibrium cooperation faction markedly differ from each other, but we should note that the degree of difference among the three strategies shown in Fig. 3.36 is not entirely consistent with that shown in Fig. 3.24. This fact must be attributed to different assumptions in initial distribution and mutation. Although detailed discussion will be presented in Supplemental discussion B, even at a glance, we note that the continuous strategy in Fig. 3.36(c) (BCH) shows less cooperation than that in Fig. 3.24(c), whereas in BSH, the result in Fig. 3.36(d) shows more cooperation than that in Fig. 3.24(d).

Previously we showed the comparison for the assumption of uniform distribution without mutation for continuous and mixed strategies and equal proportions of C and D (i.e., binary) without mutation for discrete strategy. We justify this

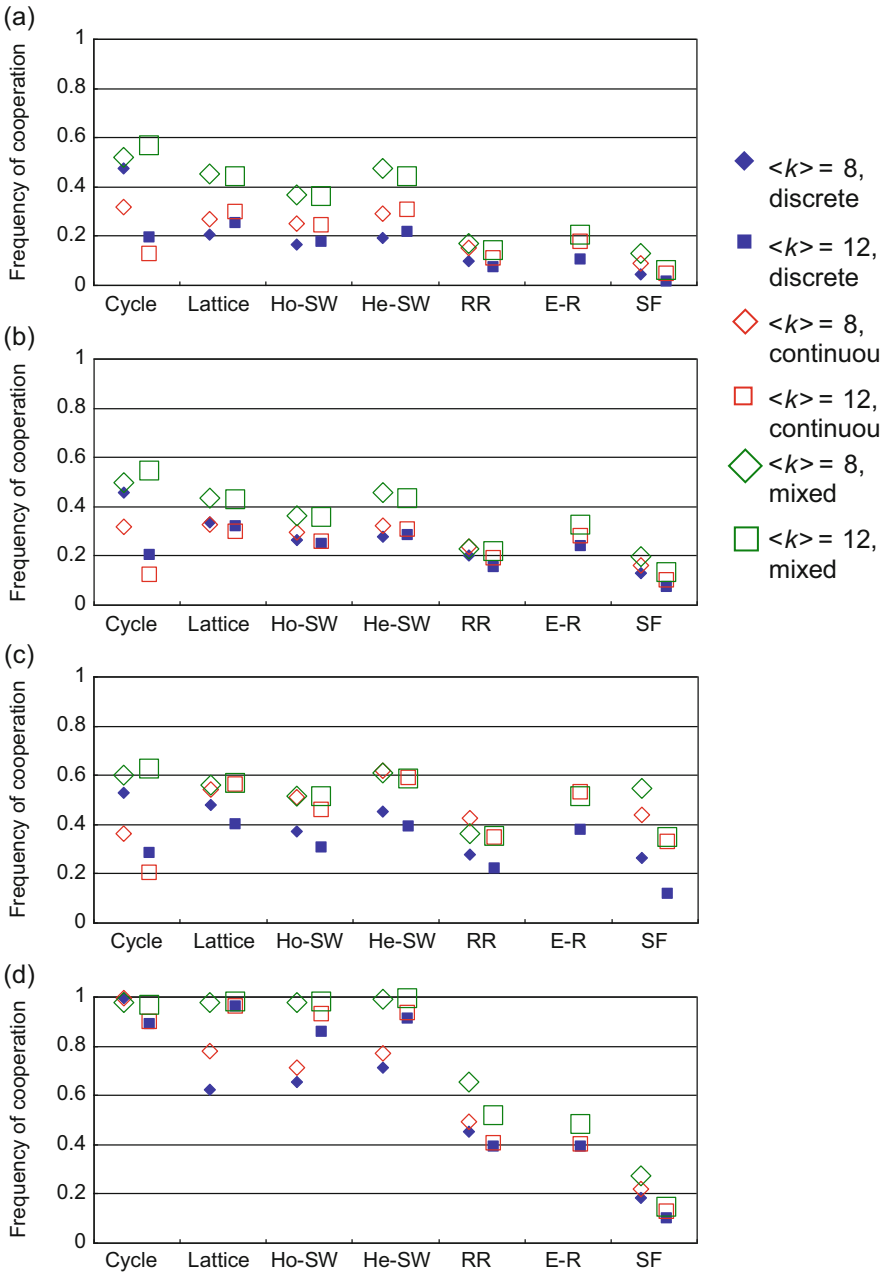

Fig. 3.36 Averaged cooperation proportions of three strategy games for (**a**) AllPD, (**b**) DRG, (**c**) BCH, and (**d**) BSH within the limit of $0 \leq D_g \leq 1$ and $0 \leq D_r \leq 1$. Games are played on seven network structures: Cycle, Lattice, Ho-SW, He-SW, RR, E-R, and SF, and two average degrees: 8 and 12. The initial distribution assumed here is the same as that of a discrete strategy game, where half the agents are perfect cooperators (expressed by $s_i = 1$) and the remaining half are perfect defectors (expressed by $s_i = 0$). We also assumed a mutation after copying the neighbor's

assumption because the strategy mutation setting inevitably causes the difficult problem that any practical assumption of mutation for both continuous and mixed strategies might not be consistent with that for a discrete strategy. In fact, a certain mutation probability for both continuous and mixed strategies does not have the same impact on the discrete strategy case, because in the former case, a mutation means $s_i \rightarrow s_i + \sqrt{0.002}*Gaussian\_Rnd[]$, whereas in the latter case, a mutation indicates either C to D ($1 \rightarrow 0$) or D to C ($0 \rightarrow 1$). Thus, when we plausibly propose that the three strategies (continuous, mixed, and discrete) must be consistent in mutation setting, the only choice is to assume no mutation process. Further, when we propose that the three cases should be consistent in initial distribution, the only possible choice is the binary setting, which, however, requires the mutation process for continuous and mixed strategies so that they operate as described. Therefore, it is not realistic to establish the binary setting as the initial strategy distribution for all three cases.

Supplemental Discussion B

This appendix sub-section discusses continuous or mixed strategy's influences on equilibrium depending on the assumptions regarding initial strategy distribution and whether a mutation event occurs. Thus, we here discuss the differences between Fig. 3.24 and Fig. 3.36. Hereafter, for simplicity, we express the conditions of Fig. 3.24 and Fig. 3.36 as *Condition A* (uniform distribution without mutation) and *Condition B* (binary distribution with mutation), respectively. In this section, we also discuss BCH and BSH separately as in Sects. 3.4.3.1 and 3.4.3.2.

We first discuss features in BCH. Observing both Figs. 3.24(c) and 3.36(c), we note that the influence of both continuous and mixed strategies on equilibrium results from the assumptions about initial strategy distribution and whether a mutation event occurs and is classified into following three categories: (1) considerable influence on only continuous strategy games and no influence on mixed strategy games (cycle and lattice); (2) negligible influence on both continuous and mixed strategy games (Ho-SW, He-SW, RR, and E-R); and (3) considerable influence on both continuous and mixed strategy games (SF).

We begin with cycle and lattice structures, where equilibria are influenced only when a continuous strategy is assumed. Figure 3.36(c) shows a cooperation level lower compared with that in Fig. 3.24(c). We limit this discussion to degree $k = 8$ as we did previously.

Figures 3.37 and 3.38 show the equilibrium cooperation proportions drawn from 100 realizations based on a continuous strategy in BCH. In addition to *Conditions A* and *B*, we added *Condition C*, in which the initial distribution is given by a uniform

Fig. 3.36 (continued) strategy so as to enable the agent to search the strategy space $s_i \in [0, 1]$, which was applied to only continuous and mixed strategies

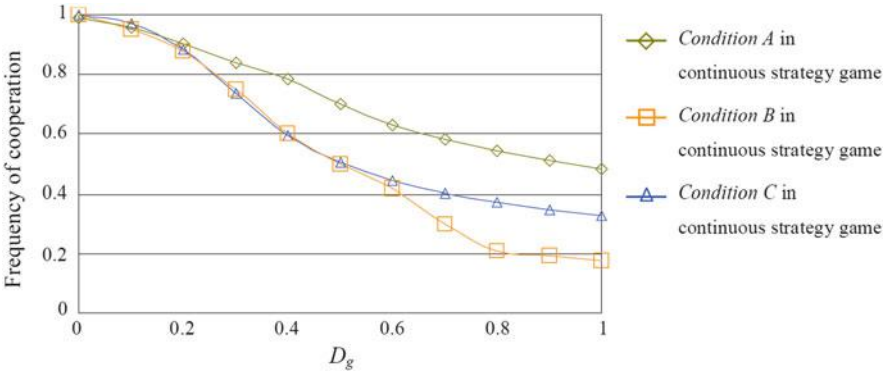

Fig. 3.37 Averaged cooperation proportion of a continuous strategy game for uniform distribution without a mutation event (*Condition A*), binary distribution with a mutation event (*Condition B*), and uniform distribution with a mutation event (*Condition C*). Games are played on lattice networks with the average degree $< k > = 8$. Dilemma subclass is BCH

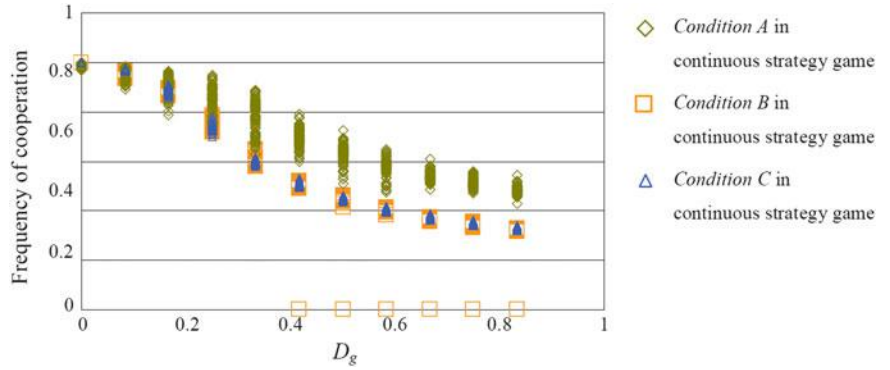

Fig. 3.38 Equilibrium cooperation proportion of each episode in a continuous strategy game for uniform distribution without a mutation event (*Condition A*), binary distribution with a mutation event (*Condition B*), and uniform distribution with a mutation event (*Condition C*). Games are played on lattice networks with the average degree $< k > = 8$. The dilemma subclass is BCH

distribution: $s_i \in [0, 1]$ with a mutation event. Comparing *Conditions A* and *C*, we note that the cooperation level assumed with a mutation event is lower than that without a mutation. Moreover, when presuming mutation, the cooperation level in a binary initial setting is inferior to that of a uniform initial distribution setting. From Fig. 3.38, we observe that the equilibrium in *Condition B* shows bi-stable-like feature when D_g becomes relatively large. As mentioned in Sect. 3.1, in continuous and mixed strategy games, a reasonable cooperation level can be established by forming a "mid-C cluster" consisting of mid-cooperative strategies even when a strong Chicken-type dilemma is imposed. However, it might be also true in strong dilemma games with binary initial distribution that some episodes can establish an

equilibrium consisting of only D-players before players attain a mid-cooperative level because D invasions in the early stage of an evolutionary process strengthen as the dilemma becomes stronger (see Figs. 3.33, 3.34, and 3.35). This leads to the result that cooperation in *Condition B* attains a level lower than that of *Condition* C. Except for those realizations where the cooperation proportion at equilibrium is 0, *Condition B* is comparable to *Condition C*. Deviation among realizations of *Condition A* is always large irrespective of the dilemma strength, which differs from that of *Condition C*. This fact implies that there is an instinct difference in equilibrium depending on whether mutation occurs, even if the same initial distribution (uniform distribution) is assumed. In the main discussion in the previous sub-section, we thought it appropriate to assume *Condition A* in order to compare discrete strategy cases with mutation excluded in order to consider in the evolutionary process.

However, there is less significant influence on the equilibrium of mixed strategy games from the assumed initial distribution. This relates to the "come-from-behind" victory probabilistically occurring in mixed strategy games. In mixed strategy games, which take a considerably long time to reach equilibrium, mid-cooperative strategies derived from mutation can be transmitted to all the agents through this "come-from-behind" victory event. That phenomenon explains why there is no difference between *Conditions A* and *B* in mixed strategy games (Figs. 3.24(c) and 3.36(c)).

Next, let us discuss Ho-SW, He-SW, RR, and E-R, where the equilibria are nearly independent of the assumptions about the initial setting and whether a mutation event occurs, for either continuous or mixed strategy games. In general, average path lengths of these four networks are relatively short compared with regular networks. Thus, a mid-cooperative strategy derived from mutation in these four networks is transmitted to all the agents more easily than that in cycle and lattice networks, which have relatively long average path lengths. Therefore, in these four networks, each episode does not exhibit bi-stable-like equilibrium but the same internal (polymorphic) equilibrium (not shown). This leads to the presence of no differences between Fig. 3.24(c) and Fig. 3.36(c).

Finally, let us discuss SF, where equilibrium depends on the assumptions about the initial setting and whether a mutation event occurs, for either continuous or mixed strategy. Figure 3.39 shows the respective cooperation fractions within the limits of $0 \leq D_g \leq 1$ and $0 \leq D_r \leq 1$ based on continuous and mixed strategy games played on SF networks with the average degree $< k > = 8$. As we confirmed, in SF, the initial assumed distribution's influence on equilibrium is larger than that from the assumption of whether mutation event occurs. As mentioned before, an equilibrium cooperation proportion of a SF network depends on a hub agent's strategy value at the beginning of an episode. When we assume a binary initial setting, hub agents can have either a perfect cooperative strategy or a perfect defective strategy. Thus, continuous and mixed strategy games exhibit the same feature as discrete strategy games, whose phase diagram clearly shows whether cooperation can survive.

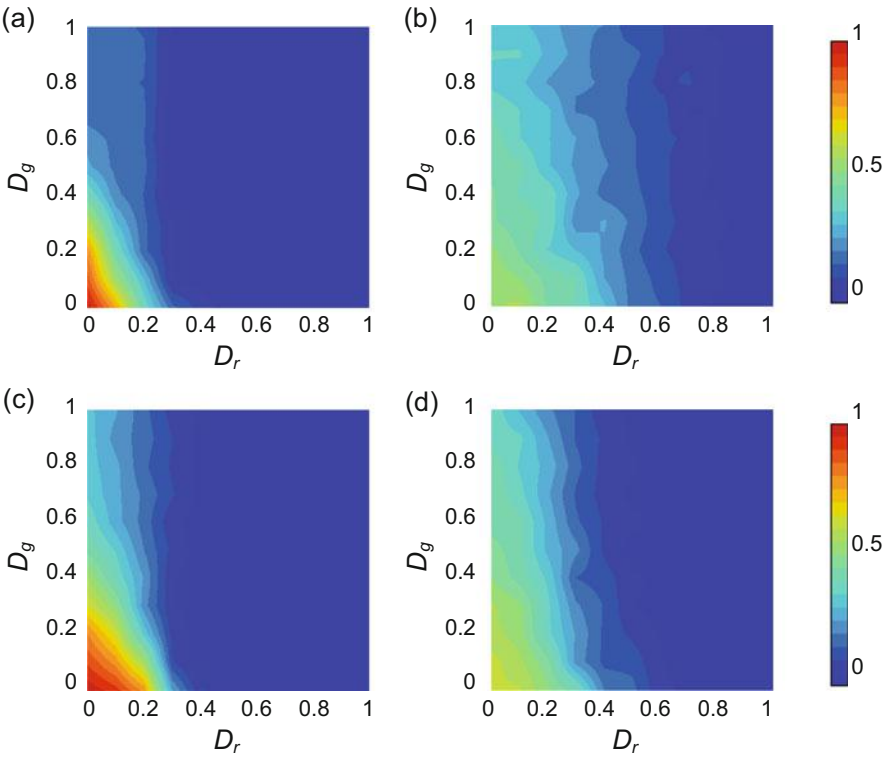

Fig. 3.39 Averaged cooperation proportion within the limit of $0 \leq D_g \leq 1$ and $0 \leq D_r \leq 1$ based on (**a**) *Condition B* in a continuous strategy game, (**b**) *Condition C* in a continuous strategy game, (**c**) *Condition B* in a mixed strategy game, and (**d**) *Condition C* in a mixed strategy game. Games are played on SF networks with the average degree $< k > = 8$

Next, let us discuss features in BSH. Observing both Figs. 3.24(d) and 3.36(d), we also note, as in BCH, that the influence of either continuous or mixed strategy, depending on assumptions about initial strategy distribution and whether a mutation event occurs, on equilibrium can be classified into the following three categories: (1) considerable influence on only continuous strategy games and no influence on mixed strategy games (cycle and lattice); (2) negligible influence on both continuous and mixed strategy games (Ho-SW, He-SW, RR, and E-R); and (3) considerable influence on both continuous and mixed strategy games (SF).

First, let us discuss cycle, lattice, Ho-SW, and He-SW structures, where equilibria are influenced only in continuous strategy games. Figure 3.36(d) shows a higher cooperation level compared with Fig. 3.24(d). For the sake of discussion here, we also limit the lattice network with the degree $k = 8$. Figure 3.40 shows the equilibrium cooperation proportion derived from 100 episodes based on a continuous strategy in BSH. Let us consider the critical dilemma strength D_{r_cr}. We define D_{r_cr} by the threshold Stag-Hunt-type dilemma strength when the equilibrium

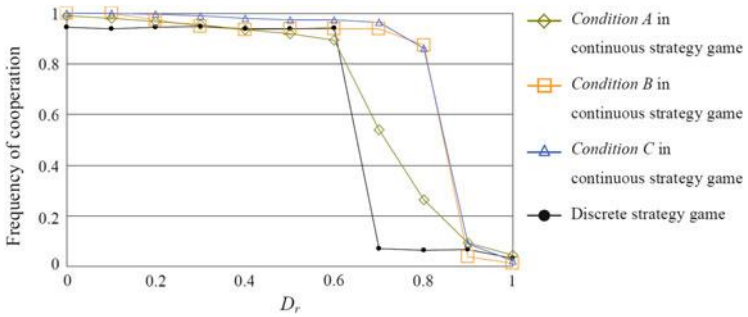

Fig. 3.40 Averaged cooperation proportion for *Condition A* in a continuous strategy game, *Condition B* in a continuous strategy game, *Condition C* in a continuous strategy game, and discrete strategy game. Games are played on lattice networks with the average degree $< k >= 8$. The dilemma subclass is BSH

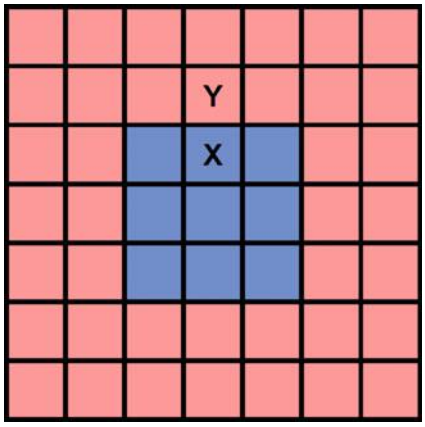

Fig. 3.41 A blue square illustrate a C-player, a red one illustrates a D-player, and the topology is an 8-neighbor lattice. The strategy values of player X and player Y are s_x and s_y, respectively

cooperation proportion falls below 0.1. Observing Fig. 3.40, we can see that D_{r_cr} of a discrete strategy game is obviously inferior to that of a continuous strategy game. Moreover, a continuous strategy game with a mutation has a larger D_{r_cr} than that of a continuous strategy game without a mutation. As mentioned, the most important core-mechanism to explain network reciprocity is how initially allocated C clusters can survive D invasions in the early stage of an evolutionary process and how robustly these C-clusters can expand to the surrounding D area after the initial ordeal. Therefore, we can say that D_{r_cr} is almost the same dilemma strength that determines whether a C-cluster can expand in a D population. Let us take an example shown in Fig. 3.41 to discuss D_{r_cr} that determines whether a C-cluster can expand in a D population. In Fig. 3.41, a blue square illustrates relatively

cooperative players, a red square indicates relatively defective players, and the topology is an 8-neighbor lattice. As long as we assume Imitation Max (IM) as the strategy update rule, we can derive D_{r_cr} by comparing the benefit of Agent X ($s_X = x$) with that of Agent Y ($s_Y = y$) in Fig. 3.41. We can derive $D_{r\_cr} = \frac{2}{8-5(x+y)}$. The sum of x and y must always be 1 ($x + y = 1$) in a discrete strategy game, but it can be larger than 1 ($x + y > 1$) in both continuous and mixed strategy games. Thus, the relationship between the critical dilemma strength of a discrete strategy game $D_{r\_cr\_discrete}$ and that of a continuous strategy game $D_{r\_cr\_continuous}$ obeys $D_{r\_cr\_discrete} < D_{r\_cr\_continuous}$, which is consistent with Fig. 3.40. The reason that $D_{r\_cr\_continuous}$ in a mutation event is considered as larger than that in the mutation excluded condition is as follows. For a continuous strategy game with uniform initial distribution and mutation excluded, it is difficult for perfect cooperators (e.g., $s_i > 0.9$) to survive in the early stage of an episode and C-clusters tend to be eliminated because the proportion of perfect cooperators is lower (see Sect. 3.1). Assuming a mutation event tends to relax the drawback that the cooperative agents cluster consists of fewer agents. This leads to the fact that D_{r_cr} becomes larger, which is consistent with what we observed in Fig. 3.40.

Next, let us discuss RR and E-R, whose equilibria are nearly independent of the assumption about initial setting and whether a mutation event occurs, for either continuous or mixed strategy games. Because these two networks have a relatively lower clustering coefficient than do the previous four networks, the underlying topology of these two networks exhibits a feature such as a well-mixed situation, with no difference of equilibria between discrete and continuous strategies (Vincent and Cressman 2000). Therefore, as long as we assume a large enough number of agents ($N >> 1$), the assumed initial distribution and possibility of a mutation become irrelevant to equilibrium.

Finally, let us discuss SF, where the equilibrium depends on assumptions regarding the initial setting and whether mutation event occurs, for either continuous or mixed strategy game. The observed result is caused by the crucial fact that hubs are occupied by either a perfect cooperative or perfect defective strategy. This is the same as what we discussed for BCH.

Supplemental Discussion C

As mentioned, in the model we assumed that an agent synchronously updates her strategy every τ step based on the accumulated payoffs with all neighbors during τ steps. We have assumed $\tau = 1$ thus far. In this sub-section, we assume $\tau > 1$, which implies the speed of strategy updating is slower than that of game progress. Figure 3.42 shows how mixed strategy games approach continuous strategy games if $\tau \to \infty$. We note that Fig. 3.42(d) is almost consistent with Fig. 3.25(b).

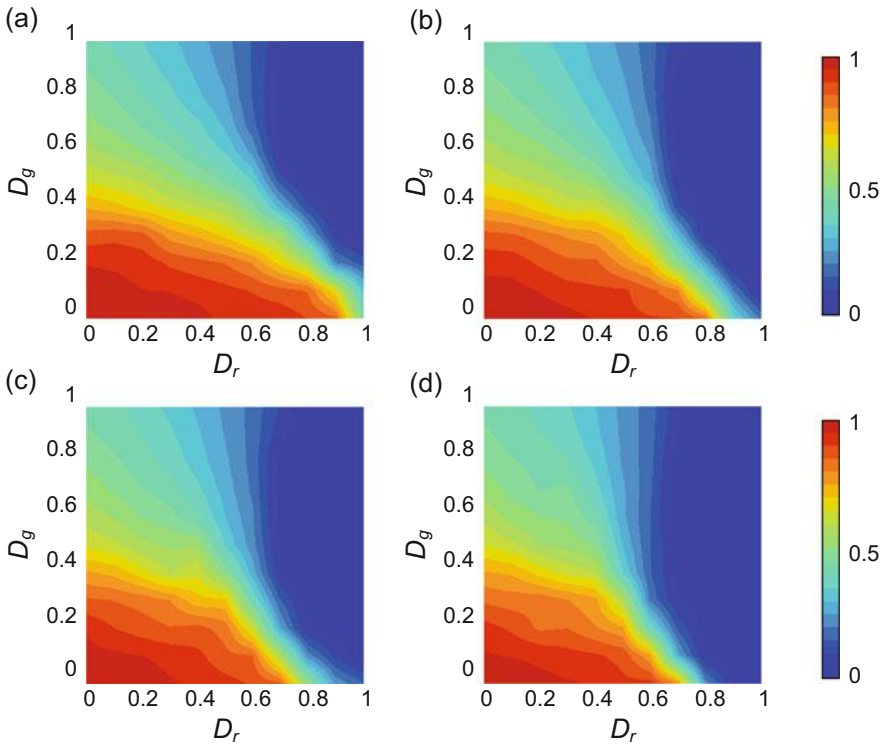

Fig. 3.42 Averaged cooperation proportion within the limit of $0 \leq D_g \leq 1$ and $0 \leq D_r \leq 1$ based on a mixed strategy game with (**a**) $\tau = 10$, (**b**) $\tau = 25$, (**c**) $\tau = 50$, and (**d**) $\tau = 100$ assumed. Games are played on 8-neighbor lattices ($k = 8$) with 4900 agents. These data are the average values of 20 trials

Supplemental Discussion D

Thus far, we limited our study to the prisoner's dilemma game (PD), where $0 \leq D_g \leq 1$ and $0 \leq D_r \leq 1$. In this appendix, we consider another important social dilemma class: Chicken game (CH game), where $0 \leq D_g \leq 1$ and $-1 \leq D_r \leq 0$. In CH game, sub game class depends on the case whether $S+T$ $(= -D_r + D_g + 1)$ is larger than $2R$. If $S+T > 2R$, alternating S and T is more effective than mutual R, which simply means ST-reciprocity is better than R-reciprocity. Therefore, it is not appropriate to evaluate how efficient reciprocity is achieved via averaged cooperation proportion. Figure 3.43 shows averaged payoff per link instead of averaged cooperation proportion. It is obvious that averaged payoff per link of continuous and mixed strategy games are larger than that discrete strategy game. Especially in the in the region $S+T > 2R$ and $D_g > 0.7$, the later becomes very low. In addition, discrete strategy game has no region where averaged payoff per link is larger than 2 $(= 2R$, amount of R reciprocity bringing).

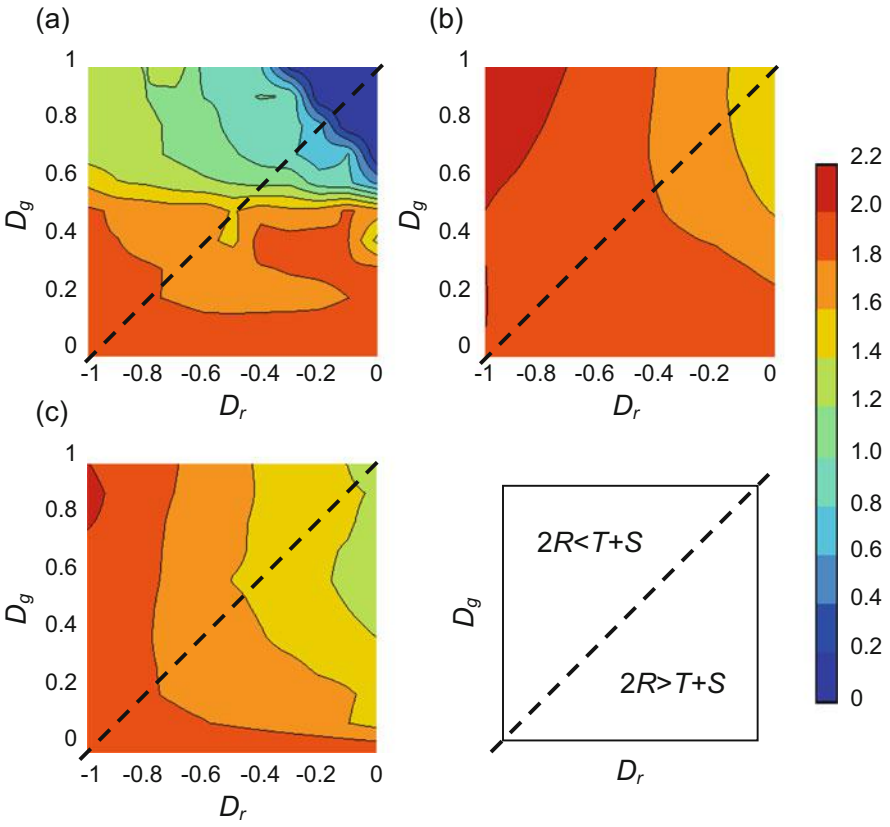

Fig. 3.43 Averaged payoff per link within the limit of $0 \leq D_g \leq 1$ and $-1 \leq D_r \leq 0$ (CH game) based on (**a**) discrete, (**b**) continuous, and (**c**) mixed strategy games. Games are played on 8-neighbor lattices ($k = 8$) with 4900 agents. The region above the broken line is $2R < T + S$

3.4.4 Summary

We thoroughly investigated the differences in terms of game equilibrium among continuous, mixed, and discrete strategies in spatially structured populations. We found that there are substantial differences among these strategies, which cannot exist in well-mixed populations. These findings might raise a significant question as to whether the previous approach to network reciprocity, presuming only binary C or D strategies, is really appropriate.

By a series of comprehensive and systematic numerical simulations, we showed how different equilibria among the three strategies can be established, assuming various underlying topologies as well as different average degrees in fundamentally Prisoner's Dilemma games.

The results imply that BCH (boundary games to Chicken) and BSH (boundary games to Stag Hunt) have different mechanisms encouraging significant differences in equilibria between continuous or mixed strategy and discrete strategy games.

In BCH games with continuous and mixed strategies, mid-cooperative clusters consisting of mid-cooperative strategies, which can establish reasonable cooperation, are formed.

In BSH games with mixed strategy, a "come-from-behind" victory event, where a more cooperative agent defeats a defective agent, occurring probabilistically, and causes a higher cooperation level than adopting either discrete or continuous strategy.

Furthermore, the underlying topology, whether SF or others, causes inconsistencies in equilibria among the three strategies. In general, hub agents play an important role in diffusing a strategy to the entire society, because they have many neighbors. Hub agents in continuous and mixed strategy games would become less cooperative as well as less defective than their initial strategies. Therefore, when the underlying topology is SF, the cooperation levels of continuous and mixed strategy games are almost consistent with each other but different from that of discrete strategy games.

3.5 A Substantial Mechanism of Network Reciprocity

So far in this chapter, we have discussed various aspects of network reciprocity, which is one of the five fundamental mechanisms for enhancing cooperation in evolutionary games classified as prisoner's dilemma.

In recent decades, there have been a great number of papers, perhaps hundreds or even thousands, reporting a "new SPD model" that can show more enhanced cooperation than the conventional SPD model when enhanced by typical network reciprocity. But, in most cases, the question of why each particular enhancement works is neglected, or at least, is treated with less concern. This is because finding a new enhancement model alone is meaningful as well as valuable. It would now be a good idea to look back at this affluent supply of work so as to take this discussion a step further. Here, let us inquire ourselves into what network reciprocity really means, and what we mean when we say the substance of network reciprocity. Figure 3.11 gives us a good start for seeking an answer to this inquiry. The social viscosity resulting from network reciprocity should be considered to have two main aspects, END and EXP, which we have defined in the previous discussion. As mentioned previously, END refers to a period when the global cooperation fraction decreases, after starting out on an evolutionary path, from the initial arrangement of cooperators and defectors. Most previous studies assumed that an equal number of cooperators and defectors are randomly placed on the vertices of a presumed underlying network. EXP, which takes place following END in the same evolutionary path, refers to a period when the global cooperation fraction increases. However, if the particular path is absorbed by an all-defectors-state in END, EXP never happens.

One acceptable idea is that if a certain mechanism could make the probability of absorption by an all-defectors-state in END lower than the usual network reciprocity, we would call that particular mechanism more enhanced than the usual network

reciprocity. If a mechanism could make the level of cooperation in EXP increase more significantly than typical network reciprocity does, we could regard that particular mechanism as more enhanced than usual network reciprocity. This concept enables us to evaluate to what extent each of the enhancement models proposed in the previous studies can bolster the network reciprocity in either END or in EXP, making the real substance of network reciprocity transparent.

For the sake of simplicity, in the following discussion, we concern ourselves with the case in which we presume a lattice and Imitation Max (IM) as the underlying network and strategy update rule, respectively. We do not introduce a degree-heterogeneous graph, such as Scale-Free, or a stochastic strategy update, such as Pairwise Fermi. This is because those features, like degree distribution, random connection among agents, and stochastic perturbation in the strategy update rule, make it more ambiguous for us to observe the natural effect resulting from the enhanced network reciprocity.

3.5.1 Simulation Settings and Evaluating the Concept of END & EXP

In the following investigation, we assume a Donor & Recipient (D & R) game, one of the representative sub-classes of Prisoner's Dilemma (PD) games, where a chicken-type dilemma strength, D_g $(= P - S)$ is consistent with a stag hunt-type dilemma strength, D_r $(= T - R)$. Without a loss of generality, we adopt Eq. (3.1) with $R = 1$ and $P = 0$. As mentioned before, we adopt a lattice of $k = 8$ for the underlying network, with a size N of 100×100, and IM with synchronous strategy updating. Each simulation starts from equal number of cooperators and defectors randomly assigned to each vertex of the network to obtained quasi-equilibrium. We evaluate cooperation fraction by ensemble average formed from 100 independent simulations.

The key point is how we measure the effectiveness of network reciprocity in END and EXP. Here, let us define the following two parameters.

E_{END} **Effectiveness in END**. We define E_{END} as the average cluster shape, SH_C, at the end of END, when initial cooperation fraction of 0.5 is imposed. As originally defined by Eq. (3.2) in Sect. 3.2, the shape of a i is defined by $SH_{Ci} = (2l_{CC} - O_{CD}) / (2l_{CC} + O_{CD})$, where l_{CC} is the number of C-C links within the C-cluster i and O_{CD} is the number of C-D links that connect the C-cluster i with the surrounding defectors. The value of SH_C, defined on a scale of $[-1,+1]$, is obtained by averaging over all SH_{Ci} and weighted by its size. A negative SH_C means that cooperators are placed dissortatively in a domain, which implies that cooperative clusters have convexo-concave boundaries with defectors surrounding them. Contrariwise, a positive SH_C means that cooperators are placed assortatively, which implies cooperators' clusters have clumpy shapes with fewer convexo-concave

boundaries surrounded by defectors. Obviously, a positive SH_C is expected to lead to a favorable EXP, in which a C-cluster can smoothly expand to the surrounding region mainly occupied by defectors. If there is a single cooperator in a domain, this cluster shape is evaluated as $SH_C = (2 * 0 - k) / (2 * 0 + k) = -1$. Thus, we presume $SH_C = -1$, in the case of an all-defectors-state, as the ultimate situation, although the original definition by Eq. (3.2) becomes indefinite. Without losing the generality of the argument so far, we can rescale SH_C from $[-1, +1]$ to $[0, 1]$ by applying a transform of $0.5 * SH_C + 0.5$. The definition of E_{END} means the following. If a simulation episode is absorbed by an all-defectors-state in END, its E_{END} is evaluated to be zero. When an E_{END} close to 1 (0) is observed, the C-clusters surviving in END have good (bad) shapes for growing with high probability.

E_{EXP} **Effectiveness in EXP**, which is defined as the cooperation fraction at equilibrium averaged over 100 realizations, when each realization begins with the initial setting of a "perfect C-cluster," where a block of nine ($= 3 \times 3$) cooperators are placed in the center of the domain while the other vertices are occupied by defectors. Let us presume a perfect C-cluster in a sea of defectors as shown in Fig. 3.44(a). Agent (D-1) neighboring the perfect C-cluster most effectively exploits the neighboring cooperator, who gets $3T + 5P$. This is rewritten as $3 \cdot (1 + D_g)$ when substituting into Eq. (3.1). His neighbor, cooperative agent (C-1) is exploited by three neighboring defectors, and thus only earns $5R + 3S = 5 - 3 \cdot D_r$. However, one of his neighbors, agent (C-2), at the center of the perfect C-cluster, gains a high payoff, $8R = 8$. Even if an agent is severely exploited by his defective neighbors, the IM rule compels him to keep cooperating as long as he has a cooperative neighbor who obtains a high payoff. For these reasons, we can infer that a perfect C-cluster, initially placed in the center of an all-defectors domain, never perishes, as long as $D_g < \frac{5}{3}$. We also infer that this perfect C-cluster can expand in the domain, as long as $D_g + D_r < \frac{2}{3}$. These two particular conditions are shown in Fig. 3.44(b), in which the green and blue regions meet at the first

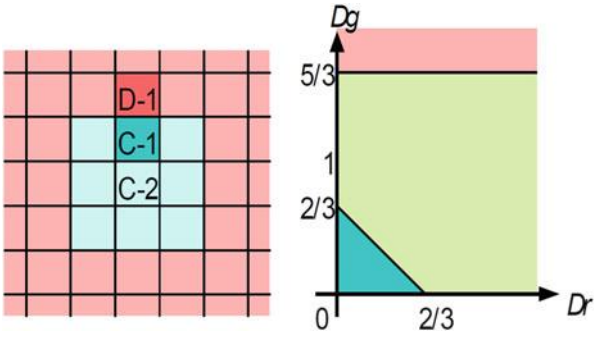

Fig. 3.44 Conditions in which a perfect can survive and expand in the case in which and IM are assumed. (**a**) Cooperators and defectors around a Perfect C-Cluster, (**b**) D_g - D_r diagram

inequality, and the blue region represents where (,) satisfies the second inequality. Therefore, we can deduce that a dynamical episode starting with a single perfect C-cluster in a sea of defectors and satisfying the second inequality could ultimately attain an all-cooperators-state if we assume a sufficiently large domain. Paraphrasing this, as long as $0 \leq D_g \leq 1$ and $0 \leq D_r \leq 1$ are satisfied, any evolutionary path implemented with the usual mechanism can never be absorbed by an all-defectors-state, and that at least the initial nine cooperators will always remain, which implies there is actually no . Instead, this particular initial setting ensures that every evolutionary path starts immediately in the , not undergoing any END period as cooperation can grow immediately from this initial situation.

In the following discussion, we focus in particular on the following ten enhanced mechanisms as representative ones.

Enlarging interaction neighborhood (IN) and learning neighborhood (LN): In a commonly-shared assumption in SPD games, a gaming neighborhood, or IN (the range of neighbors with which games can be played) is presumed to be equivalent to the strategy adaptation neighborhood, or LN (the range of neighbors from which the focal agent copies its strategy). Recently, Xia et al. (2013) delivered a rebuttal to this, in which they explored simulations to see what happens if IN and LN expand independently. They found that appropriately selecting IN and LN, if they are respectively larger than a first neighborhood, enhances network reciprocity. But they do not clearly explain what causes the appropriate IN and LN size to bolster network reciprocity and this has been comprehensively assessed by Ogasawara et al. (2014) very recently. Here, we apply a second Moore neighborhood, with $k = 24$, as the enlarged IN and LN as compared to the default $k = 8$, the first Moore neighborhood.

Void site: Vainstein and Arenzon (2001) found that the cooperation in SPD games is significantly enhanced by considering site diluted lattices. But, exactly speaking, they assumed spatial Public Goods Games with Pairwise Fermi for updating rule, which is different from the current discussion. Here, we vary the ratio of void sites to be 1 %, 5 %, 10 %, and 25 % out of N.

Time delay: Pan et al. (2013) found that the cooperation in SPD games is reasonably enhanced by introducing a time delay between the time-step when payoff information is acquired and the time-step when strategy update actually happens. Here, we apply time delay of $\tau = 1$ time step, which indicates an agent updates his strategy based on his accumulated payoff in the previous time-step.

Copy error: Cong et al. (2010) found that a small amount of copy error can promote cooperation in SPD, because copy error adds some noise into the dynamical system that may work effectively for enhancing cooperation in some situations, like with the resonance effect, but may work counterproductively in other situations. One point that should be noted is that they premise a scale-free graph as the underlying network rather than a lattice in their study. Here, we vary the copy error between 1 %, 5 %, 10 %, and 25 %.

Facilitator: Szolnoki et al. (2014) identified significant cooperation enhancement by introducing "facilitators" who behave as mirrors to their neighbors—they cooperate with cooperators and defect with defectors—but they do not participate in the exchange of strategies. Here, we vary the ratio of facilitators between 1 %, 5 %, 10 %, and 25 %.

Action error: Dai et al. (2010) found that adding action error but not copying error is able to significantly improve cooperation compared to the network reciprocity in the usual SPD model. Here, we vary the action error between 1 %, 5 %, 10 %, and 25 %.

Cumulative payoff: Ren and Wang (2014) reported more enhanced cooperation in SPD games if an agent updates based on the cumulative payoff based on all payoffs from the beginning of an episode instead of the temporal payoff obtained in a particular time-step.

Selecting game opponent: Berde (2011) found more enhanced cooperation in SPD games if an agent only plays selective neighbors stochastically selected based on their payoff, where a neighbor who obtains much more payoff than the focal agent is more frequently elected as a game opponent.

Payoff noise: Perc (2006a, b, 2007), also Tanimoto (2007b), found that adding noise to the payoff matrix can significantly bolster network reciprocity, which is equivalent to the so-called stochastic resonance effects commonly observed in many physical phenomena.

3.5.2 Results and Discussion

Figure 3.45 shows the E_{END} and E_{EXP} of the above ten enhanced models as compared with the default model where typical network reciprocity is presumed. The cross point of the horizontal and vertical coordinates represents (E_{END}, E_{EXP}) of the default model. Thus, each E_{END} (E_{EXP}) of the ten models represents how much the model bolsters network reciprocity in END (EXP) as compared with the default model if E_{END} (E_{EXP}) has a positive value. The plot's size (area) represents the averaged cooperation fraction at equilibrium over the region of $0 \leq D_g\ (= D_r) \leq 1$, in which we let each of the evolutionary episodes start from the initial state where an equal number of cooperators and defectors are randomly distributed in the domain. Thus, we can evaluate whether the network reciprocity of each of the ten models is superior to the default model or not by comparing the areas of the plots.

Firstly, it is worthwhile to note that mechanisms showing larger E_{END} and E_{EXP} than those of the default case, such as "selecting game opponent," all cases of "action error," and the 25 % case of "facilitator," show more enhanced network reciprocity than the default case. Whereas, on the other hand, cases of "enlarging IN" and "copy error" provide much more meager network reciprocity as a whole vis-à-vis the default case, because of the smaller E_{END} and E_{EXP} values than in the default case. The point to be addressed here is that the map can let you capture

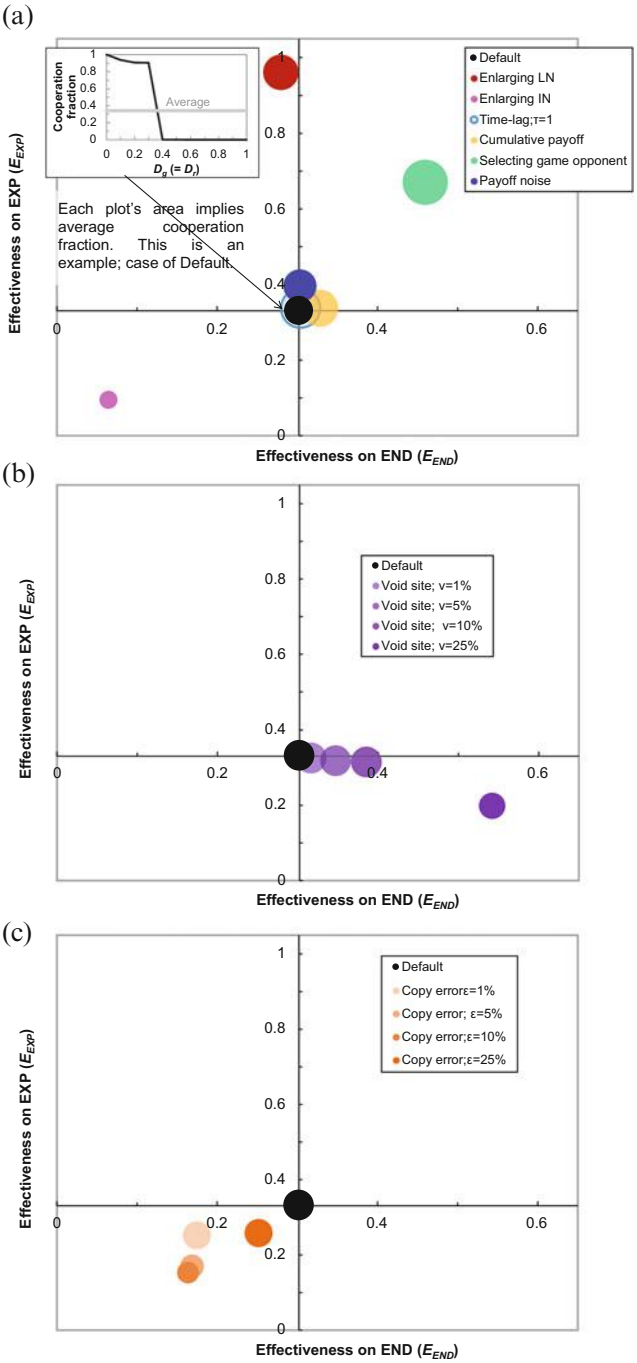

Fig. 3.45 (continued)

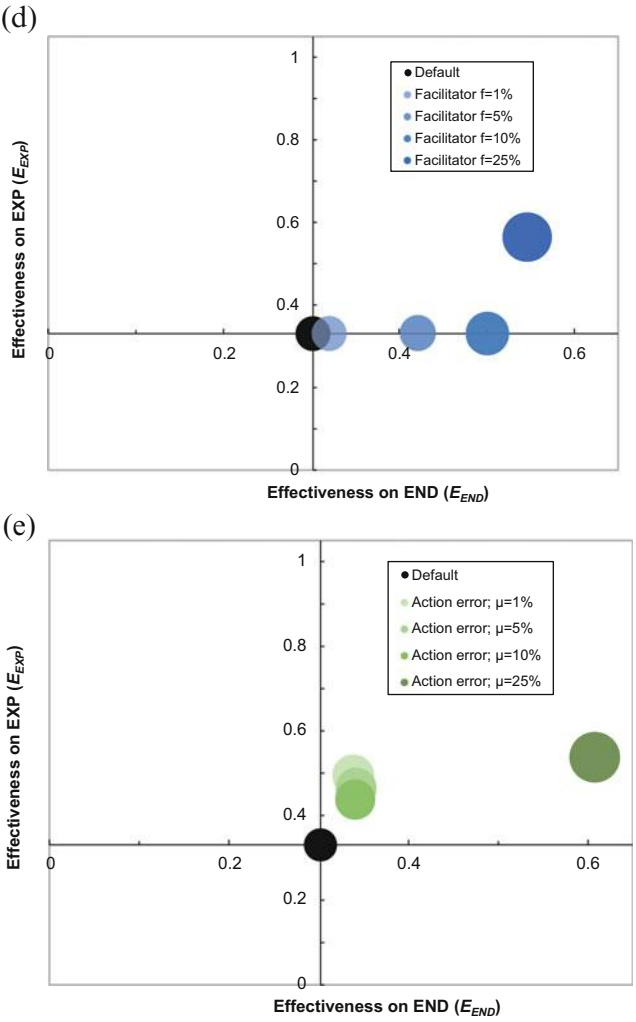

Fig. 3.45 (E_{END}, E_{END}) and holistic network reciprocity (represented by the plot's area) comparing the default model with (**a**) models enhanced by enlarging IN, enlarging LN, time delay, cumulative payoff, and selecting game opponents, (**b**) a model enhanced by a void site, (**c**) a model enhanced by copy error, (**d**) models enhanced by a facilitator, and (**e**) a model enhanced by action error

clearly, almost at a glance, which models are likely to perform with more enhanced cooperation than the default model by comparing the E_{END} and E_{EXP} values with those of the default case.

Let us start with "enlarging LN and IN." Enlarging LN makes END a little worse than the default. This results from the situation in which cooperators, initially distributed in a random arrangement, convert to defectors by copying defection

from a neighbor who efficiently exploits from plural cooperators, which relatively increases the probability of absorption by an all-defectors-state in END, or just allows SH_C to be worse even if fortunate C-clusters can survive. However, enlarging LN improves E_{EXP} a great deal. This is obviously because even a defector who is the secondary neighbor of a C-cluster converts to a cooperator, which inevitably makes it difficult for a defector to remain in a gap between plural C-clusters by efficiently exploiting cooperators in a general case of dynamics. In fact, as we can confirm by comparing the sizes of plots of "enlarging LN" cases and the default case, enlarging LN allows much more prosperous cooperation. Contrariwise, enlarging IN seems hopeless at increasing cooperation, which devastates both in END and EXP. This is not surprising in a way, because even a cooperator in the center of a perfect C-cluster is exploited by his secondary neighboring defectors. Thus, the surviving probability of C-clusters initially placed in the domain to avoid absorption of all-defector-state decreases, and the chance of expansion of C-clusters is depressed in EXP even if they survive the END period.

As reported by Cong et al. (2010), the model of "copy error" might work only for degree-heterogeneous networks like scale-free. Because of this, both E_{END} and E_{EXP} are inferior to the default case. Thus, it leads to a very poor result compared to the default case.

The highest cooperation fraction of equilibrium, expressed by each plot size, among the ten models, is found in the case of "selecting game opponent," which shows both E_{END} and E_{EXP} to be improved. This particular option allows a cooperator on the border of a C-cluster, facing defectors, to play only with a neighboring cooperator and earn $8R$, avoiding interaction with defectors, in games hosted by that particular cooperator, even though he is exploited by his neighboring defectors in the games hosted by those defectors. This system works to depress the probability of absorption by an all-defectors-state, as well as to convert more defectors to cooperation.

Interestingly, although the cases of "time delay" and "cumulative payoff" only show a slightly improved E_{END}, these holistic network reciprocities vis-à-vis the default case are reasonably improved. An improvement in E_{END} creates a situation where surviving C-clusters have appropriate shapes for growing with high probability. This fact might bring significant amelioration in these two models.

More interestingly, although the case of the "void site" with a rate of 25 % can result in an improved E_{END} compared to lower percentile cases (but a worse E_{EXP}), the holistic network reciprocity is devastated as compared with the default case. This is because a worse E_{EXP} has a more significant effect in this particular model. In fact, we can easily imagine that a larger number of void sites will destroy a spatially smooth expansion of C-clusters in EXP that have survived END.

The cases of "facilitator" and "action error" show improved E_{EXP} as well as E_{END}, except for the lower percentile cases in "facilitator," which show no improvement in E_{EXP}. This is why the level of network reciprocity of these two settings is much better than that in the default case. As previously mentioned regarding the "selecting game opponent" case, these two mechanisms can simultaneously realize the following two things: (1) the probability of C-clusters surviving in good shape

until the end of END increases and (2) the spatially smooth expansion of those C-clusters in EXP can be improved. Thus, a high level of equilibrium cooperation fraction, as observed in the "selecting game opponent" case, is attained.

The case of "payoff noise" shows a very subtle improvement in terms of the cooperation level compared with the default case, because of just a slightly better E_{EXP} than the default case.

3.5.3 *Relation Between Network Reciprocity and E_{END} & E_{EXP}*

Here, we pursue a most interesting and important question in Sects. 3.3, 3.4, and 3.5. That question is what mechanism determines network reciprocity, in other words, how qualitatively influential END is on the improved cooperation by a certain network reciprocity mechanism, and likewise, how influential EXP is.

Figure 3.46(a) shows the correlation between averaged cooperation fractions covering the whole range of $0 \leq D_g\ (= D_r) \leq 1$ (that is, equivalent to the area, size of each of the plots in Fig. 3.45) and E_{END}. Figure 3.46(b) shows another correlation with E_{EXP}. Although both contributing ratios, $R^2 = 0.425$ and 0.506, respectively shown in the figures do not seem too bad, we observe some shattered plots away from the respective regression lines. Needless to say, this is because the network reciprocity by each model including the default setting is not only influenced by END but also by how much EXP is improved.

	Degree of freedom	F-value	Significant F-value
Regression	1	17.3	**4.50E-04**
Residual	21		
Total	22		
	Standard Error (SE)	**t-value**	**P-value**
Intercept	0.076	1.25	0.225
E_{END}	0.209	**4.15**	4.50E-04

	Degree of freedom	F-value	Significant F-value
Regression	1	23.5	**8.61E-05**
Residual	21		
Total	22		
	Standard Error (SE)	**t-value**	**P-value**
Intercept	0.057	2.48	0.022
E_{EXP}	0.137	**4.85**	8.61E-05

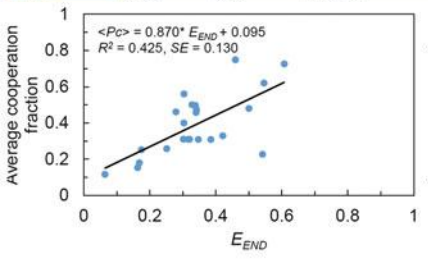

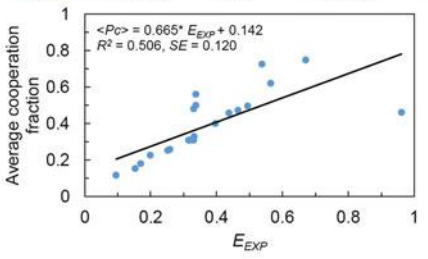

Fig. 3.46 Single regression analysis between the average cooperation fraction and (**a**) E_{END}, or (**b**) E_{END}. The regression equation with the correlation coefficient is provided in the figure. Table shows the results of statistical test. In the upper part, a regression line is significant if "Significant *F*-value" (*bold number*) is less than 0.05. While, in the lower part of the table, a regression coefficient is significant if the absolute value of "*t*-value" (marked by bold as well) is more than 2.2. Thus, both regressions are evaluated statistically robust

One plausible idea is to take correlation with $E_{END} * E_{EXP}$. The fact that EXP takes place following END in a single episode lets us expect that the product of E_{END} and E_{EXP} has a high correlation with the final equilibrium cooperation level. The result is shown in Fig. 3.47. Note that R^2 is much improved from the results of the respective single regression analyses presented in Fig. 3.46.

Another alternative idea is to apply multiregression analysis. The result is shown in Fig. 3.48, where a better R^2 is obtained than for the results of the respective single regression analyses.

These two regression analyses imply that a great contribution to the network reciprocity resulting from any models, including the default model, can be

	Degree of freedom	F-value	Significant F-value
Regression	1	70.8	**3.63E-08**
Residual	21		
Total	22		
	Standard Error (SE)	t-value	P-value
Intercept	0.032	4.99	6.09E-05
$E_{END} * E_{EXP}$	0.199	**8.41**	3.63E-08

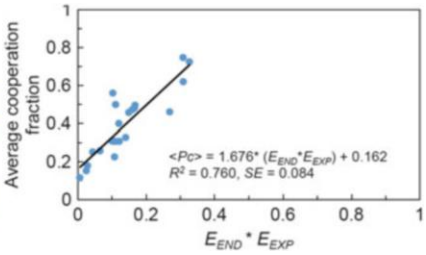

Fig. 3.47 Single regression analysis between the average cooperation fraction and the product of E_{END} and E_{EXP}. Table shows the results of statistical test

	Degree of freedom	F-value	Significant F-value	
Regression	2	23.2	**6.22E-06**	
Residual	20			
Total	21			
	Standard regression coefficient	Standard Error (SE)	t-value	P-value
Intercept	0.35E-17	0.062	0.99	0.929
E_{END}	0.451	0.174	**3.36**	0.003
E_{EXP}	0.544	0.123	**4.05**	6.25E-04

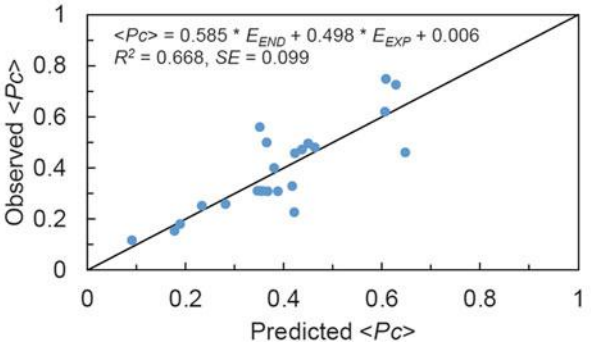

Fig. 3.48 Multiregression analysis between the average cooperation fraction and E_{END} & E_{EXP}. Table shows the results of statistical test

explained by the behavior during END and EXP in its evolutionary path, which can be evaluated using E_{END} and E_{EXP}.

3.5.4 Summary

The procedure presented here might be meaningful, because it enables transparent dissection of holistic network reciprocity, a certain newly-proposed model involving two different factors. One is how well the model can lead to good C-cluster shapes at the end of END by avoiding absorption by an all-defectors-state in END, a parameter that is measured as E_{END}. The second factor is how well the model helps spatially smooth the expansion of C-clusters that successfully survive END in EXP, measured as E_{EXP}.

This concept, supported by the idea that we should consider an evolutionary path as divided into END and EXP periods, helps us to understand the nature of network reciprocity.

In a sense, END is the period in which the dynamical system introduced by a particular network reciprocity model takes time to relax the influence resulting from the initial noise impact caused by the initial configuration of agents in the domain, usually assumed to be a random assignment of half cooperators and half defectors. As is commonly recognized in statistical physics, adding a reasonable level of noise can improve system efficiency, because of the so-called resonance effect. This fact seems consistent with the result that all models backed by a stochastic process except for "copy error" show better E_{END} than that of the default case (both "enlarging LN and IN" contain deterministic processes).

EXP is the period during which a cooperation fraction, which originally decreased, recovers. E_{END} represents the level of cooperation to which the model achieves in this period.

The simulation result amazingly reveals that most of the network reciprocity in any specific model can be quantitatively evaluated by E_{END} and E_{EXP}. Thus, the concept of dissecting the holistic network reciprocity into two processes, END and EXP, is fully justified.

This discussion has presumed IM and a lattice of $k = 8$ as the update rule and underlying topology, which is defined as entirely deterministic. We can immediately apply this procedure to different strategy update rules, even to stochastic ones such as Pairwise-Fermi, one of the most commonly-used update rules in previous studies. If Fermi-PW is assumed as a base-line, evaluating E_{END} might be less influential on the holistic network reciprocity effect, because Pairwise-Fermi adds some noise effect into the dynamics when referring to what happens in IM. A more serious problem for this application is how we apply this concept to degree-heterogeneous topologies such as Scale-Free and Small-World networks. This is because the idea of E_{EXP} premises the perfect C-cluster to measure. The question that occurs to us is how we define a perfect C-cluster in the case of degree-heterogeneous networks.

References

Barabasi, A.L., and R. Albert. 1999. Emergence of scaling in random networks. *Science* 286: 509–512.

Berde, M. 2011. Playing against the fittest: A simple strategy that promotes the emergence of cooperation. *EPL* 94: 30003.

Bollobás, B. 1985. *Random graphs*. London: Academic.

Brede, M. 2011. Playing against the fittest A simple strategy that promotes the emergence of cooperation. *EPL* 94: 30003.

Chen, X., F. Fu, and L. Wang. 2009. Social tolerance allows cooperation to prevail in an adaptive environment. *Physical Review E* 80: 051104.

Cong, R., Y–.Y. Qiu, X–.J. Chen, and L. Wang. 2010. Robustness of cooperation on highly clustered scale-free networks. *Chinese Physical Letters* 27(3): 030203.

Dai, Q., H. Li, H. Cheng, Y. Li, and J. Yang. 2010. Double-dealing behavior potentially promotes cooperation in evolutionary prisoner's dilemma games. *New Journal of Physics* 12: 113015.

Day, T., and P.D. Taylor. 2003. Evolutionary dynamics and stability in discrete and continuous games. *Evolutionary Ecology Research* 5: 605–613.

Fu, F., T. Wu, and L. Wang. 2009. Partner switching stabilizes cooperation in coevolutionary prisoner's dilemma. *Physical Review E* 79: 036101.

Fu, F., M.A. Nowak, and C. Hauert. 2010. Invasion and expansion of cooperators in lattice populations: Prisoner's dilemma vs. snowdrift games. *Journal of Theoretical Biology* 266: 358–386.

Gomez-Gardenes, J., M. Campillo, L.M. Floria, and T. Moreno. 2007. Dynamical organization of cooperation in complex topologies. *Physical Review Letters* 98: 108103.

Grilo, C., and L. Correia. 2007. What makes spatial prisoner's dilemma game sensitive to asynchronism?. *Proceedings of the 11th international conference on the simulation and synthesis of living systems*.

Hamilton, W.D. 1964. The genetical evolution of social behavior. 1. *Journal of Theoretical Biology* 7: 1–16.

Kirchkamp, O. 1999. Simultaneous evolution of learning rules and strategies. *Journal of Economic Behavior & Organization* 40: 295–312.

Li, W., X. Zhang, and G. Hu. 2007. How scale-free networks and large-scale collective cooperation emerge in complex homogeneous social systems. *Physical Review E* 76: 045102.

Moyano, L.G., and A. Sanchez. 2009. Evolving learning rules and emergence of cooperation in spatial prisoner's dilemma. *Journal of Theoretical Biology* 259: 84–95.

Newman, M.E.J. 2002. Assortative mixing in networks. *Physical Review Letters* 89: 208701.

Nowak, M.A. 2006. Five rules for the evolution of cooperation. *Science* 314: 1560–1563.

Nowak, M.A., and R.M. May. 1992. Evolutionary games and spatial chaos. *Nature* 359: 826–829.

Ogasawara, T., Tanimoto, J., Fukuda, E., and N. Ikegaya. 2014. Effect of a large gaming neighborhood and a strategy adaptation neighborhood for bolstering network reciprocity in a prisoner's dilemma game. *Journal of Statistical Mechanics: Theory and Experiment* 2014: P12024.

Ohtsuki, H., C. Hauert, E. Lieberman, and M.A. Nowak. 2006. A simple rule for the evolution of cooperation on graphs and social networks. *Nature* 441: 502–505.

Pacheco, J.M., A. Traulsen, and M.A. Nowak. 2006. Coevolution of strategy and structure in complex networks with dynamical linking. *Physical Review Letters* 97: 258103.

Pan, Q., S. Shi, Y. Zhang, and M. He. 2013. Cooperation in spatial prisoner's dilemma game with delayed decisions. *Chaos, Solitons & Fractals* 56: 166–174.

Perc, M. 2006a. Coherence resonance in a spatial prisoner's dilemma game. *New Journal of Physics* 8: 22.

Perc, M. 2006b. Chaos promotes cooperation in the spatial prisoner's dilemma game. *Europhysics Letters* 75(6): 841–846.

Perc, M. 2007. Transition from Gaussian to Levy distributions of stochastic payoff variations in the spatial prisoner's dilemma game. *Physical Review E* 75: 022101.
Perc, M., and M. Marhl. 2006. Evolutionary and dynamical coherence resonances in the pair approximated prisoner's dilemma game. *New Journal of Physics* 8: 101016.
Perc, M., and A. Szolnoki. 2010. Coevolutionary games – A mini review. *Biosystems* 99: 109–125.
Perc, M., and Z. Wang. 2010. Heterogeneous aspiration promotes cooperation in the prisoner's dilemma game. *PLoS ONE* 5(12): e15117.
Pestelacci, E., M. Tomassini, and L. Luthi. 2008. Evolution of cooperation and coordination in a dynamically networked society. *Biological Theory* 3: 139–153.
Poncela, J., J. Gomez-Gardenes, L.M. Flora, and Y. Moreno. 2007. Robustness of cooperation in the evolutionary prisoner's dilemma on complex networks. *New Journal of Physics* 9: 101088.
Poncela, J., J. Gomez-Gardenes, L.M. Floria, A. Sanchez, and Y. Moreno. 2008. Complex cooperative networks from evolutionary preferential attachment. *PLoS ONE* 3: e2449.
Ren, G., and X. Wang. 2014. Robustness of cooperation in memory-based prisoner's dilemma game on a square lattice. *Physica A* 408: 40–46.
Roca, C.P., J.A. Cuesta, and A. Sanchez. 2006. Time scales in evolutionary dynamics. *Physical Review Letters* 97: 158701.
Roca, C.P., J.A. Cuesta, and A. S'anchez. 2009. Effect of spatial structure on the evolution of cooperation. *Physical Review E* 80: 046106.
Rong, Z., X. Li, and X. Wang. 2007. Roles of mixing patterns in cooperation on a scale-free networked game. *Physical Review E* 76: 027101.
Santos, F.C., J.M. Pacheco, and T. Lenaerts. 2006a. Evolutionary dynamics of social dilemmas in structured heterogeneous populations. *Proceedings of the National Academy of Science of the United States of America* 103(9): 3490–3494.
Santos, F.C., J.M. Pacheco, and T. Lenaerts. 2006b. Cooperation prevails when individuals adjust their social ties. *PLoS Computational Biology* 2(10): 1284–1291.
Schuessler, R. 1989. Exit threats and cooperation under anonymity. *Journal of Conflict Resolution* 33: 728–749.
Shigaki, K., J. Tanimoto, Z. Wang, and E. Fukuda. 2013. Effect of initial fraction of cooperators on cooperative behavior in evolutionary prisoner's dilemma. *PLoS ONE* 8(11): e76942.
Szabo, G., and G. Fath. 2007. Evolutionary games on graphs. *Physics Reports* 446: 97–216.
Szolnoki, A., and M. Perc. 2009a. Resolving social dilemmas on evolving random networks. *EPL* 86: 30007.
Szolnoki, A., and M. Perc. 2009b. Emergence of multilevel selection in the prisoner's dilemma game on coevolving random networks. *New Journal of Physics* 11: 093033.
Szolnoki, A., M. Perc, and M. Mobilia. 2014. Facilitators on networks reveal optimal interplay between information exchange and reciprocity. *Physical Review E* 89: 042802.
Tang, C.-L., W.-X. Wang, X. We, and B.-H. Wang. 2006. Effects of average degree on cooperation in networked evolutionary game. *European Physical Journal B* 53: 411–415.
Tanimoto, J. 2007a. Dilemma-solving effects by the coevolution of both networks and strategy in a 2×2 game. *Physical Review E* 76: 021126.
Tanimoto, J. 2007b. Promotion of cooperation by payoff noise in a 2×2 game. *Physical Review E* 76: 041130.
Tanimoto, J. 2009. Promotion of cooperation through co-evolution of networks and strategy in a 2×2 game. *Physica A* 388(6): 953–960.
Tanimoto, J. 2010. Effect of assortativity by degree on emerging cooperation in a 2×2 dilemma game played on an evolutionary network. *Physica A* 389: 3325–3335.
Tanimoto, J. 2011. A study of a quadruple co-evolutionary model and its reciprocity phase for various Prisoner's Dilemma games. *International Journal of Modern Physics C* 22(4): 401–407.
Tanimoto, J. 2014. Simultaneously selecting appropriate partners for gaming and strategy adaptation to enhance network reciprocity in the prisoner's dilemma. *Physical Review E* 89: 012106.

Tanimoto, J., M. Nakata, A. Hagishima, and N. Ikegaya. 2011. Spatially correlated heterogeneous aspirations to enhance network reciprocity. *Physica A* 391(3): 680–685.

Tomassini, M., L. Luthi, and E. Pestelacci. 2007. Social dilemmas and cooperation in complex networks. *International Journal of Modern Physics C* 18(07): 1173–1185.

Tomochi, M. 2004. Defectors' niches: Prisoner's dilemma game on disordered networks. *Social Networks* 26(4): 309–321.

Vainstein, M.H., and J.J. Arenzon. 2001. Disordered environments in spatial games. *Physical Review E* 64: 051905.

Van Segbroeck, S., F.C. Santos, T. Lenaerts, and J.M. Pacheco. 2009. Reacting differently to adverse ties promotes cooperation in social networks. *Physical Review Letters* 102: 058105.

Vincent, T.L., and R. Cressman. 2000. An ESS maximum principle for matrix games. *Theoretical Population Biology* 58: 173–186.

Vukov, J., G. Szabo, and A. Szolnoki. 2006. Cooperation in noisy case: Prisoner's dilemma game on two types of regular random graphs. *Physical Review E* 73: 067103.

Wang, Z., and M. Perc. 2010. Aspiring to the fittest and promoted of cooperation in the prisoner's dilemma game. *Physical Review E* 82: 021115.

Watts, D.J., and S.H. Strogatz. 1998. Collective dynamics of 'small-world' networks. *Nature* 393: 440–442.

Xia, C., Q. Miao, and J. Zhang. 2013. Impact of neighborhood separation on the spatial reciprocity in the prisoner's dilemma game. *Chaos, Solitons & Fractals* 51: 22–30.

Xulvi-Brunet, R., and I.M. Sokolov. 2004. Reshuffling scale-free networks: From random to assortative. *Physical Review E* 70: 066102.

Yamauchi, A., J. Tanimoto, and A. Hagishima. 2010. What controls network reciprocity in the prisoner's dilemma game? *Biosystems* 102(2–3): 82–87.

Yamauchi, A., J. Tanimoto, and A. Hagishima. 2011. An analysis of network reciprocity in prisoner's dilemma games using full factorial designs of experiment. *Biosystems* 103: 85–92.

Zhong, W., S. Kokubo, and J. Tanimoto. 2012. How is the equilibrium of continuous strategy game different from that of discrete strategy game? *Biosystems* 107(2): 89–94.

Zimmermann, M., and V. Eguiluz. 2005. Cooperation, social networks, and the emergence of leadership in a prisoner's dilemma with adaptive local interactions. *Physical Review E* 72: 056118.

Chapter 4
Evolution of Communication

Abstract In this chapter, we discuss several interesting applications of evolutionary game theory. The chapter first takes up one possible scenario for why and how animal communication evolves. A series of numerical experiments based on an evolutionary game elucidates that one of the key points is time flexibility in the evolutionary trail. A social dilemma situation in a static environment only requires time-constant -reciprocity that can be emulated by Prisoner's Dilemma (PD) games, which does not give rise to any communication at all. On the other hand, a dynamic environment needs -reciprocity to solve a social dilemma. This compels communication to emerge among agents so that they can obtain a high payoff, leading to Fair Pareto optimum. This kind of constructivist approach suggests that a PD game seems less appropriate as an argument for the inception of communication, but Leader or Hero might be better.

4.1 Communication; as an Authentication Mechanism

With respect to what this section noting, a reader can consult with Tanimoto (2008). Communication is widely observed in various animal species and human language is its highly evolved form. The question of what initially brought about animal communications (including human language) and how it evolved is one of the most challenging problems, in terms of interdisciplinary viewpoint, which is still unsolved. For example, some analysts and anthropologists are seeking proof that relates language acquisition and basicranial curves. One crucial impediment to this research is that communication is only software; it is impossible to find biological evidence such as fossils and bones. To circumvent this limitation, an approach based on artificial life and complex sciences seems useful, as it can effectively shed some light on the process of emergence of animal communication. By means of this kind of approach, one establishes a model based on a hypothesis. And if a simulation result by the model is consistent with an observatory proof, one can say that the hypothesis might be likely. It is generally called a constructivism approach, which powerfully works for problems where none of direct and hard evidence is not brought about, and

J. Tanimoto, *Fundamentals of Evolutionary Game Theory and its Applications*,
Evolutionary Economics and Social Complexity Science 6,
DOI 10.1007/978-4-431-54962-8_4

of which background mechanism is sought to be clarified. A question of how a communication evolves might be one of typical applications.

Rationale mechanisms observed in animal communication have given several useful mathematical frameworks, which have been applied to many engineering fields. The ant system, initially proposed by Dorigo et al. (1996), is widely used to solve optimization problems such as the traveling salesman problem (e.g., Kawamura et al. (1998)). The ant system assumes that a group of ants develop pheromone communication in order to maximize their fitness.

Let us be concerned on the question of why and how communication evolves. Van Baalen and Jansen (2003) studied the communication strategies of bird alarm calls, using a Spaced-Chicken type dilemma game. When a dilemma tempting an agent to exploit is relatively small, the population uses a single signal for its alarm call. However, with growing dilemma strength, reliability of the alarm call decays, because of an increase in the number of mimics (who use false signals). The social system begins to fluctuate between cooperative (reliable alarm call) and defective (false information) eras. This is a perturbation phase, commonly observed in various unsteady dynamic systems. Later, assuming a strong dilemma, the communication value of the alarm call is completely disrupted, leading to a situation called the Tower of Babel.

Several previous studies dealt with emerging (self-organizing) communication processes. Grim et al. (2004) demonstrated a multi-agent simulation, where agent's action (gesture), which was initially meaningless, can acquire meaning, in order to share specific information about a predator or prey with other agents.

Buzing et al. (2005) investigated the relationship between environment and communication using their sugarscape-like multi-agent simulation. They insist that pressure to cooperate leads to the evolution of communication skills, which facilitate cooperation. Furthermore, higher levels of cooperation pressure coming from the environment encourage high-density communication.

These previous studies see communication as a way of increasing individual fitness. An animal's struggle for existence has been regarded as a social dilemma game, where a player intends to increase his fitness to produce more offspring than others. In the last decade, dilemma games based on the evolutionary game theory have been extensively investigated. The central question they ask is how the game dilemma disappears or is ameliorated? What additional game option should be imposed on the original dilemma games to dilute those that are mostly emulated by 2×2 Prisoner's Dilemma (PD)? To the end, as we mentioned in the previous chapters, Nowak (2006) sums that those additional options to solve dilemma should be called mechanisms to add social viscosity to a social system where one can classifies five frameworks under several assumptions: kin selection, direct reciprocity, indirect reciprocity, network reciprocity and group selection (see Sect. 2.6). All of those mechanisms to add social viscosity can compress "anonymity" in a society. If a society has infinite agents and is defined as well-mixed, the society assures perfect anonymity. In this situation, none of agents has incentive to mutually cooperate because probability of the opponent, to whom a focal agent gives help, giving help in return, is zero. Thus, a framework to dilute or disappear a social

dilemma is paraphrased to be a provision to identify whether an opponent is appropriate one to cooperate or not in a social context.

Following these works, we can possibly guess that communication evolved as one of those schemes, and has the same "function"—to increase fitness by means of identifying appropriate opponents from others who have a non-reciprocity attitude. But is that true?

Sato et al. (2007) developed a simulation model for proto-communication, which emulates a turf war between two fixed agents. The two agents face each other in one-dimensional space, and try to occupy the opponent's space. The agents have cognitive faculty for whether his opponent's light is on or off, which means nothing exists at the beginning of each simulation episode. The agent can also control his own light status and action. Actions are defined as either going forward or pulling back. This study suggested that the two agents, even without any initial knowledge, could develop reciprocity in an interactive game campaign, by bilaterally alternating the actions of going forward and pulling back. This provides them a high payoff. Amazingly, this coordinated alternating reciprocity action is synchronized with the sequence of light on/off for both the agents. Sato et al. insisted that this co-evolution system—a combination of the actions (offering "going forward" or "pulling back") and lighting (switching "on" or "off")—could contribute to the emergence of protopathic communication.

This particular game, seems to have the structure of a Leader ($T > R$ & $S > P$ and $S + T > 2R$ & $T > S$) or Hero ($T > R$ & $S > P$ and $S + T > 2R$ & $S > T$) game with a Chicken-type dilemma, where *ST*-reciprocity is more preferable than *R*-reciprocity as discussed in Sect. 2.8. Because an alternating set of "going forward" and "pulling back" actions is thought to be equivalent to the fair Pareto Optimum of both the Leader and Hero game, an alternating set of (C, D) (namely S) and (D, C) (T) is preferred to maximize equal payoffs.

4.2 An Evolutionary Hypothesis Suggested by Constructivism Approach

The work by Sato and his colleagues is persuasive, and their approach obviously relies on constructivism. In fact, what they showed implies one of the possible scenarios of how a primitive communication evolves. However, the game defined by Sato et al. seems more particular than the other universal and general games. Also, their game presumes an infinite iteration, the results of which cannot explain how communication works in an indirect reciprocity situation. Therefore, in the discussion of this chapter, we assume one-shot 2×2 games, covering the entire set of game structures, including PD, Chicken, Stag Hunt (ST), Leader, Hero, and even Trivial games. Our primary intention in the discussion study is to show how a game structure (dilemma feature and its strength) affects the emergence of an agent's communication.

4.2.1 Model Setup

Game Setting

Standing on what was assumed in the previous chapters, we describe all classes of 2×2 game by assuming payoff matrix; $\begin{pmatrix} R & S \\ T & P \end{pmatrix}$. As we discussed in Sect. 2.7, if we rely on the scalding parameter expressed by Eq. (2.39); ${D_g}' = \frac{T-R}{R-P} = \frac{D_g}{R-P}$ and ${D_r}' = \frac{P-S}{R-P} = \frac{D_r}{R-P}$, the all four 2×2 game classes can be reproduced by varying ${D_g}'$ and ${D_r}'$. If both ${D_g}'$ and ${D_r}'$ are positive, a game is Prisoner's Dilemma (PD). In contrast, in case of both negative, it belongs to Trivial Game that has none of dilemma at all. If only ${D_g}'$ is positive, it is Chicken, while if only ${D_r}'$ is positive, it belongs to Shag Hunt. Moreover, A game becomes Leader, which is a sub-class of Chicken, when ${D_g}' > 0$, ${D_r}' < 0$, $S + T > 2R$ and $T > S$. Also, it is a Hero game, another sub-class of Chicken, when ${D_g}' > 0$, ${D_r}' < 0$, $S + T > 2R$ and $S > T$. All other dilemma games than Leader and Hero become fair Pareto Optimum meaning social payoff maximum when R-reciprocity where mutual cooperation offering is realized. On the other hand, ST-reciprocity, where alternating S and T happening, makes Leader and Hero be a fair Pareto Optimum.

Finite State Machine (FSM)

Let us assume a well-mixed population consisting of n agents.

Each agent has two finite state machines (FSM), having a receptor and a reactor, as shown in Fig. 4.1. Through FSM #2, the agent receives information about previous game consequences—whether P, R, S, or T occurred at the receptor. Using a 4-bit processing system, he determines his action for the current time-step offering—whether his light should be switched on or off. Following that, he recognizes the input information about his and his opponents' lighting status in the current time step, through the receptor of FSM #1. Also, using the 4-bit processing system, he determines his next action—offering C or D in the current time step.

This total of eight bits used for both FSMs comprise an agent's gene.

In each generation, each agent plays M one-shot games, changing opponents randomly. The sum of the obtained payoffs during a generation is regarded as the fitness. At the end of each generation, the genetic evolutionary process of the total population is operated. In the GA (genetic algorithm) process, the probability of crossover is 1, in which one-point crossover is imposed. Also, there exists 1 % mutation, where one of 8-bit binary codes is flipped.

At the beginning of each simulation episode, the agent's 8-bit gene codes are randomly shuffled.

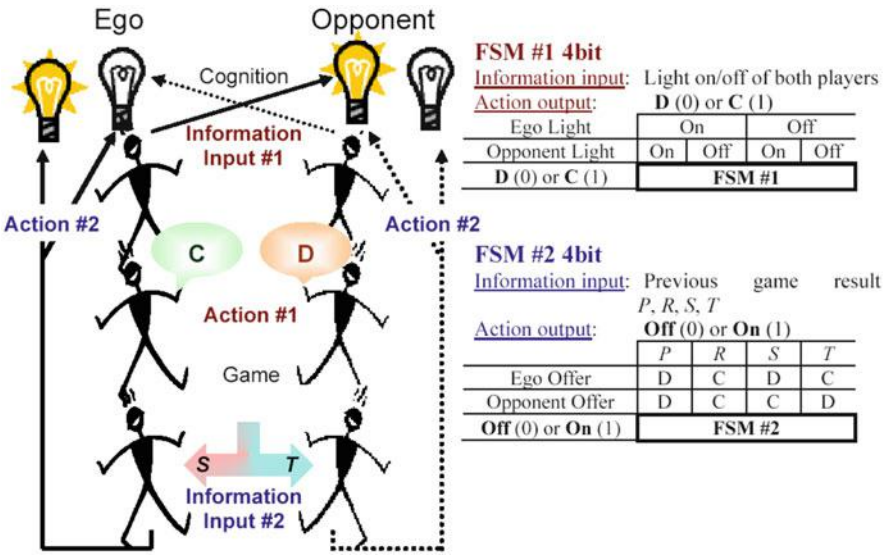

Fig. 4.1 Structure of assumed FSMs and game flow

Numerical Simulation

We assume total population; $n = 100$, number of one-shot 2×2 games in one generation; $M = 10$. Each episode is calculated up to 20,000 generations. We adopt an average of 10,000–20,000 generations as a quasi-equilibrium solution. We finally observe an ensemble average based on five simulation episodes.

4.2.2 Results and Discussion

Generative Transition of Hero and PD

Figure 4.2 shows a generative transition of $D_g' = 0.31$ and $D_r' = -1.66$ Hero game, with 0–10,000 generations. Figure 4.3 is a counterpart of a $D_g' = 0.5$ and $D_r' = 0.5$ PD case. These indicate (a) average payoff and cooperation fraction (P_C), (b) lighting fraction (P_{on}), (c) occurring fractions of P, R, S, and T, (d) information

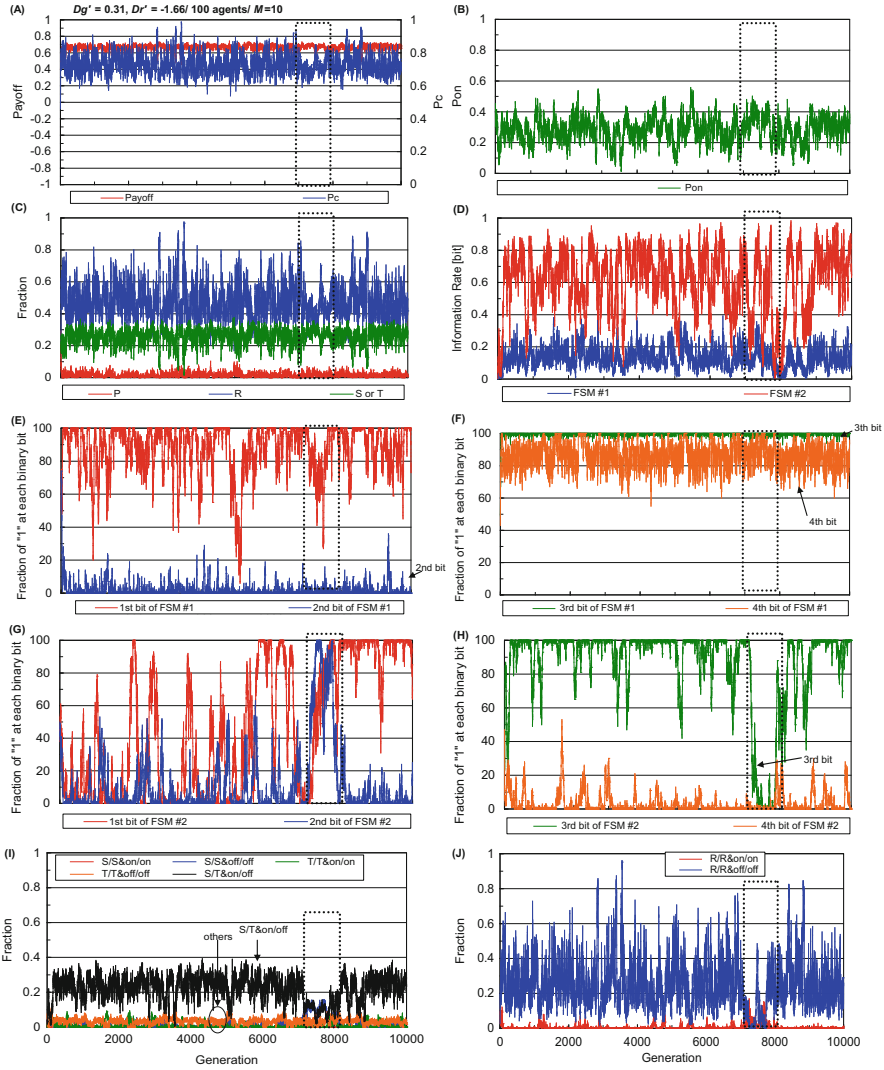

Fig. 4.2 Generative transition of $D_g' = 0.31$ and $D_r' = -1.66$ Hero game assumed 100 agents and $M = 100$. (**a**) Average payoff and cooperation fraction, (**b**) lighting fraction, (**c**) fractions of P, R, S and T, (**d**) information rate of FSM #1 and FSM #2, (**e**) fraction of "1" on either first or second bit of FSM #1, (**f**) fraction of "1" on either third or fourth bit of FSM #1, (**g**) and (**h**) same for FSM #2, (**i**) fractions of two sequence games resulting in S & on after S & on; S & off after S & off; T & on after T & on; T & off after T & off; S (or T) & on (or off) after T (or S) & off (or on), and (**j**) fractions of two sequence games resulting in R & on after R & on; R & off after R & off

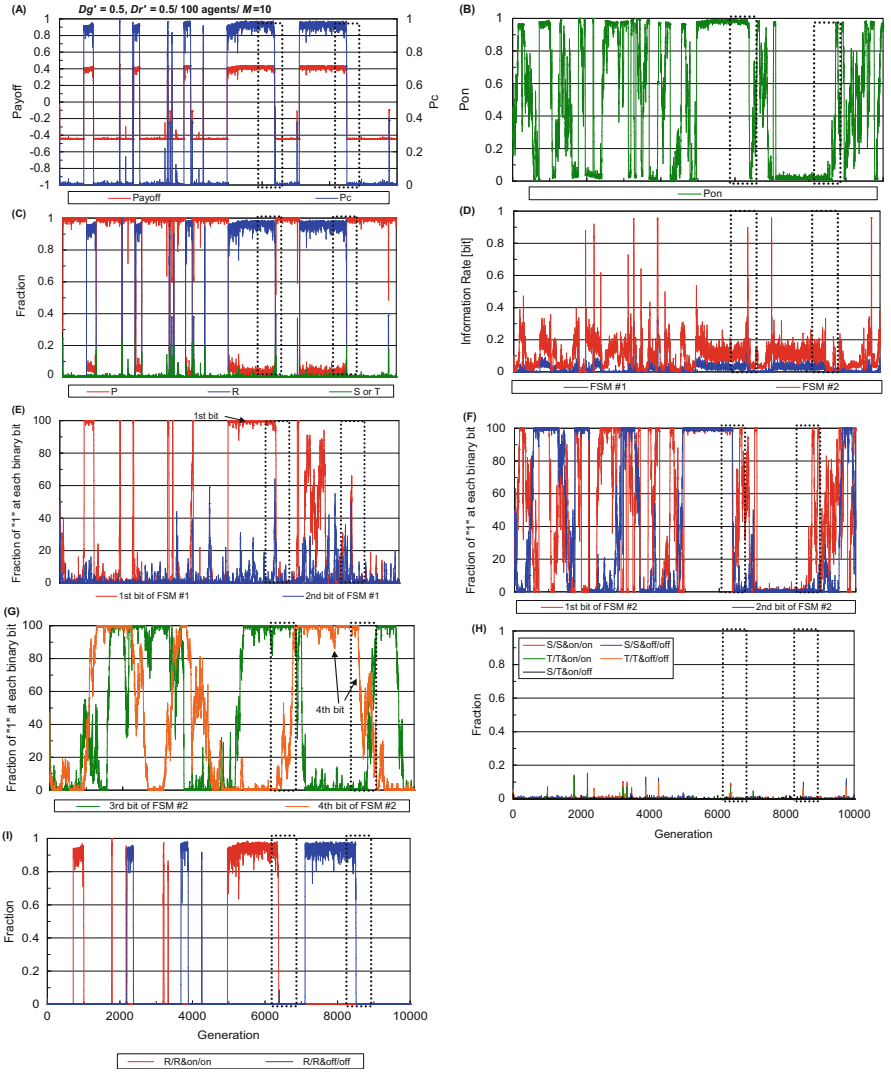

Fig. 4.3 Generative transition of $D_g{}' = 0.5$ and $D_r' = 0.5$ PD game. Same setting of Fig. 4.2 is applied

(a) The case of θ = - 10 deg, r = 1.0.

FSM #1				FSM #2			
on/on	on/on	off/on	off/off	P	R	S	T
C	**D**	**C**	C	*	*	**on**	**off**

C, **D**, **on** and **off** indicate almost perfect *C*, *D*, *on* and *off*, respectively.
C and D indicate predominant *C* and *D*.

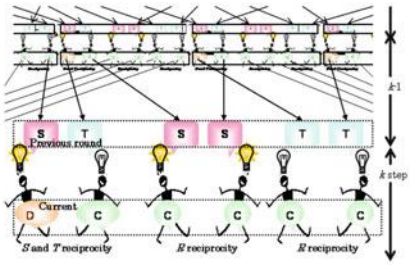

(b) The era after 8000 generation in the case of θ = 90 deg,

1 0 FSM #1				FSM #2			
on/on	on/on	off/on	off/off	P	R	S	T
*	D	D	**C**	**off**	**off**	**off**	**on**

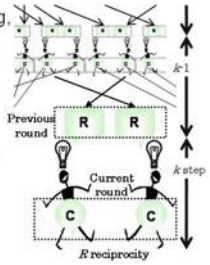

Fig. 4.4 Summary content of FSMs and possible happening game events of (**a**) $D_g' = 0.31$ and $D_r' = -1.66$ Hero game case and (**b**) the era after 8000 generation of $D_g' = 0.5$ and $D_r' = 0.5$ PD. Each table summary of both FSM #1 and FSM #2 makes an event happening drawn in the right panel scheme. (**a**) The case of $\theta = -10$ deg, $r = 1.0$. (**b**) The era after 8000 generation in the case of $\theta = 90$ deg, $r = 1.0$

rate of FSM #1 and FSM #2,[1] (e) fraction of "1" on either first or second bit of FSM #1, (f) fraction of "1" on either third or fourth bit of FSM #1, (g) and (h) same for FSM #2, (i) fractions of two sequence games resulting in *S* & on after *S* & on; *S* & off after *S* & off; *T* & on after *T* & on; *T* & off after *T* & off; *S* (or *T*)& on (or off) after *T* (or *S*) & off (or on), (j) fractions of two sequence games resulting in *R* & on after *R* & on; *R* & off after *R* & off.

In PD (see Fig. 4.4), there are unstable fluctuations perturbing between *R* reciprocity (with $P_C \cong 1$) and mutual defection (with $P_C \cong 0$). This is because of a

[1] The Information Entropy $H_{act|sense}$[bit] of action outputting x_k under information inputting y_i can be defined as;

$$H_{act|sense} = -\sum_{j=1}^{} \sum_{k=1}^{} p\left(x_k, y_j\right) \cdot \log_2 p\left(x_k | y_j\right),$$

where $p(x_k, y_j)$ is the compounded probability of x_k and y_i, and $p\left(x_k | y_j\right)$ is the conditional probability of x_k under y_i. The Information Rate I_{sense}[bit] is defined as the difference between information entropy without any information input H_{act} [bit] and $H_{act|sense}$,

$$I_{sense} = H_{act} - H_{act|sense}.$$

mutant mimic, who defects even though signaling like other cooperators, can invade the *R* reciprocity population and increase by exploiting cooperators. During the *R* reciprocity eras, lighting on or off is a signal to cooperate (see Fig. 4.3(j)). Once either lighting on or off is established as a signal, it will not change until it is corrupted by a mimic invasion. Therefore, during *R* reciprocity, the signal can be considered as a superficial symbol, which is different from the dynamic signaling of an *S & T* reciprocity, which will be explained in the following text. Furthermore, the signal in an *R* reciprocity era functions like a Tag, to discriminate cooperators from others, and is not robust enough to defend mimic invasions. Consequently, the signal sometimes shifts from generation to generation.

Here, a question may arise regarding how an *R* reciprocity era is eroded, leading to mutual defection, once cooperation is established. Consider two examples, one just after 6000 and the other after 8000 generations. These are highlighted as dotted rectangles in Fig. 4.3. The respective signals in both *R* reciprocity eras are lighting on and off (see Fig. 4.3(j)).

In the first era, after 6000 generations, an agent agrees to offer C when he recognizes a signal of mutual lighting on. It is confirmed by the fact that the first bit of FSM #1 is almost "1" (see Fig. 4.3(e)). However, in the latter part of this era, a rapidly increasing number of agents offer C, with a signal of mutual lighting off (who have "1" in the fourth bit of FSM #1, see Fig. 4.3(f)). This implies that there are agents offering C with mutual lighting on and also off. When these agents increase in the population, a game, matching agents with lighting on against those with lighting off, inevitably takes place. In this game, the consequence is mutual defection (*P*), even though they are instinctively cooperative. This leads to the corruption of *R* reciprocity.

In the second era, after 8000 generations, an agent agrees to offer C when he recognizes the signal of mutual lighting off. It is confirmed by the fact that the fourth bit of FSM #1 is almost "1" (see Fig. 4.3(f)). In Fig. 4.3(h), we notice that the fourth bit of FSM #2 is almost "1". This means that agents share using the "signal of confession," in which the light is put on whenever he accidentally exploits his opponent by obtaining *T*. However, in the last period of this era, a mimic mutant having "0" in the fourth bit of FSM #2 can successfully invade, and his offspring immediately spreads in the population. Hence, the "signal of confession," which can function as a protocol preventing mutual defection (a so-called "safety-net" for *R* reciprocity) is destroyed.

There are many dynamic patterns that shift from *R* reciprocity to mutual defection, but we discussed only two examples here. *R* reciprocity has various possible trails leading to mutual defection due to erosion of a particular bit of an FSM by mimic agents, which consequently leads to unstable reciprocity-defection cycles—the perturbation phase.

What happens in the Hero game shown in Fig. 4.2?

Payoff transition is more stable than the PD (see Fig. 4.2(a)), in which *R* reciprocity and *S & T* reciprocity are combined (see Fig. 4.2(c)). Generally speaking, a Hero game has less dilemma than PD, since D_r' of the Hero is negative while that of the PD is positive. This is qualitatively attributable to the fact that the Hero has

more stable payoff transition than PD, by avoiding mutual defection. Amazingly, the very efficient *S* & *T* reciprocity obtaining *S* and *T* by turns occurs significantly (see Fig. 4.2(i)), although *R* reciprocity through a lighting signal (off) is observed more frequently (see Fig. 4.2(j)). This *ST*-reciprocity is same as the CAD-type coordinate alternating reciprocity discussed in Sect. 2.8. The most important point is that obtaining *S* and *T* by turns is synchronized with switching signals—either lighting off after on or lighting on after off. This implies that information processing by switching light on and off plays an important role in attaining indirect reciprocity in such an anonymous matching one-shot game. This is confirmed by larger information rate (Fig. 4.2(d)), than in the PD case (Fig. 4.3(d)). In Fig. 4.2(e) and (f), we notice a manifest protocol, in which a focal agent offers D when his own light is turned on and his opponent's light is off (the second bit of FSM #1 is almost "0"); he offers C when both his and his opponent's lights are either on or off, simultaneously (the first and fourth bits of FSM #1 are almost "1"). This is attributable to the high performance of CAD-type *ST*-reciprocity in the Hero game. As discussed, continuous lighting on or off, to produce *R* reciprocity in the PD, works as a superficial symbol, and is static during the evolution period. In the Hero, however, this phenomenon results in the emergence of CAD-type *ST*-reciprocity followed by primitive communication.

Note that there exists a slightly eroded period of CAD-type *ST*-reciprocity, based on communications, after 7000 generations, highlighted by a dotted rectangle in Fig. 4.2(i). In this period, *R* reciprocity is also eroded, as shown in Fig. 4.2(j). Because the third bit of FSM #2 decreases rapidly from almost "1" to "0," the disturbance brought by mimic invasion destroys the "help call," in which a focal agent turns his light on when he is exploited by his opponent obtaining *S*. When the "help call" malfunctions, not only *R*-reciprocity but also *ST*-reciprocity are affected.

Why *R*-Reciprocity in PD Is More Fragile than *ST*-Reciprocity in Hero?

Figure 4.4 schematically shows a summary of the content of FSMs and possible game events of (a) $\theta = -10$ deg and $r = 1.0$ Hero game case and (b) during the era after 8000 generations of $\theta = 90$ deg and $r = 1.0$ PD. Observing Figs. 4.5(b) and 4.4, in the era after 8000 generation, typically two agents with lights off meet and mutually offer C, thus obtaining *R*. This is a single game event.

As opposed to this, in the Hero game shown in Figs. 4.4(a) and 4.2, there are mainly three game events. If a lighting-on agent meets a lighting-off agent, *ST*-reciprocity occurs. In cases where agents with the same signal meet, they coincidently offer C to obtain *R*, which is the second highest payoff combination after *S* & *T*. In this society, both lighting-on and lighting-off agents co-exist (see P_{on} in Fig. 4.2(b)), which implies that these three game events can respectively occur at certain frequencies. Therefore, the binary bits of both FSMs shown in Fig. 4.4(a) are meaningful, except for the first and second bits of FSM #2, which are expressed by wild card marks. In other words, if any single bit of those significant binary bits is

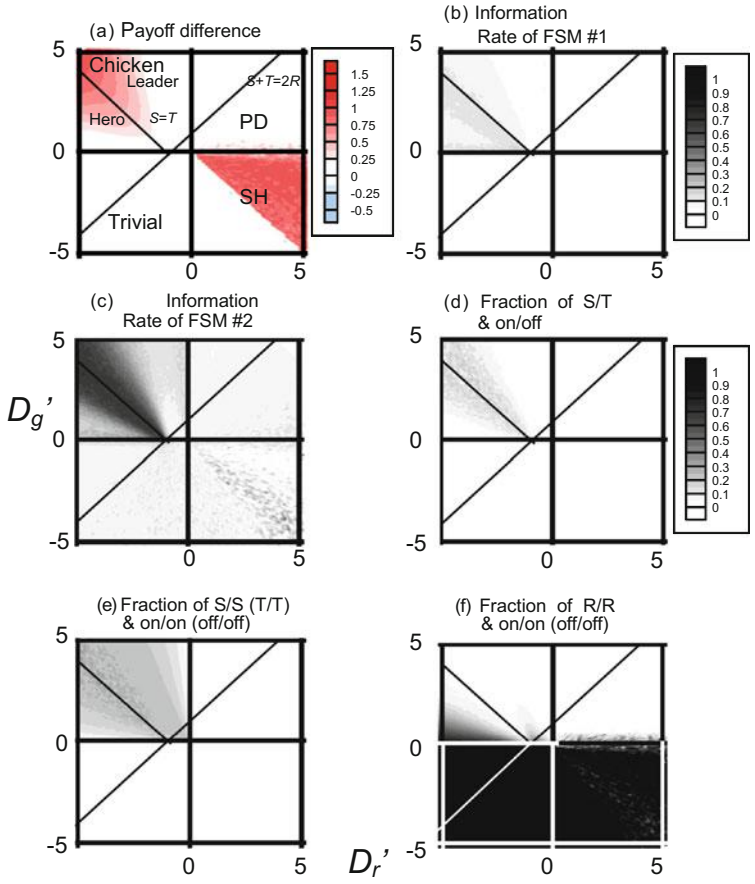

Fig. 4.5 Holistic pictures covering a 2×2 game world for (**a**) payoff difference between the present model and an analytic solution by replicator dynamics, (**b**) information rate of FSM#1, (**c**) information rate of FSM#2, (**d**) fraction of *S*/*T* & on/off, (**e**) fraction of *S*/*S*(*T*/*T*) & on/on(off/off), and (**f**) fraction of *R*/*R* & on/on(off/off)

mutated, reciprocity would never work. Once reciprocity is established, a mimic who mutated a single bit among those significant binary bits finds it hard to invade and settle in the population. This is why the reciprocity observed in the Hero game is robust and sustainable.

In the PD shown in Figs. 4.4(b) and 4.3, the situation is completely different. Once reciprocity has been established, only the fourth bit of FSM #1 and the second bit of FSM #2 are significant, because most of the agents in the population offer C and light off (see P_C and P_{on} in Fig. 4.3(a) and (b)). Therefore, binary bits other than these two are not significant in sustaining the *R* reciprocity once it is built. This is why a mutant with a malfunctioning "signal of confession" can invade the population. As explained in the previous section, after spreading this particular mutant,

signaling with lighting does not make any sense, and the situation is very vulnerable to attack by a mutant who defects in the case of mutual lighting off.

Equilibrium Features of the 2×2 Games

Figure 4.5 indicates quasi-equilibrium solutions covering the entire 2×2 game world, derived from an ensemble average of five simulation trials. Figure 4.5(a) shows payoff difference obtained with an analytical solution based on replicator dynamics, without any supporting provisions for cooperation such as memory, tag, network, and others. Figure 4.5(b) and (c) shows isographs of the information rates of both FSM #1 and FSM #2. Figure 4.5(d), (e), and (f) indicates fractions of two sequence games resulting in S (or T)& on (or off) after T (or S) & off (or on), S (or T) & on (or off) after S (or T) & on (or off), and R & on (or off) after R & on (or off).

Figure 4.5(a) indicates that the present model can gain larger payoff than the analytical solution in the areas of SH close to PD. However, the model only provides the same meager payoff (zero) of the analytical solution in PD area. Although the agents in the model equip memory and light as a sophisticated tool to support communication, the well-mixed situation only allowing one-shot game sequence is severe to emerge R-reciprocity in PD games as noted above. But, in SH where none of chicken-type dilemma exists anymore, the model makes R-reciprocity in function. Amazingly, the model in the areas of Leader and Hero where $S+T > > 2R$ is satisfied indicating much more incentive for ST-reciprocity, can provide larger payoffs than the analytical solution even in the larger dilemma (namely larger $D_g{}'$) case. This area is consistent with the region where the information rates of both FSMs (especially FSM #2) are large (Fig. 4.5(b), (c)) and high frequency of CAD-type S & T reciprocity is observed (Fig. 4.5(d)).

As shown in Fig. 4.3, the information rate of FSM #1 describes how the information input derived from lighting status affects the action output—whether an agent offers C or D. In addition, the information rate of FSM #2 implies how the information input derived from previous game consequences affects the action output—whether an agent lights are on or off. In brief, the former and the latter are orders of degree of the action strategy regulating C or D and the communication protocol (language distribution).

The above-mentioned discussion might imply that, in terms of reciprocity being synchronized with communication, both Hero and Leader games with CAD-type ST-reciprocity seem more important than PD with R-reciprocity. This can be explained by our observation that R-reciprocity in PD can only work as a time-static symbol, like the Tag system, but CAD-type ST-reciprocity in Hero and Leader can convey meaningful information by means of intermittent lighting on/off. In addition, R reciprocity seems vulnerable against dilemma strength, which can be confirmed by the fact that there is mutual defection, the Nash Equilibrium, in PD (Fig. 4.5(a)). On the contrary, the CAD-type ST-reciprocity is robust. We can see that larger payoff for larger $D_g{}'$ (Fig. 4.5(a)) and the CAD-type

ST-reciprocity is maintained to some extent (Fig. 4.5(d)). Again, the most important feature of both Hero and Leader, which are different from PD and pure Chicken, is the condition $S+T>2R$. Extrapolating, we can say that primitive communication among animals was encouraged by a particular dilemma situation, represented by Hero and Leader, where agents could only solve the dilemma by sharing unequal roles (C or D). If so, PD, which is the focus of most previous work concerning evolutionary game theory, cannot explain the question.

Relation to the Co-evolution Model of Norm and Action Strategy by Chalub et al.

Our model presented here is deeply related to the co-evolution model of norm and action strategy proposed by Chalub et al (2006). In their model, an agent having different action strategies plays one-shot 2×2 games with opponents who live on the same island, where a norm is commonly shared by all inhabitants. The action strategy is defined as a look-up table (same as an FSM) regulating a focal agent's strategy (C or D) under the input information of his opponent's image score (originally proposed by Nowak and Sigmund (1998)). The norm determines the relationship between actions and image scores. For example, consider three norms: One in which a cooperator's cooperation with a cooperator increases the focal cooperator's image score; another in which a cooperator's cooperation against a defector decreases the focal cooperator's image score; and the last one in which defector's defection against a defector increases the focal defector's image score. The second statement is the so-called protection code for the second-order free-rider. The third one is called the "safety-net" protocol for losers (those who have a low image score). The norm regulates the good or bad actions on each island. Chalub et al. report that a stable cooperative society can be obtained by the co-evolution of the individual agent's action strategy and respective island norms.

The action strategy is the counterpart of our FSM #1 and the norm accounts for FSM #2. However, there are two major differences between their theory and this study. The first difference is that not only FSM #1 but also FSM #2 are individually variable in this study. In other words, the counterpart of their norm, FSM #2, is not commonly shared with other agents in the population. This complicates the dilemma problem. The second notable difference is that the viewpoint of their norm is defined as an objective (because the norm is shared with others). On the other hand, in our model, the method to determine whether lighting is on/off, FSM #2, is defined subjectively (because the individual level defines FSM #2). In that sense, FSM #2 can be called a norm in which a focal agent can determine his own image score based on his own ideas. This also complicates the dilemma, because a vicious agent can easily diffuse false information in the society. Despite these crucial differences, in our model, we can observe the emergence of several phases of reciprocity as previously discussed. Ohtsuki and Iwasa (2004) addressed how different standpoints of the norm affect the possibility of emerging cooperation.

Summary

In order to shed some light on how animal communication evolved and led to reciprocity, we built a 2-layer co-evolution model. This model contains two FSM layers that express an agent's intelligence via two information input-action output machines for a well-mixed population only allowing agents one-shot games. The first one (FSM #1) regulates the agent's offer in a game, whether C or D, based on the light on/off status for himself and his opponent. The second one stipulates his lighting on/off status, based on information from previous game results—whether P, R, S, or T. Compared with the analytical solution derived from the replicator dynamics, where no cooperation support mechanism is assumed, our model provides higher payoffs in various dilemma games. In Particular, combining R-reciprocity and ST-reciprocity in Hero and Leader areas is observed. Time evolution in the PD is prone to unstable fluctuation between R-reciprocity and mutual defection. The R-reciprocity is unstable, and intermittently succumbs to mimic invasion, leading to defection periods. Time evolution in Hero and Leader, however, seems stable, in which the CAD-type ST-reciprocity is intermixed with R-reciprocity.

From the communications point of view, R reciprocity in PD seems only to work as a time-static symbol, just like the Tag system, although it affords some flexibility, as one can change lighting from on to off (or off to on) for use as a signal. CAD-type ST-reciprocity in Hero and Leader can convey meaningful information by alternating lighting on and off. This implies that primitive communication among animals was encouraged by a particular dilemma situation, represented by Hero and Leader, where agents could only solve the dilemma by sharing unequal roles (C or D). If so, studies based on PD or pure Chicken, which have been well investigated in the evolutionary game theory, cannot answer the question.

Our study and the studies of Chalub et al. (2006) and Ohtsuki and Iwasa (2004) are compared in terms of 2-layer co-evolution. The present model is unique in that, FSM #2, a counterpart to the norm in Chalub et al. (2006), is assumed to evolve at an individual-agent level, and lighting on or off is determined by his will, rather than a commonly shared norm.

References

Buzing, P.C., Eiben, A.E., and Schut, M.C. 2005. Emerging communication and cooperation in evolving agent societies. *Journal of Artificial Societies and Social Simulation* 8(1). http://jasss.soc.surrey.ac.uk/8/1/2.html.

Chalub, F.A.C.C., F.C. Santos, and J.M. Pacheco. 2006. The evolution of norms. *Journal of Theoretical Biology* 241: 233–240.

Dorigo, M., V. Maniezzo, and A. Colorni. 1996. The ant system: Optimization by a colony of cooperating agents. *IEEE Transactions on Systems, Man and Cybernetics – Part B* 26(1): 29–41.

Grim, P., T. Kokalis, A. Alai-Tafti, N. Klib, and P. St Denis. 2004. Making meaning happen. *Journal of Experimental & Theoretical Artificial Intelligence* 16(4): 209–243.

Kawamura, H., M. Yamamoto, T. Mitamura, K. Suzuki, and A. Ohuchi. 1998. Cooperation search based on pheromone communication for vehicle routing problems. *IEICE Transactions on Fundamentals of Electronics, Communications and Computer Sciences* E81-A-6: 1089–1096.

Nowak, M.A. 2006. Five rules for the evolution of cooperation. *Science* 314: 1560–1563.

Nowak, M.A., and K. Sigmund. 1998. Evolution of indirect reciprocity by image scoring. *Nature* 393: 573–577.

Ohtsuki, H., and Y. Iwasa. 2004. How should we define goodness?—reputation dynamics in indirect reciprocity. *Journal of Theoretical Biology* 231: 107–120.

Sato, T., Uchida, E., and Doya, K. 2007. Learning how, what, and whether to communicate: Emergence of protocommunication in reinforcement learning agents. *Proceeding of The Twelfth International Symposium on Artificial Life and Robotics 2007* (*AROB 12th '07*). Beppu (Japan).

Tanimoto, J. 2008. What initially brought about communications? *Biosystems* 92(1): 82–90.

Van Baalen, M., and V. Jansen. 2003. Common language or tower of Tower of Babel? On the evolutionary dynamics of signals and their meanings. *Proceedings of the Royal Society B* 270: 69–76.

Chapter 5
Traffic Flow Analysis Dovetailed with Evolutionary Game Theory

Abstract In this chapter, we concern ourselves with traffic flow as another meaningful example of a situation in which evolutionary game theory can be applied. Although the study of traffic flow was originally thought to be best explained using fluid dynamics, a multi-agent simulation technique that has been widely used in the field of evolutionary games has been applied to the problem, under the name of cellular automaton (CA). In this chapter, we first explain how traffic flow can be modeled. Next, we discuss how evolutionary game theory can be applied to this traffic flow. One can consider the dynamics of traffic flow to be like a multi-player game, with vehicles being controlled by drivers who compete to access to a road as a finite resource in order to reduce their personal travel time. This implies that traffic flow may change its phase depending on traffic density, and that it entails a social dilemma that might also change its game class, depending on the density. We reveal that various social dilemmas are hidden behind different aspects of traffic flows, which may be considered remarkable. Traffic flow is a game committed by agents – drivers, which seems some sort of human drama unlike we naturally think that traffic flow is governed by rigid physics because the theory of fluid dynamics, one of the representative hard-core physics fields, has been applied to it.

5.1 Modeling and Analysis of the Fundamental Theory of Traffic Flow

In studies concerning traffic flow, especially simulation studies, model reproducibility might be the most important issue. Roughly speaking, there have been two main physical approaches (see Fig. 5.1) to the studies concerning traffic flow: continuum models and discrete models including cellular automaton (CA) models. Continuum models view traffic flow as fluid flow, which is a macroscopic feature, Eulerian in scope. The latter, discrete or microscopic models, view traffic flow as vehicle granular dynamics from a Lagrangian viewpoint.

It has struck many physicists as interesting that traffic flow can be interpreted as a self-driven multi-particle system, which is linked to a second concept, the

J. Tanimoto, *Fundamentals of Evolutionary Game Theory and its Applications*,
Evolutionary Economics and Social Complexity Science 6,
DOI 10.1007/978-4-431-54962-8_5

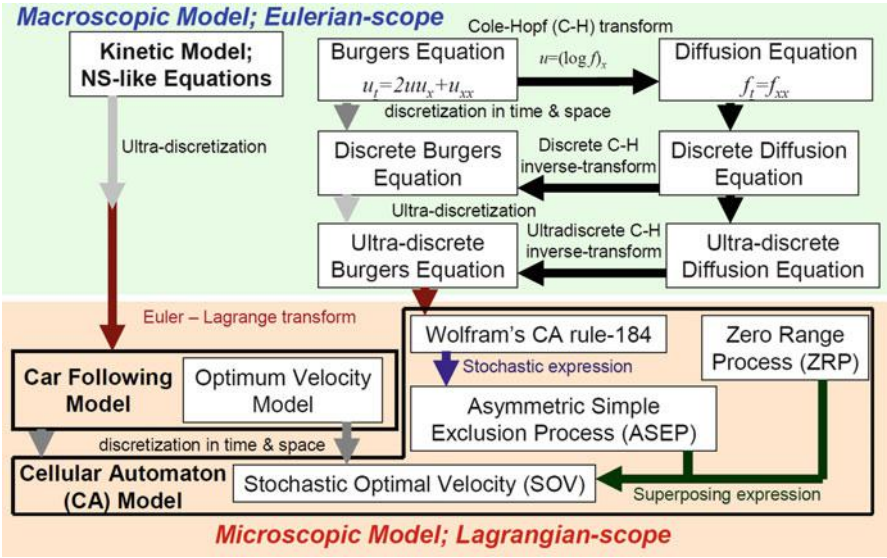

Fig. 5.1 Overview of traffic models: the macroscopic and microscopic approaches

microscopic model or Lagrangian viewpoint. Among several traffic models, such as the kinetic gas theory (e.g., Lighthill and Whitham 1955), fluid dynamical model (e.g., Kerner and Konhäuser 1994; Helbing 1995), and car-following model (e.g., Pipes 1953; Gazis et al. 1961), the cellular automaton (CA) model has been the most heavily investigated. In addition, there is a very intriguing consistency from a theoretical standpoint between the CA traffic model and traffic flow kinetics. In fact, a series of studies revealed that Burgers' equation, which governs one-dimensional shock wave propagation, is exactly equivalent to the asymptotic behavior of elementary CA rule 184 (Wolfram 1986), when the Cole–Hopf transformation is applied to the ultra discrete diffusion equation (Nishinari and Takahashi 1998).

It is not just all of this background work, but also an increase in computational power that has attracted heavy attention to the CA model, as a CA model is far more flexible than other models in taking account of the plausible motions by each of the vehicles such as lane-changing, influences from an intersection and signals, another road merging with or exiting from the focus road, lane closing, and all other likely realistic scenarios. In fact, a lot of observational data have proved that CA models are able to replicate real traffic flows in various situations (e.g., Neubert et al. 1999; Kerner et al. 2013).

Concerning CA models, the first milestone model we must cite is by Nagel and Schreckenberg (1992) (abbreviated as the NaSch model or NS model). Although the NS model is simple and considers the dynamics of a vehicle that accelerates its unit velocity if possible, and also probabilistically decelerates its unit velocity according to random brake probability, it roughly reproduces a realistic traffic

flow. In fact, the NS model reasonably reproduces a free flow phase, in which every vehicle is driving at maximum speed, and a congested phase in the so-called fundamental diagram that indicates a relation between traffic flow and density (namely the slope of the interpolated line over points indicating speed). Therefore, due to this success, many works have made use of the NS model. However, the NS model has drawbacks resulting from its simplicity, because, of course, actual driving behavior possesses rich complexity. One of the state-of-the-art models is the stochastic Nishinari–Fukui–Schadschneider (S-NFS) model (Sakai et al. 2006), which takes into account the motions that are commonly observed in real vehicles: slow-to-start (S2S), quick start (QS), and random braking (RB). S2S implies an inertial effect, which importantly produces metastable states in the fundamental diagrams. Metastable phases are observed and thought to be an important feature in real traffic flow, where a group of vehicles with less heading distance (implying reasonable middle traffic density) drive at reasonably high speed (referred to as "platoon driving"), showing maximum flux, but this is a volatile situation and it easily phase-shifts to a congested phase irreversibly. QS is the result of acceleration or deceleration by a driver who is anticipating the intentions of both the preceding vehicle and several further preceding vehicles.

One important thing to be noted is that variants of the NS model including the S-NSF model suffer when a high speed vehicle shows an unrealistic slow-down manner like a sudden stop by bumping with a heading vehicle. This is because the NS-based models always accelerate irrespective of heading distance and do not decelerate gradually when approaching to a vehicle ahead, which seems unlikely if we remember what happens in reality. On the other hand, we consider the optimum velocity (OV) model (Bando et al. 1994, 1995), one of the Car Following models, categorized as a microscopic model with a spatiotemporally continuous view point as shown in Fig. 5.1, and the stochastic optimum velocity (SOV) model (e.g., Shigaki et al. 2011), which is one of the CA models as also shown in Fig. 5.1, and regarded as a powerful tool due to having two exact solutions: zero range process (ZRP) and asymmetric simple exclusion process (ASEP) at the two limits of the stochastic parameter range: 0 and 1. These two models both provide good performance, because they modulate acceleration or deceleration according to a heading distance related to the traffic density around the focal vehicle. The lack of this particular feature brings unlikely phase transition from free phase (F) to jam phase (J), while free (F) to jam (J) through a synchronous phase (S) is what really happens, as claimed by Kerner (2009) in the three phase theory.

To end this discussion, we would say it is necessary to establish a CA model, considered as plausible, which is possible at reproducing real driving dynamics, while maintaining high flexibility to extend its framework by adding the lane-change sub-model. For example, Kokubo et al. (2011) have successfully produced one possibility by introducing the Revised S-NFS model, refining RB in the S-NFS model to improve the reproducibility of Kerner's three phase theory.

5.2 A Cellular Automaton (CA) Model to Reproduce Realistic Traffic Flow

In this section, the revised S-NFS model is explained.

In real flow fields, the field-observations confirm many complex phases, for example, some of these phases imply that two congested phases may coexist. Spontaneous phase transition from free flow to wide moving jam (F → J transition) is not observed in a real traffic as mentioned above. A wide moving jam can emerge spontaneously only in synchronized flow (S → J transition). Therefore, a wide moving jam emerges spontaneously because of a sequence of F → S → J transitions. This is what Kerner's three phase theory insists. However, in most of the conventional CA models based on the NS model, synchronized flow is not reproduced very well. On the other hand, several previous authors have reported that the synchronized flow can be reproduced by considering the appropriate deceleration process of each vehicle depending on the velocity difference or heading distance with a preceding car (e.g., Gao et al. 2007, 2009; Knospe et al. 2000).

Another problem, previously mentioned as well, is that most NS-based CA models show unrealistic deceleration dynamics for each vehicle agent. If there is a relatively slower vehicle ahead, a real vehicle would gradually decelerate when approaching the preceding vehicle. However, most CA models based on the NS model only reproduce an unrealistic rapid deceleration where the focal vehicle stops by a collision

Note that the above-mentioned two problems, namely, reproduction of the three phase theory and appropriate deceleration dynamics, are mutually related, because an unrealistic abrupt deceleration would cause a rapid growth of a stop-and-go wave, which rarely permits synchronized flow to emerge. If a model overestimates stopping probability, the excessive stop-and-go wave inevitably occurs. On the other hand, if a vehicle is allowed to gradually decelerate when approaching the tail-end of a jam, the stopping probability would be decreased. Thus, an occurrence of this excessive stop-and-go wave would be discouraged and synchronized flow could result.

5.2.1 Model Setup

The updating rules of the Revised S-NFS model can be written as follows.

Rule 1 "Acceleration"

$$v_i^{(1)} = \min\left[V_{\max}, v_i{}^{(0)} + 1\right] \tag{5.1}$$

(only if $g_i \geq G \cup v_i{}^{(0)} \leq v_{i+1}{}^{(0)}$ then Rule 1 is applied).

Rule 2 "Slow-to-start"

$$v_i^{(2)} = \min\left[v_i{}^{(1)}, x_{i+s_i}^{t-1} - x_i^{t-1} - s_i\right] \tag{5.2}$$

(only if rand() $\leq q$ then Rule 2 is applied) and (if rand() $\leq r$ then $s_i = S$ else $s_i = 1$).

Rule 3 "Perspective (Quick start)"

$$v_i^{(3)} = \min\left[v_i{}^{(2)}, x_{i+s_i}^{t} - x_i^{t} - s_i\right] \tag{5.3}$$

Rule 4 "Random brake"

$$v_i^{(4)} = \max\left[1, v_i{}^{(3)} - 1\right] \tag{5.4}$$

(only if rand() $< 1 - p_i$ then Rule 4 is applied).

$$\text{if}(g_i \geq G)$$

$$ip_i = P_1 \tag{5.5-1}$$

$$\text{if}(g_i < G)$$

$$p_i = P_2 \quad \text{for } v_i^{(0)} < v_{i+1}^{(0)} \tag{5.5-2}$$

$$p_i = P_3 \quad \text{for } v_i^{(0)} = v_{i+1}^{(0)} \tag{5.5-3}$$

$$p_i = P_4 \quad \text{for } v_i^{(0)} > v_{i+1}^{(0)} \tag{5.5-4}$$

Rule 5 "Avoid collision"

$$v_i^{(5)} = \min\left[v_i{}^{(4)}, x_{i+1}^{t} - x_i^{t} - 1 + v_{i+1}{}^{(4)}\right] \tag{5.6}$$

Rule 6 "Moving forward"

$$x_i^{t+1} = x_i^{t} + v_i^{(5)} \tag{5.7}$$

where x_i^t is the position of vehicle i at time t, $v_i^{(0)}$ is the velocity $v_i^{(5)}$ at the previous time step $t-1$, defined by $x_i^t - x_i^{t-1}$, s_i is the number of precedent vehicles from the ith driver's perspective, g_i is the gap between vehicle i and vehicle $i+1$ (thus, $g_i = x_{i+1}^t - x_i^t$), and $V_{\max}$ is the maximum velocity. The notation rand()

represents a random number drawn from the uniform distribution on [0, 1]. The quantities G, q, r, S, P_1, P_2, P_3, and P_4 are model parameters. The probability of random braking is given by $1 - p_i$. We presume $P_1 > P_2 > P_3 > P_4$.

5.2.2 Model Performance Explored by Simulations

We assumed model parameters as follows: $q = 0.99$, $r = 0.99$, $S = 2$, $V_{\max} = 5$, $p = 0.96$, $P_1 = 0.999$, $P_2 = 0.99$, $P_3 = 0.98$, $P_4 = 0.01$, and $D = 15$. The simulations are implemented under the open boundary condition.

5.2.3 Discussion on the Deceleration Dynamics of Vehicle Particles

First, let us discuss the reproducibility of the real deceleration process by the proposed model. The first simulation is implemented when all vehicles are required to stop in the vicinity of the exit by assuming outflow probability at the posterior open boundary: $\beta = 0$. The system length L is set to 500. Figure 5.2 shows spatiotemporal diagrams that show trajectories of several successive vehicles in this episode. Each line shows the trajectory of a car. Because the vertical axis is the position of vehicles and the horizontal axis is time step, the slope indicates the velocity of each vehicle. In the default S-NFS model, no vehicle ever decelerates before being caught up in the tail of the jam. On the other hand, the deceleration process by the Revised S-NFS model seems to reproduce well the gradual dynamics showing smooth curves. In the NS model, on which many CA models are based, any velocity-adjusting process that considers the velocity difference and heading distance with respect to the preceding vehicle, which is the so-called optimal velocity model, is not taken into account. This process is also disregarded in the S-NFS model, even though it takes into account the slow-to-start and perspective effects. In the proposed

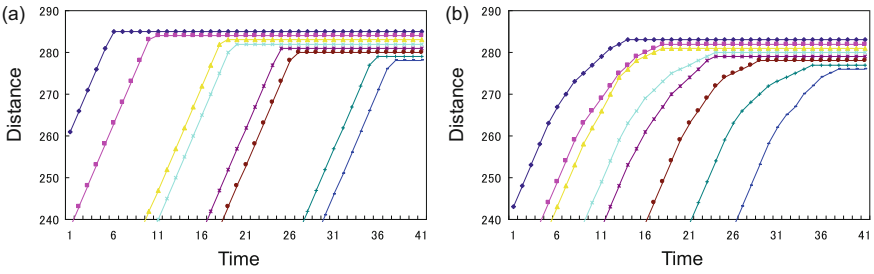

Fig. 5.2 Spatiotemporal diagram for a set of sequential eight cars facing the tail of jam by: (**a**) the pure S-NSF model, (**b**) the Revised S-NFS

Table 5.1 Number of collision-like deceleration events occurring

	S-NFS model	Present study
$v_i^{t-1} - v_i^t = 5$	211	0
$v_i^{t-1} - v_i^t \geq 4$	562	1
$v_i^{t-1} - v_i^t \geq 3$	929	8

model, the random braking effect, where the probability changes in relation to velocity difference and distance, substitutes this specified process.

Next, we extend the system length for it to be sufficiently large, $L = 2500$, which has a dead-end at the end of the system. In order to measure the deceleration extent, we cause 1000 vehicles to drive from the upper open boundary. Table 5.1 shows the number of decelerating events having more than three velocity units for a single time step, which implies an unrealistic rapid deceleration such as a collision. In the S-NFS model, this unrealistic deceleration event is observed more than half the time, while the events in the Revised S-NFS are considerably decreased.

Summing up, we conclude that the proposed model embedded into S-NFS, which modifies the variable random braking probability depending on velocity difference and heading distance, is able to prevent the occurrence of unrealistic deceleration events.

5.2.4 Discussion of Three Phase Theory

In this section, we discuss whether the proposed model is able to reproduce synchronized flow to agree with the three phase theory.

Figure 5.3 shows the fundamental diagrams of the S-NFS model and the proposed model. There are unusual line-like plots with flux of about 0.1 which is independent of the density, and some unusual blanks which exist in the line of free flow and the wide moving jam. These drawbacks are caused by the open boundary condition we assumed. First, let us discuss the unusual line. Because we got the results of Fig. 5.3 by controlling both inflow probability at the upper open boundary and outflow probability at the posterior open boundary within the region [0.0, 1.0] by 0.1 increments, the extreme situation when outflow probability is very low, $\beta = 0.1$ brings this unusual line-like plots. Next, let us discuss the unusual blanks. There are two causes for this specific problem: (i) Because the simulation is implemented with the open boundary condition which is controlled by the procedure above mentioned, we cannot always catch smoothly and continuously stringed plots. (ii) Because the results are drawn from each 30-trial ensemble average observed from the 3001st to the 3500th time step, instantaneous results are not included. For those reasons, the variety of the results which can be obtained is limited. Anyhow we see those are technical problems, not crucial drawbacks. Hence, as shown in Fig. 5.3, it is worthwhile to confirm that the proposed model

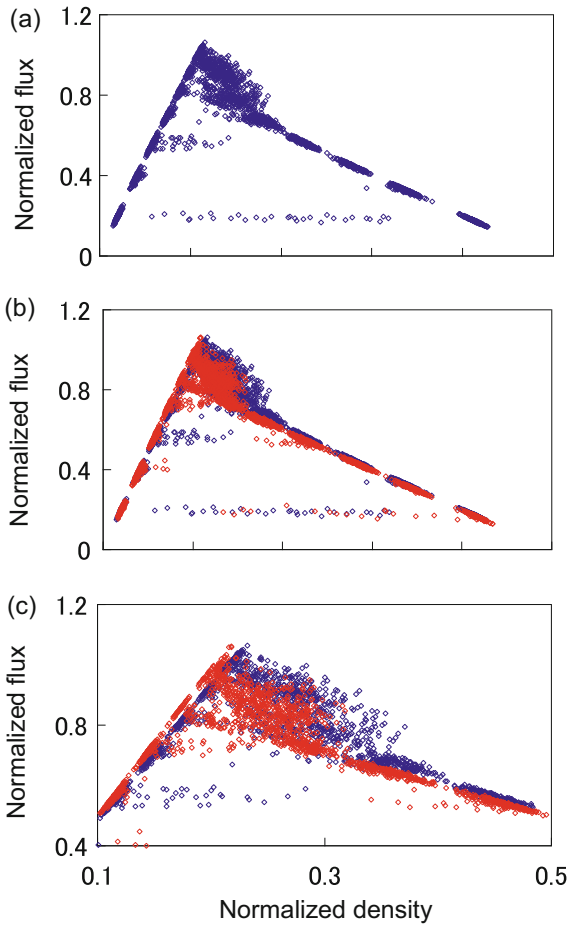

Fig. 5.3 Fundamental diagrams: (**a**) the proposed model, (**b**) comparison of the proposed model and the S-NFS models, (**c**) macrograph of the region of $0.1 <$ (normalized density) < 0.5 & $0.4 <$ (normalized flux) < 1.2 in panel (**b**). *Red* and *blue* plots indicate results by S-NFS and the proposed models, respectively

reproduce a plausible fundamental diagram, which the original S-NFS model was, of course, able to show.

Although the two models indicate equivalent peak fluxes at the metastable phase, the following points should be noted. First, the S-NFS shows slightly larger normalized flux than the proposed model when the normalized density ranges from 0.1 to 0.2 (see Fig. 5.2(b) and (c)). However, as the second point, the proposed model contrastingly shows larger flux than the S-NFS model in a density range 0.2–0.5. The reasons for these points are possibly as follows:

Concerning the first point, the proposed model assumes slightly larger random braking owing to the variable probability with increasing density even in free flow phase than that of S-NFS with constant random braking probability.

With respect to the second point, the original S-NFS model only reproduces an unrealistic deceleration process, which causes frequent stop-and-go waves. Lack of a synchronized flow phase inevitably leads to a smaller flux. However, in our

model, synchronized flow might be reproduced properly, which can cause a reasonably larger flux than that of the S-NFS model in the J phase.

Figure 5.4 shows velocity distributions of the respective two models in relation to the normalized density. It is obvious that the distribution of the S-NFS model in a density range of 0.2–0.5, largely consists of the maximum ($V_{\max} = 5$) and minimum ($v = 0$) velocities, while the proposed model is composed of various velocity vehicles. Observing the proposed model (Fig. 5.3(b)) in a density range of 0.1–0.2, we note that not only $v = 5$ but also $v = 4$, the second largest velocity, appear in its distribution. This also explains why our model is featured with slightly less flux than the S-NFS model in free flow phase, which was discussed previously.

Summarizing the above discussion, we would conclude that the proposed new model is able to reproduce not only the F and J phases but also the S phase reasonably.

Focusing on a density range of 0.2–0.5, let us observe the spatiotemporal diagrams. Figure 5.5 shows a comparison of two models having equivalent densities. The S-NFS model suffers from a huge wide moving jam, which causes smaller flux, 0.815, than that of the proposed model, 0.92. On the other hand, the new model evidently shows a different congested cluster from that of the S-NFS model, where

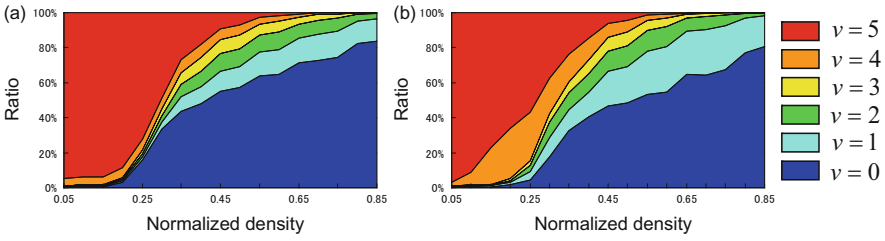

Fig. 5.4 Velocity distribution in relationship with normalized density: (**a**) S-NFS model, (**b**) the proposed model

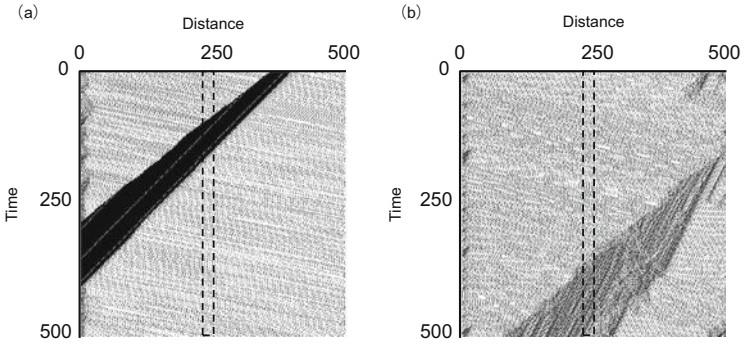

Fig. 5.5 Spatiotemporal diagrams for comparison: (**a**) a flow by the S-NSF model under the normalized density condition, 0.269, and normalized flux, 0.805, (**b**) a flow by the proposed model under the condition of normalized density, 0.268, and normalized flux, 0.997

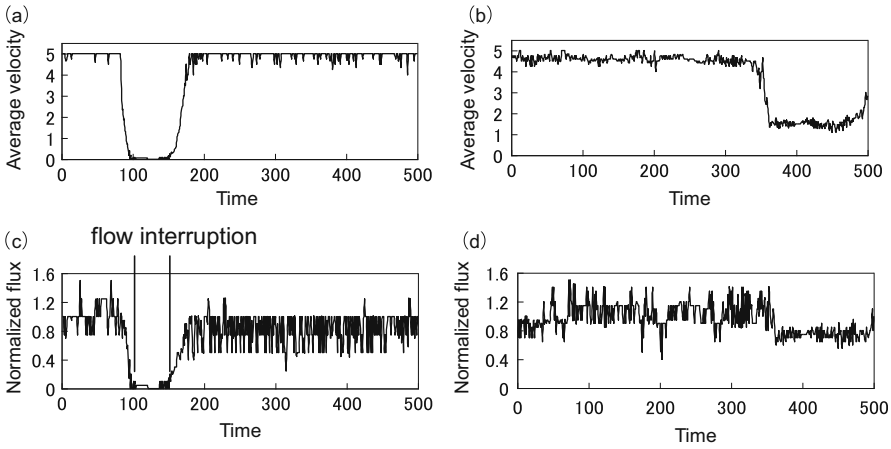

Fig. 5.6 Time-series of the flow in the region of $229 < x < 250$ shown in Fig. 5.5 (a), (b) (regions surrounded by *broken line*). Both local average velocities by S-NFS and the proposed model are shown in (**a**) and (**b**), which are consistent with Fig. 5.5 (a) and (b) respectively. Likewise local average fluxes by S-NFS model and the proposed model are shown in (**c**) and (**d**)

vehicles are able to maintain nonzero velocity, implying synchronized flow might occur.

Figure 5.6 shows the time-series of local velocities and local fluxes of both flows (Fig. 5.5(a) and (b)) observed at $229 < x < 250$. The different feature of each cluster shown in Fig. 5.5(a) and (b) can be confirmed by Fig. 5.6. As shown in Fig. 5.5 (a) and (c), it is confirmed that the traffic flow is interrupted by the cluster of Fig. 5.5 (a) which is regarded as wide moving jam. On the other hand, as shown in Fig. 5.6 (b), (d), it is confirmed that the traffic flow is not interrupted by the cluster of Fig. 5.5(b), which is regarded as synchronized flow.

Concerning reproducibility for both free flow and jam phase, the proposed model seems appropriate as confirmed in Fig. 5.7.

To show that the proposed model can secure a phase transition F $\rightarrow$ S $\rightarrow$ J, we conducted another simulation. We presumed the road with a on- ramp bottleneck at the position $x = 249$ and $x = 250$, where new vehicles having velocity with $V_{\max}$ appear at sites $x \in \{249, 250\}$ with probability $\alpha_{on} = 0.05$. Three panels in Fig. 5.8 indicate different spatiotemporal diagrams under different in-coming and out-flowing open boundary conditions. Obviously, Fig. 5.8(a) shows F $\rightarrow$ S transition, while (b) and (c) indicate appearing S $\rightarrow$ J transition just after the bottle neck.

We further confirm that the proposed model shows acceptable reproducibility for synchronized flow in terms of time series analysis. We emulate a road with a bottleneck in the region of $2499 < x < 2700$, where a velocity limitation of $V_{\max} = 2$ is implemented. We assume a system length, $L = 3000$, and inflow probability at the upper open boundary $\alpha = 0.65$ (Fig. 5.9). We see several wide moving jams in the original S-NFS model. However, in the proposed model, a single flow state with

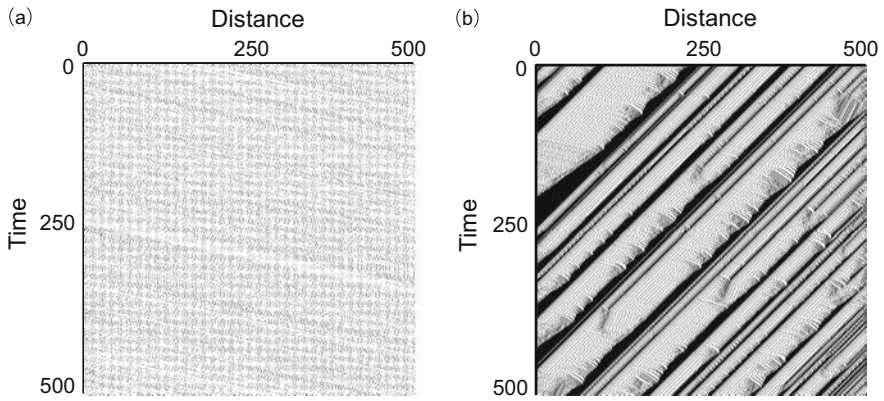

Fig. 5.7 Spatiotemporal diagrams by the proposed model: (**a**) a free flow under the condition of normalized density, 0.196, and normalized flux, 0.910, (**b**) a wide moving jam flow under the condition of normalized density, 0.402, and normalized flux, 0.573

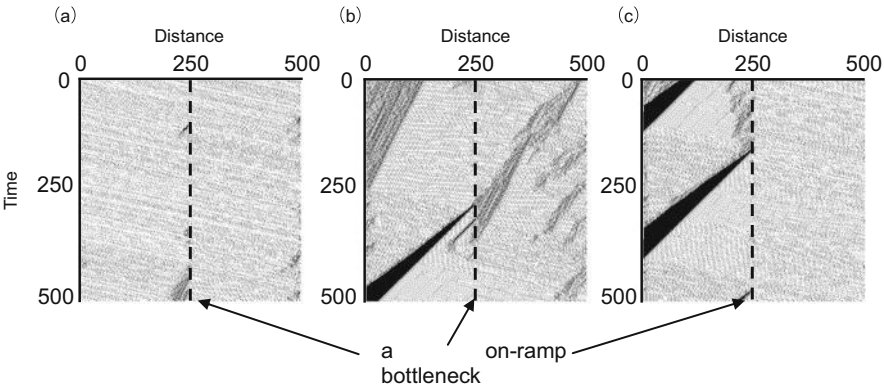

Fig. 5.8 Spatiotemporal diagrams by the proposed model with a on-ramp bottleneck observed in independently different time series: (**a**) showing F → S transition under the open boundary condition, $\alpha = 0.50$ and $\beta = 0.80$, (**b**) S → J transition under the open boundary condition, $\alpha = 0.90$ and $\beta = 0.80$, (**c**) S → J transition under the open boundary condition, $\alpha = 1.00$ and $\beta = 0.90$

low velocity emerges, which belongs to a synchronized flow phase. We estimate both autocorrelation functions of density, flux, and velocity, and a cross-correlation function between density and velocity, based on the data measured within the region of $2479 < x < 2500$ for 60 steps. Figure 5.10 shows the results. Because there are no correlations, we can conclude that the flow filed observed here is classified as synchronized flow.

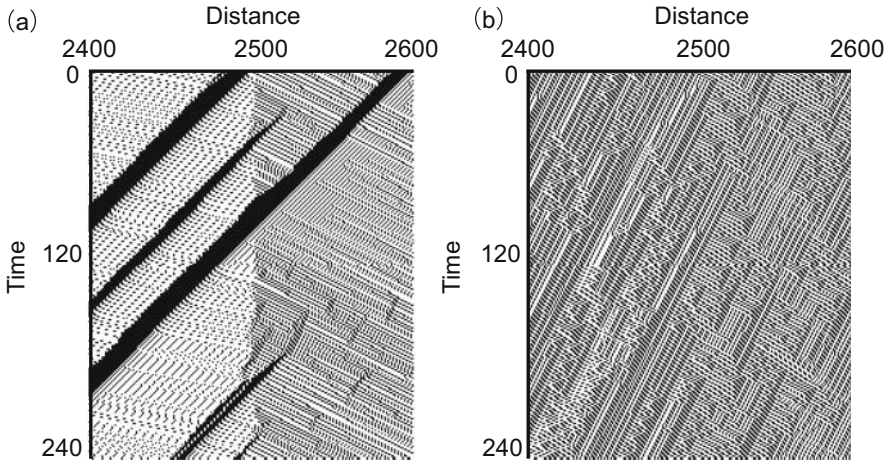

Fig. 5.9 Spatiotemporal diagrams for comparison to reproduce a bottleneck flow by: (**a**) the S-NSF model, (**b**) the proposed model

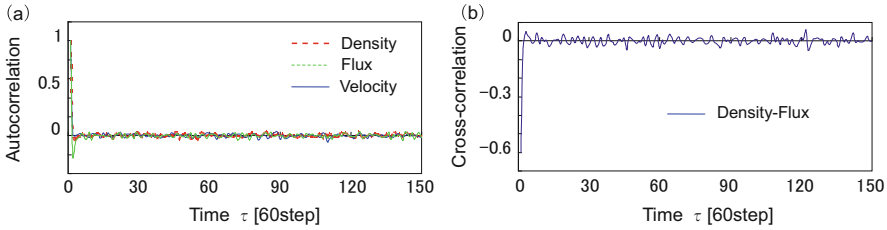

Fig. 5.10 Time-series analysis for the flow shown in Fig. 5.6 (b): (**a**) autocorrelation functions of local average density, flux, and velocity, (**b**) cross-correlation function of local density–flux

5.2.5 Summary

We developed a new model based on S-NFS, which adjusts the occurrence probability of random braking depending on velocity difference and heading distance with a preceding vehicle.

A series of simulations for a single lane flow with the open boundary condition reveals that the model revision is able to reproduce realistic smooth deceleration dynamics, which never causes a vehicle collision in a stopping event.

This model revision also improves reproducibility for Kerner's three phase theory, which reproduces not only free flow and jam phases but also synchronized flow phase by suppressing excessive occurrence of stop-and-go waves.

5.3 Social Dilemma Structure Hidden Behind Various Traffic Contexts

Traffic flow can be treated as a multi-player game with agents as drivers who wish to minimize their own travel time compared to others by competing for a road that is a finite recourse. Going back to the original question of what creates a dilemma situation, as discussed in Chap. 2, we remember that there is a social dilemma if a fair Pareto Optimum, meaning a best possible solution for all, is inconsistent with an individual best solution. This suggests that in real-life traffic, excessive speed, intrusion into a line of vehicles, frequent lane-changing, or other egocentric driving behaviors likely reduce a focal driver's travel time but also have a negative impact on and create annoyance for surrounding drivers, causing inefficiency in terms of whole the traffic flow. For example, a dangerous intrusion gives rise to turbulence in the traffic flow that may create a traffic jam. If this is the case, the vehicle that resorts to the dangerous intrusion successfully exploits others in order to move ahead, but the move is detrimental to other drivers/vehicles and reduced efficiency is inflicted on the system as a whole. This implies a typical social dilemma. The hypothesis that a social dilemma lies behind traffic flow may be surprising, because analysis of traffic flow is one of the problems that pure physics—namely, fluid dynamics—can deal with, and therefore seems far from a problem dominated by human decision making like an evolutionary game. In this sense, whether the hypothesis is valid or not is a meaningful and interesting question to be explored from a scientific viewpoint. Moreover, this could be followed by another challenging question, whether each of the traffic phases: the free, metastable, congested, and jam phases, can be related to each of the dilemma classes, i.e., the prisoner's dilemma (PD), chicken, stag hunt (SH), and trivial games. In this section, we further discuss this fascinating subject.

5.3.1 Social Dilemma Structures Hidden Behind a Traffic Flow with Lane Changes

With the background noted in the previous paragraph, we detected that several social dilemma structures, represented by n-person Prisoner's Dilemma (n-PD) games, appear in certain traffic flow phases at a bottleneck caused by a lane closing (e.g., Yamauchi et al. 2009; Nakata et al. 2010). We confirmed that an n-PD game structure appears in the high-density phase area, but no social dilemma exists in the free-flow and jam phases. It seems plausible for a social dilemma to underlie such traffic flows because closing a lane creates an obvious bottleneck. Thus, our next challenge is whether a social dilemma still lies beneath traffic flow that does not involve any explicit bottleneck like a lane closing, on-ramp (merging), off-ramp (exit), or uphill travel. Although there have been several reports of work addressing dilemmas in traffic flow, none have considered the issue we raise here. Thus, this

sub-section addresses whether or not only lane-changing actions by drivers can give rise to a social dilemma in an ordinal two-lane road system with cyclic boundaries.

We applied the Revised S-NFS model, explained in the previous section, for driving vehicles forward.

Lane-Changing Rule

We applied the lane-changing rule used by Kukida et al. (2011) in the CA model. That rule is defined as follows:

$$\textbf{Incentive criterion}: \ gap_p^f \leq v_i^{(p)} - v_{i+1}^{(p)} \cap gap_n^f > v_i^{(p)} - v_{i+1}^{(n)}, \tag{5.8}$$

$$\textbf{Safe criterion}: \quad gap_n^b \geq v_{i-1}^{(n)} - v_i^{(p)}. \tag{5.9}$$

Here, gap_p^f is the number of unoccupied sites in front of the focal vehicle (agent i) in the same lane, gap_n^f is the number of unoccupied sites in front of the focal vehicle in the opposite lane, and gap_n^b is the number of unoccupied sites behind the focal vehicle in the opposite lane. If a vehicle meets the two criteria (5.8) and (5.9), an actual lane change occurs with probability P_{LC}. This lane-change rule applies symmetrically in the two lanes.

Agent and Simulation Flow

In the system there are two types of agents: cooperators (C-agents) remain in the lane initially assigned without making any lane changes, and defectors (D-agents) change lanes according to the rule in Sect. 2.2. We use cyclic boundary conditions to keep the vehicle density constant during a single simulation episode. The procedure in a single simulation episode, repeats the following steps (i) to (v) in which steps (ii) to (v) correspond to one time step.

(i) N_S vehicles are generated and placed at random positions in the system. The C (D)-agent fraction among N_S is P_c $(1 - P_c)$.
(ii) Only D-agents decide whether or not to change lanes, based on (8) and (9).
(iii) The random brake probability, $1 - p_i$, of all agents is determined according to (5–1)–(5–4).
(iv) The next step velocity of all agents is determined from (1)–(4) and (6).
(v) All agents update their positions in the system by (7).

Simulation Setting

In the actual numerical experiments, we set the system length to $L = 500$ and assumed the following values for model parameters: $q = 0.99$, $r = 0.99$, $S = 2$,

$V_{\max} = 5$, $P_1 = 0.999$, $P_2 = 0.99$, $P_3 = 0.98$, $P_4 = 0.01$, $G = 15$, and $P_{LC} = 1$. We basically varied N_S from 50 to 950 in increments of ten vehicles, although for cases in the middle density region ($012 \leq \rho \leq 0.35$), we used N_S increments of 1 due to the high sensitivity in that region because it contains a metastable phase. We also varied P_c from 0 to 1 in increments of 0.1.

All results were drawn from 100 independent realizations. We evaluated the average velocity of each agent by L/(travel time), and then averaged those over all C-agents (D-agents) for the average payoff of each strategy. For the social payoff, we used the time-averaged traffic flux.

Each realization (a single simulation episode) involved a run-up period (RU-period) to attain a fully developed flow, followed by an observation period (O-period) in which the above simulation results were evaluated. Because a developed flow may contain unsteady features, the run-up and observation periods differed depending on traffic density.

For $\rho \leq 0.65$, RU-period = 10,000 time steps and O-period = 500 time steps.

For $0.65 \leq \rho \leq 0.82$, RU-period = 25,000 time steps and O-period = 2500 time steps.

For $0.82 \leq \rho \leq 0.95$, RU-period = 50,000 time steps and O-period = 5000 time steps.

Results and Discussion

Figure 5.11 shows fundamental diagrams for (a) $P_c = 1$ and (b) $P_c = 0$ in which each dilemma class discussed below is identified by a different color. Figure 5.11(a) shows that flows of all cooperators can exhibit the so-called metastable phase, while Fig. 5.11(b) shows that no metastable phase occurs in flows of all defectors. This seems plausible because a flow in relatively high-density regions can be stable with high traffic flux so long as none of the vehicles change lanes. In contrast, a flow with lane changes becomes volatile, since turbulence caused by frequent lane changes promotes traffic jams. Behaviors of the observed dilemma classes are explicitly discussed below; here, we merely note that only the Prisoner's Dilemma (including quasi-PD and quasi-little PD) class appears in the middle density region with relatively high traffic fluxes. The Trivial game and Neutral game also appear there, but these are not categories of social dilemmas.

Effects of Vehicle Density

Figure 5.12 shows the payoff functions and velocity frequencies for Case A in Fig. 5.11(a) ($\rho = 0.1$), which is in the free-flow phase. Panel 2(a) shows that all payoffs for Case A are insensitive to the cooperation fraction; this implies a kind of gameless situation. So we denote this as a Neutral game class. This is not surprising because most of the vehicles in Case A run at maximum velocity (see Panel 2(b)), so lane changes in the system are rare.

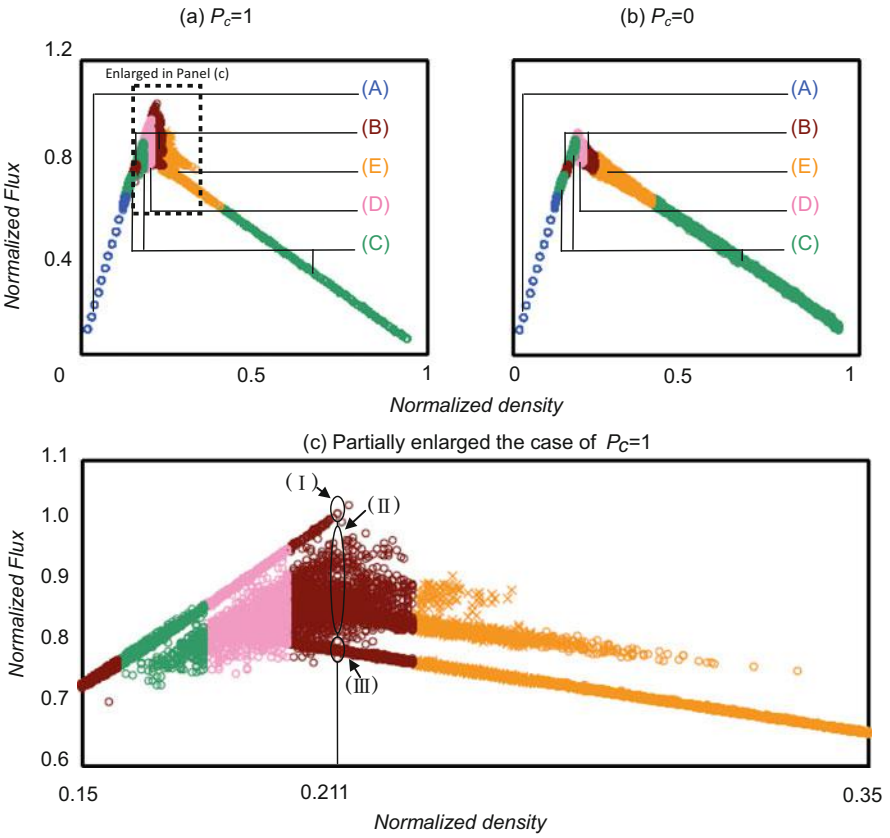

Fig. 5.11 Fundamental diagrams (normalized flux vs normalized density) for situations with (**a**) all cooperators ($P_c = 1$) and (**b**) all defectors ($P_c = 0$). Colored symbols identify (A) Neutral game, (B) Prisoner's Dilemma game at two densities in Panels (**a**) and (**b**), (C) D-dominate Trivial game at three densities in Panels (**a**) and (**b**), (D) D-dominate quasi-PD game, and (E) D-dominate quasi-light-PD game (see the main text). Panel (**c**) shows an enlarged portion of Panel (**a**)

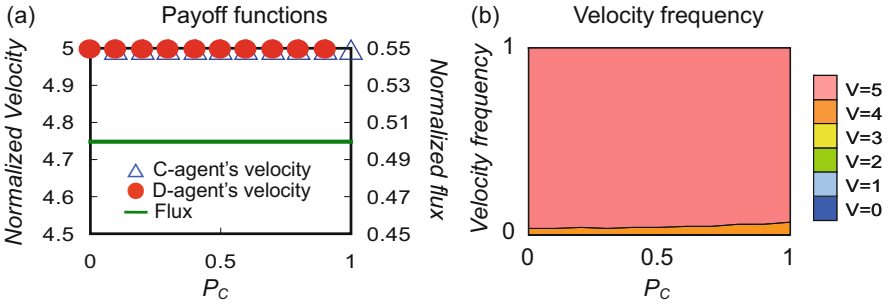

Fig. 5.12 Results for $\rho = 0.1$ at point A in Fig. 5.11 (a). (**a**) Effect of fraction of cooperators (P_c) on payoff functions (velocity and flux). *Red closed circles* are average payoffs of defectors, and *blue triangle* are average payoffs of cooperators. *Green bold line* indicates traffic flux as a social payoff. (**b**) Effect of fraction of cooperators (P_c) on velocity frequency. This behavior corresponds to a Neutral game

Figures 5.13, 5.14, 5.15, 5.16, 5.17, 5.18, and 5.19 show counterparts of Fig. 5.12 for the other cases explicitly marked in Fig. 5.11(a). The situation in Fig. 5.13 ($\rho = 0.141$) can be called a Trivial game because Nash equilibrium (NE)

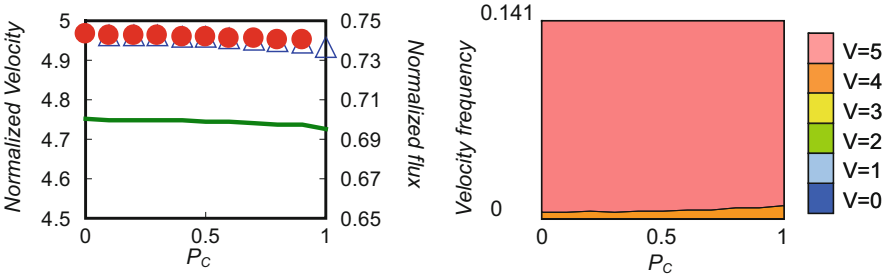

Fig. 5.13 Same as in Fig. 5.12, except at, which corresponds to one of the three points C in Fig. 5.11 (a). This behavior corresponds to a D-dominate Trivial game. (**a**) Payoff functions (**b**) Velocity frequency

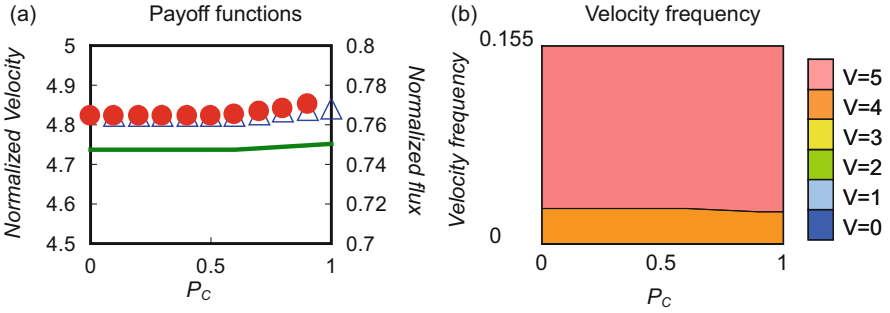

Fig. 5.14 Same as in Fig. 5.12, except at, which corresponds to one of the two points B in Fig. 5.11 (a). This behavior corresponds to a weak Prisoner's Dilemma game. (**a**) Payoff functions (**b**) Velocity frequency

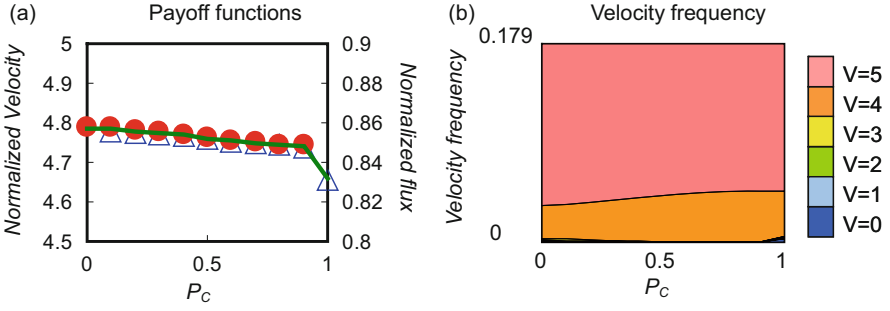

Fig. 5.15 Same as in Fig. 5.12, except at, which corresponds to one of the three points C in Fig. 5.11 (a). This behavior corresponds to a D-dominate Trivial game. (**a**) Payoff functions (**b**) Velocity frequency

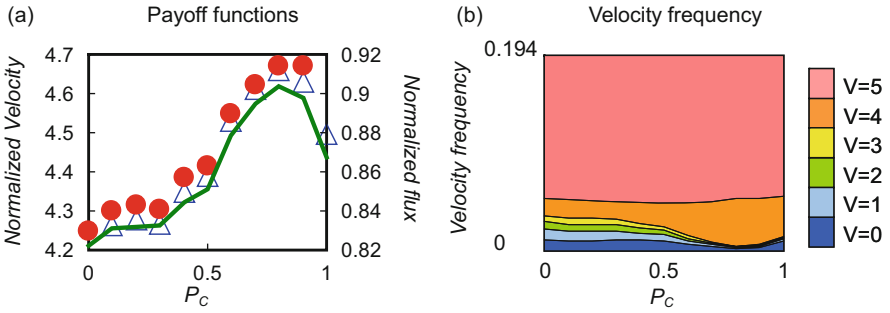

Fig. 5.16 Same as in Fig. 5.12, except at, which corresponds to point D in Fig. 5.11 (a). This behavior corresponds to a D-dominate quasi-Prisoner's Dilemma game. (**a**) Payoff functions (**b**) Velocity frequency

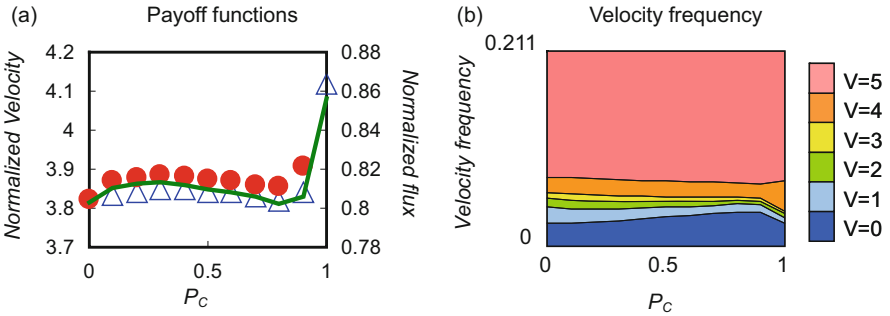

Fig. 5.17 Same as in Fig. 5.12, except at, which corresponds to one of the two points B in Fig. 5.11 (a). This behavior corresponds to a weak Prisoner's Dilemma game. (**a**) Payoff functions (**b**) Velocity frequency

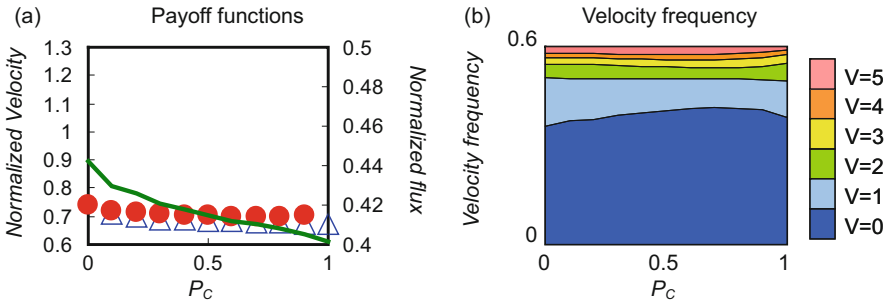

Fig. 5.18 Same as in Fig. 5.12, except at, which corresponds to point E in Fig. 5.11 (a). This behavior corresponds to a D-dominate quasi-light PD game. (**a**) Payoff functions (**b**) Velocity frequency

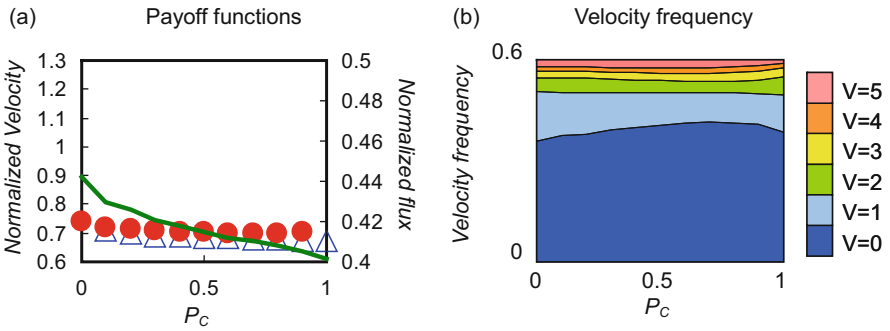

Fig. 5.19 Same as in Fig. 5.12, except at, which corresponds to one of the three points C in Fig. 5.11 (a). This behavior corresponds to a D-dominate Trivial game. (**a**) Payoff functions (**b**) Velocity frequency

accords with the fair Pareto Optimum (FPO) at $P_c = 0$. This game is dominated by defection, since the defector's payoff is always larger than that of the cooperator. However, the maximum social payoff also appears at all defector states. In a nutshell, we call this a D-dominate Trivial game, which implies that more frequent lane changing is preferable in this density region from both social and individual points of view.

Figures 5.15 ($\rho = 0.179$) and 5.19 ($\rho = 0.6$) show the same tendencies as in Fig. 5.13. Thus, all these should be classified as D-dominate Trivial games. The fact that the jam phase belongs to the D-dominate Trivial game (Fig. 5.19) seems reasonable because lane changes into even a slightly small vacant space between jamming vehicles brings benefits for not only the focal vehicle who changes lanes but also for the society as a whole, even if its frequency is low.

Figure 5.14 ($\rho = 0.155$) suggests a weak Prisoner's Dilemma (PD). This is confirmed by the following facts. At $P_c = 0$, NE is trapped because the defector's payoff is always greater than that of the cooperator. EPO appears at $P_c = 1$ because the social payoff increases with increasing cooperation fraction, although the effect is subtle. The same tendency appears in Fig. 5.17 ($\rho = 0.211$), although the extent of this dilemma (discussed in latter) seems more severe than that in Fig. 5.14. In Fig. 5.17, the social payoff function does not monotonically increase with the increase in the cooperation fraction, as observed in Fig. 5.14; rather, it shows an N-character shape, in which a local peak (much smaller than FPO at $P_c = 1$) appears at a lower cooperation fraction. This point is carefully discussed in latter.

Figure 5.16 ($\rho = 0.194$) differs slightly from the simple PD because FPO is not observed at $P_c = 1$, although NE is trapped at $P_c = 0$. At any rate, FPO is largely inconsistent with NE since FPO, which is the peak of social payoff, appears above $P_c = 0.5$. Therefore, we call this game structure a D-dominate quasi-Prisoner's Dilemma game.

Figure 5.18 ($\rho = 0.244$) seems odd; it looks analogous to a D-dominate quasi-PD Game (Fig. 5.16), but it differs. FPO defined by the peak of social payoff appears below $P_c = 0.5$ and is relatively close to NE found at $P_c = 0$. Therefore, we call this a D-dominate quasi-light PD game.

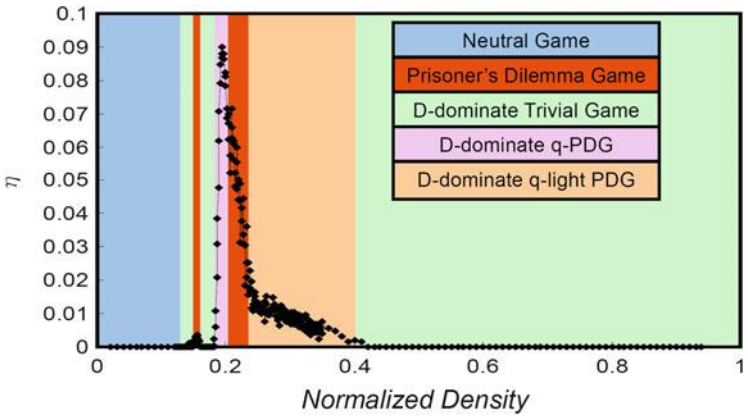

Fig. 5.20 Effects of vehicle density on dilemma strength, η. Each color identifies one of the dilemma classes shown in Fig. 5.11 (a): (A) Neutral game, (B) Prisoner's Dilemma game, (C) D-dominate Trivial game, (D) D-dominate quasi-PD game, and (E) D-dominate quasi-light-PD game

Figure 5.20 shows the effects of vehicle density on the strength of dilemma, η, defined by Nakata et al. (2010) and expressed by;

$$\eta = \frac{q_{EPO} - q_{NE}}{q_{EPO}}. \tag{5.10}$$

Here q_{EPO} and q_{NE} are the fluxes at FPO and NE, respectively. Figure 5.20 shows that the density at severe dilemma strength is consistent with the density observed in the high-flux region, including the metastable phase (Fig. 5.11(a)). This seems physically plausible because, in this density region, a driver has a strong incentive for changing lanes to exploit other drivers and ensure his own benefit is maximized (smaller travel time). However, when one driver changes lanes, others might follow. Therefore, states with high flux, say in the metastable phase, collapse with the phase shifting to the jam phase.

Multiple Game Structures at One Vehicle Density

As discussed above, Fig. 5.17 ($\rho = 0.211$) shows the general tendency of the Prisoner's Dilemma game class, although the social payoff function has an N-character shape rather than a monotonic increase. We discuss this point later. Figure 5.11(c) shows that, even when the same traffic density is presumed ($\rho = 0.211$), the equilibrium points are scattered. Obviously, there are three different subphases in this particular density region, denoted by I, II, and III in Fig. 5.11 (c). Figure 5.11 shows all 100 realizations for $\rho = 0.211$, sorted by the fluxes, for $P_c = 1$. The inset panels in Fig. 5.21 indicate the typical payoff functions for the subphases I, II, and III when we vary P_c. Note that the subphase with the higher flux

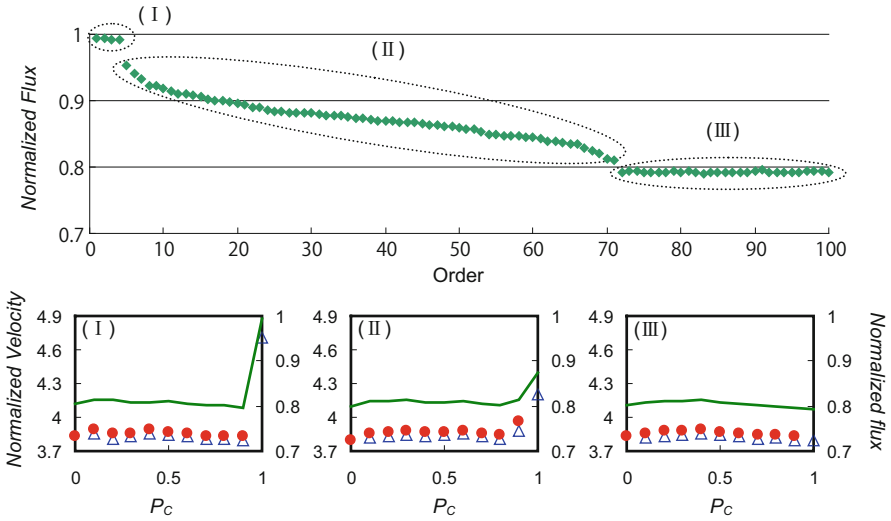

Fig. 5.21 *Upper panel* shows results from all 100 realizations for $P_c = 1$ and $\rho = 0.211$. The results are sorted by fluxes into the three subphases I, II, and III. *Lower panels* show the corresponding payoff functions for subphases I, II, and III

(I) shows an obvious PD tendency; however, for the subphase with the lower flux (III), the three payoff functions are insensitive to the cooperation fraction, so the presence of PD behavior is ambiguous. This implies that the N-character appears in Fig. 5.17 because the payoff functions in Fig. 5.17 were drawn from averages over all the data shown in Fig. 5.21.

Figure 5.22 shows spatiotemporal diagrams for both lanes at $P_c = 0$ and $P_c = 1$ for subphases I, II, and III. At $P_c = 0$ in which all drivers are defectors, a huge stop-and-go wave—a jam—occurs in all realizations. However, at $P_c = 1$, some realizations successfully avoid forming a jam; these correspond to high fluxes and, consequently, appear in subphase I. In some other realizations, a jam only happens in one of the two lanes; these correspond to reasonable fluxes and appear in subphase II. In other realizations, both lanes suffer jams; this significantly reduces the flux and appear in subphase III. This particular bifurcation into the three subphases I, II, and III is caused by the initial random allocation of vehicles between C and D.

In short, we can say that in the density region near $\rho = 0.211$, where scattered points occur in Fig. 5.11(c) (and which is almost consistent with the density region found in Fig. 5.20 for large dilemma strength), the flow field potentially contains several different fully developed states or equilibrium states. This means that several dilemma games may form with slightly different structures. This is why the N-character shape appears in Fig. 5.17, and why the dilemma class underlying that shape is not obvious. Nevertheless, we can identify the game class and dilemma strength, as a whole, by referring to Fig. 5.20 at any arbitrary density.

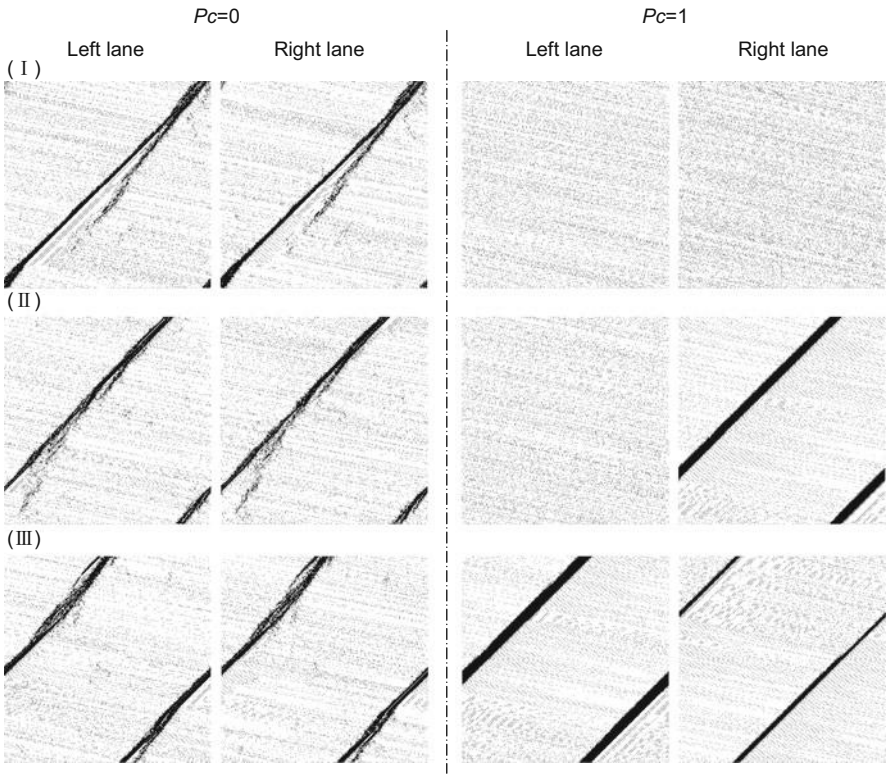

Fig. 5.22 Spatiotemporal diagrams at $\rho = 0.211$ for both lanes at (*left*) $P_c = 0$ and (*right*) $P_c = 1$. Results are shown for each of the three subphases identified in Fig. 5.21: (*top row*) subphase I, (*middle row*) subphase II, and (*bottom row*) subphase III

5.3.2 Summary

For ordinal traffic flows, we have successfully demonstrated that there are hidden social-dilemma structures evoked by drivers' decisions whether or not they should change lanes. This was confirmed by a series of numerical simulations using the revised S-NFS cellular automaton model combined with a lane-changing model that we developed and applied with cyclic boundary conditions.

Interestingly, social dilemmas, as classified by the Prisoner's Dilemma game or its variants, were only observed in situations of middle vehicle density; these situations correspond to the region on the fundamental diagram, including the metastable phase, in which data are scattered. This seems plausible because, when a driver is surrounded by other vehicles, that driver has a serious incentive to change lanes. However, if all drivers make the same decision, social efficiency declines phenomenally and huge traffic jams emerge. We also evaluated the relation between dilemma strength and density of vehicles.

Our results imply that social-dilemma structures used by game theorists may underlie traffic flow phenomena that are commonly believed to be mere physics problems. Although the current model assumes symmetric lane-changing rules and makes no distinctions among vehicles, asymmetric lane-changing behaviors and mixed-flow situations should be considered if we want to model what happens in real traffic flows. These kinds of realistic cases should be investigated in future work.

References

Bando, M., K. Hasebe, A. Nakayama, A. Shibata, and Y. Sugiyama. 1994. Structure stability of congestion in traffic dynamics. *Japan Journal of Industrial and Applied Mathematics* 11: 203–223.

Bando, M., K. Hasebe, A. Nakayama, A. Shibata, and Y. Sugiyama. 1995. Dynamical model of traffic congestion and numerical simulation. *Physical Review E* 51: 1035–1042.

Gao, K., R. Jiang, S.X. Hu, H. Wang, and Q.S. Wu. 2007. Cellular-automaton model with velocity adaptation in the framework of Kerners three-phase traffic theory. *Physical Review E* 76: 026105.

Gao, K., R. Jiang, B.H. Wang, and Q.S. Wu. 2009. Discontinuous transition from free flow to synchronized flow induced by short-range interaction between vehicles in a three-phase traffic flow mode. *Physica A* 388: 3233–3243.

Gazis, C., R. Herman, and R.W. Rothery. 1961. Nonlinear follow-the-leader models of traffic flow. *Operations Research* 9: 545–567.

Helbing, D. 1995. Improved fluid-dynamic model for vehicular traffic. *Physical Review E* 51: 3164–3169.

Kerner, B.S. 2009. *Introduction to modern traffic flow theory and control*. Berlin: Springer.

Kerner, B.S., and P. Konhäuser. 1994. Structure and parameters of clusters in traffic flow. *Physical Review E* 50: 54–83.

Kerner, B.S., H. Rehborn, R.-P. Schafer, S.L. Klenopv, J. Palmer, S. Lorkowski, and N. Witte. 2013. Traffic dynamics in empirical probe vehicle data studied with three-phase theory: Spatiotemporal reconstruction of traffic phases and generation of jam warning messages. *Physica A* 392: 221–251.

Knospe, W., L. Santen, A. Schadschneider, and M. Schreckenberg. 2000. Toward a realistic microscopic description of highway traffic. *Journal of Physics A* 33: L477–L485.

Kokubo, S., J. Tanimoto, and A. Hagishima. 2011. A new Cellular Automata Model including a decelerating damping effect to reproduce Kerner's three-phase theory. *Physica A* 390(4): 561–568.

Kukida, S., J. Tanimoto, and A. Hagishima. 2011. Analysis of the influence of lane changing on traffic-flow dynamics based on the cellular automaton model. *International Journal of Modern Physics C* 22(3): 271–281.

Lighthill, M.J., and G.B. Whitham. 1955. On kinematic waves. II. A theory of traffic flow on long crowded roads. *Proceedings of the Royal Society of London Series A* 229: 317–345.

Nagel, K., and Schreckenberg, M. 1992. A cellular automaton model for freeway traffic. *Journal de Physique France* II:2221–2229.

Nakata, M., A. Yamauchi, J. Tanimoto, and A. Hagishima. 2010. Dilemma game structure hidden in traffic flow at a bottleneck due to a 2 into 1 lane junction. *Physica A* 389: 5353–5361.

Neubert, L., L. Sante, A. Schadschneider, and M.L. Schreckenberg. 1999. Single-vehicle data of high traffic: A statistical analysis. *Physical Review E* 60: 6480.

Nishinari, K., and D. Takahashi. 1998. Analytical properties of ultradiscrete Burgers equation and rule-184 cellular automaton. *Journal of Physics A: Mathematical and General* 31: 5439–5450.

Pipes, L.A. 1953. An operational analysis of traffic dynamics. *Journal of Applied Physics* 24: 274–281.

Sakai, S., K. Nishinari, and S. Iida. 2006. A new stochastic cellular automaton model on traffic flow and its jamming phase transition. *Journal of Physics A: Mathematical and General* 39: 15327–15339.

Shigaki, K., J. Tanimoto, and A. Hagishima. 2011. A revised stochastic optimal velocity model considering the velocity Gap with a preceding vehicle. *International Journal of Modern Physics C* 22(9): 1005–1014.

Wolfram, S. 1986. *Theory and applications of cellular automata*. Singapore: World Scientific.

Yamauchi, A., J. Tanimoto, A. Hagishima, and H. Sagara. 2009. Dilemma game structure observed in traffic flow at a 2-to-1 lane junction. *Physical Review E* 79: 036104.

Chapter 6
Pandemic Analysis and Evolutionary Games

Abstract Human social networks are a central theme to which evolutionary game theory has been applied because the complexity of the underlying network serves as the key factor in determining game equilibrium. The spread of an epidemic throughout such a network is mathematically described by percolation theory, which is an archetype of the physics of diffusion processes. Vaccination, which is driven by individual decision making, inhibits the spread of infectious diseases. In addition, if the so-called herd immunity is established, a free-rider, who pays no cost for vaccination, can escape infection. Obviously, there is a conflict between individual and social benefits; in short, a conflict between individual rational choices: trying to avoid vaccination, or everyone taking the vaccine achieving the fair Pareto optimum. This conflict is why we introduce evolutionary game theory into epidemiology; vaccination can be viewed as a game in a complex social network. In this chapter, we examine pandemic analysis as another application to which evolutionary game theory can be applied.

6.1 Modeling the Spread of Infectious Diseases and Vaccination Behavior

Pre-emptive vaccination is one of the best public health measures for preventing epidemics of infectious diseases as well as reducing morbidity and mortality (Anderson and May 1991). However, most societies entrust vaccination to the autonomy of the individual: vaccination is usually voluntary, despite some national or local governments providing subsidies for it. Therefore, decision making at the individual level may be the result of a trade-off between protection and perceived risks and costs of vaccination and infection. Furthermore, it might be that an individual's decision is influenced by the vaccination behaviors of others (Chapman and Coups 1999, 2006; Basu et al. 2008). The only example of a vaccination campaign completely eradicating a vaccine-preventable disease is smallpox, while cyclic (seasonal) epidemics of other infectious diseases, such as flu-like diseases and influenza, remain a serious threat to mankind.

J. Tanimoto, *Fundamentals of Evolutionary Game Theory and its Applications*,
Evolutionary Economics and Social Complexity Science 6,
DOI 10.1007/978-4-431-54962-8_6

One major reason for the difficulty in eradicating vaccine-preventable diseases is related to an inherent *paradox in epidemiology*. As vaccination coverage increases over a population, the proportion of immunized individuals finally exceeds a critical level above which the disease can no longer persist; this point is called the *herd immunity*. Once the herd immunity is attained, the remaining unvaccinated individuals are quite unlikely to become infected since they are indirectly protected by vaccinated individuals. Thus, unvaccinated individuals obtain benefits from the herd immunity without considering the perceived risks associated with vaccination, such as complications, side effects, and financial costs. There is less incentive for them to get vaccinated, and then, the so-called first-order free-rider problem[1] arises. Some reports suggest that the welfare of a society can be threatened if too many individuals perceive the herd immunity as a public good (Asch et al. 1994). As a result, too much self-interest destabilizes the herd immunity state, and the disease resurges. This paradox makes complete eradication of the disease difficult under a voluntary vaccination policy, and it causes a conflict between the optimal vaccination behavior for each individual and the sufficient level of vaccination needed to protect the whole society via the herd immunity (e.g., Cullen and West 1979; Fine and Clarkson 1986; Geoffard and Philipson 1997; Bauch et al. 2003; Bauch and Earn 2004). In addition, the number of vaccinated individuals may be reduced by underestimates of infection risk due to lack of knowledge about the disease and/or by overestimates of vaccine risk based on scientifically groundless information (Jansen et al. 2003).

Interrelations among vaccination coverage, disease prevalence, and the vaccination behaviors of individuals are complicated, and we should duplicate and dynamically as well as quantitatively predict the consequences of these interrelations if we intend to develop effective public health measures for preventing epidemics of infectious diseases. In this regard, many studies of the vaccination dilemma have applied a game theoretic framework to a population wherein each individual tries to maximize his or her own payoff. These studies have provided highly fruitful results (e.g., Bauch 2005). Previous analyses of vaccination behavior by game theory have assumed a static game wherein individuals always act with perfect information on their probability of becoming infected. In reality, individuals cannot precisely know this probability. Moreover, the game should allow individuals to update their strategies through learning by imitating others who appear to have adopted more successful strategies. In this context, *imitating others* means adapting one's strategy based on his or her own personal experience and based on information from media (the former and latter can be called active and passive information, respectively). To describe this process explicitly, we should construct a model that combines mathematical epidemiologic dynamics with game-theoretic

[1] In 2×2 games, a defector who is harmful to cooperators is called a *first-order free-rider*. When a costly punishment scheme for defectors exists, there can be defined a strategy of the masked good guy, who cooperates with others but never punishes defectors; such an individual is called a *second-order free-rider*. There is much literature on the second-order freerider problem. For example, Olson (1965), Axelrod (1986), Yamagishi (1986).

dynamics. For example, Bauch constructed and analyzed a model that combines epidemiological dynamics with replicator dynamics of evolutionary game theory to capture the imitative behavior of individuals during outbreaks of diseases; he found that imitative behavior provokes periodic outbreaks of diseases (e.g., Bauch 2005). Vardavas et al. (2007) proposed an individual-level adaptive decision-making model that was inspired by Minority Game methodology. By solving the model numerically and analytically, they showed that incentive-based vaccination programs are indispensable to control epidemics of infectious disease but that misuse of these programs may lead to a severe epidemic.

These studies have assumed that the population is homogeneously mixed and that individuals are fully rational in the sense that they make decisions to pursue maximum personal utility based on their perceived risks. Yet, in reality, there are always spatial structures for networks of both disease transmission and an individual's contacts, and any individual's behavior is not completely rational. Accordingly, Fu et al. (2011), for example, elevated a model to that of evolutionary game theory to explore the effects of individual adaptation behavior and population structure on vaccination when a population is faced with an epidemic of an infectious disease.

Let us revisit the term *paradox in epidemiology* in the context of a game theoretical application. Any rational individual has a strong incentive to exploit the public good by free-riding on the herd immunity. However, this incentive, wherein the individual pays nothing but still obtains a benefit, only works as long as the majority in the community spontaneously receive the vaccination. In contrast, if the majority disregards vaccination, then doing nothing is no longer a better option because infection is likely. In this case, spontaneous vaccination becomes the rational option. This difference implies that the best choice for an individual is to always adopt the strategy of the social minority; either free-ride when the herd immunity is well established or take the vaccination when most people neglect to do so. This situation obviously contains the structure of a Minority Game, as Vardavas pointed out (Vardavas et al. 2007). A Minority Game (e.g., Challet et al. 2005), originally defined as the El Farol Bar problem (Brian Arthur 1994), is a typical social dilemma that can be observed in many real situations. The most heavily concentrated applications are in financial markets. In a Minority Game, any individual has the incentive to adopt the strategy of the minority under any circumstance. This duality might be interpreted as a Chicken-type dilemma wherein the fair Pareto optimum is realized when two strategies coexist, as discussed in Chap. 2.

From the perspective of evolutionary game theory, a simple, honest question might be raised: does a Chicken-type dilemma really appear in a particular expected situation wherein individuals live in a complex social network on which an epidemic is spreading? If so, what impact does the dilemma strength have? Dilemma strength is influenced by the underlying network topology. Furthermore, what social provisions can be taken to prevent a pandemic? For example, can the government provide subsidies to encourage people to take the vaccine? And do such actions really contribute to preventing outbreaks of a disease?

To start the discussion, let us focus on the following point: what classes of game structures apply to those social dilemmas and dilemma strengths that underlie the paradox in epidemiology?

6.1.1 *Infinite & Well-Mixed Population*

We start our discussion with the simplest situation (Fu et al. 2011). We presume that a population is infinite and well mixed, which implies the lack of any of the so-called social viscosity that was discussed in Chap. 2. In this context, the dynamics can be formulated by a set of ordinary differential equations (ODEs). To model disease transmission, we apply the susceptible-infectious-recovered (SIR) model[2] wherein the population is divided into three groups: susceptible individuals (S), who are currently healthy but may or may not be infected with the disease; infectious individuals (I), who are currently infected and will recover; and recovered individuals (R), who are never infected again (see Fig. 6.11). Immunity is acquired by either recovering from the disease or by pre-emptive vaccination. The immunity is presumed to be effective over an individual's life span. The SIR model is expressed by

$$\frac{\mathrm{d}S(t)}{\mathrm{d}t} = -\beta \cdot S(t) \cdot I(t),$$
$$\frac{\mathrm{d}I(t)}{\mathrm{d}t} = \beta \cdot S(t) \cdot I(t) - \gamma \cdot I(t),$$
$$\frac{\mathrm{d}R(t)}{\mathrm{d}t} = \gamma \cdot I(t),$$

and

$$S(t) + I(t) + R(t) = 1, \tag{6.1}$$

where β and γ indicate the disease transmission rate per capita and the rate of recovery, respectively. Obviously, the SIR process always takes place in a unilateral direction, $S \rightarrow I \rightarrow R$, which is unlike the SIS model (Hethcote and van den Driessche 1995) wherein immunization efficacy is neglected. Therefore, we can deduce the final epidemic size at the equilibrium of the dynamics: $R(\infty)$ is the fraction of individuals who were once infected with the disease. According to Eq. (6.1) with initial conditions $S(0) \approx 1$, $R(0) = 0$, $I(\infty) = 0$, and $S(\infty) = 1 - R(\infty)$, we derive

[2] The SIR model is widely applied to infectious diseases, such as influenza and measles. An example can be found in Keeling and Eames (2005).

$$R(\infty) = 1 - \exp[-R_0 \cdot R(\infty)]. \tag{6.2}$$

Here, $R_0 \equiv \beta/\gamma$ is called the *basic reproduction ratio*, which is the number of secondary infections caused by a single infected individual. Let x be the fraction of the total population that is vaccinated, so the remaining fraction $1-x$ is not. Then, we can rewrite the final epidemic size at the equilibrium of the dynamics when the fraction of pre-emptive vaccination is $x, R(x, \infty)$, by solving the following equation:

$$R(x, \infty) = (1 - x) \cdot (1 - \exp[-R_0 \cdot R(x, \infty)]). \tag{6.3}$$

This equation is obviously nonlinear and transcendental. Technically, we cannot derive an exact analytic solution, but we can obtain a numerical solution by, for instance, using the Newton–Raphson method. The solution is in Fig. 6.1, which shows the relation between $R(x, \infty)$ and x. One important factor wherein we are interested is the infection point at which $R(x, \infty)$ rises from zero with a decreasing vaccination rate. Let us call this value the *critical vaccination rate*, x_{cr}, because the epidemic cannot be suppressed if the vaccination rate decreases below this critical value. The value of x_{cr} can be obtained by solving the nonlinear Eq. (6.3) to obtain,

$$x_{cr} = 1 - \frac{1}{R_0}. \tag{6.4}$$

The critical value x_{cr} is the so-called *herd immunity threshold*; if x exceeds x_{cr}, further propagation of the disease cannot occur in the population ($R(x_{cr}, \infty) = 0$).

Now, let us extend the discussion further, leading to evolutionary game theory. A fair Pareto optimum, defined in Chap. 2, means a state wherein the accumulated social payoff is maximal but fairness is maintained among all individuals. This concept has already been applied in the discussion in Chap. 5 wherein we

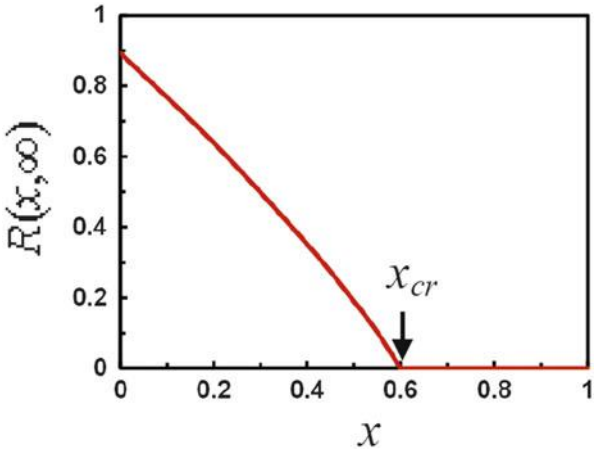

Fig. 6.1 Relation between $R(x, \infty)$ and x when $R_0 = 2.5$

considered a social dilemma structure hidden in various traffic contexts. Being concerned with the payoff structure functions for both cooperators and defectors as well as that of society as a whole, we regarded the fair Pareto optimum as a state at which the maximum social flux appeared. By determining whether or not this maximum social payoff is consistent with Nash equilibrium, we can identify the dilemma class; whether a PD (defection-dominate), Chicken (polymorphic), or SH (bistable) dilemma exists in the model. In the current discussion, we can derive a vaccination rate at which a social payoff is maximized, $x_{\text{social}-\max}$, which identifies a state at which the epidemic is successfully suppressed ($R(x_{\text{social-max}},\infty)=0$) by a minimum vaccination rate. We want the minimum vaccination rate because both vaccination and infection are costly. The maximum social payoff is attained when the vaccination rate is

$$x_{\text{social}-\max} = \begin{cases} x_{cr} = 1 - \dfrac{1}{R_0} & \text{if } R_0 > 1, \\ 0 & \text{if } R_0 \leq 1. \end{cases} \tag{6.5}$$

An important point is that Eq. (6.5) does not cover $C_r = 0$, which should be considered as the limit. This omission is present because, when the range of x which exceeds x_{cr}, every value of x corresponds to that of $x_{\text{social-max}}$. It is qualitatively obvious that $x_{\text{social}-\max} = 1$ when $C_r = 0$.

The next step is to find the Nash equilibrium. The vaccination rate, which is the *strategy* in this game, is defined as continuous. In a game defined with a continuous strategy, the Nash equilibrium was provided by Doebeli et al. (2004). We follow their development. Let us presume a resident strategy x. Suppose, here, a small proportion of the resident, defined as ε, which is called mutant, converts from x to y ($x \neq y$). The new average social strategy, p, for example, the new vaccination rate, is obtained from $p = x \cdot (1-\varepsilon) + y \cdot \varepsilon$. The expected payoffs (average social payoffs) of mutants y are as follows:

$$E(y, p) = -y \cdot C_r + (1 - y) \cdot R(p, \infty), \tag{6.6}$$

where, again for confirmation, C_r is the vaccination cost normalized by the infection cost of 1. The necessary and sufficient conditions that x_{NE} is a stable equilibrium are the following:

$$\left.\frac{\partial E(y,p))}{\partial y}\right|_{y=x_{NE}} = 0 \text{ and } \left.\frac{\partial^2 E(y,p))}{\partial y^2}\right|_{y=x_{NE}} \leq 0. \tag{6.7}$$

These two equations lead us to the explicit form for x_{NE},

$$x_{NE} = \begin{cases} 1 & \text{if } C_r = 0, \\ 1 + \dfrac{\ln(1 - C_r)}{C_r \cdot R_0} & \text{if } 0 < C_r \leq R_0(0, \infty), \\ 0 & \text{if } R_0(0, \infty) < C_r. \end{cases} \tag{6.8}$$

Figure 6.2 shows how $x_{\text{social-max}}$ and x_{NE} are affected by the vaccination cost (relative cost of vaccination to infection) when we assume $R_0 = 2.5$. At the point $C_r = 0$, the social maximum is consistent with Nash equilibrium; thus, we would say it is a Trivial game, or, more precisely, a C-dominate Trivial game. At the point $C_r = 0$, Nash equilibrium becomes discontinuous, as described in Eq. (6.8). If the vaccination cost increases, the Chicken game class appears because its dynamics are absorbed by an internal equilibrium. With additional increases in cost, the Prisoner's Dilemma (PD) class is finally observed, and the absorbed state is an all-defectors-state. Note that this Chicken-type game is a game wherein *ST*-reciprocity, which was discussed in Sect. 2.8, is more appropriate than *R*-reciprocity. This characteristic is confirmed by the fact that the vaccination rate for the maximum social payoff is not an all-cooperators state, $x = 1$, but one that has $x = x_{cr} = 0.6$.

As the final product of this discussion, Fig. 6.3 shows the phase diagram on the cost-R_0 plane. In the figure, the upper panel shows Nash equilibrium with x_{NE} indicating the vaccination rate as the final game result. The lower panel shows the normalized dilemma strength, which varies from 0 to 1 according to the definition by Nakata et al. (2010), and is formulated by

$$\eta = E(x_{\text{social}-\max}) - E(x_{NE}). \tag{6.9}$$

In Fig. 6.3, the region $R_0 \leq 1$ has no dilemma because an epidemic is completely suppressed even though $x_{\text{social}-\max} = 0$. Thus, this game belongs to the defectors-dominate (D-dominate) but still Trivial game class (hereafter, D-dominate Trivial

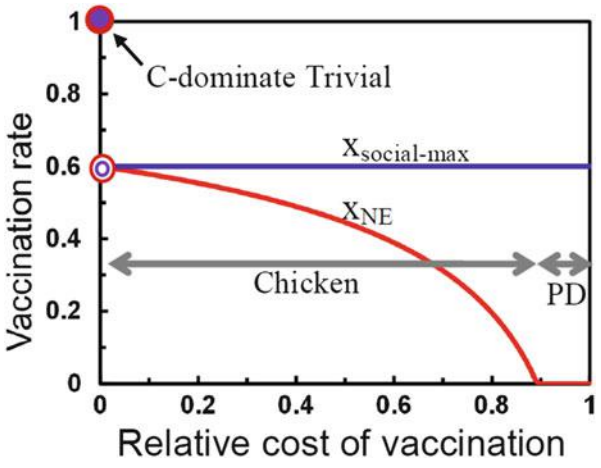

Fig. 6.2 Vaccination rate at the social maximum payoff and Nash equilibrium when $R_0 = 2.5$

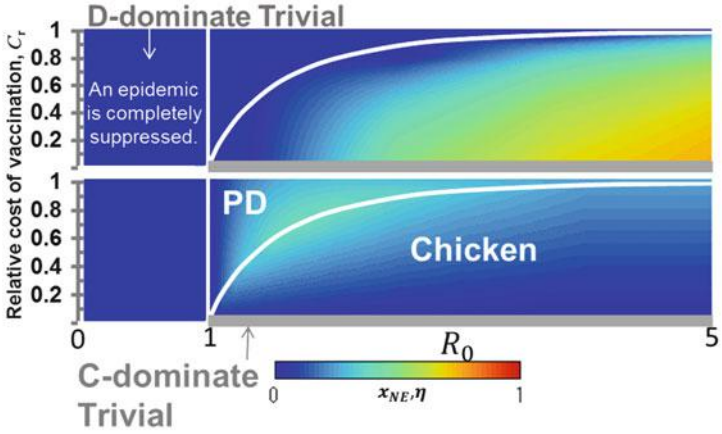

Fig. 6.3 Phase diagram on the cost-R_0 plane with colored contours indicating Nash equilibrium x_{NE} (*upper panel*) and dilemma strength η (*bottom panel*)

or D-Trivial). The region $C_r = 0$ and $R_0 > 1$, highlighted by the bold gray line, is a cooperators-dominate (C-dominate) and Trivial game, as mentioned in Fig. 6.2 (hereafter, C-dominate Trivial or C-Trivial), wherein all individuals take a vaccine, so no infection occurs.

A social dilemma only appears in the region $C_r > 0$ and $R_0 > 1$. As the relative cost of vaccination increases, the PD replaces the Chicken-type game. In the PD region at extremely high cost, the dilemma strength is rather relaxed because too much increased vaccination cost does not differ from the cost of infection, which, for the individual, is not only socially unacceptable but also rather hopeless. The highest social dilemma occurs on the boundary between PD and Chicken in the middle range of the basic reproduction ratio, $1.5 < R_0 < 2.5$. This range of R_0 corresponds to typical influenza.

Large values of R_0 make the entire region (except for $C_r = 0$) belong to a Chicken-type game, and the game becomes less sensitive to further increases in R_0. Sensitivity to cost also becomes less than that for small R_0. Moreover, the dilemma strength with large R_0 gradually becomes small. This decrease occurs because large R_0, implying higher likelihood to be infected, instinctively motivates more people to take the vaccine (letting x_{NE} increase with the increase in R_0, which is manifestly understood by Eq. (6.9) as well as the upper panel of Fig. 6.3). Thus, the discrepancy between x_{NE} and $x_{\text{social-max}}$ becomes relatively small. At the extreme limit of $R_0 \to \infty$, there is only a C-dominate Trivial game for any C_r, although Fig. 6.3 does not extend that far. In this sense, a middle level of epidemic infection, rather than a high level, evokes a social dilemma (this claim can be confirmed by the fact that the light yellow region spreads around $1.5 < R_0 < 2.5$). This interesting result crucially affects people's decisions regarding whether or not to be vaccinated.

6.1.2 Topological Influence

The discussion in the previous subsection assumes an infinite and well-mixed population. No doubt our real society is built on a certain human network wherein an epidemic spreads from one individual to others. So, let us extend the previous discussion to those situations. Since we can no longer apply an analytical approach, we must rely on a numerical route.

Here, we assume N individuals are placed on vertices of an underlying network. In the following, the assumed topologies of the underlying network are complete graphs, a lattice with $k = 4$, and a Barabási-Albert scale-free (BA-SF) network (Barabási and Albert 1999) with $\langle k \rangle = 4$, where k and $\langle k \rangle$ indicate degree and average degree of the topology.

At the beginning of a simulation episode, we randomly place l_0 infectious individuals and presume a vaccination rate that remains constant over a single simulation episode. At the initial state of a simulation episode, $x{\cdot}N$ vaccinated individuals are randomly placed on vertices of the underlying network. After that, we track the time-evolution of epidemiological dynamics by the Gillespie algorithm (Gillespie 1977) based on the SIR model. At equilibrium, we measure a final epidemic size. This process is repeated 100 times to obtain the ensemble average of the final epidemic size for a certain vaccination rate, x.

Unlike in the analytical approach in the previous section, we cannot directly control R_0. Again, let us confirm that the disease transmission rate through a link is defined as β [day^{-1} person^{-1}] and the recovery rate is γ [day^{-1}]. Because of the locality caused by the topology, R_0 is not consistent with β/γ in the network context. However, by recalling that R_0 qualitatively implies how easily the epidemic spreads, we can translate R_0, used in the analytical approach above, to β and γ, used in the simulation approach here. In the following discussion, we set $\gamma = 1/3$. Thus, in a multi-individual simulation with a certain underlying network, the counterpart variable must be β if γ is fixed. To determine the β that is the counterpart to a certain R_0, we proceed as follows. Based on a given R_0 and presuming a vaccination rate $x = 0$, we seek a β value that reproduces the same final epidemic size that the analytic solution yields, $R(0, \infty)$. This particular β depends on the underlying topology. For example, for BA-SF ($N = 4900$ and $\langle k \rangle = 4$) with $R_0 = 2.5$, the counterpart β must be 0.55. Figure 6.4 shows how the final epidemic size decreases with increasing vaccination rate when we presume BA-SF and $\beta = 0.55$; this distribution is actually the counterpart of Fig. 6.1. The intercept with the Y-axis is the final epidemic size, showing that both the analytical solution and simulation are consistent. Unlike what we observed in Fig. 6.1, in the simulation approach it is difficult to clearly define the critical vaccination rate x_{cr} because the random drift resulting from the presumed random numbers introduces some stochastic uncertainty. Therefore, we define the critical vaccination rate in simulations as the vaccination rate that can subdue a final epidemic size to less than $2 \cdot I_0/N$. The criterion "2" adopted here comes from the literature (Fu et al. 2011).

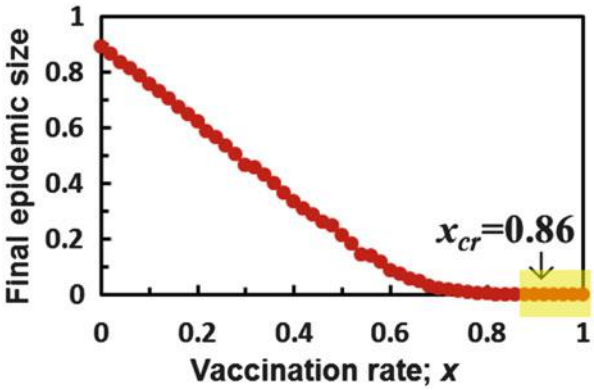

Fig. 6.4 Relation between vaccination rate and final epidemic size for BA-SF ($N = 4900$ and $\langle k \rangle = 4$) and $\beta = 0.55$ with $l_0 = 5$

As shown in Fig. 6.4, the critical value is 0.86 in this example. The yellow highlighted region indicates the vaccination rate that attains herd immunity.

Over a series of simulations wherein vaccination cost, C_r, and β are varied, we can identify both the game class and dilemma strength defined by Eq. (6.9). As an example, Fig. 6.5 shows how we perform this identification; in this example, we used BA-SF ($N = 4900$ and $\langle k \rangle = 4$), $\beta = 0.55$, and $l_0 = 5$. For $C_r = 0$, the vaccination rate yielding the maximum social payoff, $x_{\text{social-max}}$, is identified by the peak of the social payoff function, $\langle \pi_{\text{social}} \rangle$, and Nash equilibrium, x_{NE}, is identified by the crossing point of the defectors payoff function, $\langle \pi_D \rangle$ and that for cooperators, $\langle \pi_C \rangle$. The top panel of Fig. 6.5 shows that the vaccination rate for maximum social payoff and Nash equilibrium are consistent at $x_{cr} = 0.86$. Thus, this situation belongs to the C-Trivial game class.

For $C_r = 0.5$, $x_{\text{social-max}}$ appears in the middle of [0, 1], which indicates an internal equilibrium that differs from Nash equilibrium, x_{NE}. Therefore, this situation belongs to the Chicken game class. The game for the bottom panel, where $C_r = 0.96$ is presumed, belongs to the PD game class because Nash equilibrium is an all-defectors-state, $x_{NE} = 0$, and is inconsistent with $x_{\text{social-max}}$. In this analysis, we should disregard plots for $x > x_{cr} = 0.86$ (highlighted by yellow in Fig. 6.5) because the simulation results are contaminated with the random drift, as mentioned above.

The last result we show here is Fig. 6.6, which should be compared with Fig. 6.3. Again, we assume BA-SF of $N = 4900$, $\langle k \rangle = 4$, $\beta = 0.55$, and $l_0 = 5$. The upper panel in Fig. 6.6 shows Nash equilibrium, x_{NE}, indicating vaccination rate as the final game result. The lower panel shows the dilemma strength. The red dotted line is for $\beta = 0.55$, which we discussed in relation to Fig. 6.5.

In comparing Fig. 6.6 with Fig. 6.3, the most important point is that dilemma strength is relaxed by introducing an underlying network, BA-SF in this case. In other words, introducing a network strongly motivates individuals to receive the vaccine. The reason is as follows. In a BA-SF network, a pandemic can easily occur if hub individuals, who have relatively large numbers of neighbors, are infected; this feature is called the *super-spreader* effect. Unless vaccinated, both individual

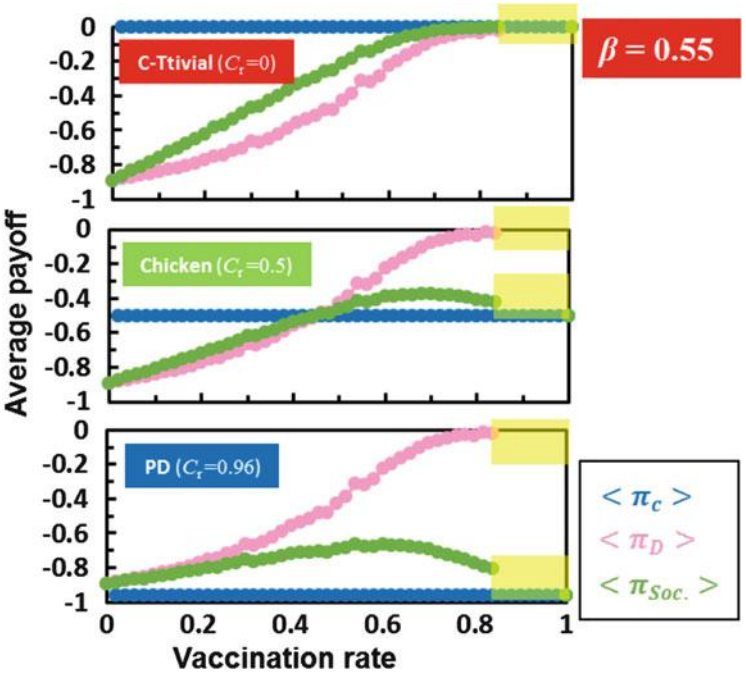

Fig. 6.5 Payoff structure functions for three different vaccination costs using BA-SF ($N = 4900$ and $\langle k \rangle = 4$), $\beta = 0.55$, and $l_0 = 5$

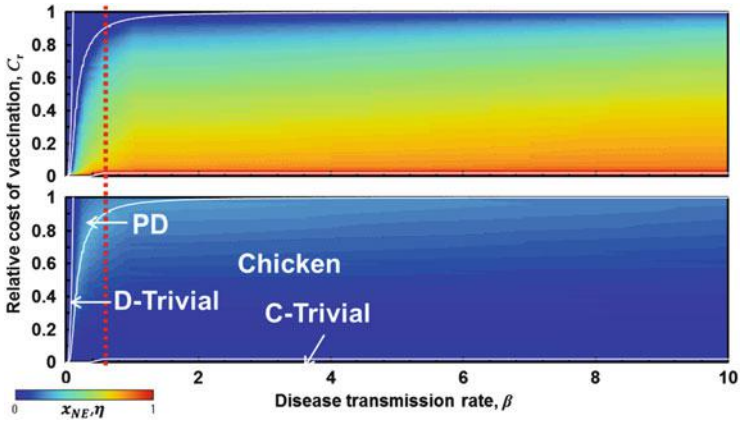

Fig. 6.6 Phase diagram on the cost-β plane with colored contours indicating Nash equilibrium x_{NE} (*upper panel*) and dilemma strength η (*bottom panel*) for BA-SF with $N = 4900$, $\langle k \rangle = 4$, and $l_0 = 5$. The *red dotted line* indicates $\beta = 0.55$

and social payoffs inevitably deflate. In this social context, getting vaccination is an acceptable solution to avoid infection rather than attempting to free ride on the herd immunity. In fact, the upper panel of Fig. 6.6 shows a relatively high vaccination rate as long as the vaccination cost is relatively low. Despite subtle differences, a slightly larger dilemma region appears on the border of Chicken and PD, where the vaccination cost is relatively large and β is less than 1 but not too small. Although Fig. 6.6 does not extend to very large β, unlike the case of well-mixed and infinite populations in Fig. 6.3, the C-dominate Trivial game does not occupy all regions of relative cost of vaccination even in the extreme limit of $\beta \to \infty$. This feature occurs because the effects of spatial (population) structure allow several individuals, who can avoid infection without vaccination (free-riding on herd immunity), to remain in the system even if the environment becomes extremely infectious. This tendency is also true when using a lattice.

Figure 6.7 shows the results for a 2D lattice of $N = 4900$, $k = 4$, and $l_0 = 5$. Compared with the results for BA-SF, the vaccination rate as the final game result (upper panel) is less. Because of this decrease, a relatively larger dilemma occurs vis-à-vis the BA-SF (lower panel). In particular, the region with high vaccination cost and lower β is marked with a higher dilemma compared to that in the case of BA-SF. The relatively longer average path length of the lattice compared to that of BA-SF tends to inhibit spreading of the epidemic, which makes individuals less motivated to receive the vaccine as compared with those in the case of BA-SF. This difference occurs because, in situations with low possibility of infection, no vaccination might be beneficial due to free-riding on the herd immunity. Consequently, more social dilemma is present in the lattice than in the BA-SF network.

Since the horizontal axis in Fig. 6.3 (R_0) differs from those in Figs. 6.6 and 6.7 (β), a candidate for comparing with Fig. 6.3 is shown in Fig. 6.8, for which a complete graph for $N = 1000$ and $l_0 = 5$ was used. Using a complete graph certainly indicates a well-mixed situation, but it does not mean an infinite population.

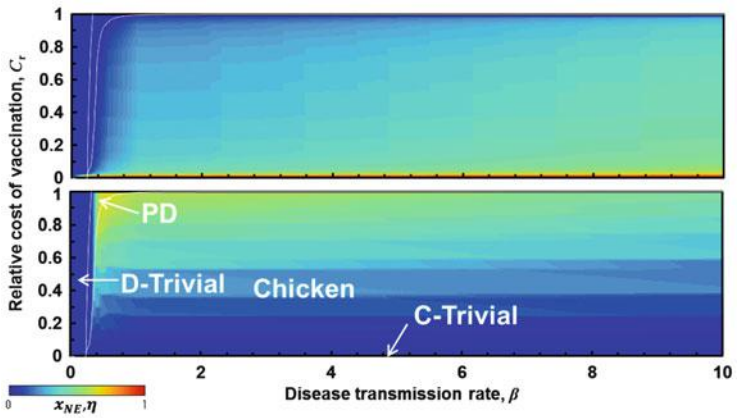

Fig. 6.7 Phase diagram on the cost-β plane with colored contours indicating Nash equilibrium x_{NE} (*upper panel*) and dilemma strength η (*bottom panel*) for a lattice of $N = 4900$, $k = 4$ and $l_0 = 5$

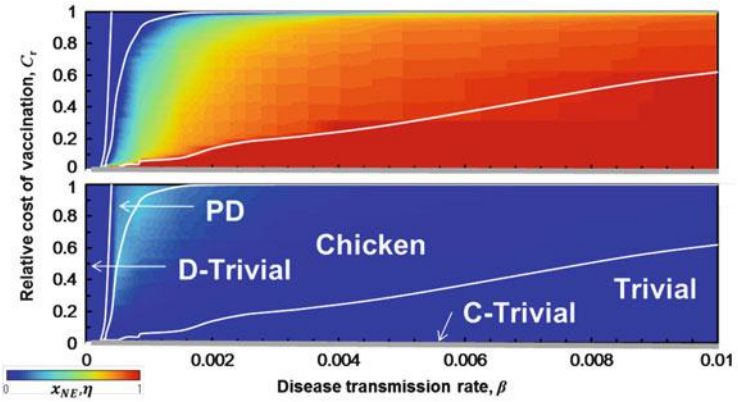

Fig. 6.8 Phase diagram on the cost-β plane with colored contours indicating Nash equilibrium x_{NE} (*upper panel*) and dilemma strength η (*bottom panel*) for a complete graph with $N = 1000$ and $l_0 = 5$. The game class "Trivial" means that no dilemma game was absorbed by either the all-defectors state (D-Trivial) or all-cooperators state (C-Trivial)

Because of this difference, Fig. 6.8 is not strictly comparable to Fig. 6.3. Figure 6.3 only covers the left part of Fig. 6.8, so, again, there are substantial differences between Figs. 6.3 and 6.8. Many of those differences are due to differences in population size: Fig. 6.8 applies to a finite population of $N = 1000$, while Fig. 6.3 applies to an infinite population.

6.1.3 Summary

In this section, we proposed new tools for addressing the vaccination dilemma. One tool is a phase diagram that allows us to identify the dilemma class that underlies the problem. Another is the combined use of dilemma strength and final vaccination rate, provided that the epidemic transition rate and vaccination cost vary independently.

A Chicken-type dilemma, which should be expected in *ST*-reciprocity but not in *R*-reciprocity, appears as the main underlying dilemma class. At high vaccination costs, a PD class dilemma appears with relatively large dilemma strength. Increasing the transition rate can relax the dilemma because a high likelihood of being infected becomes more important, regardless of the cost of vaccination.

The topology of the underlying network has a significant impact on the structure of the vaccination dilemma. Generally, a network with a small average path length can relax the vaccination dilemma because a long distance between any two arbitrarily selected individuals effectively prevents rapid spread of infection through the society. This separation allows agents to stray in whether they take the vaccination or try to free-ride on the herd immunity.

6.2 Vaccination Games in Complex Social Networks

In the previous section, the game we studied did not include any evolutionary process. What we discussed was whether or not the process leading to a particular payoff structure contained a dilemma; if so, then we wanted to identify the dilemma game class. An important point might be how the instinct dilemma can be diluted by each of the various subsidy campaigns that might be invoked to motivate vaccination, which might be meaningful for public health officials.

In this section, let us take a further realistic step wherein not only epidemic spreading but also an individual's decision for or against voluntary vaccination are both time-evolving on a complex social network (Fukuda et al. 2014). This kind of exploration was originally reported by Fu and his colleagues (Fu et al. 2011). They constructed a model wherein the network of disease transmission was just the same as that of strategic interactions among individuals on complex networks, and they found that vaccination coverage sensitively depends on the cost of vaccination.

More precisely, their model has two stages. The first stage is decision making. Each individual in a population (represented by a node (vertex) in a social network) makes a decision whether or not to get vaccinated; this decision corresponds to his or her choice of strategy. The second stage is an epidemic season. To describe the epidemiologic dynamics in a structured population, their combined model uses SIR dynamics on a social network. In the SIR model, a fixed population is divided into three groups: susceptible (S), infected (I), and recovered (R) (or vaccinated (V)). Each group develops temporally according to a certain mathematical structure. Those who decide not to be vaccinated are included in the susceptible group. At the end of the epidemic season, the epidemic transmission on the network determines whether each susceptible individual has been infected or not. According to the final epidemic state, a stipulated payoff is assigned to each individual. After that, each individual re-examines his or her strategy regarding vaccination via an imitation process. In Fu's work, an individual compares his or her payoff to the payoff of a randomly chosen neighbor. If that neighbor earned a higher payoff than he or she did in the last epidemic season, this individual may imitate the selected neighbor's strategy with higher probability. This concept has been commonly adopted in spatial versions of 2×2 games, such as the prisoner's dilemma and snow drift (chicken) games.

However, it is not always true that an individual relies only on the payoff of his or her neighbor to make a decision regarding whether or not to imitate. For example, mass media, such as television, radio, and newspapers, have the potential to powerfully influence people's behaviors; for this discussion, those media can present objective information about a currently spreading disease. Consequently, each individual can take into account a survey on the social circumstances wherein an infectious disease spreads, and that survey could affect his or her decision concerning vaccination. That is, an individual can adjust the probability of getting vaccinated based on the level of the epidemic. This adjustment might be crucially important in attempting to reproduce how each individual behaves in a real social context.

This situation is closely linked to the evolution of cooperation in the usual evolutionary game theory wherein network reciprocity helps emerging cooperation—getting vaccination instead of defection—which we discussed in Chap. 3. Shigaki et al. (2012) constructed a model of the prisoner's dilemma as a typical 2×2 game for a network wherein an individual extracts the number of other individuals who adopt a strategy s_j, depending on some sampling rate, and compares his or her own payoff to the payoff averaged over those extracted individuals for strategy adaptation. In particular, they studied the effects of sampling rate on the frequency of cooperation. They found that cooperative behavior was most often promoted when the sampling rate was relatively low. An average with a low sampling rate generally fluctuates around its overall average; thus, the average exceeds the overall average over some durations and falls below the average in other durations. They proved that this instantaneous spiking of the average sampled payoff among cooperators over the overall average plays a key role in promoting cooperation. This feature indicates that cooperative behavior is more likely when people put trust in so-called anecdotal information, meaning someone's "success story," rather than in public information that reflects the whole of society. This contrast is thought to be meaningful in the sense that the evolutionary game is able to show a possible scenario on how mass media work to significantly enhance cooperation in a modern society. Then, such scenarios might be applied to other situations, like what we have just argued—how we can control a spreading epidemic by means of vaccination.

Motivated by the above reasons, in this section, we assume that an individual in a population grasps the whole situation in the society; that is, he or she obtains complete information about the society and updates his or her strategy based on that information. Namely, an individual determines his or her strategy-updating probability, not based on the payoff of a selected opponent among neighbors, but on the averaged payoff that is obtained by averaging the payoffs over those who adopt the same strategy that the individual's opponent adopts. We analyze in detail how this newly proposed strategy-updating rule affects vaccination coverage and the final proportion of the population who are infectious. The results might be interesting in relation to Shigaki's network reciprocity as one of the supporting mutual-cooperation frameworks for 2×2 games.

6.2.1 Model Setup

In this section, we describe the basic model introduced originally by Fu et al. (2011), which presumes an individual-based risk assessment for strategy update. Then, we propose a new model in which each individual assesses risks based on the averaged payoff resulting from adopting a certain strategy (Fig. 6.9).

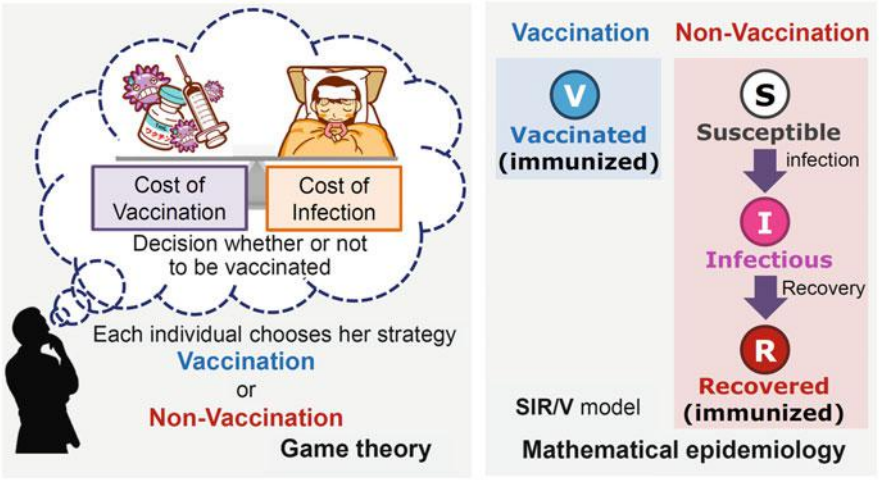

Fig. 6.9 Model at a glance

Model Assumption

Consider a population in which each individual on a social network decides whether to be vaccinated. Seasonal and periodical infectious diseases, such as flu, are assumed to spread through such a population. The protective efficacy of a flu vaccine persists for less than a year because of waning antibodies and year-to-year changes in the circulating virus. Therefore, under a voluntary vaccination program, individuals must decide every year whether to be vaccinated. Thus, the dynamics of our model consists of two stages: the first stage is a vaccination campaign, and the second is an epidemic season.

The First Stage: The Vaccination Campaign

Here, in this stage, each individual makes a decision whether to get vaccinated before the beginning of the seasonal epidemic, i.e., before any individuals are exposed to the epidemic strain. Vaccination imposes a cost C_v on each individual who decides to be vaccinated. The cost of vaccination includes the monetary cost and other perceived risks, such as adverse side effects. For simplicity, we assume that the vaccination provides perfect immunity to an individual against the disease during a season; however, an unvaccinated individual faces the risk of being exposed to infection during a season.

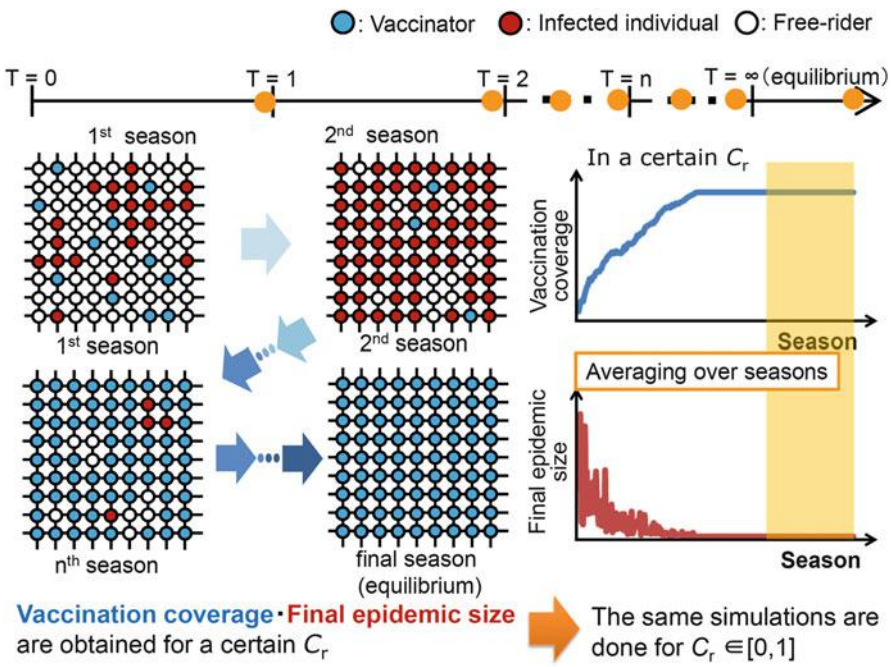

Fig. 6.10 Time evolution covering the first and second stage

The Second Stage: The Epidemic Season

Here, at the beginning of this stage, the epidemic strain enters the population, and a number I_0 of randomly selected susceptible individuals are identified as the initially infected ones. Then, the epidemic spreads according to SIR dynamics (Fig. 6.10).

SIR Dynamics in Finite Populations on Social Networks

The classic SIR model is given by coupled (integro-) differential equations and does not assume any spatial structure for the population. Using SIR model, a short-range and local epidemic outbreak of infectious diseases such as plague are modeled (Kermack and McKendrick 1927). Here, we use an extended SIR model that involves a spatial structure for the whole population. This structure is represented by a network consisting of nodes and links. The dynamics of SIR on a spatially structured population is not captured by a system of differential equations; thus, we numerically simulate an epidemic spreading on a network by using the Gillespie algorithm (Gillespie 1977) to the extended SIR model.

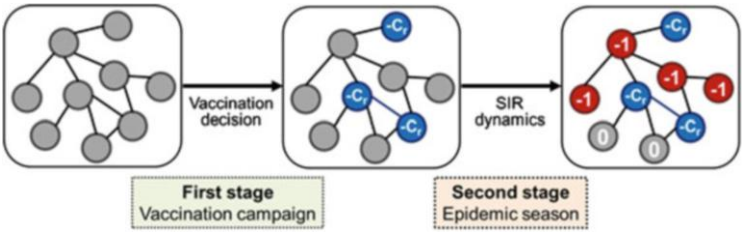

Fig. 6.11 Schematic of the SIR model. In this model, the population is divided into three categories on their epidemiological states: susceptible individuals (S), infected individuals (I), and recovered individuals (R), respectively. We assumed that R who had come down the infectious disease and recovered acquires perfect immunity. Therefore, they do not get infected again within the same epidemic season

In the model, the whole population N is divided into three sub groups: susceptible (S), infected (I), and recovered (R) individuals (see Fig. 6.11). The disease parameters are β, which is the transmission rate per day per person, and γ, which is the recovery rate per day (i.e., the inverse of the mean number of days required to recover from the infection).

In this study, we consider three typical networks: a square lattice, a random regular graph (RRG), and the Barabási-Albert scale-free (BA-SF) networks (Barabási and Albert 1999). An epidemic spreads much more easily on the RRG and the BA-SF network, even when the transmission rate is lower than that on the square lattice (Keeling and Eames 2005; Pastor-Satorras and Vespignani 2001). In this study, we set the disease transmission rate β to ensure that the risk of infection in a population with only the unvaccinated individuals is equivalent for all three network structures. That is, we calibrate the value of β such that the final proportion of infected individuals across the networks will be 0.9. Accordingly, we set $\beta = 0.46$ day^{-1} person^{-1} for the square lattice, $\beta = 0.37$ day^{-1} person^{-1} for the RRG, and $\beta = 0.55$ day^{-1} person^{-1} for the BA-SF network (see Fig. 6.13). We set the recovery rate $\gamma = 1/3$ day^{-1}. A typical flu is assumed to determine these disease parameters.

An epidemic season lasts until no infection exists in the population. Each individual who gets infected during the epidemic season incurs the cost of infection, C_i. However, the cost paid by a "free-rider" who does not vaccinate and still is free from infection is zero. For simplicity, we renormalize these costs (payoffs) by defining the relative cost of vaccination $C_r = C_v/C_i$ ($0 \leq C_r \leq 1$). Then, the payoff for every individual after the end of an epidemic season is summarized according to her state in Table 6.1.

Table 6.1 The payoff for the three types of individuals' strategy and state in the population after the epidemic season

Strategy/State	Healthy	Infected
Vaccination	$-C_r$	
Non-vaccination	0	-1

We assume that vaccinators acquire perfect immunity by vaccination to the seasonal infectious disease during the epidemic season. Therefore, there is no simultaneously vaccinated and infected individual in the population

Strategy Adaptation: The Original Individual-Based Risk Assessment (IB-RA)

After the above two stages, every individual again examines vaccination decision-making at the beginning of next season. The rule of strategy adaptation is given as follows. A certain individual i chooses randomly individual j among all of her neighbors. Let $\pi_{i,}$, π_j denote the payoffs of individual i and j respectively. The probability $P\left(s_i \leftarrow s_j\right)$ that the individual i (whose strategy is s_i) imitates the individual j's strategy, s_j, is given by a pairwise comparison of their payoff difference according to the Fermi function, which has been repeatedly appeared in previous chapters;

$$P\left(s_i \leftarrow s_j\right) = \frac{1}{1+\exp\left[\frac{\pi_i - \pi_j}{\kappa}\right]}, \tag{6.10}$$

where the term "strategy" implies an individual's decision to be vaccinated and κ is the sensitivity of individuals to the difference in the payoff. For $\kappa \to \infty$ (weak selection pressure), an individual i is insensitive to the payoff difference $\pi_i - \pi_j$ against another individual j and the probability $P\left(s_i \leftarrow s_j\right)$ approaches 1/2 asymptotically, regardless of the payoff difference. For $\kappa \to 0$ (strong selection pressure), individuals are sensitive to the payoff difference, and they definitely copy the successful strategy that earns the higher payoff, even if the difference in the payoff is very small. In the present study, we set $\kappa = 0.1$, which has been used as a typical selection pressure in most previous studies. This value of κ implies that, in most situations, individuals adopt any successful strategy; however, occasionally they end up imitating a worse performer with a lower payoff. Such erratic decision making is a reflection of irrationality or mistakes made by ordinary individuals. Figure 6.12 shows the flow of the model described so far.

The Proposed Model: The Strategy-Based Risk Assessment (SB-RA)

Equation (6.10) indicates that as the negative payoff difference increases, the probability that an individual will change her strategy to that of her successful neighbor increases. Observing (6.10) from a different viewpoint, this rule of

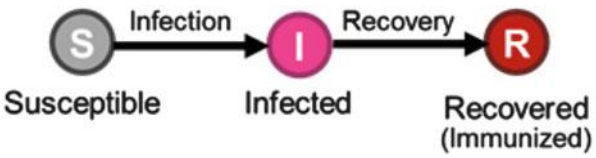

Fig. 6.12 The flow of the model we used. That dynamics is modeled as a two-stage dynamics. In the first stage (vaccination campaign), each individual decides whether or not to get vaccinated. An individual who decides to get vaccinated incurs the cost of vaccination C_v, and acquires perfect immunity to the infectious disease. In the second stage (epidemic season), the epidemic spreads according to SIR dynamics. Each infected individual incurs the cost of infection C_i. Successful individuals who are unvaccinated and remain healthy (free-riders) avoid any cost, and they are indirectly free-riding off the vaccination efforts of others. For simplicity, we set $C_i = 1$, and rescale the payoffs by introducing the relative cost of vaccination $C_r = C_v, / C_i$ $(0 \leq C_r \leq 1)$

strategy adaptation can be interpreted as follows: each individual evaluates both the risk of maintaining her own strategy and imitating her opponent's strategy and then selects the one with the smaller risk. In this method, each individual i assesses the risk based only on one certain individual j because (6.10) uses only the payoff of i's opponent (individual j). Thus, we call the updating rule (6.10) as individual-based risk assessment updating rule (IB-RA).

However, when we assume that the information regarding the consequences of adopting a certain strategy are disclosed to the society and everyone in the population has access to those consequences, then individuals no longer rely heavily on the payoff of any one neighbor. Instead, in adapting their strategy, they tend to assess the risk based on a socially averaged payoff that results from adopting a certain strategy.

To reflect the above situation, we propose a modified imitation probability, which is as follows.

$$P\left(s_i \leftarrow s_j\right) = \frac{1}{1 + \exp\left[\frac{\pi_i - <\pi_{s_j}>}{\kappa}\right]}, \tag{6.11}$$

where $< \pi_{s_j} >$ is an average payoff obtained by averaging a collective payoff over individuals who adopt the same strategy as that of a randomly selected neighbor j of the individual i. The sampling number is a control parameter that ranges from only one individual (i.e., only one of i's neighbors, j) to all individuals among the whole population who adopt the strategy same as that of j. That is, if s_j is the strategy of vaccination (Cooperation, C), then $< \pi_{s_j} >= -C_r$ (since the payoff of a vaccinated individual is uniquely determined); whereas, if s_j is the strategy of no-vaccination (Defection, D), then $< \pi_{s_j} >$ takes a value between 0 and 1, depending on the fractions of infected and healthy individuals (free-riders) with the strategy s_j in the population at the end of the epidemic. Moreover, if sampling is impossible because the population size of individuals with the strategy s_j is too small, the individual i uses the payoff of one randomly selected neighbor instead of $< \pi_{s_j} >$ in (6.11),

which leads to an expression that is same as (6.10). Thus, when the sampling rate is set to zero, (6.11) reduces to (6.10).

Equation (6.11) implies that an individual i assesses the risk of changing her strategy based on the payoff attained by adopting a certain strategy, and not the payoff attained by a certain other individual. Thus, we call the updating rule (6.11) as strategy-based risk assessment updating rule (SB-RA). Note that, for a vaccination strategy, risk assessment based on the consequences of that strategy is the same as that based on a unique individual because the immune effect of vaccination is perfect during an epidemic season. However, for the no-vaccination strategy, the risk may differ from season to season because the degree of the epidemic may differ.

Simulation Assumption

Initially, equal fractions of the vaccinated and unvaccinated individuals are randomly distributed among the population allocated on the network. The vaccination coverage and the fraction of infected individuals are updated by iterating each two-stage process (the vaccination campaign and the epidemic season). The equilibrium results shown in Figs. 6.14 and 6.16 represent average fractions over the last 1000 from among 3000 iterations in 100 independent simulations. In the present study, we show only the results for which the population size $N = 4900$ and the sampling rate when collecting individuals who adopt the strategy s_j was 100 %. We confirmed that the results show no differences unless the sampling rate was changed to as low as 0.1 % and the population size was set to $N = 1600$. In such cases, sampling becomes quite difficult.

6.2.2 Results and Discussion

Figure 6.14 shows equilibrium values for vaccination coverage and final proportion infected individuals as functions of the relative cost of vaccination C_r. Generally, vaccination coverage in the RRG shows better results than that on the square lattice (Fig. 6.14(a1) and (b1)), and that the BA-SF network is superior to the RRG at the same values of C_r (Fig. 6.14(b1) and (c1)). As a result, the RRG shows lower final proportions of infected individuals than that shown by the square lattice (Fig. 6.14 (a2) and (b2)), and the BA-SF network can show even lower proportions than that shown by the RRG (Fig. 6.14(b2) and (c2)). These tendencies are because the RRG and the BA-SF network make it easier for infectious diseases to spread due to the randomness or heterogeneity of the networks, which is basically confirmed in Fig. 6.13. Ease of epidemic spreading makes it difficult to achieve the herd immunity state; thus, it is difficult for both free-riders and selfish individuals to remain uninfected. Consequently, both the randomness of the RRG and the

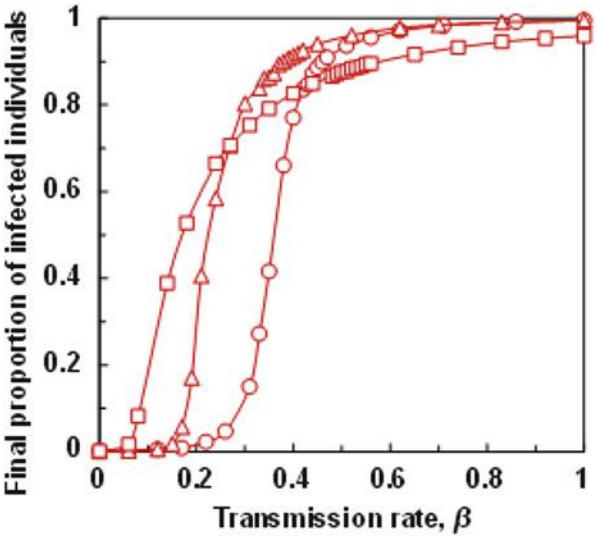

Fig. 6.13 Final proportion of infected individuals as a function of transmission rate β when no individuals are vaccinated on each network: square lattice (*circles*), random regular graph (RRG) (*triangles*), Barabási-Albert scale-free (BA-SF) network (*squares*). For the lattice (*circles*): population size $N = 70 \times 70$ with von Neumann neighborhood, recovery rate $\gamma = 1/3$ day^{-1}, seeds of epidemic spreading $I_0 = 5$. For RRG (*triangles*): population size $N = 4900$, degree $k = 4$, recovery rate $\gamma = 1/3$ day^{-1}, seeds of epidemic spreading $I_0 = 5$. For BA-SF network (*squares*): population size $N = 4900$, average degree $< k > = 4$, recovery rate $\gamma = 1/3$ day^{-1}, seeds of epidemic spreading $I_0 = 5$. Each plotted point represents an average over 100 runs

heterogeneity of the BA-SF network enhance the voluntary vaccination of individuals. The results for each network have been shown separately in the following sections.

Lattice Populations

From Fig. 6.14(a1), (a2), one can find that for wider range of C_r (roughly $C_r < 0.7$), the SB-RA can suppress the final proportion in infectious by increasing the equilibrium vaccination coverage compared to the case of the IB-RA. Figure 6.15 illustrates snapshots of the system with different risk assessment schema when $C_r = 0.05$ after approaching equilibrium. As can be seen from these figures, the SB-RA promotes the growth of larger clusters of vaccinators which work as bulwarks to infectious disease. Therefore, the risk assessment based on the strategy for imitation has a large impact on the suppression of epidemics for wider range of C_r. The difference in the results due to the different risk-assessment schema fades out at large value of C_r, the reason of which will be explained qualitatively as follows.

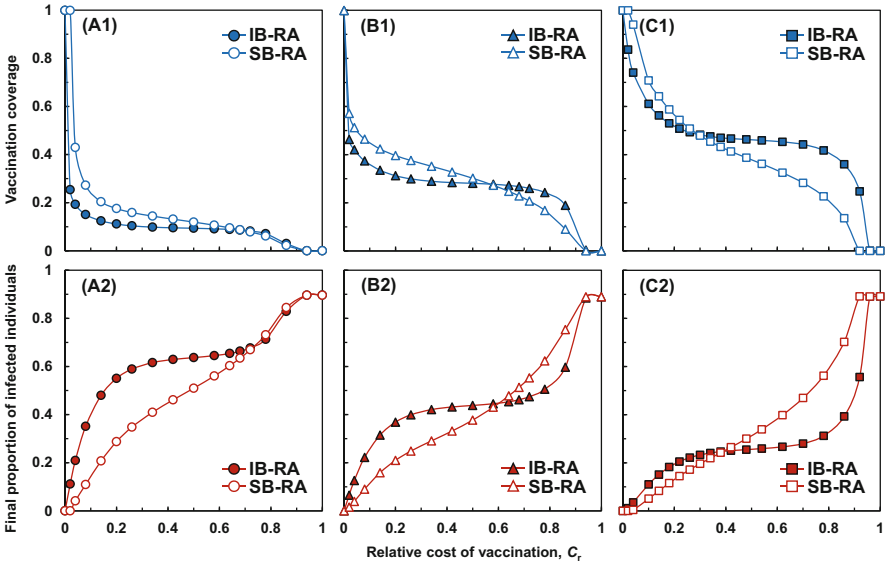

Fig. 6.14 Vaccination coverage (*upper three panels*) and final proportion of infected individuals (*lower three panels*) as functions of relative cost of vaccination C_r for each network: lattice population (*circles* in Panels **a**1 and **a**2), RRG network (*triangles* in Panels **b**1 and **b**2), and BA-SF network (squares in Panels **c**1 and **c**2). Filled symbols are for the original individual-based risk assessment updating rule (IB-RA). Open symbols are for the proposed strategy-based risk assessment updating rule (SB-RA). For the lattice (*circles*): transmission rate $\beta = 0.46$ day^{-1} person^{-1}. For the RRG (*triangles*): transmission rate $\beta = 0.37$ day^{-1} person^{-1}. For BA-SF network (*squares*): transmission rate $\beta = 0.55$ day^{-1} person^{-1}. Other parameters used in the simulation are given in the caption to Fig. 6.13

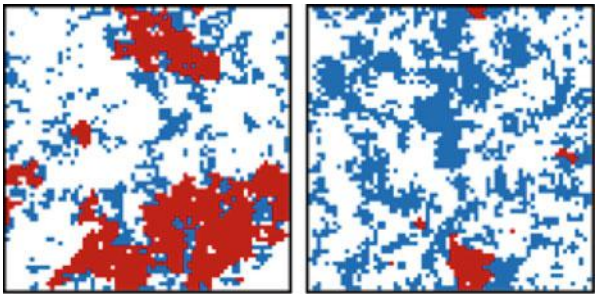

Fig. 6.15 Typical snapshots of systems in the equilibrium state for $C_r = 0.05$ on the lattice network utilizing (**a**) original IB-RA and (**b**) proposed SB-RA. Blue denotes a vaccinated individual, red an infected individual, and white a free-rider. For the original IB-RA in (**a**), the vaccinated individuals form some small clusters whose fraction is about 18 % of the population. For the proposed SB-RA in (**b**), the vaccinated individuals form some larger clusters whose fraction is about 59 % of the population

In the square lattice, infectious disease is relatively more difficult to spread than other kinds of network (e.g. the BA-SF treated in this paper). Thus each individual ceases to get vaccinated even if C_r is small, finally leading to relatively higher level of final proportion in infectious. In turn, the number of infected individuals is larger than that of free-riders and so an individual i has quite a few opportunities to keep her own strategy. That is, if a focal i's opponent j is a free-rider, the payoff of i cannot be larger than that of j under the IB-RA updating rule, while $< \pi_{s_j} >$ which is calculated under the SB-RA updating rule may be smaller than i's payoff, meaning that the focal i can keep her original strategy. Meanwhile if i's opponent j is infected, $-C_r > < \pi_{s_j} >$ may hold when C_r is moderately low and then the focal i who adopt the cooperative strategy (vaccinator) is unlikely to imitate the defective strategy (non-vaccinator) of her focal j for the SB-RA updating rule. (The cooperator i basically do not imitate the defective strategy of an infected opponent j under the IB-RA.)

Increase of C_r decreases the vaccination coverage and then increases the final fraction of infection, thus resulting in $-C_r \cong < \pi_{s_j} >$. Hence it cannot be expected that the SB-RA helps vaccinators to keep their cooperative strategy. Additionally free-riders basically keep their defective strategy because the payoff difference between a free-rider and a vaccinator becomes large at larger C_r. This is the case for both the IB-RA and the SB-RA. In other words, the possibility for defectors (free-riders) to change the strategy from D to C cannot be enhanced by applying the SB-RA updating rule. That is the reason why the SB-RA gives no enhancement effect at larger C_r.

Barabási-Albert Scale-Free Networks

For the BA-SF network, we found that, unlike the other networks, the SB-RA leads to lower vaccination coverage and higher levels of final proportion of infected individuals over a narrower range of C_r (approximately $C_r > 0.4$) (Fig. 6.14(c1) and (c2)). Figure 6.16 shows the fraction of vaccinated individuals as the functions of the number of neighbors for $C_r = 0.1$ and 0.6. This figure shows that highly connected individuals (hubs) who have larger risks of infection are active to voluntary vaccination; whereas, individuals with smaller number of neighbors ride freely on the benefits brought by the voluntary vaccination of the hubs. A risk assessment based on strategy is effective for suppressing the spread of an epidemic when the relative cost of vaccination C_r is small; however, it has the opposite effect when C_r is large. The explanation is as follows.

When $C_r = 0.1$ (low cost of vaccination), 70 % of the overall population gets vaccinated and 5 % are infected at the equilibrium state (Fig. 6.14(c1) and (c2)), then the averaged payoff for the defective strategy $< \pi_{s_j} >$ is nearly -0.17. Thus, a cooperative individual is likely to maintain her strategy even if her opponent j is a defector, since $-C_r > < \pi_{s_j} >$ holds. As mentioned earlier, any defective individual has the same imitation probability under the IB-RA and SB-RA.

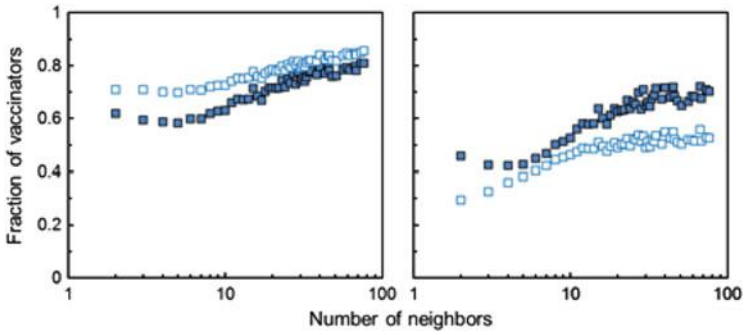

Fig. 6.16 Fraction of the vaccinated individuals on the Barabási–Albert scale-free network as a function of the number of neighbors (degree) for (**a**) $C_r = 0.1$ and (**b**) $C_r = 0.6$. *Open squares* are for the proposed SB-RA. *Filled squares* are for the original IB-RA

In Fig. 6.16(a), the SB-RA provides higher vaccination coverage for all number of neighbors, and enhancement is more remarkable for fewer neighbors. The SB-RA enhances the tendency for cooperators to maintain their cooperative strategy; however, it cannot increase the vaccination coverage of hubs. Those hubs naturally have strong tendencies to get vaccinated, irrespective of the risk assessment schema. However, individuals with few neighbors become more likely to get vaccinated by imitating the cooperative hubs, and the SB-RA gives an additional impetus for them to maintain their cooperative strategy. Thus, the result is shown in Fig. 6.16(a).

An infectious disease is well known to spread easily on a scale-free network with heterogeneity in the neighbor distribution due to the presence of hubs as super-spreaders. Therefore, the final proportion of infected individuals cannot be inhibited effectively unless individuals with large number of neighbors are more likely to get vaccinated.

Thus, we conclude that the SB-RA helps the hubs in maintaining their cooperative strategy. This increases the frequency for individuals with few contacts to change their strategy from defection to cooperation and cooperators to maintain their cooperative strategy. This finally results in slightly improved vaccination coverage for small values of C_r. However, the SB-RA does not have a significant impact on suppressing the final proportion of infected individuals because it has little influence on the decision-making processes of highly connected individuals.

When $C_r = 0.6$ (a moderately higher cost of vaccination), the average payoff brought about by adopting a defective strategy $< \pi_{s_j} >$ is nearly -0.57. Since the average payoff of the defective strategy is larger than that of the cooperative strategy, cooperative individuals find it difficult to maintain their own strategy. For defective individuals, there is no difference in the imitation probability between the IB-RA and SB-RA. Figure 6.16(b) shows the fraction of vaccinated individuals as a function of number of neighbors when $C_r = 0.6$. The results are explained as follows.

Compared to IB-RA, the result of vaccination coverage using SB-RA is lower for all the degrees of contact, and the difference is larger for higher number of neighbors. Moreover, the level of vaccination coverage using IB-RA for number of nodes $k = 3, 4, 5$ are lower than that for $k = 2$ with IB-RA. To understand this, note that the number of nodes with $k = 2$ is very large, which implies that the number of individuals who connect to the hubs is also very large. Then, the decision making of individuals with $k = 2$ is considerably affected by the decisions of the hubs. When the vaccination coverage of hubs is high, individuals with $k = 2$ can ride freely on the preventive ability of hubs against infectious diseases. However, for IB-RA, the influence of the attitude of cooperation by hubs on individuals with $k = 2$ surpasses the temptation for free-riding, and thus the vaccination coverage of individuals with $k = 2$ is superior to that with $k = 3, 4, 5$.

For SB-RA, the decline in vaccination incentive due to larger values of C_r remarkably influences vaccination coverage. Generally, the BA-SF network consists of a great majority of individuals with few contacts and relatively few hubs. Thus, even if only one hub selects the defective strategy (no -vaccination), it causes a large reduction in vaccination coverage. Because of this reduction in vaccination coverage of hubs, those with fewer contacts who connect to hubs tend to decline to get vaccinated (C to D) or maintain their defective strategy (D to D). As discussed previously, the average payoff of the defective strategy is larger than that of the cooperative strategy. These two factors induce individuals with fewer contacts to adopt the defective strategy, yielding the result shown in Fig. 6.16(b).

Summing up, for moderately large values of the cost C_r, a strategy-based risk assessment makes it difficult for each individual to maintain the cooperative strategy of vaccination, and thus vaccination coverage declines and a large epidemic ensues.

Random Regular Graphs

Figure 6.14(b1) and (b2) show that, compared to IB-RA, SB-RA can suppress the final proportion of infected individuals by increasing the equilibrium vaccination coverage over a moderately wider range of C_r (approximately $C_r > 0.6$). Moreover, this threshold value of C_r is greater than that for the square lattice, but smaller than that for the BA-SF network. This is because the RRG is not only homogeneous in its degree distribution, like a square lattice, but also random in its network structure. In general, an epidemic spreads more easily through a network in which the average path length is small, such as an RRG or BA-SF network. Hence, on these networks, the vaccination behavior of individuals can be promoted to more than that on a square lattice. Further, in a BA-SF network, cooperative hubs can allow many neighboring individuals to imitate the behavior of the hub individual. For these reasons, in the RRG, all fractions of each possible state (vaccinated, infected, and free-rider) and the value of $< \pi_{s_j} >$ for a certain C_r are between those of the other kinds of networks. Thus, in the RRG, the threshold value of C_r crossing $-C_r$ and

$< \pi_{s_j} >$ (i.e., the inversion of whether SB-RA or IB-RA effectively works better to deter the spread of an epidemic) occurs at an intermediate value of C_r between that of the square lattice and the BA-SF network.

6.2.3 Summary

In this study, we investigated how the method of risk assessment affects (1) an individual's decision to get vaccinated against a spreading epidemic and (2) the aggregate vaccination behavior of the population. In most previous studies, risk assessment has been based at the individual level in the sense that a focal individual compares her payoff to that of one of her randomly selected neighbor. However, in this paper, we propose a strategy-based risk assessment in which a focal individual compares her payoff to an average payoff that is realized by adopting a strategy adopted by one of her neighbors.

Consequently, a more effective method of risk assessment to prevent the spreading of an infectious disease depends on both the network structure and the cost of vaccination. In the RRG and the BA-SF network, the average path lengths between individuals are smaller than that on a square lattice; thus, an infectious disease spreads more easily. Moreover, the infection of hub individuals induces a pandemic in a heterogeneous graph, such as the BA-SF network. This implies that the vaccination of hubs is more important in a heterogeneous network. However, in a homogeneous network, vaccination of any individual helps to suppress the final proportion of infected individuals.

Based on our results, it is suggested that, for a society to select the preferable method of risk assessment, each individual should know the spatial structure of the network in which she is involved, or at the regional level, an administrative agency should disclose the information on the status of an infectious disease after identifying the network structure. At low values of vaccination cost C_r, our proposed method of risk assessment enhances vaccination coverage and reduces the final proportion of infected individuals, irrespective of network structure. Thus, if the cost of vaccination can be lowered, we can prevent the spread of an infectious disease, irrespective of the underlying network structure, so long as individual actions are based on public information and not on merely imitating their immediate neighbors. This argument provides supporting evidences for subsidizing people to get vaccinated.

For simplicity, we assumed that individuals acquire perfect immunity from vaccination against a seasonal infectious disease during an epidemic season. That is, the probability that a vaccinated individual gets infected is 0 % during an epidemic season. In reality, the efficacy and effectiveness of a vaccination are not always perfect for some infectious diseases. In future work, vaccine efficacy must be considered for allowing us to make a more realistic proposal for preventing epidemics.

References

Anderson, R.M., and R.M. May. 1991. *Infectious diseases of humans*. Oxford/New York: Oxford University Press.

Asch, D.A., J. Baron, J.C. Hershey, H. Kunreuther, J. Meszaros, I. Ritov, and M. Spranca. 1994. Omission bias and pertussis vaccination. *Medical Decision Making* 14: 118–123.

Axelrod, R. 1986. An evolutionary approach to norms. *American Political Science Review* 80(4): 1095–1111.

Barabási, A.L., and R. Albert. 1999. Emergence of scaling in random networks. *Science* 286: 509–512.

Basu, S., G.B. Chapman, and A.P. Galvani. 2008. Integrating epidemiology, psychology, and economics to achieve HPV vaccination targets. *Proceedings of the National Academy of Science of the United States of America* 105: 19018–19023.

Bauch, C.T., and D.J.D. Earn. 2004. Vaccination and the theory of games. *Proceedings of the National Academy of Science of the United States of America* 101: 13391–13394.

Bauch, C.T. 2005. Imitation dynamics predict vaccinating behavior. *Proceedings of the Royal Society B* 272: 1669–1675.

Bauch, C.T., A.P. Galvani, and D.J.D. Earn. 2003. Group interest versus self interest in smallpox vaccination policy. *Proceedings of the National Academy of Science of the United States of America* 100: 10564–10567.

Brian Arthur, W. 1994. Inductive reasoning and bounded rationality. *American Economic Review* 84: 406–411.

Challet, D., Marsili, M., and Zhang, Y.C. 2005. *Minority games: Interacting individuals in financial markets*. Oxford: Oxford University Press.

Chapman, G.B., and E.J. Coups. 1999. Predictors of influenza vaccine acceptance among healthy adults. *Preventive Medicine* 29(4): 249–262.

Chapman, G.B., and E.J. Coups. 2006. Emotions and preventive health behavior: Worry, regret, and influenza vaccination. *Health Psychology* 25: 82–90.

Cullen, J., and West, P. 1979. *The economics of health. An introduction*. Oxford: Martin Robertson.

Doebeli, M., C. Hauert, and T. Killingback. 2004. The evolutionary origin of cooperators and defectors. *Science* 306: 859–862.

Fine, P., and J. Clarkson. 1986. Individual versus public priorities in the determination of optimal vaccination policies. *American Journal of Epidemiology* 124: 1012–1020.

Fu, F., D.I. Rosenbloom, L. Wang, and N.A. Nowak. 2011. Imitation dynamics of vaccination behavior on social networks. *Proceedings of the Royal Society B* 278: 42–49.

Fukuda, E., S. Kokubo, J. Tanimoto, Z. Wang, A. Hagishima, and N. Ikegaya. 2014. Risk assessment for infectious disease and its impact on voluntary vaccination behavior in social networks. *Chaos, Solitons & Fractals* 68: 1–9.

Geoffard, P., and T. Philipson. 1997. Disease eradication: Private versus public vaccination. *American Economic Review* 87: 222–230.

Gillespie, D.T. 1977. Exact stochastic simulation of coupled chemical reactions. *Journal of Physical Chemistry* 81: 2340–2361.

Hethcote, H.W., and P. van den Driessche. 1995. An SIS epidemic model with variable population size and a delay. *Journal of Mathematical Biology* 34: 177–194.

Jansen, V.A., N. Stollenwerk, H.J. Jensen, M.E. Ramsay, W.J. Edmunds, and C.J. Rhodes. 2003. Measles outbreaks in a population with declining vaccine uptake. *Science* 301: 804.

Keeling, M.J., and K.T.D. Eames. 2005. Networks and epidemic models. *Journal of the Royal Society Interface* 2: 295–307.

Kermack, W.O., and McKendrick, A.G. 1927. A contribution to the mathematical theory of epidemics. *Proceedings of Royal Society of London, Series A* 115: 700–721.

Nakata, M., A. Yamauchi, J. Tanimoto, and A. Hagishima. 2010. Dilemma game structure hidden in traffic flow at a bottleneck due to a 2 into 1 lane junction. *Physica A* 389: 5353–5361.

Olson, M. 1965. *The logic of collective action*. Cambridge University Press.
Pastor-Satorras, R., and A. Vespignani. 2001. Epidemic spreading in scale-free networks. *Physical Review Letters* 86: 3200.
Shigaki, K., J. Tanimoto, Z. Wang, S. Kokubo, A. Hagishima, and N. Ikegaya. 2012. Referring to the social performance promotes cooperation in spatial prisoner's dilemma games. *Physical Review E* 86: 031141.
Vardavas, R., R. Breban, and S. Blower. 2007. Can influenza epidemics be prevented by voluntary vaccination? *PLoS Computational Biology* 3(5), e85.
Yamagishi, T. 1986. The provision of a sanctioning system as a public good. *Journal of Personality and Social Psychology* 51: 110–116.

Index

J. Tanimoto, *Fundamentals of Evolutionary Game Theory and its Applications*,
Evolutionary Economics and Social Complexity Science 6,
DOI 10.1007/978-4-431-54962-8